UNIVERSITY OF LONDON THESIS

Degree PhD Year 2006 Name of Author MAVROMATAKIS Yannis

Role of the forkhead transcription factor *Foxa2* in the development of the ventral mesencephalon: A study using conditional mouse mutants

Yannis Emmanuel Mavromatakis

Presented for the degree of Doctor of Philosophy
August 2006

Division of Developmental Neurobiology
National Institute for Medical Research
The Ridgeway, Mill Hill
London NW7 1AA

Department of Anatomy and Developmental Biology
University College London
University of London

ProQuest LLC
789 East Eisenhower Parkway
P.O. Box 1346
Ann Arbor, MI 48106-1346

Declaration of Authenticity

I, **Yannis Emmanuel Mavromatakis**, confirm that the work presented in this thesis is my own. Where information has been derived from other sources, I confirm that this has been indicated in the thesis

Yannis Emmanuel Mavromatakis

28/08/2006

Abstract

The developing mesencephalon consists of two distinct domains. The dorsal domain, the tectum, gives rise to the superior and inferior colliculi, which in the adult receives information from the optic and auditory systems respectively. The ventral domain gives rise primarily to 3 distinct nuclei which are involved in the control of motor movement, such as the mesencephalic dopaminergic neurons, which are the neurons affected in Parkinson's disease, the oculomotor complex and the red nucleus. Forkhead transcription factors of the A subgroup, *Foxa1* and *Foxa2,* are expressed in the ventral midbrain, in addition to being expressed in the notochord, floorplate and gut during embryonic development.

In this study, I focused on the role of *Foxa2*, a member of the forkhead/winghelix family of transcription factors in the specification of the ventral mesencephalic neurons. To address the role of *Foxa2* specifically in the mesencephalon, we have generated a conditional allele of *Foxa2*, referred to as $Foxa2^{flox}$ and crossed this mouse line with *Wnt1-Cre* transgenic animals. Inactivation of *Foxa2* protein in mesencephalic progenitors of *Wnt1-Cre;* $Foxa2^{flox/flox}$ embryos occurred by E8.5. Severe reduction in the numbers of $Islet1^{+}$ oculomotor, $Brn3a^{+}$ red nucleus and *tyrosine hydroxylase*$^{+}$ dopaminergic neurons were observed in *Foxa2* conditional mutant embryos at E12.5, which were preceded by changes in the expression of the morphogen *Shh* as well as *Foxa1* and Nkx transcription factors. Detailed phenotypic characterization by histology, RNA *in-situ* hybridization and immunohistochemistry has revealed novel roles for *Foxa2* in regulating the patterning of mesencephalic progenitors as well as their differentiation. In collaboration with another postdoctoral fellow in the laboratory, we have also shown that *Foxa1* plays a very similar role and can compensate for the function of *Foxa2* in the ventral mesencephalon.

Acknowledgements

I would like to mention and thank the people who contributed to my thesis work.

Firstly, I would like to thank my supervisor for providing me with an interesting and challenging project. I would like to thank every member of the Ang laboratory, from the past (Bertrand) and from the present. I would especially like to thank Anna for her help on the *Foxa2* project and for sharing her data with me for this thesis and Carol for her excellent skills in embryo culture. I have worked closely with Anna and Carol throughout the final stages of my project and would not have been able to achieve any of my goals if it were not for their help and friendship. Finally I would like to thank Wei for providing me with the challenge of obtaining results whilst combating his famous Chinese jinxes. I would also like to thank members of the Briscoe and Wilkinson labs for their suggestions and for their reagents.

I would like to acknowledge Prof. Steven Wilson and Marc for critically reading my manuscript and helping me during the writing stages of the thesis by providing unlimited suggestions on things I should read (mainly telling me I need to read more fish papers).

Finally I would like to thank my family and Chiara who always supported me throughout my studies and encouraged me when work in the laboratory seemed to reach a dead end.

Table of Contents

List of Figures

Introduction:

Results:

Foxa2 CKO

Tables:

Graphs:

List of Abbreviations

-/-	Knockout (e.g. Ptc -/- : Ptc knockout)
5-HT	5-hydroxytryptamine (serotonin)
6-OHDA	6-hydroxydopamine
AADC	L-aromatic amino acid decarboxylase
ABB	Alar-basal boundary
ADHD	Attention deficit hyperactivity disorder
ANR	Anterior neural ridge
APC	Adenomatous Polyposis Coli
AVE	Anterior visceral endoderm
b-HLH	Basic helix loop helix
BMP	Bone morphogenic protein
Brd-U	Bromodeoxyuridine
cDNA	Complementary DNA
Ci	Cubitus interpuptus
Ci-155	Full length cubitus interuptus
Ci-R (Ci-75)	Repressor form of cubitus interuptus
CKO Foxa2 χ	Foxa2 chimaeric embryos
CNS	Central nervous system
Cos2	Costal 2
D1R	Dopamine receptor type 1
D2R	Dopamine receptor type 2
DA	Dopamine
DAB	3,3-diamino-benzidine
DAT	Dopamine transporter
DIG	Digoxigenin
DNA	Deoxyribonucleic acid
E	Embryonic day (e.g. E8.5: embryonic day 8.5)
En1	Engrailed 1
En2	Engrailed 2
FGF	Fibroblast growth factor
Foxa(1 or 2)	Forkhead box (a1 or a2)

Foxa2 CKO	Foxa2 conditional knockout mice
Fu	Fused
GABA	γ-aminobutyric acid
GDNF	Glia derived neurotrophic factor
GFP	Green fluorescent protein
Gli3-R*	Gli3 repressor form
Gli3 XT	Gli3 extra toe mutants
GSK-3β	Glycogen Synthase Kinase 3β
HH	Hamilton hamburger stage (stage of chick development)
Hh	Hedgehog
Hh-C	Hedgehog carboxyl terminal fragment
Hh-N	Hedgehog amino terminal fragment
Hh-NP	Hedgehog amino terminal fragment with signalling moiety
HNF3(α, β or γ)	Hepatocype nuclear factor 3(α, β or γ)
IsO	Isthmic organiser
kDa	Kilo Dalton (unit)
L-DOPA	L-dihydroxyphenylalanine
mesDA	Mesencephalic dopaminergic neurons
MHB	Midbrain-hindbrain boundary
MPTP	1-methyl-4-phenyl-1,2,3,6-tetrahydropyridine
OMC	Oculomotor complex
PD	Parkinson's disease
PKA	Protein kinase A
pMN	Motor neuron progenitor cells
Ptc	Patched
r1	Rhombomere 1
RA	Retinoic acid
RN	Red nucleus
RNA	Ribonucleic acid
RRF	Retrorubral field
Shh	Sonic hedgehog
Shh CKO	Shh conditional knockout mice
Smo	Smoothened

SNpc	Substantia nigra pars compacta
Su(fu)	Suppressor of fused
TF	Transcription factor
TGF	Transforming growth factor
TH	Tyrosine hydroxylase
TUNEL	TdT-mediated dUTP nick end labelled
VMAT	Vesicular monoamine transporter type 2
VTA	Ventral tegmental area
WT	Wild type (embryos/cells/mice)
ZLI	Zona limitans intrathalamica

Introduction

Development of the Mesencephalon

The mesencephalon is one of the least studied regions of the central nervous system (CNS), but it provides a good paradigm to study the mechanisms of how neural tissues are patterned and subdivided to generate distinct structures. Different neuronal populations within the mesencephalon have differing essential functions, with neurons controlling movement located ventrally (tegmentum) and neurons processing acoustic or optic information located dorsally (tectum). These functionally diverse neuronal populations are generated in specific spatial locations along both the anterior-posterior and dorsal-ventral axes in response to signals emanating from signalling centres positioned along the neural tube. In order to appreciate the mechanisms involved in the generation of neuronal diversity within the mesencephalon, it is important to understand the events which are critical for the correct specification and patterning of the mesencephalon from the primitive neural tube.

1. The primitive neural tube is divided along the anterior-posterior and dorsal-ventral axes to create functionally diverse compartments

During the process of neurulation, pattern formation is imposed upon the cells within the neural plate along the anterior-posterior axis in response to a combination of signals emanating from primary signalling centres, such as the anterior visceral endoderm (AVE) and the node, and retinoic acid (RA) emanating from the mesoderm (Beddington and Robertson, 1999; Stern, 2001; Wurst and Bally-Cuif, 2001). In response to these signals the anterior cerebral vesicle is initially subdivided into three distinct domains; the prosencephalon, the mesencephalon and the rhombencephalon (Wurst and Bally-Cuif, 2001; Zervas et al., 2005). The posterior regions neural tube do not undergo a

similar expansion in size, and remain generally cylindrical giving rise to the spinal cord (Gilbert, 2003).

Subsequently, the prosencephalon undergoes a further subdivision to yield the telencephalon and the diencephalon. The telencephalon will give rise to the cerebral hemispheres, while the diencephalon will contain the hypothalamus. The rhombencephalon also undergoes a further subdivision, yielding the metencephalon, which gives rise to the cerebellum and the pons, and the myelencephalon, which gives rise to the medulla (see figure A). The rhombencephalon is also characterised by periodic swellings called rhombomeres running along its anterior-posterior axis which give rise to distinct neuronal populations. However, unlike the primary vesicles in the developing brain, the mesencephalon does not undergo any further subdivision (Gilbert, 2003).

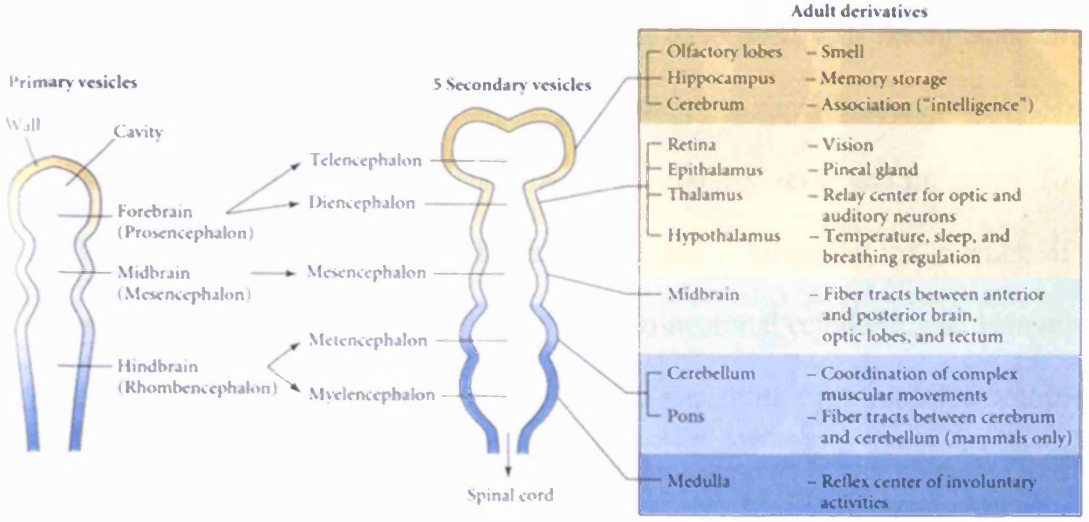

Figure A: Compartmentalisation of the neural tube: The anterior region of the neural tube forms specialised vesicles along the anterior-posterior axis and regions of the adult brain are derived from these vesicles.

Figure A continued: Due to an increase in the proliferation of cells which occupy this domain three primary vesicles are created, the prosencephalon, the mesencephalon and the rhombencephalon. These primary vesicles then sub-divide to create two extra vesicles further specialising the neural tube. Diagram taken from Gilbert, 2003.

Following neurulation the neural tube is further refined along the anterior-posterior axis, to yield further diversity. The prosencephalon and mesencephalon are patterned in response to signals emanating from secondary signalling centres, while the pattern formation of the rhombencephalon and spinal cord are generally controlled by the differential expression of the Hox genes in combination with some signalling mechanisms (Amoyel et al., 2005; Echevarria et al., 2003; Kiecker and Lumsden, 2005; Rubenstein et al., 1998). Secondary signalling centres can be defined as focal transverse domains with morphogenetic activity across the anterior-posterior axis (Echevarria et al., 2003).

At present three such secondary signalling centres have been well documented in the anterior neural tube; the anterior neural ridge (ANR), the zona limitans intrathalamica (ZLI) the isthmic organiser (IsO) (Echevarria et al., 2003; Kiecker and Lumsden, 2005). The ANR is derived from the anterior neural plate and is located at the junction of the most anterior section of the neural tube and the non-neuronal ectoderm, and is involved in patterning of the telencephalon. The ZLI is the signalling centre located within the diencephalon and is involved in patterning the three segments of this domain (Kiecker and Lumsden, 2004; Kiecker and Lumsden, 2005). The best studied of the secondary organisers is the IsO, located at the constriction which separates the mesencephalon with rhombomere 1 (metencephalon) and is also referred to as the midbrain-hindbrain boundary (MHB) (Bally-Cuif and Wassef, 1995). It is critical for the correct

development of neuronal populations of the mesencephalon and the metencephalon and will be discussed in detail below (Echevarria et al., 2003; Simeone, 2000; Wurst and Bally-Cuif, 2001). Recently another secondary signalling centre has been identified within the anterior neural tube, located within rhombomere 4, which is involved in the patterning and specification of the adjacent rhombomeres (rhombomeres 3, 5 and) (Irving et al., 2002; Maves et al., 2002).

Although the most striking transformations of the primitive neural tube occur along its anterior-posterior axis, important transformations also occur along the dorsal-ventral axis. Patterning along this axis is determined by the antagonistic interactions between ventralising and dorsalising signals, which ultimately create four distinct regions of the neural tube; the floor plate, the basal plate, the alar plate and the roof plate (Echelard et al., 1993; Jessell, 2000; Lee and Jessell, 1999; Marti et al., 1995a; Roelink et al., 1995).

In summary, the developing neural tube is patterned along both the anterior-posterior and dorsal-ventral axes in response to inductive signals. Although these primary patterning events generate diverse domains within the developing neural tube, the vast diversity of neuronal populations evident within the adult CNS are generated when signalling mechanisms along both these axes interact creating a Cartesian grid of positional information. This theme will be discussed for each neuronal population of the ventral mesencephalon in a later chapter (see neuronal populations of the ventral mesencephalon).

2. Positioning of the IsO at the interface of *Otx2* and *Gbx2* expression domains

The IsO is known to be necessary and sufficient for the initial development of the mesencephalic and metencephalic structures (Wurst and Bally-Cuif, 2001), and its positioning along the anterior-posterior axis is governed by the interaction of cells expressing two homeodomain transcription factors; *Otx2* and *Gbx2* (Simeone, 2000; Wurst and Bally-Cuif, 2001; Zervas et al., 2005). *Otx2* is expressed from the anterior neural tube occupying the presumptive prosencephalon and mesencephalon forming a border at the presumptive MHB (Acampora et al., 1995; Ang et al., 1996), while *Gbx2* expression is present in a domain posterior to the MHB (Wassarman et al., 1997; Wurst and Bally-Cuif, 2001).

Genetic analysis of mutant mice for *Otx2* and *Gbx2* has demonstrated their importance in the correct positioning of the IsO within the MHB. Mice with a homozygous deletion of *Otx2* (*Otx2-/-*) display a loss of the forebrain and mesencephalon (Acampora et al., 1995; Ang et al., 1996), while *Gbx2* knockout mice (*Gbx2 -/-*) lack the anterior rhombencephalon and display a posterior expansion of the mesencephalic *Otx2* positive domain (Millet et al., 1999; Wassarman et al., 1997). Interestingly the dosage of Otx proteins is also an important factor in the positioning of the IsO at the MHB. Embryos which only have one functional allele of *Otx2* in an *Otx1* null background (*Otx1 -/- ; Otx2 +/-*) display a transformation of the posterior diencephalon and the mesencephalon into an enlarged metencephalon (Acampora et al., 1997). Ectopic expression studies using either *Otx2* or *Gbx2* have produced similar results (Broccoli et al., 1999; Millet et al., 1999). All these results clearly demonstrate that the IsO is positioned in the MHB between the expression domains of *Otx2* and *Gbx2*, and that the correct position of the

IsO is critical for determining the size of the mesencephalon and metencephalon. Recently it has been demonstrated that the establishment and specification of the IsO at the MHB is not dependent on the actions of either *Otx2* or *Gbx2*, as genes normally expressed in a restricted manner at the MHB are still observed in *Otx2/Gbx2* double mutants (Li and Joyner, 2001; Martinez-Barbera et al., 2001).

3. Secreted signalling molecules from the IsO pattern the mesencephalon and metencephalon

The inducing capability of the IsO has been studied extensively in recent years. Transplant experiments demonstrated that ectopically placing tissue from the MHB region into the host diencephalon or metencephalon can induce a new MHB region around the transplanted tissue (Liu and Joyner, 2001a; Nakamura et al., 2005). Two classes of signalling molecules, Wnts and FGFs are known to be expressed at the MHB, with initial studies indicating that *Wnt1* (Wilkinson et al., 1987) and *Fgf8* (Crossley and Martin, 1995) gene expression were localised around this domain. *Wnt1* was originally identified as an oncogene due to frequent insertions of the mouse mammary tumour virus which lead to the over-expression of its transcript (Nusse and Varmus, 1982), and is first expressed at the first somite stage and by the 6-8 somite stage is expressed throughout the presumptive mesencephalon (Echelard et al., 1994; Wilkinson et al., 1987). The expression of *Wnt1* in the mesencephalon gradually becomes restricted to the ventral and dorsal midlines and to a small semi-circular domain at the posterior limit of the *Otx2* domain (Zervas et al., 2004). *Fgf8* is first expressed during gastrulation and is eventually restricted to several signalling centres along the anterior-posterior axis (Crossley and Martin, 1995). The expression of *Fgf8* within the MHB region is

restricted posterior to the expression of *Wnt1*, and forms a semi-circular domain of expression around the MHB (Crossley and Martin, 1995; Meyers et al., 1998).

Wnt1 is essential for the development of the MHB, as this region is lost in *Wnt1* knockout (*Wnt1* -/-) embryos (McMahon and Bradley, 1990; McMahon et al., 1992), but it has been shown that *Wnt1* is only required for the proliferation and survival of this region (Danielian and McMahon, 1996; McMahon et al., 1992). Furthermore, *Wnt1* does not posses the inducing properties of the IsO as demonstrated in gain of function studies (Danielian and McMahon, 1996).

FGFs, in particular *Fgf8* were demonstrated to posses the inducing capabilities of the IsO. Fgf8-soaked beads can transform the anterior diencephalon into a MHB region (Crossley et al., 1996; Liu et al., 1999; Martinez et al., 1999). The requirement for *Fgf8* during the development of the MHB was also demonstrated by using *Fgf8* conditional knockout mice, as classical knockout mice have gastrulation defects (Sun et al., 1999). The loss of *Fgf8* from the MHB results in the loss of the mesencephalon and anterior metencephalon (Chi et al., 2003; Meyers et al., 1998). Recent analysis has revealed that apart from *Fgf8*, *Fgf17* and *Fgf18* also play a role in the inducing capabilities of the MHB region (Liu et al., 2003). It has also been demonstrated that different isoforms of *Fgf8* posses different roles in the patterning of regions adjacent to the MHB domain. *Fgf8a* is involved in the specification of the mesencephalon while *Fgf8b* specifies the metencephalon (Liu et al., 1999). Furthermore, another role for FGF signalling from the IsO has been described in zebrafish. Fgf8 signals acting in concert with the *Engrailed* genes are important in the maintenance of the boundary between the mesencephalon and the diencephalon (Scholpp et al., 2003).

4. Other factors involved in the maintenance of the IsO/MHB domain and the specification of the mesencephalon

Following the expression of *Otx2* and *Gbx2* and the positioning of the IsO at the correct location within the MHB, a network of transcription factors are involved in the maintenance and further patterning of the presumptive mesencephalon and metencephalon. *Pax2*, a member of the paired-rule family of transcription factors, is expressed prior to somitogenesis, followed by the expression of *Engrailed-1* (*En-1*), a member of the segmentation family of transcription factors and *Lmx1b*, a member of the LIM homeodomain transcription factors. *Pax5* and *En-2* become expressed at the 5-somite stage of embryogenesis. These genes are initially expressed in broad overlapping domains spanning the presumptive mesencephalon and the presumptive rhombencephalon, which are later refined and restricted to distinct locations within the mesencephalon, metencephalon and also the MHB (Wurst and Bally-Cuif, 2001; Zervas et al., 2005).

Numerous gain-of-function and loss-of-function assays have elucidated the role that each gene plays in the maintenance of the MHB region. The gain-of-function and loss-of-function experiments for *Otx2*, *Gbx2*, *Wnt1* and *Fgf8* have been described earlier. *Pax2* knockout (*Pax2 -/-*) mice display a loss of the posterior mesencephalon and metencephalon with the severity of the phenotype depending upon the genetic background of the mice (Schwarz et al., 1997). *Pax5* knockout (*Pax5 -/-*) mice display a much less severe phenotype than the *Pax2 -/-* with a loss of the inferior colliculi and the anterior cerebellum (Schwarz et al., 1997). Double *Pax2 -/-; Pax5 -/-* mice show a complete loss of the mesencephalon and metencephalon (Schwarz et al., 1997). *En1*

knockout mice (*En1* -/-) display an almost complete loss of mesencephalic and anterior metencephalic tissue (Wurst et al., 1994), whereas *En2* knockout (*En2* -/-) mice display only mild alterations to the foliation of the cerebellum (Millen et al., 1994).

Through the analysis of the gain-of-function data, a clearer image of the intricate relationships between the genes of the developing MHB region can be drawn. It becomes evident that all of the genes which are expressed throughout the developing mesencephalon and MHB region are either sufficient to induce or repress each other's expression. The ectopic expression of *Otx2* can induce *Lmx1b* and *Wnt1* but repress *Gbx2*, while ectopic *Gbx2* can repress *Otx2*, *Lmx1b* and *Wnt1*. *Lmx1b* is able to induce the expression of *Otx2* and *Wnt1* but represses *Fgf8* (Adams et al., 2000; Matsunaga et al., 2002). In the same study it was shown that *Wnt1* can induce *Fgf8* and *En1*, but not *Lmx1b*. *En1* has the ability to induce *Fgf8* and *Pax2* (Shamim et al., 1999), while *Pax2* alone is sufficient to induce the expression of *Fgf8* (Ye et al., 2001). Ectopic expression of *Fgf8* induces *Wnt1*, *Lmx1b*, *Gbx2*, *Pax5*, *En1* and *En2* whilst repressing the expression of *Otx2* (Martinez et al., 1999).

Taken together, these data demonstrate the tight relationship between all the genes within this region of the brain. Interestingly these genes are sufficient to induce the expression of the other genes within the MHB region but are not necessary for their induction. The genes of the developing MHB region are induced independently from each other, but once induced form a tight regulatory mechanism to maintain each others expression. A clear example of this phenomenon can be seen from the *En1* -/-; *En2* -/- double knockout mice. Although there is a loss of the entire mesencephalic and metencephalic region, *Fgf8* and *Wnt1* were induced, but due to the loss of *En1* and *En2*

there was no maintenance of the *Fgf8* and *Wnt1* gene expression and both were subsequently lost (Liu and Joyner, 2001b).

To summarise, once the mesencephalic region has been specified within the developing embryo a complex series of interactions occur to maintain its identity. In addition to maintaining the structure and identity of the mesencephalon, signalling molecules from the IsO interact with signals from the floor plate further refine, pattern and specify distinct neuronal populations along its neuraxis. The mechanisms for the specification of neurons along the dorsal-ventral axis will be discussed in the following chapter, and the interactions of signals emanating from the anterior-posterior and dorsal-ventral axes will be discussed for each of the neuronal populations individually in the subsequent chapters.

Patterning the Neural Tube along the Dorsal-Ventral Axis

The developing neural tube is patterned along both the anterior-posterior and dorsal-ventral axes by signalling molecules to specify populations of functionally diverse neurons at specific locations along the neuraxis. The initial patterning of the neural tube along the dorsal-ventral axis generates four domains; the floor plate, basal plate, alar plate and the roof plate. In similar fashion to the patterning along the anterior-posterior axis, signals emanating from signalling centres are responsible for the cell type specification along the dorsal-ventral axis. The two signalling centres along this axis are the roof plate (dorsally) and the floor plate (ventrally), and neurons are specified along this axis due to the interactions of dorsal and ventral signals (Jessell, 2000).

The developing spinal cord is the best characterised region of the CNS as it presents the simplest model for dorsal-ventral patterning. The physiology and anatomy of the neurons are well defined and functions have already been assigned to many of the identified neurons (Briscoe and Ericson, 2001). The neurons which are generated within the developing neural tube can be categorised into three classes. Neurons which are involved in the processing and relaying of sensory information are located within the dorsal regions of the neural tube, whereas neurons involved in the processing of motor output reside in the ventral region (Briscoe and Ericson, 2001; Jessell, 2000). Different classes of interneurons, which connect the sensory and motor systems, are found at stereotypical locations along the dorsal-ventral axis (Jessell, 2000) (see figure B). The mechanisms which have been described in the developing spinal cord apply throughout the entire neuraxis, with slight variations occurring in the more anterior domains of the neural tube.

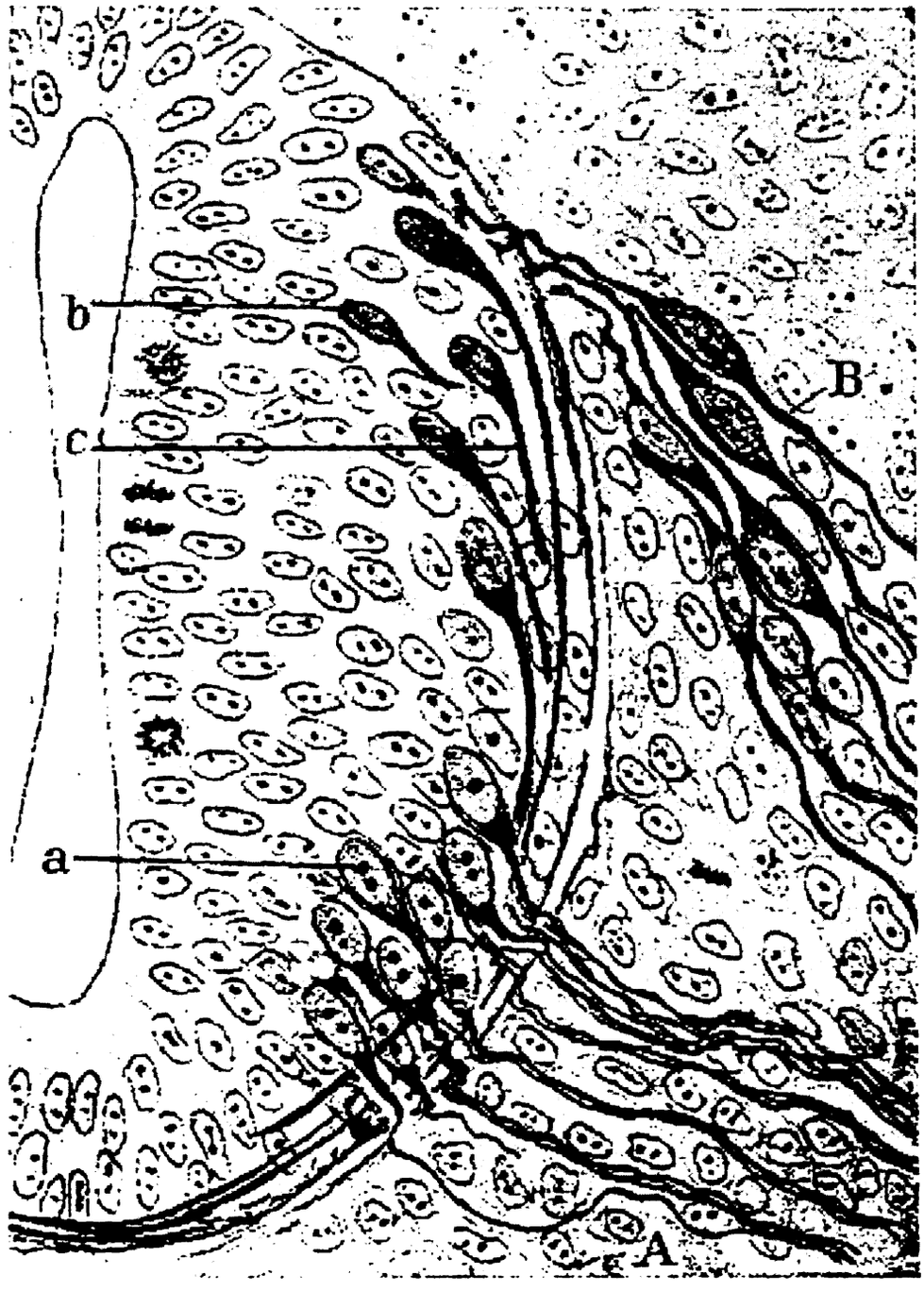

Figure B: Cross section of developing chick spinal cord: A drawing from Ramon y Cajal's Nobel prize winning lecture in 1906 showing schematic cross section of the developing spinal cord from a 3 day old chicken embryo. Sensory neurons are generated and located dorsally (b) while motor neurons are located ventrally (a). (B) Shows sensory ganglions emanating from the dorsal neural tube. (A) Shows anterior root ganlglion cells. A commissural interneuron which whose axon crosses the midline of the neural tube is represented at position (c) (Ramon y Cajal, 1906).

Ramon y Cajal described that motor neurons were generated in a spatially restricted region of the ventral spinal cord, and that they were generated at a much earlier period in development than more dorsally located neurons (Ramon y Cajal, 1906). This observation raised the question as to what controlled the position of the progenitor cells and the subsequent progeny along the dorsal-ventral axis.

5. Mechanism of Sonic Hedgehog signalling

The signalling molecule responsible for patterning the neural tube along the dorsal-ventral axis is Sonic Hedgehog (Shh), the vertebrate homologue to the *Drosophila* segment polarity gene *hedgehog* (Hh), which is expressed in the notochord and the floor plate (Chang et al., 1994; Echelard et al., 1993; Marti et al., 1995b; Riddle et al., 1993; Roelink et al., 1994). Initially Shh is expressed in the notochord and later induces its own expression in the overlying neural plate generating the floor plate (Echelard et al., 1993; Roelink et al., 1994). Secreted Shh diffuses along the dorsal-ventral axis and is responsible for the patterning of the neural tube along this axis (Jessell, 2000).

The mechanism of Shh signalling was first described in the *Drosophila* and thus has been best characterised in this model, but is well conserved throughout many species (Ingham and McMahon, 2001). Hh is initially produced as a 46kDa precursor protein and acquires its inducing capabilities following an autocatalytic intramolecular proteolysis which creates two distinct fragments; an amino-terminal 19kDa fragment (Hh-N) and a carboxyl 27kDa fragment (Hh-C) (Bumcrot et al., 1995; Ingham and McMahon, 2001; Lee et al., 1994). It has been demonstrated that the Hh-C fragment induces the intramolecular proteolysis causing a cleavage between the Glycine and

Cystine residues which are found in an ultra-conserved tri-peptide sequence (Lee et al., 1994; Porter et al., 1995).

After this cleavage event occurs, the Hh-N fragment receives further refinement by the addition of a cholesterol molecule which provides the molecule with its processed signalling moiety (Hh-Np) (Porter et al., 1996a; Porter et al., 1996b). Confirmation of the size of the Hh-Np fragment was provided from analysis of its crystal structure (Hall et al., 1997). Further studies revealed that the Hh-Np fragment is active throughout Hh signalling, while no other function has been assigned to the Hh-C apart from the autocatalytic processing involved in producing the Hh-N fragment (Ingham and McMahon, 2001). The Hh-Np molecule is bound by the extracellular domain of the 12-transmembrane receptor *Patched (Ptc)* (Fuse et al., 1999; Marigo et al., 1996a; Marigo et al., 1996b; Marigo and Tabin, 1996; Stone et al., 1996), and when this extracellular domain is deleted, the Hh-Np molecule can not be bound (Briscoe et al., 2001). Studies on *Ptc* mutants in both mouse and *Drosophila* have revealed that *Ptc* activity suppresses the actions of Shh, and that the Shh ligand functions by suppressing the action of *Ptc* (Goodrich et al., 1997; Ingham and McMahon, 2001). In the absence of Hh-Np ligand the activity of the 7-transmembrane protein *Smoothened* (*Smo*) is repressed by *Ptc* (Taipale et al., 2002). In the presence of the Hh ligand, the repression of *Smo* by *Ptc* is abolished, allowing *Smo* to induce a signalling cascade which results in the transcription of Hh target genes. The Hh signalling in *Drosophila* is mediated by the actions of a zinc-finger transcription factor Cubitus interuptus (Ci). There are three *Ci* homologues in vertebrates; *Gli1 -2 -3* whose roles will be addressed later (Ingham and McMahon, 2001).

In the absence of an Hh ligand *Smo* is unable to translocate to the plasma membrane and *Ci* is sequestered in the cytoplasm by a protein complex consisting of *Costal 2* (*Cos-2*), *Fused* (*Fu*) and *Suppressor of Fused Su(Fu)* (Huangfu and Anderson, 2006; Jia et al., 2003; Lum et al., 2003a; Lum et al., 2003b; Ogden et al., 2003; Ruel et al., 2003; Zhu et al., 2003). This protein complex allows for the phosphorylation of *Ci* by PKA, and ultimately the proteolytic cleavage of the full length *Ci* (*Ci-155*) protein into a repressor form (*Ci-R or ci-75*) (Jia et al., 2004). This repressor form translocates to the nucleus where it functions to repress Hh target genes. In the presence of the Hh ligand, *Smo* is phosphorylated by PKA inducing the release of *Ci* from the protein complex, allowing *Ci-155* to enter the cell nucleus and function as an activator of Hh target genes (see figure C) (Briscoe and Therond, 2005; Collins and Cohen, 2003; Huangfu and Anderson, 2006; Ingham and McMahon, 2001).

Evidence of the transducing properties of *Smo in-vivo* has been demonstrated by the presence of activated forms of *Smo* in basal cell carcinomas, usually a sign of excessive Hh signlling. Transgenic mice which expressed a mutated form of *Smo* in the epidermis also showed evidence of basal cell carcinoma suggesting a role for *Smo* in transducing the Hh pathway (Xie et al., 1998). Consistent with the hypothesis that *Smo* plays a positive role in the transduction of the Hh pathway, ectopically expressing mutated forms of *Smo* in the neural tube triggered the cell autonomous expression of Hh target genes (Hynes et al., 2000). It was later discovered that carcinomas common to the over-activity of the Hh pathway can be reversed by the administration of a plant derived teratogen, cyclopamine (Taipale et al., 2000).

A In Absence of Hh Ligand

B In Presence of Hh Ligand

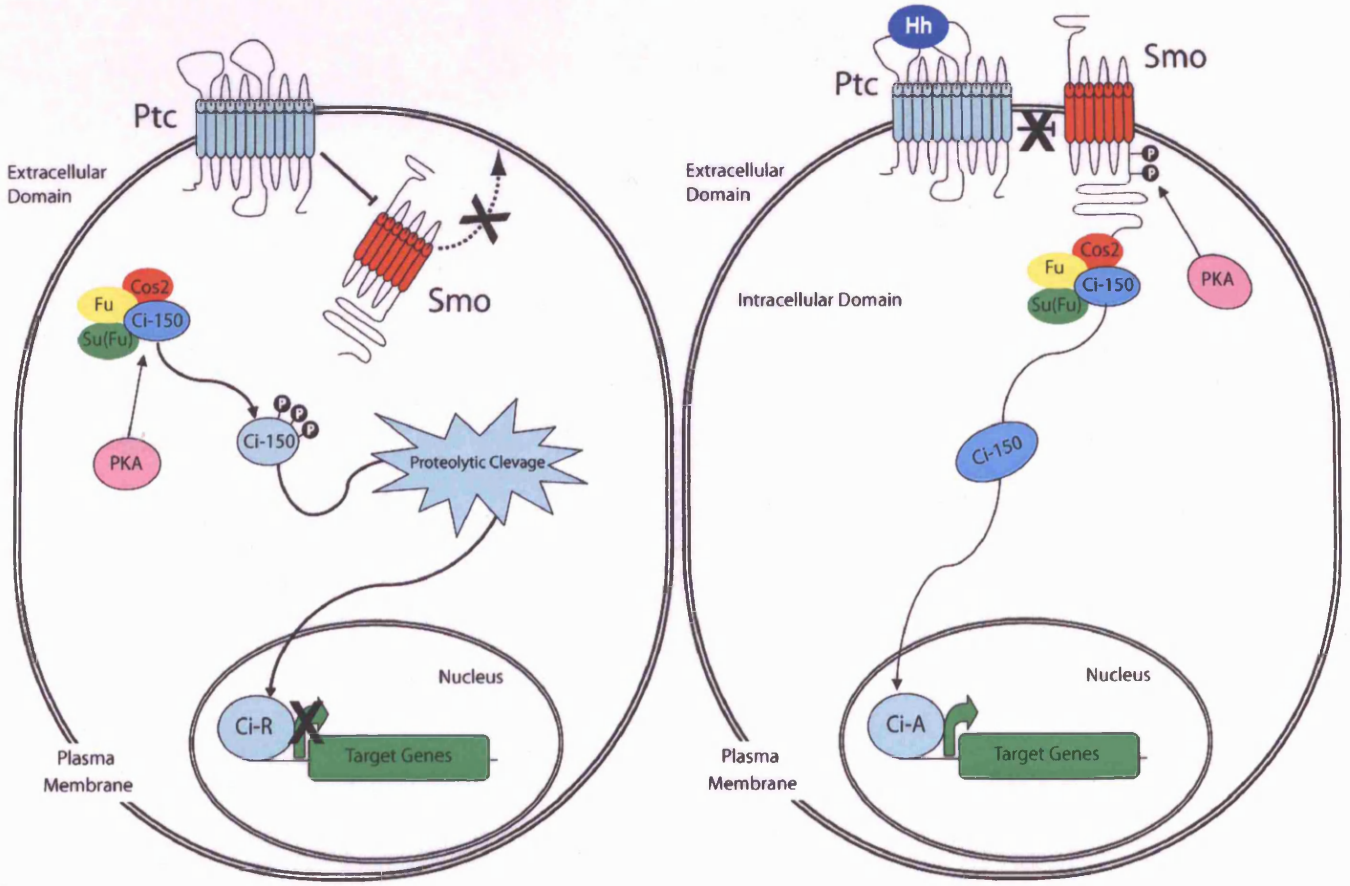

Figure C: The Hedgehog (Hh) signalling cascade in Drosophila: (A) In the absence of the Shh ligand the activity of the 7-transmembrane protein Smo is repressed by the 12-transmembrane receptor protein Ptc. Downstream of Smo, Ci is sequestered in the cytoplasm by the Cos2-Fu-Su(Fu) complex, where it is phosphorylated by PKA and subsequently cleaved into a repressor form which enters the nucleus and represses transcription of Hh target genes. (B) In the presence of the Hh signal, there is no repression of Smo from Ptc. Due to the phosphorylation of the Smo protein by PKA, Ci is no longer bound to the Cos2-Fu-Su(Fu) complex allowing the full length activating form of Ci to enter the nucleus inducing the transcription of Shh target genes. In vertebrates there are three homologues of Ci; Gli1, Gli2 and Gli3, and the signalling cascade is generally identical. Based on diagrams by (Briscoe and Therond, 2005; Litingtung and Chiang, 2000a; Ruiz i Altaba et al., 2002)

It was later shown that this effect was due to the cyclopamine binding to the Smo protein and inhibiting its activity (Chen et al., 2002a). The blocking of *Smo* activity now seems to be a major aim for pharmaceutical companies in a bid to provide therapeutic benefits to patients suffering from carcinomas related to aberrant Hh signalling (Chen et al., 2002b).

Further evidence for the role that *Smo* plays in the transduction of the Shh signalling pathway was provided from the analysis of *Smo* knockout mice (*Smo* -/-). The loss of *Smo* activity causes embryonic lethality at embryonic day 9 (E9), with analysis of embryos prior to their death revealing that the phenotype resembles that of embryos deficient in hedgehog signalling activity (Zhang et al., 2001).

6. Shh signalling induces the generation of distinct neuronal populations along the dorsal-ventral axis

Following the identification of Shh as the inducible factor derived from the notochord and subsequently from the floor plate, many studies were carried out in order to determine which fragment of the Shh molecule possessed the inducing capabilities.

Experimental evidence revealed that Shh-Np possessed the inducing capabilities of the signalling molecule (Marti et al., 1995a; Roelink et al., 1995). Furthermore, the application of different concentrations of the Shh-Np molecule to cultured cells produced different populations of neural cell types. Low concentrations of Shh-Np produced motor neurons and no floor plate cells, while the exposure of the cells to high concentrations of Shh-Np produced floor plate cells in expense of motor neurons (Roelink et al., 1995).

The importance of Shh-Np in the patterning of the ventral neural tube and the specification of ventral neuronal types was later demonstrated by blocking the Shh signal with the use of antibodies *in-vitro* (Ericson et al., 1996) and *in-vivo* by creating Shh knockout mice (*Shh* -/-) (Chiang et al., 1996). By adding a Shh antibody specific for the Shh-Np fragment to neural plate explants it was possible to sequester the endogenous Shh molecules and inhibit the endogenous Shh signalling cascade. This blockade of the endogenous Shh activity resulted in the lack of floor plate formation and the absence of motor neurons from the explants (Ericson et al., 1996). Direct evidence for the necessity of Shh signalling to induce the floor plate and the ventral neuronal populations came from the analysis of the *Shh* -/- mice. The *Shh* -/- mutants were unable to establish or maintain the notochord and floor plate structures, and subsequently displayed a loss of all ventral neuronal populations. This loss was accompanied by the expansion of dorsal neural tube markers to ventral locations (Chiang et al., 1996).

The following year it was demonstrated that the concentration of the Shh-Np signal influences the final fate of the progenitor cells of the ventral neural tube. Using the

chick explant system, it was shown that incremental ~2-fold increases in the concentration of Shh-Np were sufficient to generate either motor neurons or two distinct classes of interneurons, V1 & V2 interneurons, along the ventral neural tube (see figure D) (Ericson et al., 1997). V1 interneurons which are located further away from the floor plate required the least concentration of Shh to be induced, while motor neurons required ~4 times that concentration to be generated (Ericson et al., 1997). The observation that different neuronal populations were generated according to the distance from the ventral midline suggested that Shh signalling functions in a graded manner and acts as a long range signalling molecule to pattern the neural tube into five distinct progenitor domains (Ericson et al., 1997; Jessell, 2000; Price and Briscoe, 2004).

These results raised the question as to how the cells received the inducing capabilities of the Shh signal. It had been shown to act over a long range to pattern different neuronal populations, but no direct *in-vivo* evidence of a gradient of Shh-Np molecules in the ventral neural tube could be found. Due to the lack of *in-vivo* evidence that Shh was forming a protein gradient, and in line with work performed in the *Drosophila* wing, it was suggested that Shh acts over a short distance inducing a cell-cell interaction relay signal. Direct evidence that the graded Shh signalling in-vivo was acting as a long range signalling molecule was provided by the ability to block an individual cell's ability to response to the Shh-Np signal. A mutated form of the *Ptc* receptor (*Ptc-Δ-loop*), which lacked the extracellular Shh binding domains and acted as a dominant inhibitor of Shh signalling even in the presence of Shh ligand was generated (Briscoe et al., 2001).

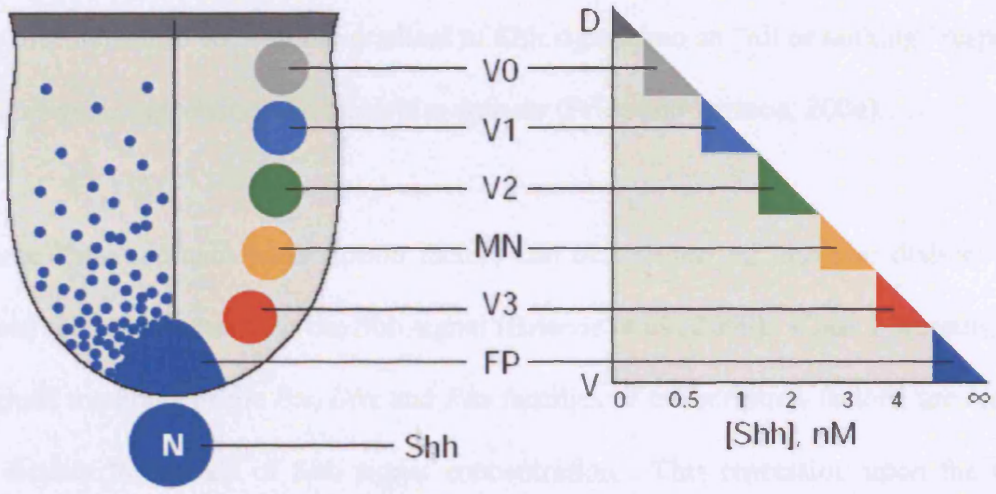

Figure D: Increments of Shh protein pattern the neural tube along the dorsal-ventral axis: Specific increments of Shh-Np concentration provide an all or nothing response to generate 5 distinct neuronal populations within the ventral neural tube. The requirement for a specific concentration of Shh-Np is dependant on the distance from the source of the Shh-Np signal, with ventral neuronal populations requiring higher concentrations of Shh-Np than neuronal located in more dorsal regions. Diagram taken from review by (Jacob and Briscoe, 2003)

Electroporating the *Ptc-Δ-loop* construct into the neural tube demonstrated that the target cells did not respond to Shh signalling, and produced cell autonomous inhibition of the generation of different classes of ventral neuronal populations, depending on the dorsal-ventral location of the target cells (Briscoe et al., 2001). This result demonstrated that Shh acts directly on the progenitor cells along the dorsal-ventral axis, and not through a relay system of cell-cell signalling.

7. How neural progenitor cells interpret the graded Shh signal

It was evident that different populations of neurons were generated at distinct locations along the dorsal-ventral axis of the neural tube, in response to graded Shh signalling. However, it was still not understood how the cells interpreted this signal. Due to their expression patterns within the progenitor cells of the ventral neural tube of both the

chick and the mouse, it was suggested that homeodomain transcription factors provided the mechanism to convert the gradient of Shh signal into an "all or nothing" response to induce gene expression of a particular domain (Price and Briscoe, 2004).

These homeodomain transcription factors can be categorised into two distinct classes based on their response to the Shh signal (Briscoe et al., 2000). Class I proteins, which include members of the *Irx*, *Dbx* and *Pax* families of transcription factors, are repressed at distinct thresholds of Shh signal concentration. This repression upon the Class I proteins limits the extent of their ventral gene expression. In contrast Class II proteins, which include members of the *Nkx* family of transcription factors, are induced by specific concentrations of Shh signal. This induction of gene expression at specific thresholds of Shh concentration of the Class II genes determines the extent of their dorsal expression (Briscoe et al., 2000).

Data from gain-of-function analysis on chick neural tube, coupled with loss-of-function data generated in the mouse have now demonstrated a mechanism by which sharp boundaries of homeodomain gene expression are created to produce five distinct progenitor domains, which correspond to the five distinct neuronal populations of the ventral neural tube (see figure E). It was shown that the sharp boundaries of gene expression were generated due to the cross-repressive interactions between the Class I and Class II proteins, which are expressed in adjacent domains (Briscoe et al., 2000; Ericson et al., 1997). By ectopically inducing the expression of either Class I or Class II proteins, it was possible to alter the fate and position of the generation of individual neuronal populations (Briscoe et al., 2000). Additionally, the generation of knockout mice for specific Class I or Class II proteins revealed similar results. The inactivation

of the Class I protein *Pax6*, caused an expansion of the V3 interneuron population expressing *Nkx2.2* in expense of the motor neurons normally located in this domain (Ericson et al., 1997). The inactivation of *Nkx2.2* induced the expansion of the motor neuron domain in expense of the V3 interneurons (Briscoe et al., 1999). One further example of this mechanism can be seen from the inactivation of *Dbx1*, a gene expressed within the V0 progenitor domain. There was an expansion of the V1 interneuron population in expense of the V0 interneuron population (Pierani et al., 2001).

The roles of the homeodomain transcription factors are best understood for the generation of the motor neurons. The combinatorial action of three homeodomain proteins, *Irx3-Nkx6.1-Nkx2.2*, establishes the location of the motor neuron progenitor cells within the ventral neural tube (see figure E) (Briscoe and Ericson, 1999; Briscoe and Ericson, 2001; Briscoe et al., 2000). Motor neurons are restricted within the specific pMN domain due to the restrictive actions of *Nkx2.2* ventrally and *Irx3* dorsally. This interaction ensures that the motor neurons are not generated outside of this domain. From this restricted domain, *Nkx6.1* was shown to induce the expression of transcription factors essential for motor neuronal development, the basic-Helix-loop-helix (b-HLH) transcription factor *Olig2* and motor neuron determinant gene MNR2 (*Hb9* in mouse) (Novitch et al., 2001; Tanabe et al., 1998). *Olig2* has been shown to be required for the acquisition of pan-neuronal properties and subtype characteristics of the differentiating motor neurons.

The ectopic expression of *Olig2* in the ventral neural tube was demonstrated to be sufficient to repress the expression of *Irx3*, thus alleviating the repression of motor neuron generation outside of the previously defined domain (Novitch et al., 2001),

whilst the loss of *Olig2* causes a loss of motor neuron differentiation (Zhou and Anderson, 2002). It was shown that MNR2 is expressed in the motor neuron progenitor cells during their final cell division, and ectopic expression of MNR2 is sufficient to induce ectopic motor neurons without altering the expression of the endogenous Class I or Class II genes (Tanabe et al., 1998).

Thus, the homeodomain transcription factors are involved in interpreting the graded Shh signal and converting this signal into distinct regions of gene expression from which distinct neuronal populations are generate. The cross repressive interactions between the Class I and Class II proteins function to maintain the identity of the progenitor cells within the five distinct neuronal progenitor domains. However, it has also been shown that Shh-independent mechanisms are also involved in the specification of neurons within the V1 and V0 domains. Although Shh is sufficient to induce the expression of *Dbx* genes in the V1 and V0 domain, it is not required for this *in-vivo* or *in-vitro*. A parallel pathway was shown to involve RA in mediating the differentiation of the interneurons at this level of the dorsal-ventral axis (Pierani et al., 1999).

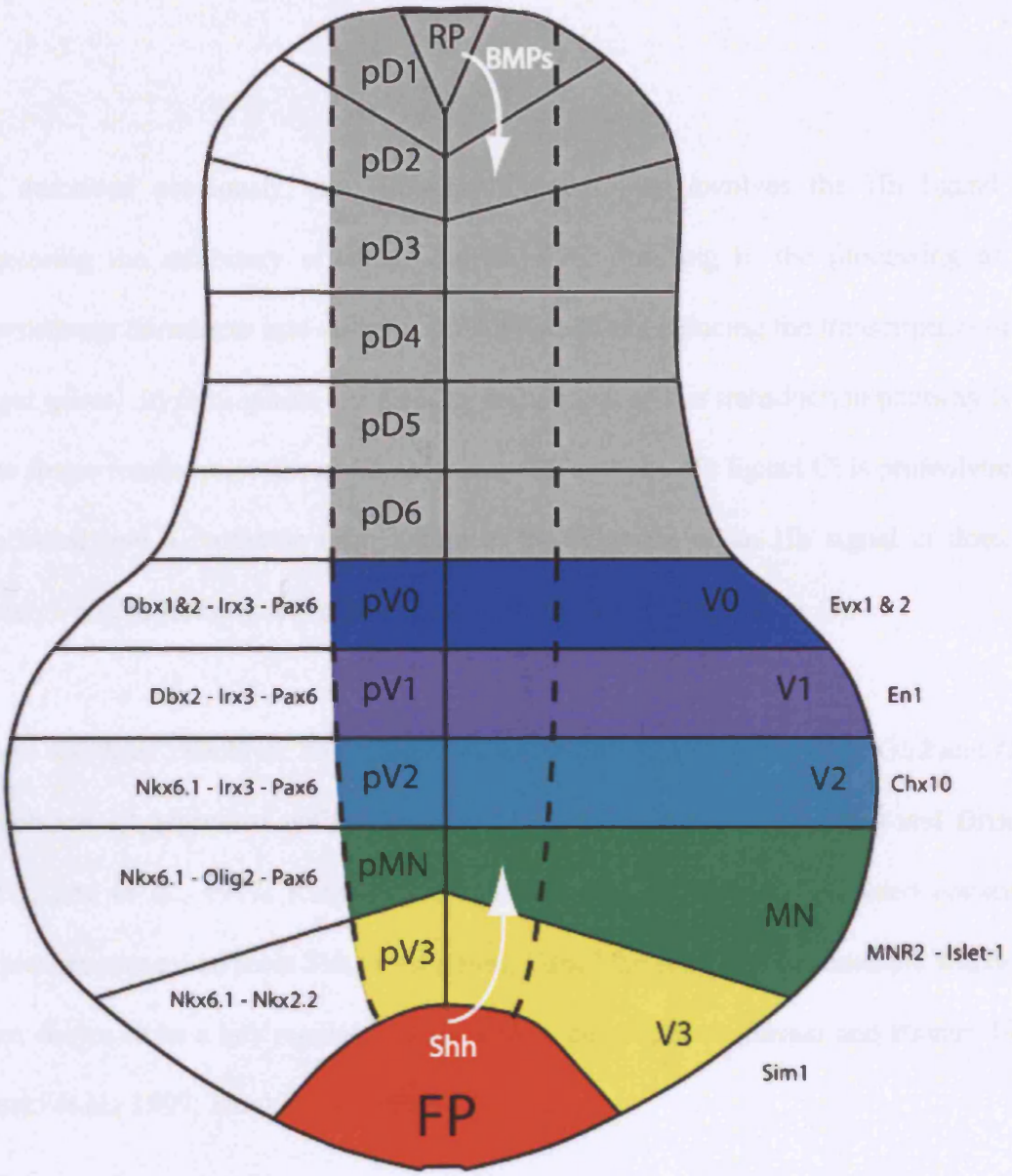

Figure E: Progenitor domains of developing spinal cord: The locations of specific progenitor domains which eventually give rise to the distinct neuronal populations present in the adult spinal cord. In the ventral half of the neural tube, Shh is secreted from the floor plate (FP) and forms a concentration gradient. Distinct neuronal progenitor domains are created in response to this grade Shh signal due to the actions of homeodomain transcription factors, which correspond to the distinct neuronal populations generated, e.g. V3 interneurons expressing Sim1 are generated in the pV3 progenitor domain expressing homeodomain proteins Nkx2.2 and Nkx6.1. The dorsal neural tube is patterned by members of the bone morphogenic proteins (BMP) which belong to the TGFβ superfamily of transcription factors, being secreted from the roof plate (RP) creating distinct progenitor domains which correspond to the sensory neurons generated in the dorsal neural tube. Progenitor domains within the ventricular zone are within dotted lines. Diagram adapted from (Wilson and Maden, 2005)

8. Transduction of the Shh signal by the zinc finger transcription factor(s) Ci/*Gli1 -2 -3*

As described previously, the Hh signalling pathway involves the Hh ligand de-repressing the inhibitory effect of *Ptc* on *Smo*, resulting in the processing of the downstream transducer into an activator form and thus inducing the transcription of Hh target genes. In *Drosophila*, the primary component of this transduction pathway is the zinc finger transcription factor Ci. In the absence of any Hh ligand Ci is proteolytically processed into a repressor form, while in the presence of an Hh signal ci does not undergo any processing and retains its activating abilities (see figure C).

There are three vertebrate homologues to the *Drosophila* Ci gene, *Gli1*, *Gli2* and *Gli3*, which are all expressed within the neural tube (Hui et al., 1994; Jacob and Briscoe, 2003; Lee et al., 1997; Ruiz i Altaba, 1998), and all bind to Ci-related consensus sequences present on most Shh target genes, *Foxa2* the most notable example which has been shown to be a key regulator of floor plate development (Sasaki and Hogan, 1994; Sasaki et al., 1997; Sasaki et al., 1999).

Gene expression studies have revealed that *Gli1* is localised to the ventral region of the neural tube adjacent to the Shh expression domain, and is dependent on Shh signalling (Bai et al., 2002; Platt et al., 1997). It has been shown that *Gli1*, unlike Ci, does not undergo any proteolytic processing and functions as an activator to induce Shh target genes (Lee et al., 1997; Ruiz i Altaba, 1998). Experimental evidence for the activator ability of *Gli1* was provided when ectopically inducing *Gli1* mimicked Shh signalling and activated Shh target genes (Hynes et al., 1997). However it is still maintained that

Gli1 is unlikely to mediate the early response to the Shh signal, which was confirmed by the absence of any visible developmental defects in *Gli1* knockout mice (*Gli1 -/-*) (Bai et al., 2002; Park et al., 2000).

Both *Gli2* and *Gli3* are expressed in the neural tube prior to its closure and in the developing spinal cord *Gli3* expression is confined to the dorsal domain while *Gli2* expression is uniform throughout (Hui et al., 1994; Lee et al., 1997). Unlike *Gli1*, it has been revealed that *Gli2* and *Gli3* possess both a repressor and activator domain similar to Ci (Ruiz i Altaba, 1999; Sasaki et al., 1999), with *Gli2* considered to be the primary activator and *Gli3* the primary repressor (Jacob and Briscoe, 2003).

Gli2 knockout mice (*Gli2 -/-*) display multiple developmental defects in the skeletal structures and in the lungs. In addition to these defects, in the neural tube there is an absence of the floor plate structure and the majority of the V3 interneurons, but other neuronal populations remain intact. Surprisingly the motor neurons are still present even in the absence of the floor plate, but are re-located within the midline of the neural tube (Ding et al., 1998; Matise et al., 1998).

Not only do these results suggest that *Gli2* functions downstream of Shh signalling to induce the most ventral regions of the neural tube, but that the induction of the floor plate is dependent of *Gli2* function. When both *Gli1* and *Gli2* were inactivated together (*Gli1 -/- ; Gli2 -/-*) the phenotype was not more severe and resembled that of the *Gli2 -/-* single mutant (Matise et al., 1998). Taken together these results demonstrate that *Gli1* and *Gli2* are not required for the specification of neuronal populations located outside of the ventral midline, and neither is the floor pate.

Interestingly, if a *Gli2* repressor is generated it is not an essential requirement for normal development, as demonstrated when *Gli1* was knocked into the *Gli2* locus. This genetic alteration caused the rescue of the defects present in all tissues present in the *Gli2 -/-* mice (Bai and Joyner, 2001). This result therefore suggests that inductive effects of Gli2 are mediated through the transcriptional activation of Shh target genes. The following year it was demonstrated in *Ptc* mutants that *Gli2* and not *Gli1* was required for mediating the initial Shh signalling (Bai et al., 2002).

Gli3 is transformed into a repressor form in wild type embryos, and this processing can be inhibited by the ectopic expression of Shh (Litingtung et al., 2002). Suprisingly, although the full length *Gli3* protein can be detected in-vivo, an activator function for *Gli3* is not evident during normal development. However, it has been shown to behave as a weak activator in *Ptc -/-* embryos (Motoyama et al., 2003). The *Ptc -/-* develop progenitor cells for the floor plate, V3 interneurons and motor neurons in dorsal regions of the neural tube, suggesting the normal role of *Ptc* is to suppress the generation of ventral cell types in the dorsal neural tube (Goodrich et al., 1997; Motoyama et al., 2003) Further evidence that *Gli3* is able to function as a weak activator was demonstrated when *Gli3* was knocked into the *Gli2* locus, and was able to induce some floor plate cells and V3 interneurons (Bai et al., 2004).

The analysis of the *Gli3* mutants (*Gli3 -/-*) has revealed many phenotypes in multiple tissues (Hui and Joyner, 1993). The analysis of the *Gli3 -/-* mutants revealed that it functions primarily as an inhibitor of Shh signalling. In these mutants there was ectopic expression of Shh further suggesting an inhibitory role for *Gli3* in the transduction of Shh signalling (Buscher et al., 1997). The early analysis of the *Gli3 -/-*

did not reveal any obvious defects of neural tube development (Ding et al., 1998; Litingtung and Chiang, 2000b), but more careful analysis of the neural tube revealed that there was a dorsal expansion of the progenitor domains (V0-V2) within the intermediate region of the neural tube at the expense of dorsal progenitor domains (Persson et al., 2002). In the *Xenopus*, it was demonstrated that *Gli3* antagonised the induction of the floor plate by *Gli1* and it blocked the induction of motor neurons by *Gli2* (Ruiz i Altaba, 1998; Ruiz i Altaba, 1999).

Further analysis of both *Gli2* and *Gli3* mutants has revealed a functional redundancy between these two genes. In non-neural tissue this overlap of function was demonstrated in the lungs, where the *Gli2 -/-* , *Gli3 -/-* double mutant provided a more severe phenotype than either of the single mutants alone (Mo et al., 1997; Motoyama et al., 1998). In the neural tube, this functional redundancy between *Gli2* and *Gli3* was demonstrated in *Ptc -/-* mice when either *Gli2*, *Gli3* or both were inactivated in a *Ptc -/-* background (Motoyama et al., 2003). . When *Gli2* was inactivated in the *Ptc -/-*, all of the dorsal cell types were restored, while inactivation of *Gli3* in the *Ptc -/-* background produced a weaker rescue (Motoyama et al., 2003). The differences of the rescue were apparent at different positions along the anterior-posterior axis which provided different roles of *Gli2* and *Gli3* in the brain and spinal cord.

From the analysis of the *Gli2 -/- ; Gli3 -/-* double knockout mice it was observed that *Gli1* expression was absent, resulting in these mice being devoid of *Gli* activity. Therefore these mice were considered to be *Gli* mutant mice. These *Gli* mutants are able to generate motor neurons and more dorsal interneurons but have severe organisation defects along the dorsal-ventral axis (Bai et al., 2004; Lei et al., 2004).

The spatially restricted domains of gene expression are lost, suggesting that the correct patterning of the ventral neural tube is dependent on the actions of the *Gli* proteins and that *Gli* proteins act as mediators of spinal cord dorsal-ventral patterning.

To demonstrate the repressor role of *Gli3* a truncated version of the repressor form of *Gli3* (*Gli3-R**), which acts as a constitutive repressor independent of Shh signalling, was electroporated into the ventral neural tube of chick embryos and resulted in the suppression of ventral neural fates and the induction of dorsal cell fates (Meyer and Roelink, 2003; Persson et al., 2002). An interesting finding in the study by Meyer and Roelink was that in neural tube explants BMPs, specifically *BMP4*, were able to induce the expression of *Gli3*. This result might shed light on the general mechanism by which BMP signals antagonise Shh signals to generate neuronal identity along the dorsal-ventral axis (Meyer and Roelink, 2003).

An alternative study attempting to induce the inhibition of *Gli* activation using a dominant negative *Gli* caused the loss of motor neurons and the V2 interneurons, thus causing the dorsalisation of the neural tube (Persson et al., 2002). Recently it was demonstrated that the gradient of *Gli* transcriptional activity is sufficient to pattern the neural tube. Incremental changes in the concentration of Shh signal that are necessary to switch the fate of progenitors to induce alternative neuronal populations can be mimicked by small alterations of the concentration of *Gli* activity (see figure F) (Stamataki et al., 2005).

From all these results described above, a simple model was proposed, where the graded Shh signal controls the balance between *Gli* activator and *Gli* repressor activities in the progenitor cells along the dorsal-ventral axis (Jacob and Briscoe, 2003). The generation

of these opposing gradients then orchestrate the patterning of the ventral neural tube (Stamataki et al., 2005).

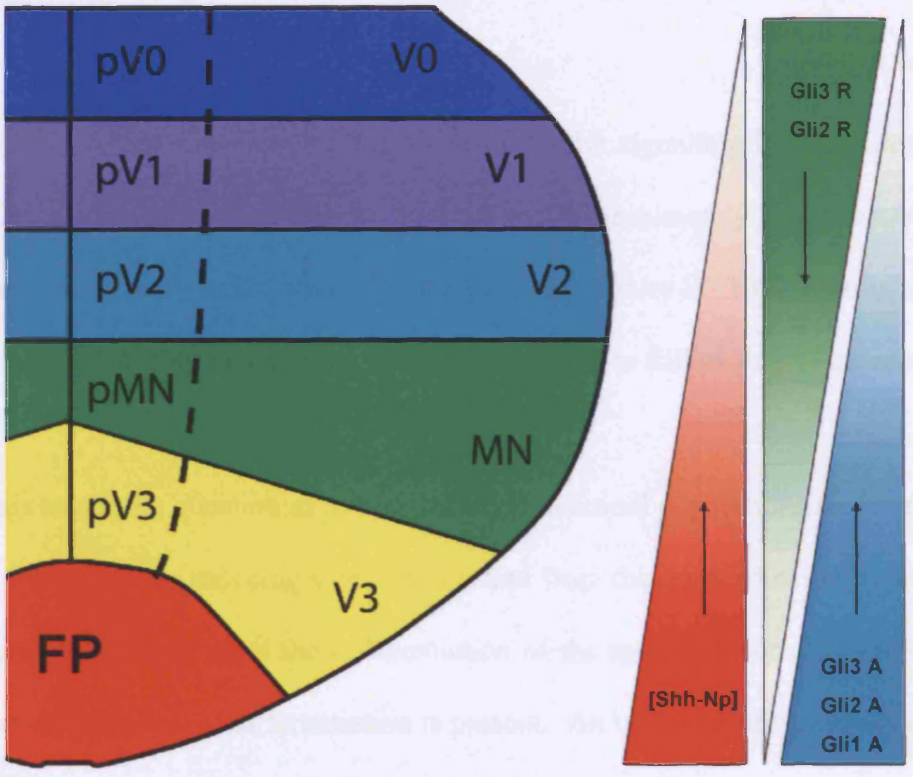

Figure F: Gli transcription factors are involved in interpreting the Shh signal: Graded Shh signalling results in the ventral neural tube initially divides this region into five distinct progenitor domains from which arise specific neuronal populations. Specific concentrations of Shh signalling control the balance between the generation of Gli-repressor against the generation of Gli-activator proteins at specific locations along the dorsal-ventral axis. Ventrally a high concentration of Shh induces the activator function of Gli2 to pattern the floor plate and the adjacent V3 interneurons. In dorsal locations, the low concentration of Shh signalling is unable to induce activator Gli proteins and thus Gli repressors are generated. Gli3 is the primary repressor protein, whilst Gli2 and Gli1 are associated with the activator functions. Diagram adapted from Stamataki et al. 2005.

9. Temporal aspects of dorsal-ventral patterning

Based on gene expression within the ventral neural tube and anatomical analysis it is evident that distinct neuronal populations are generated at specific time points reviewed by (Poh et al., 2002). This phenomenon has been best characterised in the chick neural tube.

From previous experiments it is known that Shh signalling is active during the neural plate stage during neurulation, yet it takes approximately 18 hours before the first neurons are born in the ventral neural tube (Ericson et al., 1992; Poh et al., 2002). The generation of interneurons has been demonstrated to follow that of the motor neurons.

This raised the question as to how different neuronal populations arose at different time points when the inducing signal is constant from the onset of neural tube development. Specifically looking at the differentiation of the motor neurons, it was revealed that a two step process of differentiation is present. An initial low concentration Shh signal is required to convert the progenitor cells in the ventral neural tube to a ventral fate, revealed by the repression of *Pax7* (Ericson et al., 1996). This initial signalling step is followed by a second considerably higher concentration of Shh signal (10 times higher concentration), which is required to induce the differentiation of the motor neurons (Ericson et al., 1996).

Evidence to show that Shh was initially required to ventralise the progenitor cells was provided when neural tube explants (stage 10 HH) were removed from the Shh signal and reverted back to a dorsal cell fate, signalled by the expression of *Pax7*. If the neural

tube explants were removed from the source of Shh signal 12 hours later (stage 12 HH), the progenitor cells were able to maintain their ventral identity (Ericson et al., 1996). It was also demonstrated that the concentration of the initial Shh signal was insufficient to induce the differentiation of the different neuronal populations. After the application of a 10 fold increase in the concentration of the Shh signal were motor neurons generated. Interestingly, when stage 12 chick neural tube explants were cultured in the absence of the Shh signal, and then exposed to the high second dose of Shh signal, there was no induction of the motor neurons. This result demonstrates that the competence of the motor neuron progenitor cells to the ventralising effect of the Shh signal is time dependent. After a specific period of time they become unresponsive to the signal. Thus the Shh signal could be regarded as important to prime the ventral neural tube and to restrict the progenitor cells occupying the ventral neural tube from adopting a fate other than that of the ventral neural tube.

It was later demonstrated that ectopically inducing Shh expression in the mouse neural tube from embryonic day 10.5 (E10.5) onwards was insufficient to generate an ectopic floor plate structure, whilst being able to induce the expression of ventral neural tube markers. This provided further evidence that progenitor cells which give rise to the floor plate are competent to the Shh signal only at a specific time point, and the ectopic expression of Shh in these experiments occurred once this competence has passed (Rowitch et al., 1999).

Another example of how dorsal-ventral patterning in the ventral neural tube is influenced by time is the generation of oligodendrocytes, the myelinating glial cells of the nervous system. It has been demonstrated that the progenitor cells of pMN only

generate motor neurons for a specific period of time (Ericson et al., 1992; Poh et al., 2002) after which the progenitor cells switch their developmental program and begin to produce oligodendrocytes (Richardson et al., 2000; Zhou et al., 2001). It is believed that this developmental switch is mediated by the actions of the b-HLH transcription factor *Olig2*, whose role is discussed in detail by Richardson et al. 2000.

The temporal restrictions of dorsal-ventral patterning present yet another mechanism to increase the diversity of the neuronal populations found in the adult nervous system, and this is made possible by altering the developmental program of progenitor cells to signalling molecules at different time points.

10. Overview of the Dorsal patterning of the neural tube

The patterning of the dorsal neural tube occurs simultaneously with ventral patterning, through an independent mechanism. Evidence for the existence of this independent system emerged from the analysis of chick and *Xenopus* transplants and from mouse mutants (Lee and Jessell, 1999). These experiments have been described above and were critical for the understanding of patterning within the ventral neural tube. When analysing these mutants it became evident that although there was a loss of the neuronal populations ventrally, the differentiation of dorsal neuronal cell types persisted (Ericson et al., 1992; Lee and Jessell, 1999; Liem et al., 1997; Yamada et al., 1991).

The generation of the dorsal neurons was believed to involve the same signals emanating form the notochord diffusing along the dorsal-ventral axis. The basis for this hypothesis was that when the notochord was removed, *Pax3* and *Pax7* which are both markers of the dorsal neural tube would expand ventrally (Chiang et al., 1996; Ericson

et al., 1996; Goulding et al., 1993; Yamada et al., 1991). However, upon closer analysis it became clear that no dorsal cell fates were generated within the ventral neural tube, despite the ventral expansion of dorsal genes. From these results it was suggested that "dorsalising" signals were required to induce the dorsal cell fates (Liem et al., 1997).

The generation of dorsal cell fates is now firmly attributed to the inducing activities of the *bone morphogenic proteins* (BMP) which belong to the *transforming growth factor-beta* (TGFβ) super-family of transcription factors. The inducing signals are produced from the ectoderm overlying the neural tube and from the roof plate (Lee and Jessell, 1999; Liem et al., 1997; Liem et al., 1995; Wilson and Maden, 2005).

The dorsal neural tube is divided into six distinct progenitor domains (d1-d6), which are characterised in similar fashion to the ventral neural tube, by the combinatorial expression of b-HLH, *LIM* homeodomain transcription factors and members of the *Pax* family of transcription family (see figure E) (Lee and Jessell, 1999; Wilson and Maden, 2005).

The roof plate is functionally equivalent to the notochord, and when it is ablated the expression domain of *Pax7* is reduced whilst *Pax6*, a ventral neural tube marker, expands dorsally. This reduction of the *Pax7* domain is concomitant with the loss of the neuronal populations which are generated within the progenitor domains where *Pax7* is normally expressed. It has been demonstrated that the roof plate expresses *BMP4 -5 -7*, which induce the dorsal markers *Pax3* and *Msx* leading to the specification of the dorsal neuronal subtypes. A mechanism in which graded BMP signalling from the roof plate

is responsible for the patterning of the dorsal neural tube has been proposed (Lee and Jessell, 1999; Wilson and Maden, 2005).

In addition to the actions of the *BMPs*, other signalling molecules are present in the dorsal neural tube, such as *Wnt1* and *Wnt3a* and may contribute to the patterning of specific regions of the neural tube. For a more detailed review on the patterning of the dorsal neural tube please refer to Lee & Jessell, 1999; and Wilson & Maden, 2005.

The Floor Plate

11. The history of floor plate studies

The floor plate was originally identified by morphology over a century ago by W. His, and was described as a group of cells in the ventral midline of the neural tube which possess a translucent appearance, ependymal structure and lack of any differentiated neurons (Kingsbury, 1930). These cells are involved in governing the specification of neuronal and glial cell types through the secretion of the glycoprotein Shh (Briscoe and Ericson, 1999; Kessaris et al., 2001; Marti et al., 1995a; Patten and Placzek, 2000; Placzek and Briscoe, 2005; Strahle et al., 2004). An additional function of the floor plate has been demonstrated in directing the trajectories of axons throughout the ventral neural tube by the secretion of Shh and Netrin1 (Charron et al., 2003; Placzek and Briscoe, 2005; Placzek et al., 1990a; Strahle et al., 2004).

Early experimental work performed on the floor plate was carried out solely based on morphology as no molecular markers were available. It was demonstrated that motor neurons are generated in close proximity to the floor plate and that ectopically grafting a notochord, a rod of axial cells mesodermal cells which underlies the neural tube, would generate ectopic floor plate cells adjacent to the notochord (Placzek et al., 2000; Placzek et al., 1990b; van Straaten et al., 1985a; van Straaten et al., 1985b). Conversely when the notochord is ablated the floor plate structure does not differentiate (Placzek et al., 1990b; van Straaten and Hekking, 1991).

Following the discovery of molecular markers more detailed analysis was possible. Motor neurons are lost when the notochord or the floor plate are ablated, while placing an ectopic notochord or floor plate cells at different locations throughout the neural tube

induces ectopic motor neurons (Placzek et al., 1990b; Placzek et al., 1991; Yamada et al., 1991).

Moreover the floor plate is always induced adjacent to the notochord, and motor neurons are always generated at a specific distance from the floor plate. It was therefore suggested that the notochord was sufficient to induce the floor plate and had instructive roles in the positioning and identity of the motor neurons of the ventral neural tube (Yamada et al., 1991).

Following the successful experimental design of culturing chick explants *in-vitro* it was shown that the floor plate needs direct contact with the notochord, while motor neurons are induced further away from the notochord and floor plate (Yamada et al., 1993). These results suggested that a diffusible factor is sufficient to induce the generation of motor neurons, while the induction of the floor plate requires direct contact with the source of the factor. These findings resulted in the traditional model for floor plate induction. A signal from the notochord induces the floor plate cells in the ventral midline of the neural tube which acquire and share the patterning capabilities of the notochord, and act together as a source of a patterning signal to induce motor neurons (Placzek et al., 1993; Yamada et al., 1993).

The diffusible protein was identified as Shh which is expressed in the notochord and floor plate at the time when their inducing capabilities are active (Chang et al., 1994; Echelard et al., 1993; Marti et al., 1995b; Riddle et al., 1993; Roelink et al., 1994). In gain-of-function studies, ectopic Shh induces the differentiation of ventral cell types. Furthermore, cells which are transfected with a Shh expression vector and placed into

contact with explants from naïve neural plate tissue are able to induce the differentiation of floor plate structures and also motor neurons (Roelink et al., 1994).

12. Recent challenges to the traditional model of floor plate induction

The simple model for the induction of the floor plate described above, has recently come under scrutiny. Experimental data generated from studies in mouse, chick and zebrafish have provided contrasting results which do not fit with the simple induction model (Placzek and Briscoe, 2005; Strahle et al., 2004).

The data generated from gain-of-function and knockout studies in the mouse has generally supported the role of Shh in the induction of the floor plate. *Shh* -/- mice display a complete loss of the floor plate (Chiang et al., 1996). Targeting components of the Shh signalling pathway provides further evidence that Shh signalling in involved in the induction of the floor plate in mice. *Ptc* -/- mice exhibit the ectopic generation of floor plate cells due to an increase in Shh signalling activity (Goodrich et al., 1997), while chimaeric mice generated with both wild type and *Smo* mutant cells reveal the absence of all floor plate markers (Wijgerde et al., 2002). Ectopic expression of *Gli1* mimics the endogenous Shh signalling cascade and induces and ectopic floor plate (Hynes et al., 1997), whilst *Gli2* knockout mice display a complete loss of the floor plate (Ding et al., 1998; Matise et al., 1998). Furthermore, *in-vitro* assays revealed that Shh signalling is able to induce floor plate cells in culture when exposed to notochord explants (Roelink et al., 1994). Moreover, the inactivation of *Foxa2* results in the loss of the floor plate, supported by the loss of *Shh* gene expression from the notochord (Ang and Rossant, 1994; Weinstein et al., 1994), whilst ectopic expression of *Foxa2* is

able to induce the ectopic expression of *Shh* leading to the generation of an ectopic floor plate (Sasaki and Hogan, 1994).

The floor plate structure in zebrafish can be divided into two domains based characterised by specific gene expression, termed the lateral and medial floor plate (lFP and mFP respectively). The genetic studies on zebrafish floor plate mutants have revealed that these two domains of the floor plate are induced by different mechanisms, and form the basis for challenging the traditional floor plate induction model.

Although the zebrafish homologue to *Hedgehog* was cloned at the same time as in the mouse, and was shown to posses the ability to induce *axial*, the zebrafish *Foxa2* homologue (Krauss et al., 1993), more recent analysis has revealed that the role of *Shh* in the induction of the floor plate in zebrafish to be minor in comparison to the mouse. The removal of *Shh* from the zebrafish, encoded by *sonic-you* gene (*syu*) causes the loss of the lFP cells, while the mFP cells are maintained (Schauerte et al., 1998). Moreover, when *syu* is ectopically expressed in the zebrafish embryos there is no induction of mFP cell suggesting that *syu* is not required for the induction of the mFP (Schauerte et al., 1998). To conclude whether there was any functional compensation to the loss of *syu* from the other closely related Hh genes in the zebrafish, a combinatorial knockdown of all these genes was carried out, which in similar fashion to the *syu* phenotype does not affect the specification of the mFP cells (Etheridge et al., 2001). Additionally experiments where *Smo* activity is blocked by treating the zebrafish embryos with cyclopamine does not abolish the specification of the mFP cells (Neumann et al., 1999). These results suggest that unlike the mouse model where Shh signalling is required for

the specification of the floor plate, Hh signalling in the zebrafish is required for the specification of only the lFP.

There are several classes of zebrafish floor plate mutants which can be categorised into four groups based on their phenotype. Two of these groups provide some interesting phenotypes which introduce the possibilities of other signalling mechanisms contributing to the formation of the floor plate. One such class of floor plate mutants display the impaired development of the lFP cells while possessing a normal notochord and mFP cells. Members of this category of mutants encode components of the Shh signalling pathway such as *syu* (Schauerte et al., 1998), *smoothened* (Chen et al., 2001a) and *detour* (Karlstrom et al., 2003), the zebrafish homologue of *Gli1*. These mutant embryos display an absence of *axial* from the lFP, whilst maintaining its expression in the mFP, further showing the requirement of Shh signalling in the lateral regions of the floor plate (Odenthal et al., 2000; Schauerte et al., 1998).

Another class of floor plate mutants forms the notochord and lFP but fails to differentiate the mFP, indicating that these two divisions of the floor plate can develop independent from each other (Odenthal et al., 2000; Strahle et al., 1996). Mutants in this class include *cyclops* (*cyc*) (Hatta, 1992; Hatta et al., 1991; Strahle et al., 1993; Tian et al., 2003), *one eyed pinhead* (*oep*) (Schier et al., 1996) and *schmalspur* (*sur*) (Brand et al., 1996). All these mutants still posses a notochord which expresses *Shh* therefore suggesting that the lack of the mFP specification is not due to a failure of Shh signalling. These genes were later shown to encode components of the Nodal signalling pathway, with *cyc* endoding a TGFβ signalling molecule related to the murine Nodal (Sampath et al., 1998). From the studies of the *cyc* and related mutants it became clear

that the mFP cells are dependent upon Nodal related signals for their induction, while the lFP cells are responsive to Shh related signals.

In the mouse, *Shh* expression is believed to be induced by *Foxa2* in the floor plate (Echelard et al., 1993; Hynes et al., 1995b; Ruiz i Altaba et al., 1995a) as demonstrated when *Foxa2* is ectopically expressed. Additionally it was demonstrated that there are *Foxa2* binding sites on the *Shh* promoter (Epstein et al., 1999; Jeong and Epstein, 2003). Early studies in the zebrafish also revealed a similar function of Foxa2 within the ventral midline tissue of the neural tube. When *axial* (*Foxa2*) is ectopically expressed in the zebrafish embryo, *Shh* transcription is activated (Chang et al., 1997). Coupled to this finding, it was revealed that the zebrafish *Shh* promoter has two *axial/Foxa2* binding sites which are required for the transactivation of *Shh* (Chang et al., 1997). These results therefore revealed that *Foxa2* acts as a direct regulator of *Shh* in the zebrafish as in the mouse.

It was later suggested that during floor plate induction in zebrafish, *Foxa2* within the mFP cells was acting downstream of Nodal signalling. This was demonstrated when cell autonomous activation of the Nodal signalling pathway induced the expression of *Foxa2* (Muller et al., 2000). Furthermore, it was shown that when *Foxa2* was re-introduced into the *cyc* mutants, which lack *Foxa2* expression (Strahle et al., 1993), the missing mFP cells would be restored (Rastegar et al., 2002). Taken together, all this data suggests that the induction of the floor plate in zebrafish utilises two distinct signalling pathways. Shh related signalling is required to induce the lFP cells, while the mFP cells are dependent upon Nodal related signals (Placzek and Briscoe, 2005; Strahle et al., 2004). More recently, it has been revealed that Nodal-dependent specification of

the mFP cells can occur in the absence of *Foxa2*, but their differentiation is compromised due to the absence of *Foxa2* activity (Norton et al., 2005).

Although the initial studies on the chick embryos suggested that the induction of the floor plate was dependent upon Shh signaling emanating from the notochord, recent studies in the chick (along with the data generated from the zebrafish work) have moved to challenge this original hypothesis. Recent analyses of chicken-quail chimaeras has suggested that both the notochord and some of the floor plate share the same lineage and are derived from the same precursor cells located within the chicken organizer, Henson's node (Le Douarin and Halpern, 2000; Teillet et al., 1998). Furthermore, the observation that *FOXA2* and *SHH* in Henson's node prior to the formation of the notochord and the floor plate have led to the hypothesis that the floor plate is generated when cells originating from Henson's node migrate and nest within the ventral midline of the neural tube and no induction is involved (Le Douarin and Halpern, 2000). Further studies also suggested a novel role for SHH in the development of the chick floor plate, as being required to adjust the width of the floor plate (Charrier et al., 2002), which resembles one of the functions already described in zebrafish (Strahle et al., 2004).

It was later suggested that the floor plate is different along the anterior-posterior axis of the embryo. For example, the floor plate of the mesencephalon differs from the floor plate of the spinal cord, as the mesencephalic floor plate gives rise to dopaminergic neurons (Andersson et al., 2006; Hynes et al., 1995a; Hynes et al., 1995b), while the spinal cord floor plate does not give rise to any neuronal populations. Removal of the notochord from the anterior region of the embryo does not affect the differentiation of

the floor plate in that region (Patten et al., 2003), whilst removal of the notochord in posterior regions of the embryo result in the loss of the floor plate structure (Placzek et al., 2000; Placzek et al., 1990b; van Straaten and Hekking, 1991; Yamada et al., 1991). These results demonstrate that the floor plate is induced at different time points, and in response to signals from different axial mesoderm tissues. The anterior floor plate in chick is governed by signals emanating from the prechordal mesoderm while the posterior floor plate is maintained from the notochord (Placzek and Briscoe, 2005; Strahle et al., 2004). Due to the observation that the anterior floor plate cells are not governed by notochord derived signals it is possible to speculate that these floor plate cells exist as a pre-specified population and migrate to their final destination.

In response to these challenges to the traditional floor plate induction model, studies in the mouse have focused on *Foxa2* and *Shh*. In similar fashion to the chicken, *Shh* and *Foxa2* are both detectable in the murine node prior to notochord and floor plate differentiation (Ang et al., 1993; Echelard et al., 1993; Marti et al., 1995b). However, in contrast to the chicken, the floor plate and notochord do not share the same lineage. Floor plate cells are not derived from the same precursor cells in the node as the notochord (Jeong and Epstein, 2003). Additionally the floor plate cells do not migrate from the node and integrate into the ventral midline as in the chick model, but are indeed induced from Shh signalling originating from the node (Jeong and Epstein, 2003). However, it cannot be ruled out that Nodal signalling also plays a role in the induction of the floor plate in the mouse. Unlike the inactivation of *Foxa2* in the zebrafish where the embryos survive, inactivation of *Foxa2* in mice is lethal and results in the loss of the node. Therefore it is a possibility that the loss of the notochord and floor plate are caused by the absence of nodal signalling. However, further studies

using conditional mouse mutants of *Foxa2, Shh* and *Nodal* must be conducted in order to conclude whether the traditional model of floor plate induction must be revised for all species.

The Forkhead-Box Transcription Factor *Foxa2*

13. Identification of *Foxa2*

Transcription factors are assigned to families based on the structure of their DNA-binding motif. Examples of various families are the POU-domain family and the homeodomain family of transcription families. At the beginning of the 1990s a new motif was detected within the *Drosophila* Forkhead gene product and within the rat *hepatocyte nuclear factors 3* (HNF-3). The *Drosophila* Forkhead gene is required for the correct development of terminal structures of the embryo which give rise to the anterior and posterior gut. Mutants display homeotic transformation of gut structures into head structures, creating a two pronged embryo, hence the name Forkhead (Weigel et al., 1989). Shortly after the description of the forkhead domain, a small family of hepatocyte enriched DNA-binding transcription factors was isolated.

The HNF-3 proteins for the rat were initially studied as DNA-binding sites of these proteins were required for hepatocyte specific expression of two genes which were highly expressed in the adult liver, but absent from other tissues such as the brain. From these extracts one DNA-protein complex was isolated, purified and a cDNA copy of the gene obtained (Lai et al., 1990). This gene was termed *Hepatocyte Nuclear Factor 3α* (*HNF-3α*). Following a screen using the cDNA of *HNF-3α*, two other members of this novel family of transcription factors were isolated; *HNF-3β* and *HNF-3γ* (Lai et al., 1991).

Analysis of the DNA-binding domain revealed a domain of ~110 amino acids, which were highly conserved between the HNF-3 genes, but when the sequence of the DNA-binding domain was compared with other known sequences from DNA-binding motifs

no match was generated. However when the sequences of the newly described forkhead and *HNF-3α* were compared, a 85-90% sequence similarity was described (Weigel and Jackle, 1990). Now the forkhead and *HNF-3α* are considered the founding members of a large transcription family, as this unique domain has been shown to be present within proteins of different species ranging from yeast to humans (Kaufmann and Knochel, 1996; Lai et al., 1993).

The three-dimensional structure of the forkhead domain was determined by X-ray crystallography using *HNF-3γ*. The solution of the three-dimensional structure revealed a core of 3 α-helices and β-sheets flanked by two large loops or "wings" (Clark et al., 1993). Thus the transcription factors which possessed this DNA binding were also referred to as winged-helix transcription factors.

Almost a decade after the initial identification of the forkhead/winged helix transcription factors there have been over 100 new members of this family identified within several different species (Kaestner et al., 2000; Kaufmann and Knochel, 1996). Laboratories would assign each protein with multiple names which lead to some confusion. In order to address this issue, the nomenclatures for proteins of the forkhead/winged helix transcription factors have now been standardised. Now all member of this family are referred to as Forkhead box transcription factors (Fox), with 15 specific subclasses created depending on the similarities between each protein. The HNF-3 proteins have now been allocated with the subclass A. *HNF-3α* is now *Foxa1*, *HNF-3β* is *Foxa2* and *HNF-3γ* is now *Foxa3* (Kaestner et al., 2000). This standard nomenclature will be used throughout this thesis.

14. Expression of *Foxa2* throughout the embryo

In the developing embryo the expression of *Foxa2* is first detected within a localised region of the anterior primitive streak within the epiblast cells which are about to delaminate. Once the node has formed, *Foxa2* expression can be detected throughout this structure, and along the notochord and the overlying neural plate (Ang et al., 1993; Sasaki and Hogan, 1993). At the head fold stage *Foxa2* is expressed along the notochord and the ventral midline of the neural tube (Ang et al., 1993; Sasaki and Hogan, 1993). The importance of *Foxa2* expression within the ventral midline of the neural tube will be discussed later.

The initiation of *Foxa2* expression within the ventral midline of the neural tube occurs within the presumptive mesencephalon, and then expands caudally along the embryo. However the expression of *Foxa2* along the neural tube is not uniform as can be detected by the expression within the mesencephalon being broader than any other region of the neural tube (Sasaki and Hogan, 1993).

Foxa2 is also expressed within endodermal structures of the embryo such as the lungs, pancreas, liver and the intestines (Ang et al., 1993; Sasaki and Hogan, 1993). This expression during embryonic stages is maintained and can be detected after birth and throughout adulthood (Sund et al., 2000; Sund et al., 2001; Wan et al., 2004b).

The *Foxa2* gene consists of three exons which encode the *Foxa2* protein. Analysis of the expression of the *Foxa2* protein revealed that there are 3 variants present during embryogenesis, termed L1, L2 and E with only the E transcript being preferentially

expressed throughout the developing nervous system. L1 and L2 were restricted to the liver (Sasaki and Hogan, 1994).

15. Role of *Foxa2* within developing nervous system

The role of *Foxa2* during development was initially believed to be restricted to the development of the internal organs, due to its expression within the adult liver and intestines. However closer analysis of the early embryonic stages revealed that it might also play a role in the development of the nervous system.

The expression of *Foxa2* and the *Xenopus* homologue, *Pintallavis*, within the node (celled the organiser in *Xenopus*) suggested a possible role of *Foxa2* in the specification of the embryo along both the anterior-posterior and dorsal-ventral axes. Furthermore, *Foxa2* was considered a candidate for correct floor plate development, based on the observation that *Foxa2* expression is induced in the ventral midline of the neural tube. Additionally the zebrafish mutant *cyclops* which lacks the floor plate structure does not show any expression of axial, the zebrafish homologue of *Foxa2* (Strahle et al., 1993).

To address the role of *Foxa2* in the formation of the floor plate, *Foxa2* was placed under the control of the *En-2* promoter and ectopically expressed in a region spanning the dorsal mesencephalon and metencephalon. Initial analysis reveals that the cerebellum of the transgenic embryos is decreased in size as interpreted by the initial loss of expression of the Purkinje cell specific gene *L7* (Sasaki and Hogan, 1994). Furthermore markers for the floor plate, *Foxa1* and *BMP1*, are ectopically expressed dorsally within the ectopic domain of *Foxa2* expression, suggesting that a floor plate structure has been

induced dorsally. Further evidence was provided by the repression of the dorsal marker *Pax3* and the inability to identify dorsal mesencephalic structures such as the inferior colliculi (Sasaki and Hogan, 1994). These results were identical to the data produced by ectopically expressing *Pintallavis* in the *xenopus* embryos which produce an ectopic floor plate at the site of ectopic *Pintallavis* expression (Ruiz i Altaba et al., 1993).

These results suggested that *Foxa2* is a regulator of floor plate development. It was also suggested that *Foxa2* is able to induce the morphogen Shh within the notochord and the floor plate (Echelard et al., 1993; Hynes et al., 1995b; Ruiz i Altaba et al., 1995b). Based on the observation that *Foxa2* expression precedes that of *Shh* within the same cells of axial mesoderm and floor plate, *Foxa2* was proposed to be an upstream activator of *Shh* (Ang et al., 1993; Echelard et al., 1993; Marti et al., 1995b; Sasaki and Hogan, 1993). It was later determined that as a consequence of Shh signalling, *Foxa2* is induced by *Gli1*, a downstream target of Shh, thus *Foxa2* and *Shh* expression is induced and maintained within the floor plate (Hynes et al., 1997; Sasaki et al., 1997).

These experiments did not address the possible role of *Foxa2* in the specification of the embryo along both the body axes. In 1994 two groups simultaneously generated *Foxa2* knockout mice (*Foxa2* -/-) in order to address this issue. Both groups described severe phenotypes which begin during gastrulation. There is an absence of the node, the notochord never forms and the primitive streak is truncated (Ang and Rossant, 1994; Weinstein et al., 1994). An interesting finding was that even though there is an absence of the node some neural tissues are still generated. This neural tissue does not display any severe alteration along the anterior-posterior axis, but the dorsal-ventral axis is clearly altered.

The notochord is not detectable at E8.5 along the entire embryo, confirmed by the loss of both *Shh* and *Brachyury* expression (Ang and Rossant, 1994; Weinstein et al., 1994). The neural tube is severely affected in the *Foxa2* -/- mice. The posterior region of the neural tube (developing spinal cord) does not display any evident alterations along the anterior-posterior axis. Morphological analysis of the embryos revealed that the anterior region of the neural tube is dramatically affected. In all embryos the head structures are abnormal, and in some instances no brain tissue is formed anterior to the otic vesicle (Ang and Rossant, 1994). Molecular analysis provided by expression studies using *Otx2* confirmed these results. *Otx2* is either weakly expressed at the anterior tip of the neural tube, or absent in the cases where the presumptive midbrain and forebrain are absent (Ang and Rossant, 1994).

The specification along the dorsal-ventral axis of the *Foxa2* -/- neural tube is dramatically affected. Molecular markers for the notochord, *Shh* and *Foxa1*, revealed that there is an absence of the notochord and floorplate, coupled with the loss of ventral motor neurons and the general expansion of dorsal markers. The expression domain of *Pax3*, which is usually restricted to the alar plate, expands ventrally, while *Pax6* expression is shifted ventrally and now occupies the ventral midline (Ang and Rossant, 1994; Weinstein et al., 1994). The ventral motor neuron population which is normally located adjacent to the floor plate (Ericson et al., 1995a; Ericson et al., 1992) is absent in *Foxa2* -/- embryos as confirmed by the loss of *Islet-1* expression (Ang and Rossant, 1994; Weinstein et al., 1994). Interestingly in the *Foxa2* +/- mice, the floorplate and notochord are both present, and there is no dramatic alteration within the dorsal-ventral patterning of the neural tube indicating that one functional allele of *Foxa2* is sufficient to correctly specify the neural tube (Weinstein et al., 1994).

16. Role of *Foxa2* in non-neural tissue

The role of *Foxa2* in non-neural tissue was also addressed using the *Foxa2* -/- mice. In the wild type mouse, *Foxa2* is expressed in the endoderm of the embryo and in the developing foregut. At later stages of development it is also expressed throughout the entire developing gut (Ang et al., 1993; Sasaki and Hogan, 1993). Analysis of the *Foxa2* -/- embryos revealed that the morphogenesis of the foregut is impaired whilst hindgut development is unaffected. This study is therefore suggsting that some definitive endoderm remains within the mutant embryos (Ang and Rossant, 1994).

More recent work has now provided evidence into the role of *Foxa2* in other endodermal derived structures such as the pancreas and the lungs. The expression of *Foxa2* within the adult intestine, pancreas, lungs and liver is known, but due to the embryonic lethality caused by the deletion of *Foxa2*, the role of *Foxa2* within these structures has never been addressed.

Foxa2 expression is detectable in the type II epithelial cells of the developing alveoli in the lungs and is known to regulate airway epithelial cell differentiation in the postnatal lung, and a specific temporal deletion of *Foxa2* induces neonatal respiratory failure (Wan et al., 2004a; Wan et al., 2004b). *Foxa2* has also been demonstrated to play a role within the differentiating β-cells of the pancreas. A deletion of *Foxa2* specifically in these β-cells induces a hypoglycaemic state, coupled with deregulated insulin secretion in response to administration of glucose (Sund et al., 2001).

Taken together, all results indicate that *Foxa2* is essential during early development to pattern the node, and induce and maintain the notochord and floor plate of the developing neural tissue. In addition to these roles, it has been demonstrated that *Foxa2* is also required during later embryonic development and postnatal maintenance of endoderm derived structures such as the pancreas, liver, intestine and the lungs.

Neuronal Populations of the Ventral Mesencephalon

Following the compartmentalisation of the neural tube along the anterior-posterior and dorsal-ventral axes, signals emanating from secondary signalling centres further pattern and refine each domain, and in the process generate distinct neuronal populations at specific stereotypical locations along the neural tube. Examples of this can be seen in the developing mesencephalon and rhombencephalon where distinct neuronal populations, which are involved in the control of movement, are generated in response to secreted signals emanating from the IsO and floor plate.

In the mesencephalon, secreted Shh signal from the floor plate forms a morphogen gradient along the dorsal-ventral axis, while FGFs *(Fgf8a)* and Wnts *(Wnt1)* secreted from the IsO form a concentration gradient along the anterior-posterior axis. At specific locations where these signals intersect, the neuronal progenitor cells located within these precise regions are induced to follow a specific lineage (see figure G) (Goridis and Rohrer, 2002; Hynes and Rosenthal, 1999; Ye et al., 1998). The three main neuronal populations of the ventral mesencephalon are the mesencephalic dopaminergic neurons (mesDA), the red nucleus (RN) and the oculomotor complex (OMC), and each population will be introduced individually. The generation of the serotonergic neurons (5-HT) within the rhombencephalon also follows a similar mechanism to the mesencephalic nuclei. The 5-HT progenitor cells are specified at a specific location where Shh, Fgf8b and Fgf4 signals interact (see figure G, Fgf4 signalling present during gastrulation is not shown) (Goridis and Rohrer, 2002; Hynes and Rosenthal, 1999; Wurst and Bally-Cuif, 2001; Ye et al., 1998).

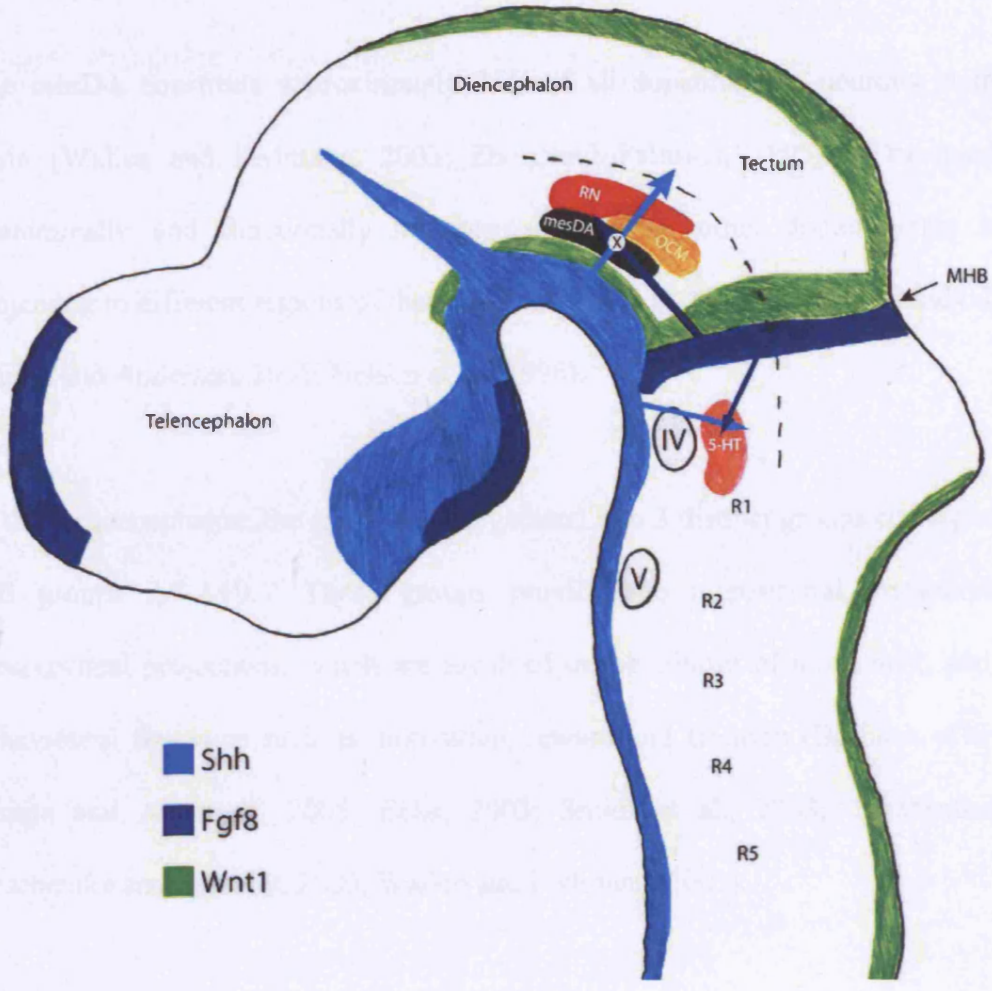

Figure G: Neuronal populations of the ventral mesencephalon: Shows the relative positions of the nuclei of the ventral mesencephalon to the floor plate and the midbrain-hindbrain boundary (MHB). Shh from the floor plate forms a concentration gradient along the dorsal-ventral axis, with the highest concentration being closest to the floor plate. Different neuronal populations are generated in response to different concentrations of the Shh signal along this axis. Fgf8 emanating from the MHB forms a concentration gradient along the anterior-posterior axis. These two signalling molecules control the specification and location of the nuclei of the ventral mesencephalon. The mesDA develop in a region adjacent to the floor plate at a position marked "X" in the diagram where the Shh and Fgf8 signals intersect. The oculomotor complex (OCM) and the red nucleus (RN) are also specified and positioned in response to these signals. The 5-HT neurons in rhombomere 1 (R1) of the hindbrain are specified at a location where Shh and Fgf8 signals intersect, but other signalling factors also contribute to their specification. The nuclei labelled IV and V represent the 4th and 5th cranial nerves respectively. The dotted line represents the division of the mesencephalon into the ventral tegmentum and the dorsal tectum. Diagram based on (Wurst and Bally-Cuif, 2001).

17. The mesencephalic dopaminergic neurons (mesDA)

The mesDA constitute approximately 75% of all dopaminergic neurons in the adult brain (Wallen and Perlmann, 2003; Zhou and Palmiter, 1995). The mesDA are anatomically and functionally heterogeneous to all other dopaminergic neurons, projecting to different regions of the brain (see figure H) (Bjorklund and Lindvall, 1984; Chinta and Andersen, 2005; Nelson et al., 1996).

In the mesencephalon, the mesDA are organised into 3 distinct groups corresponding to cell groups A8-A10. These groups provide the nigrostriatal, mesolimbic and mesocortical projections, which are involved in the control of movement, and also in behavioural functions such as motivation, reward and emotion (Burbach et al., 2003; Chinta and Andersen, 2005; Eells, 2003; Smidt et al., 2003; Tzschentke, 2000; Tzschentke and Schmidt, 2000; Wallen and Perlmann, 2003).

The neurons of cell group A10 correspond to the ventral tegmental area (VTA). Their efferent projections include the nucleus accumbens, the dorsal striatum, other limbic brain areas and also the cortex, forming the mesolimbic/cortical pathways, which are involved in the control of behaviours relating to emotion and to reward (Tzschentke, 2000; Tzschentke and Schmidt, 2000). The A9 group corresponds to the substantia nigra pars compacta (SNpc) which in the adult brain appears black due to the presence of the black pigment neuromelanin. The SNpc has projections towards the dorsal-lateral striatum forming the nigrostriatal pathway (Beckstead et al., 1979; van der Kooy, 1979), and is involved in the control of voluntary movement (Di Chiara et al., 1992).

The other dopaminergic population in the mesencephalon, group A8, corresponds to the retrorubral field (RRF) (see figure H).

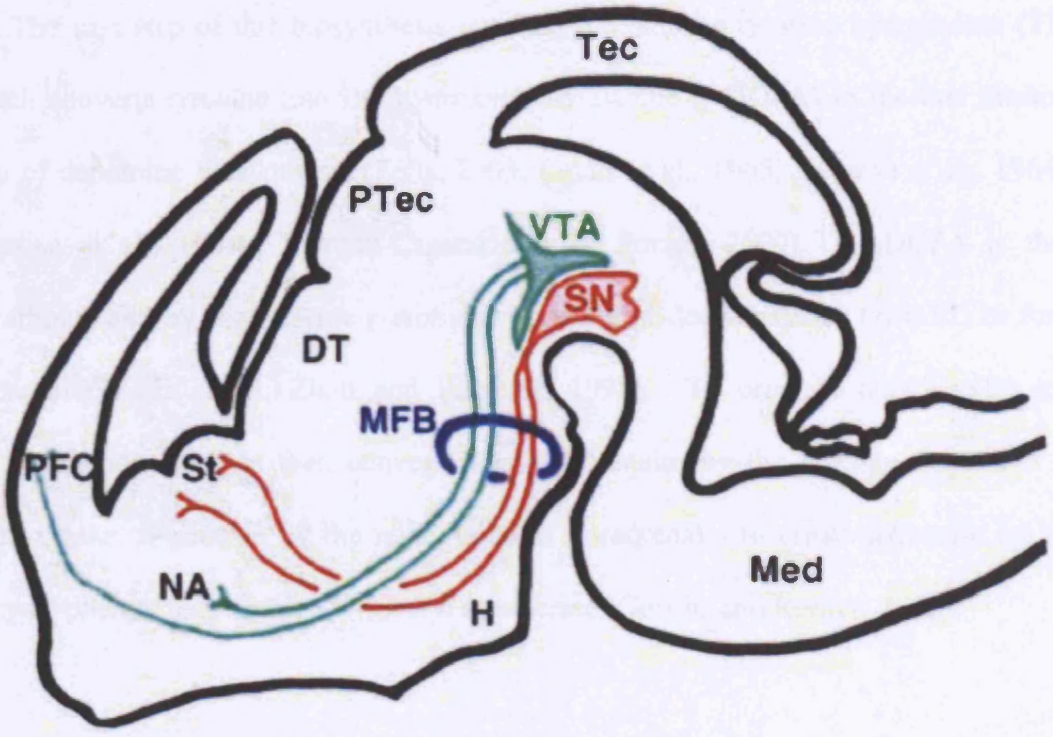

Figure H: Projections of the mesDA populations: Show the projections of the dopaminergic neurons of the ventral mesencephalon in an adult brain. The neurons from the ventral tegmental area (VTA) project through the midbrain-forebrain bundle(MFB) and form synaptic connections with the pre-frontal cortex (PFC) and the nucleus acumbens (NA), and form the bulk of the mesolimbic system. The neurons from the substantia nigra pars compacta (SN) create synaptic connections with neurons in the striatum (St) and form the nigrastriatal pathway which degenerates in patients with Parkinson's disease. Diagram taken from Lin and Rosenthal, 2003

17.1. Synthesis of the dopamine neurotransmitter and the mechanism of dopamine neurotransmission

The catecholamine neurotransmitters dopamine, noradrenalin and adrenalin are all synthesized from the amino acid tyrosine in a common biosynthetic pathway (see figure I). The first step of this biosynthesis involves the enzyme tyrosine hydroxylase (TH) which converts tyrosine into L-dihydroxyphenylalanine ($_L$-DOPA) in the rate limiting step of dopamine biosynthesis (Eells, 2003; Levitt et al., 1965; Nagatsu et al., 1964a; Nagatsu et al., 1964b; Perrone-Capano and Di Porzio, 2000). $_L$-DOPA is then decarboxylated by the enzyme $_L$-aromatic amino acid decarboxylase (AADC) to form dopamine (Eells, 2003; Zhou and Palmiter, 1995). To produce noradrenalin and adrenalin, dopamine in then converted to noradrenalin by the enzyme dopamine β-hydroxylase. Followed by the methylaion of noradrenalin to create adrenalin by the enzyme phenylethanolamine-N-methyl transferase (Goridis and Rohrer, 2002).

As described above, TH is the rate limiting enzyme for the synthesis of all catecholamines. Mice with a homozygous deletion of *TH* are embryonic lethal and display a severe loss of all catecholamines (Kobayashi et al., 1995; Zhou et al., 1995). To specifically address the role of dopamine, knockout mice (DA -/-) were created by placing the *TH* gene under the control of the of the dopamine β-hydroxylase promoter, which allowed for the synthesis of norepinephrin and epinephrine in the absence of dopamine. These mice survive development and are born despite displaying severe depletion of dopamine, but are unable to survive longer than four weeks after birth and showed severe weight loss and growth retardation (Zhou and Palmiter, 1995).

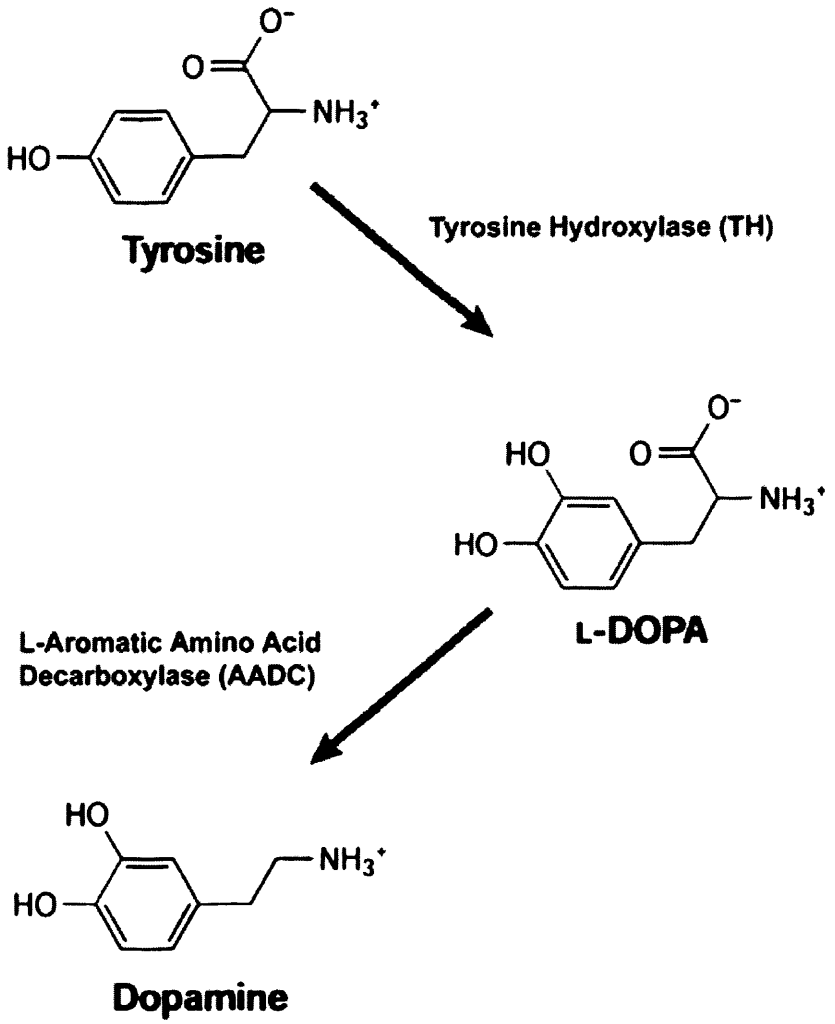

Figure I: Biosynthesis of dopamine neurotransmitter: Tyrosine Hydroxylase (TH) is the rate limiting step of dopamine synthesis and is required to hydrolyse tyrosine and produce L-DOPA. L-Aromatic Amino Acid Decaboxylase (AADC) then converts L-DOPA into dopamine. Diagram adapted from Goridis and Rohrer, 2002.

Newly synthesised dopamine is accumulated from the neuronal cytoplasm and stored into synaptic vesicles by the vesicular monoamine transporter type 2 (VMAT). When an action potential arrives at the terminus of the pre-synaptic axon, the vesicles containing the dopamine neurotransmitter fuse with the cytoplasmic membrane, and release dopamine into the synaptic cleft. Dopamine then diffuses along the synaptic cleft and can either bind to specific dopamine receptors on pre- or post synaptic membranes (Eells, 2003).

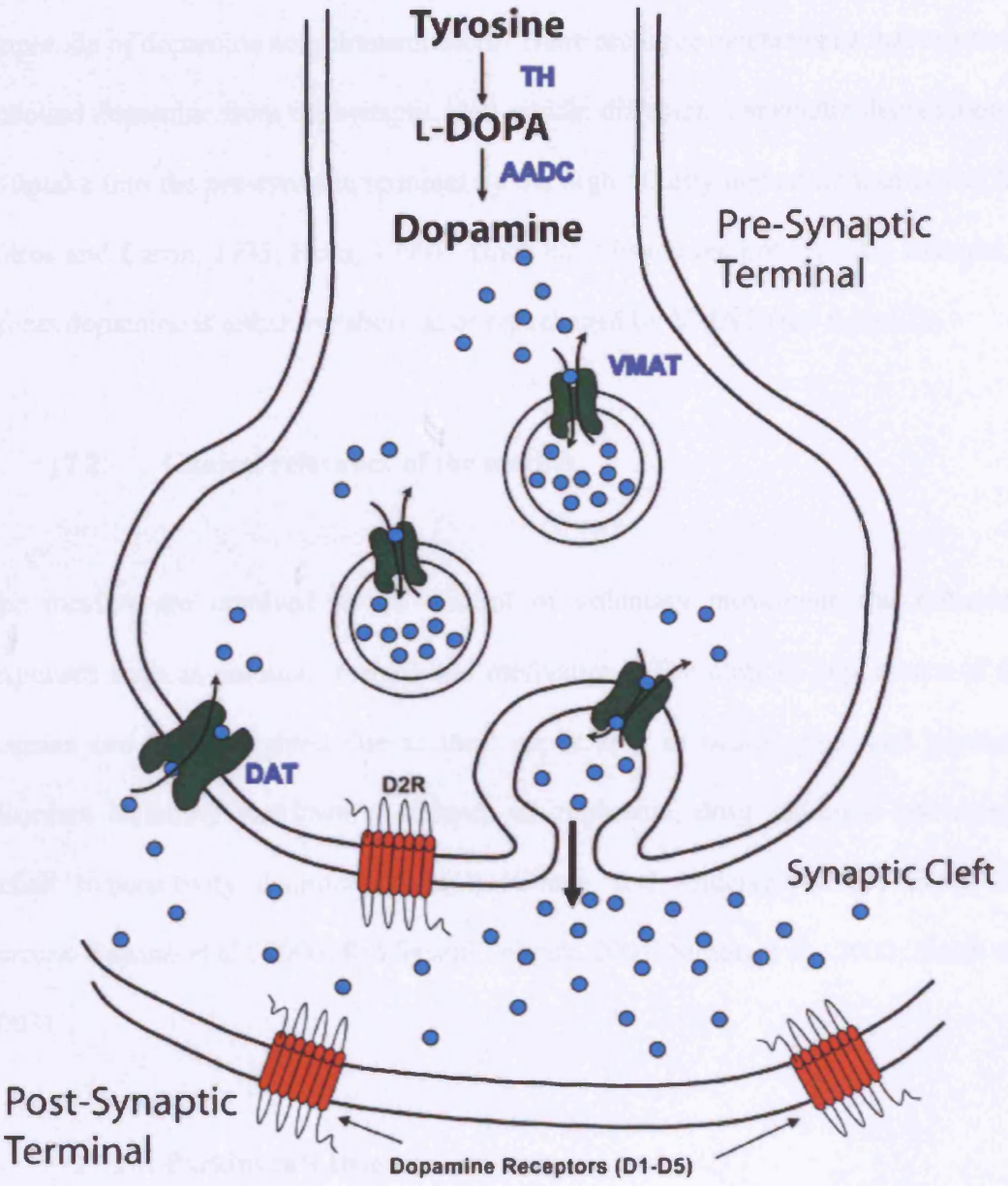

Figure J: The dopaminergic synapse: Newly synthesised dopamine in accumulated in the cytoplasm and is then packaged into vesicles by the vesicular monoamine transporter type 2 (VMAT). When an action potential arrives at the pre-synaptic terminal of the neuron, the vesicles containing the dopamine fuse to the cytoplasmic membrane of the pre-synaptic neuron releasing dopamine into the synaptic cleft. Dopamine then binds to its specialised receptors on either the pre- or post-synaptic membrane. Dopamine binding to the pre-synaptic membrane receptors allows the neuron to regulate extracellular dopamine levels.

The removal of the extracellular dopamine is critical for determining the duration and amplitude of dopamine neurotransmission. There are three mechanisms that remove the unbound dopamine from the synaptic cleft which: diffusion, enzymatic degradation and re-uptake into the pre-synaptic terminal by the high affinity dopamine transporter DAT (Giros and Caron, 1993; Horn, 1990). Once back inside the pre-synaptic terminal, the excess dopamine is either metabolised or repackaged by VMAT (see figure J).

17.2. Clinical relevance of the mesDA

The mesDA are involved in the control of voluntary movement and behavioural responses such as emotion, reward and motivation. The clinical importance of these neurons can be highlighted due to their implication in neurological and psychiatric disorders including Parkinson's disease, schizophrenia, drug addiction and attention deficit hyperactivity disorder (ADHD) (Chinta and Andersen, 2005; Eells, 2003; Perrone-Capano et al., 2000; Riddle and Pollock, 2003; Simon et al., 2003; Smidt et al., 2003).

17.2.1. Parkinson's Disease

Parkinson's disease (PD) is a progressive neurodegenerative disorder which was first characterised by James Parkinson in 1817, affecting approximately 2% of the human population over 65 years of age. The onset of PD occurs with the degeneration of the pigmented dopaminergic neurons of the SNpc resulting in a severe deficiency of dopamine neurotransmission within the striatum and excessive inhibition of the brain stem and thalamocortical neurons involved in the control of movement (Hirsch et al.,

1988; Jiang et al., 2005; Simon et al., 2003). When a minimal threshold of dopamine is attained, the clinical symptoms of PD become evident, which include bradykinesia, muscle rigidity, resting tremor, difficulties in initiating movement and postural instability (Kandel et al., 2000a; Polymeropoulos et al., 1997; Simon et al., 2003). Dopamine cell loss is also associated with the abnormal presence of intraneuronal ubiquitinated cytoplasmic protein aggregates, called Lewy bodies (Goldman et al., 1983; Trojanowski et al., 1998).

The cause of the dopaminergic cell death in PD patients remains unclear. It is thought to be a combination of exposure to environmental toxins, ageing and genetic susceptibility (Eells, 2003; Hirsch and Faucheux, 1998; Jenner, 1998; Schapira, 1997). It has been suggested that dopaminergic neurons are particularly prone to oxidative stress due to their high rate of oxygen metabolism, low levels of anti-oxidants and high iron content. Through its catabolism, dopamine is believed to generate toxic reactive oxygen species, which if accumulated within the cell can lead to cause cell death (Chinta and Andersen, 2005). However, this does not explain why only the dopaminergic neurons of the SNpc are lost in PD.

Several animal models have been created to enable scientist to recreate the pathology of Parkinson's disease. The two most common animal models are created using the neurotoxins 6-hydroxy-dopamine (6-OHDA) and 1-methyl-4-phenyl-1,2,3,6-tetrahydropyridine (MPTP). These neurotoxins have been shown to specifically induce the degeneration of the dopamine neurons of the SNpc. 6-OHDA injections are the oldest method of inducing Parkinson-like phenotypes and have been used since the 1960s (Blum et al., 2001). MPTP is a more recent neurotoxin which was discovered by

chance in 1982 when some intravenous drug users in California injected a heavily contaminated batch of synthetic heroin (MPTP was a by-product of the manufacturing process of this synthetic heroin). These drug users displayed an irreversible bradykinetic and rigid syndrome which was immediately associated with the symptoms of Parkinson's disease (Przedborski and Jackson-Lewis, 1998). Interestingly both of these neurotoxins are taken into the neuronal terminals of the dopamine neurons of the SNpc by the dopamine transporter (DAT), and where they disrupt the respiration of the mitochondria, which ultimately leads to the degeneration of the neuron (Blum et al., 2001; Przedborski and Jackson-Lewis, 1998).

The importance of genetic factors involved in Parkinson's disease has been the centre of debate for decades, and an understanding of these genetic factors could hold the key to possible therapeutic treatments. Investigations with siblings from patients of Parkinson's disease demonstrate that there is a higher possibility of developing Parkinsonian symptoms compared to the siblings of non-affected parents (Pankratz and Foroud, 2004), and several genes have now been identified which are considered to have the potential to increase the incidence of Parkinson's disease, such as *α-synuclein*, *parkin* and *DJ-1*.

17.2.2. Schizophrenia

Schizophrenia is a severe, chronic and complex neurological disorder with either psychotic (positive) or deficit (negative) symptoms. The psychotic symptoms are characterised by hallucinations and delusions, whilst the negative deficit symptoms are

characterised by major cognitive defects such as poverty of speech, and dramatic functional impairment (Egan and Weinberger, 1997; Wong and Van Tol, 2003).

The aetiology of schizophrenia remains unclear, but many studies have shown that alterations in neurotransmitter systems could play a role in the pathophysiological processes which lead to schizophrenia. The dopaminergic system has been implicated and is one of the most intensely studied neurotransmitter groups for this neurological disorder, based on the observation that agonists of dopamine can elicit psychosis on normal individuals and exacerbate psychosis on patients with schizophrenia (Eells, 2003; Egan and Weinberger, 1997). Furthermore, drugs which specifically block the D2 dopamine receptor (D2R) also serve to diminish psychotic symptoms, and patients with schizophrenia have a higher occupancy of the D2R by endogenous dopamine (Abi-Dargham et al., 2000; Berry et al., 2003; Eells, 2003).

17.2.3. Addiction

Drug addiction has long been considered as a psychological defect with subjects showing moral defects or character weakness, but recent studies are beginning to dispel this theory. Drug addiction is now considered a brain disorder caused by the repetitive use of various substances which alter the normal functioning of the central nervous system (Melis et al., 2005). The classical symptoms of drug addiction are a compulsive, out of control use of drugs despite the knowledge of the negative consequences which occur, such as tolerance, sensitization which lead to dependence and ultimately withdrawal.

Drugs of abuse include cocaine, amphetamines, heroin, nicotine, cannabis, and alcohol, and all these drugs share the common action of increasing the neurotransmission of dopamine within the mesolimbic system especially within the nucleus accumbens, but produce this action in different mechanisms (Bassareo and Di Chiara, 1997; Di Chiara and Imperato, 1988).

It has been demonstrated that cocaine binds to the DAT, preventing dopamine re-uptake, which results in the accumulation of dopamine within the synaptic cleft (Melis et al., 2005). Amphetamines are known to increase dopamine levels in the synapse by disrupting the function of VMAT causing the release of nascent dopaminergic neurotransmitter. These drugs of abuse are known to cause persistent modifications of neuronal circuits which lead to addictive behaviour (Liu et al., 2005; Nestler, 2001). It is believed that a change in synaptic plasticity of the dopaminergic neurons of the VTA contribute to circuit modification induced by drugs of abuse, including cocaine (Liu et al., 2005; Ungless et al., 2001). In a recent study, in response to the repeated exposure of cocaine, excitatory synapses to the VTA dopaminergic neurons were susceptible to the induction of long term potentiation (LTP). This finding suggests that this mechanism may be important for the drug associated "memory" seen in drug addicts (Liu et al., 2005).

17.2.4. Attention Deficit Hyperactivity Disorder

Attention Deficit Hyperactivity Disorder (ADHD) is a relatively new neurological disorder, which has been documented mainly in infants, but is also witnessed in adults. The primary symptoms include motor over-activity, inattention and impulsivity

(Solanto, 2002; Swanson et al., 1998), with the onset of symptoms believed to occur before the age of seven (Swanson et al., 1998). The motor over-activity which is characteristic of ADHD combined with neuro-imaging data suggest that dysfunction within the striatum or in the regulation of the striatum is associated in the pathophysiology of ADHD (Solanto, 2002).

It is well documented that the dorsal striatum is involved in the initiation of voluntary movement. Two parallel prefrontal-striatal-thalamic-cortical circuits are involved (Castellanos, 1997). The first pathway, "the direct pathway," runs from the pre-frontal cortex through the internal segment of the globus pallidus through to the thalamus, feeding back to exert a net amplification of the original cortical output. A depletion of dopamine within this pathway results in the difficulty initiating movements as is characteristic of PD sufferers. The second pathway, "the indirect pathway," projects through the external segment of the globus pallidus, and synapses on inhibitory projections from the subthalamic nucleus to the internal globus pallidus, thus producing a net inhibition of cortical output. A depletion of dopamine within this pathway results in excessive motor output (Solanto, 2002).

The motor hyperactivity evident in patients with ADHD could mirror the symptoms exhibited by patients of PD, largely characterised by either excessive dopaminergic activity within the internal region of globus pallidus or insufficient inhibition of the external region of the globus pallidus (Castellanos, 1997; Solanto, 2002). Furthermore, functional-MRI studies on both children and adults with diagnosed with ADHD reveal that the activation of the striatal pathway is reduced (Eells, 2003; Rubia et al., 1999; Solanto, 2002; Vaidya et al., 1998).

17.3. The development of the mesDA

As stated previously, extrinsic signalling events determine the neuronal fate of the progenitor cells giving rise to the mesDA at a distinct stereotypical location within the tegmentum (Ye et al., 1998). Once the progenitor cells have been specified, many intrinsic events involving transcription factors ultimately lead these progenitor cells to adopt a mesDA lineage (Burbach et al., 2003; Eells, 2003; Hynes and Rosenthal, 1999; Lin and Rosenthal, 2003; Maxwell and Li, 2005; Riddle and Pollock, 2003; Simon et al., 2003; Smidt et al., 2003).

The extrinsic signalling events were first discovered when it was demonstrated that the mesDA develop in the immediate vicinity of the floor plate near the MHB (Hynes et al., 1995b). *In-vitro* data established that the floor plate is sufficient to induce TH positive cells in explants at their normal positions within the ventral mesencephalon, or in ectopic dorsal regions (Hynes et al., 1995b), complimenting *in-vivo* data described for the transgenic mice where an ectopic floor plate is induced in the dorsal mesencephalon due to the ectopic expression of *Foxa2* (Hynes et al., 1995b; Sasaki and Hogan, 1994). The ectopic mesDA neurons develop at the same anterior-posterior location as the endogenous mesDA neurons. These results indicate that the mesDA neurons require contact with the floor plate cells in order to develop.

Later that year it was discovered that the mesDA neurons were being induced by Shh secreted by the floor plate cells (Hynes et al., 1995a; Wang et al., 1995). *In-vitro* experiments revealed that the generation of mesDA neurons in culture was blocked by the activation of the Shh antagonist PKA using the cAMP signalling pathway (Hynes et

al., 1995a). Furthermore, mesencephalic explants generate mesDA neurons in the absence of any floor plate tissue when cultured in a permissive medium containing Shh protein (Hynes et al., 1995a). These results, coupled with the finding that the mesDA develop in close proximity to the floor plate indicate that Shh is involved in their induction.

Further evidence for the role of Shh in the induction of the mesDA was provided by ectopically expressing *Gli1* in the dorsal mesencephalon of mice (Hynes et al., 1997). *Gli1* is a downstream target of Shh signalling in the neural tube, and when ectopically induced mimics the effect of ectopic expression of *Shh*, inducing the expression of *Ptc*, *Foxa2* and *Shh*. *Gli1* was placed under the control of the *En2* promoter and consistent with the ectopic induction of *Shh*, generated mesDA neurons in the dorsal mesencephalon (Hynes et al., 1997).

Following the observations that Shh is able to induce the generation of the mesDA and that the ectopic mesDA neurons were always located at the same anterior-posterior location suggested that another factor must be involved in the specification of the mesDA along the anterior-posterior axis. That factor was later discovered to be Fgf8 (Ye et al., 1998).

The role of Fgf8 in the positioning of the mesDA was first demonstrated when explants of non-mesencephalic origin which maintained the ventral midline and hence the floor plate, were exposed to Fgf8 and were able to induce ectopic mesDA neurons along the anterior-posterior axis (Ye et al., 1998). During the same study it was demonstrated that Fgf8 in cooperation with Shh can induce mesDA neurons in ectopic locations. When

Fgf8 was chemically blocked *in-vitro* there was no induction of the mesDA even in the presence of Shh signal. These results demonstrated for the first time that both Shh and Fgf8 were critical for the initial induction of the mesDA and that Shh positions the mesDA along the dorsal-ventral axis while Fgf8 positions the mesDA along the anterior-posterior axis (see figure G) (Ye et al., 1998).

17.4. Transcription factors involved in the development of mesDA

Shortly after the induction of the mesDA a whole range of transcription factors are expressed by the progenitor cells. Before these cells express the mesDA specific markers, they begin to express ventral mesencephalic markers, among which are *En1*, *En2*, *Lmx1b*, *Wnt1*, *Pax2* and *Pax5*. At around E10.5 the developing mesDA neurons express the orphan nuclear receptor *Nurr1* followed closely by the expression of *TH* at E11.5. The induction of *TH* is parallel to the induction of the mesDA specific marker *Ptx3*, marking the birth of the mesDA neurons (Burbach et al., 2003; Eells, 2003; Lin and Rosenthal, 2003; Riddle and Pollock, 2003; Simon et al., 2003; Smidt et al., 2003). These neurons mature and later begin to express genes which are necessary for the synthesis of dopamine and dopamine neurotransmission, such as *AADC*, *VMAT*, *DAT* and the *D2R* dopamine receptor (Eells, 2003).

17.4.1. The orphan nuclear receptor *Nurr1*

The transcription factor *Nurr1* (Nur-related factor 1) was characterised as a member of the nuclear steroid/thyroid hormone receptor superfamily of transcription factors due to its homology with an another family member *Nur77* (Law et al., 1992). The members

of this transcription superfamily are described as being orphan nuclear receptors as they lack any identified ligands. *Nurr1* is widely expressed in both the adult and the developing brain including the olfactory bulb, the cerebellum, the hippocampus, the hypothalamus, regions of the cortex and the mesDA (Saucedo-Cardenas and Conneely, 1996; Zetterstrom et al., 1996). In the mesencephalon, *Nurr1* expression can only be detected in newly differentiated mesDA neurons (~E10.5) prior to the induction of *Ptx3* and *TH* at E11.5 (Saucedo-Cardenas et al., 1998; Smidt et al., 1997; Zetterstrom et al., 1997; Zetterstrom et al., 1996), suggesting that the *Nurr1* is not involved in the specification of these neurons but plays a later role in their development (Wallen et al., 1999).

The creation of *Nurr1* knockout (*Nurr1* -/-) mice revealed a specific role for this gene in the development of the mesDA (Castillo et al., 1998; Le et al., 1999; Saucedo-Cardenas et al., 1998; Zetterstrom et al., 1997). These mice survive embryonic development and show signs of hypoactivity, but die shortly afterwards which is believed to be a direct consequence of poor suckling (Saucedo-Cardenas et al., 1998; Zetterstrom et al., 1997).

The *Nurr1* -/- newborn pups display a loss of *TH* and *Ptx3* gene expression (Saucedo-Cardenas et al., 1998), combined with the absence of other dopaminergic markers from the VTA and SNpc (Castillo et al., 1998; Zetterstrom et al., 1997). Other dopaminergic neurons of the brain (e.g. hypothalamus: groups A11, A12 and A13) are unaffected by the loss of *Nurr1* suggesting a specific role for *Nurr1* in the development of the mesDA (Saucedo-Cardenas et al., 1998).

The phenotype was originally believed to be due to the agenesis of the mesDA neurons (Zetterstrom et al., 1997). However subsequent studies revealed that the mesDA neurons are specified correctly in the *Nurr1* -/- embryos at E11.5 and express *Ptx3* and *En1/En2* (Saucedo-Cardenas et al., 1998; Wallen et al., 1999), but are not maintained and gradually degenerate resulting in the loss of the mesDA neurons described in the new born pups. This degeneration is concomitant with an increase of apoptosis in the ventral mesencephalon of the *Nurr1* -/- mice (Saucedo-Cardenas et al., 1998). Therefore there is strong evidence to suggest that the role of *Nurr1* in the mesencephalon is to maintain the mesDA neurons.

The levels of dopamine neurotransmitter are reduced dramatically in the *Nurr1* -/- mice, as seen by the complete loss of dopamine from the striatum, which is specific for the mesDA neurons as levels of norepinephrin, 5-HT and Chat remain normal (Castillo et al., 1998; Saucedo-Cardenas et al., 1998; Zetterstrom et al., 1997). The partial reduction of dopamine neurotransmitter in the *Nurr1* +/- mice suggests a role for *Nurr1* in the regulation of *TH* activity, but the mechanism by which *Nurr1* can induce *TH* has not yet been discovered (Zetterstrom et al., 1997). This reduction in dopamine neurotransmitter can be explained by the failure of the remaining mesDA neurons of the *Nurr1* -/- to migrate to their correct positions, ultimately failing to innervate the striatum (Wallen et al., 1999). To address whether the loss of the dopamine neurotransmitter in the *Nurr1* -/- mice was due to the absence of *TH* within the mesDA, pregnant females were treated with $_{L}$-DOPA throughout gestation. The rescue described in the *DA* -/- mice when they were administered $_{L}$-DOPA (Zhou and Palmiter, 1995) was not evident in the *Nurr1* -/- mice, suggesting that the loss of dopamine in this instance is not due to the depletion of *TH* (Castillo et al., 1998)

Of clinical relevance, several studies have now demonstrated that mutations of the *Nurr1* gene in humans are evident in patients with Parkinson's disease (Pankratz and Foroud, 2004; Xu et al., 2002; Zheng et al., 2003), and schizophrenia (Buervenich et al., 2000; Chen et al., 2001b). Of particular relevance to Parkinson's disease, a recent study which analysed the adult *Nurr1* +/- mice showed that age depenedent changes in *Nurr1* expression lead to the dysfunction of the nigrastriatal pathway, again strongly suggesting a role for *Nurr1* in maintaining the mesDA cells from development to adulthood (Jiang et al., 2005).

17.4.2. The paired like homeodomain transcription factor *Ptx3* (or *Pitx3*)

Ptx3 is a member of the paired-like homeodomain transcription factor family. *Ptx3* was originally discovered by two groups in 1997. One group was using a degenerate PCR approach to identify homeobox transcription factors involved in brain development (Smidt et al., 1997), whilst the other group cloned *Ptx3* from an embryonic library by homology screening using *Ptx2* (Semina et al., 1997). The name *Ptx3* was assigned due to its homology with *Ptx1* and *Ptx2*. Further studies into these three genes revealed that the homeodomain is highly conserved, with only 1-2 differences in amino acids. Interestingly they all posses a lysine residue at position 50 of the homeodomain, which is characteristic of all bicoid-related proteins (Smidt et al., 1997).

In the developing embryo *Ptx3* is expressed in the outer rim of the lens (Semina et al., 1997; Smidt et al., 2004b), in skeletal muscle with the exception of the heart (Smidt et al., 2004b), and in the VTA and SNpc of the mesDA, *Ptx3* expression completely overlaps with *TH* gene expression (Korotkova et al., 2005; Maxwell et al., 2005;

Maxwell and Li, 2005; Semina et al., 2000; Smidt et al., 2004b; Smidt et al., 1997; Zhao et al., 2004).

To determine the role of *Ptx3* in the mesDA the neurotoxin 6-OHDA was unilaterally injected into adult rat brains, resulting in the loss of *TH* and *Ptx3* gene expression on the lesioned sides of the rat brain, whilst being maintained on the contralateral side (Smidt et al., 1997). Following this result, adult human brain tissue from patients of Parkinson's disease was analysed for *Ptx3* expression, revealing a substantial decrease in *Ptx3* expressing neurons within the mesDA. These results strongly suggested a major role for *Ptx3* within the development and possibly the maintenance of the mesDA.

Fortunately, scientists who were studying eye development in the *aphakia* mouse discovered that this spontaneously occurring recessive phenotype was the result of a genomic deletion of *Ptx3*. Initial genetic analysis of these *aphakia* mice revealed that there was a deletion of the upstream enhancer of the *Ptx3* gene (Semina et al., 2000), whilst a second deletion was later shown to span the promoter area, exon1 and a region of intron1 (Rieger et al., 2001). Due to these findings, the *aphakia* mice were considered to be equivalent to *Ptx3* null mice.

Analysis of the *aphakia* mice revealed that *Ptx3* expression is absent from the neurons of the mesDA in both the developing embryo at E12.5 and at adult stages (Hwang et al., 2003; Nunes et al., 2003; Smidt et al., 2004a; Smidt et al., 2003; Smidt et al., 2004b; van den Munckhof et al., 2003). The adult *aphakia* mice also display a loss of *TH* expressing neurons which is more severe within the SNpc than the VTA. Furthermore, analysis of *TH* immunoreactivity in the adult *aphakia* striatum revealed that there is a

reduction of *TH* immunoreactivity in the dorsal striatum, the target for neurons projecting from SNpc, but not in the nucleus acumbens which is the target structure for projections from the VTA (Hwang et al., 2003; Nunes et al., 2003; Smidt et al., 2004a; Smidt et al., 2003; Smidt et al., 2004b; van den Munckhof et al., 2003).

Although there were some minor discrepancies between the laboratories working with the *aphakia* mice, the general consensus these studies was that the mesDA neurons are initially born and present at E12.5, but during later stages of development the mesDA neurons of the SNpc are lost.

With the recent generation of the *Ptx3* knockout mouse (*Ptx3* -/-), which also carries the *eGFP* reporter gene under the control of the endogenous *Ptx3* promoter (Zhao et al., 2004), quantitative analysis of the number of *Ptx3* and *GFP* expressing cells in *Ptx3* -/- embryos at E12.5 and E14.5 provided evidence that there is a 50% reduction of TH-positive GFP-positive cells, and an overall 45% reduction of TH immunoreactive cells (Maxwell et al., 2005). This dramatic reduction of *TH* expressing neurons at E12.5 had not been described in the studies using the *aphakia* mice, which provides evidence that *Ptx3* is essential for the complete development of the mesDA neurons, and that the *aphakia* mutation is hypomorphic (Maxwell et al., 2005; Maxwell and Li, 2005). Similar to the results described in the *aphakia* mice, the reduction of mesDA neurons is more evident in the SNpc than the VTA of the *Ptx3* -/- (Maxwell et al., 2005).

Potential roles for *Ptx3* in the induction of TH have previously been suggested. DNA binding studies revealed that *Ptx3* can behave as an activator of transcription on direct interaction with target genes (Smidt et al., 1997). More recent studies have illustrated that there is a single high-affinity binding site for *Ptx3* within the *TH* promoter, and that

this site is sufficient for *Ptx3* responsiveness, suggesting that *Ptx3* can activate *TH* in a cell dependent manner (Lebel et al., 2001).

However, gain-of-function studies have provided contrasting results to the possible function of *Ptx3* within the ventral mesencephalon. The over-expression of *Ptx3* in adult hippocampus-derived progenitor cells does not induce the expression of markers for the mesDA such as *AADC*, *TH*, *c-RET* and the *D2R* dopamine receptor (Sakurada et al., 1999). This result resembles the data generated from the studies of the *Lmx1b* knockout mice which revealed that *in-vivo TH* expression was independent of *Ptx3* function (Smidt et al., 2000).

It has recently been shown that the over-expression of *Ptx3* in embryonic stem cells (ES) does not have an effect on the total number of *TH* positive cells produced in the culture but rather results in a greater proportion of these cells to expressing *TH* (Maxwell et al., 2005). This recent work has now established a specific role for *Ptx3* in the acquisition of a SNpc fate for the dopaminergic progenitor cells, and it has reinforced the theory that *Ptx3* is essential for the survival of the SNpc neurons.

17.4.3. The LIM homeodomain transcription factors *Lmx1b and Lmx1a*

Lmx1b is a member of the LIM homeodomain transcription factors and was cloned during the screen from which *Ptx3* was initially cloned (Smidt et al., 1997). In the embryo *Lmx1b* is expressed in the developing limbs where it plays a crucial role in dorsal ventral patterning (Riddle et al., 1995) and in the CNS (Smidt et al., 2000). *Lmx1b* gene expression within the CNS is detectable in the subthalamic nucleus,

posterior hypothalamus continuing along the ventral mesencephalon and past the MHB where it shifts dorsally and continues through the hindbrain and along the spinal cord (Asbreuk et al., 2002; Smidt et al., 2000). In the ventral mesencephalon the onset of *Lmx1b* expression is at E7.5 and during later development it has been demonstrated to completely overlap with *TH* and *Ptx3* within the mesDA neurons where it is maintained until and throughout adulthood (Smidt et al., 2000).

The role of *Lmx1b* in the development of the neuronal populations around the MHB was determined from the analysis of the *Lmx1b* knockout (*Lmx1b* -/-), which display a loss of 5-HT neurons from the rhombencephalon (Ding et al., 2003), and a loss of the mesDA from the ventral mesencephalon (Smidt et al., 2000). The mesDA neurons are specified correctly in the *Lmx1b* -/- embryos as determined by the presence of *Nurr1* and *TH* gene expression at E12.5, but gradually degenerate and are no longer detectable by E16.5, indicating that *Lmx1b* is not required for the specification of the mesDA neurons but is important in their maintenance (Smidt et al., 2000). Additionally, *Ptx3* gene expression is not detectable at any time point in these embryos and suggests a role of *Lmx1b* in its regulation (Smidt et al., 2000). From these results the authors suggested that *Lmx1b* is the upstream regulator of *Ptx3* and that they had uncovered a pathway independent from *Nurr1* required in the development of the mesDA. The authors also suggest that *Ptx3* is not required for the expression of *TH* in the mesDA, however, in light of the recent *Ptx3* -/- which maintains the expression of *TH* within the VTA this statement is not completely accurate. Therefore we may speculate that the *TH* gene expression reported in the *Lmx1b* -/- mice could be the neurons from the VTA as *Ptx3* is specifically required for the development of the SNpc (Maxwell et al., 2005; Zhao et al., 2004).

It has been well documented that the autosomal dominant disorder, nail-patella syndrome, is attributed to a mutation of the *Lmx1b* gene. Nail-patella syndrome is characterised by pleiotropic developmental defects of dorsal limb structures such as the nails, patella and elbows, bony outgrowth of the dorsal ileum and a progressive kidney disease (Chen et al., 1998a; Dreyer et al., 1998; Knoers et al., 2000; Vollrath et al., 1998). However, more recent studies have indicated that brain sections from patients of Parkinson's diseased also exhibit a substantial decrease in *Lmx1b* positive neurons (Smidt et al., 2000). This result can be repeated in an animal model of Parkinson's disease when unilaterally injecting 6-OHDA into the brain of adult rats. This caused the complete ablation of the mesDA on the lesioned side of the brain, as detected by the absence of both *Lmx1b* and *TH* gene expression, which remained normal in the contralateral side (Smidt et al., 2000). This result suggested that *Lmx1b* plays a crucial role in the maintenance of the mesDA during development and possibly throughout adulthood.

Recently, the LIM homeodomain transcription factor *Lmx1a* which is closely related to *Lmx1b*, has been demonstrated as being a major pre-determinant of the mesDA phenotype. The removal of *Lmx1a* induces the absence of mesDA progenitor cells (Andersson et al., 2006). Another function of *Lmx1a* has also been elucidated in the same study. The transcription factor *Msx1* which allows cells to differentiate into mesDA post-mitotic cells expressing *TH* is believed to be induced by the activity of *Lmx1a* (Andersson et al., 2006). Therefore, while *Lmx1b* is crucial for the maintenance of the mesDA neurons, *Lmx1a* is essential for their initial specification.

17.4.4. The homeodomain transcription factors En1 & En2

In vertebrates, two homologues of the *Drosophila Engrailed* gene have been identified; *Engrailed1 (En1)* and *Engrailed2 (En2)*, based on their sequence similarity to the *Drosophila* gene (Joyner et al., 1985; Joyner and Martin, 1987). Their expression patterns partly overlap, but their onset of expression differs slightly. The onset of *En1* expression is at the 1st somite stage, in the region of the presumptive MHB region followed by the expression of *En2* at the 5 somite stage (Davis and Joyner, 1988). *En1* is expressed in the region from where the cerebellum and the inferior colliculi are generated and in the developing mesDA (Davis and Joyner, 1988; Simon et al., 2001). Even though *En2* expression has been described as overlapping *En1* in the mesDA, it is apparent that *En2* is more diffusely expressed and located within a subset of the mesDA (Simon et al., 2001).

To investigate the role of the engrailed genes in the development of the mesDA, knockout mice were generated. *En1* knockout mice (*En1* -/-) die at birth and display abnormalities in their forelimbs and sternum (Wurst et al., 1994). Specific analysis of the *En1* -/- brains revealed that they lack the cerebellum, the inferior colliculi, cranial nerves III and IV, but maintain the mesDA neurons (Wurst et al., 1994). Further analysis revealed that the neurons of the SNpc are unaffected, while those in the VTA display a slight alteration in their cytoarchitecture (Simon et al., 2001). Interestingly in the *En1* -/- mice there is an up-regulation of *En2*, which indicates the presence of a compensatory mechanism between these two genes (Simon et al., 2001).

The phenotype of the *En2* knockout mice (*En2 -/-*) was surprisingly mild compared to the *En1 -/-* mice. The *En2 -/-* are viable and fertile and display a minor defect in the foliation of the cerebellum (Joyner et al., 1991; Millen et al., 1994). To address whether either *Engrailed* gene can compensate for the loss of other, *En1/En2* double knockout mice (*En1 -/-; En2 -/-*) were generated. These *En1 -/-; En2 -/-* mice are not viable, and they lack the VTA and SNpc (Alberi et al., 2004; Simon et al., 2001). Analysis of the double knockout embryos revealed that the mesDA neurons are initially induced and acquired their neurotransmitter phenotype, but are lost by E14.5. This specific loss of mesDA neurons is coupled with an increase in apoptosis (Alberi et al., 2004).

Furthermore, there is a dose dependent requirement for the engrailed genes, with one copy of *En1* being sufficient to maintain the mesDA to a level indistinguishable from the wild type (Simon et al., 2001), suggesting one functional copy of the *Engrailed* genes is essential for the development of the mesDA. Of clinical relevance, the correlation between the engrailed genes and Parkinson's disease was made when α-*synuclein* (a gene implicated in the pathogenesis of Parkinson's disease) was understood to be regulated by the engrailed genes (Simon et al., 2001).

17.5. The role of Wnt proteins in the development of the mesDA

The Wnt signalling pathway is involved in many aspects of the development of the CNS and is named after its upstream ligands. The signalling mechanism is very complex and although genetic and biochemical analysis have revealed that there are two distinct pathways which act downstream of the Wnt signal, the pathway which is best understood is the canonical pathway (Huelsken and Behrens, 2002).

Simply described, this pathway is mediated by β-Catenin. In the absence of the Wnt ligand, β-Catenin is destabilised by a protein complex consisting of Axin, Adenomatous Polyposis Coli (APC) and Glycogen Synthase Kinase 3β (GSK-3β) leading to its degradation via ubiquitin-dependent proteolysis, and thus is unable to bind to the Tcf/LEF transcription factors which are constitutively bound to their target DNA sequences repressing transcription. The presence of the Wnt ligand to its receptors (Frizzled and the co-receptor LRP) activates Dishevelled which destabilises the β-Catenin degradation complex allowing β-Catenin to accumulate and activate Wnt target genes via interaction with the Tcf/LEF transcription factors (Huelsken and Behrens, 2002; Ilyas, 2005; Logan and Nusse, 2004; Taipale and Beachy, 2001).

As *Wnt1* -/- mice and mice with null alleles of downstream components of the Wnt signalling pathway (*β-Catenin* and *LRP-6* mutants) all display a complete loss of the mesencephalon and anterior rhombencephalon, the investigation of the direct role for Wnt1 in the development of the mesDA were not possible (Brault et al., 2001; McMahon and Bradley, 1990; McMahon et al., 1992; Pinson et al., 2000). Studies in the *Drosophila* have indicated that *Wnt1* is necessary for the maintenance of the *Engrailed* genes. This relationship is conserved in the mouse where the expression of *En1* is initiated in the *Wnt1* -/- mice but in the absence of *Wnt1* is not maintained (McMahon et al., 1992). Re-introducing *En1* expression in the *Wnt1* -/- mice causes the restoration of the early development of the mesencephalon and anterior rhombencephalon (Danielian and McMahon, 1996). Closer analysis of the embryos revealed that when *En1* was reintroduced in the *Wnt1* -/- embryos, there was a rescue of the mesDA re-emphasising the role of *En1* in the development of the mesDA, but also showing that *Wnt1* plays an important role in the developing mesDA by regulating *En1*

(Danielian and McMahon, 1996). Furthermore, *in-vitro* assays using *Nurr1* expressing cells of the mesDA revealed that they also express *β-Catenin* which implicates the Wnt signalling pathway playing a role in the development of the mesDA (Castelo-Branco et al., 2003).

A recent study has provided new evidence for the role of *Wnt1* in the development of the mesDA. The classic explant cultures performed by Ye et al., 1998 were repeated with the only alteration being that the explants were taken from *Wnt1* -/- mice. When Fgf8 soaked beads were placed in neural tissue from the *Wnt1* -/-, there was no induction of the mesDA (Prakash et al., 2006). This result suggests that in addition to maintaining the expression of *En1*, *Wnt1* also plays a role much earlier in the specification of the mesDA, working in concert with Shh and Fgf8 to induce the mesDA.

Further evidence to the role of *Wnt1* in the development of the mesDA came from *in-vitro* assays. From these assays it was also evident that two other members of the Wnt family were involved in the development of the mesDA; *Wnt3a* and *Wnt5a* (Castelo-Branco et al., 2003). *Wnt3a* promotes the proliferation of mesDA precursor cells expressing *Nurr1*, but does not increase the number of *TH* positive cells within the culture. In contrast *Wnt1* and *Wnt5a* both increase the number of mesDA neurons via two different mechanisms. *Wnt1* increases the proliferation of the *Nurr1* precursors, by upregulating the expression of *cyclin D1* and *D3* (mediators of cell cycle progression by *Wnt1*) and down regulating *p27* and *p57* (cell cycle inhibitors), whilst *Wnt5a* increases the proportion of *Nurr1* expressing precursors which adopt a mesDA phenotype as

detected by the expression of *Ptx3* and *c-RET* (Castelo-Branco et al., 2003). These results suggest that *Wnt1* and *Wnt5a* may act to promote mesDA neuron development.

18. The Red Nucleus (RN)

The RN can be identified in mammals as a distinct cell mass in the tegmentum at the level of the oculomotor nerve, rostral to the decussation of the brachium conjunctivum (Jerath, 1964; Massion, 1967; ten Donkelaar, 1988). Other criteria which can be used to identify the red nucleus are the mesencephalic termination of the bracium conjunctivum and its contralateral spinal projection (see figure K) (ten Donkelaar, 1988). Studies to identify the neurotransmitter phenotype of the RN neurons have revealed that both GABA and Glutamate are predominantly used for either inhibitory or excitatory responses to stimuli respectively (Billard et al., 1991; Nieoullon et al., 1988; Taguchi et al., 1989). In the brains of adult rats, 5-HT neuronal fibres have also been identified passing through the RN (Pazos et al., 1985; Pazos and Palacios, 1985), which have the ability to modulate the neurotransmission of the GABAergic neurons within the RN (Licata et al., 2001).

18.1. Structure and function of the RN

The structure and function of the RN has been studied for over a century with special interest arising when the discovery of a new tract originating from the brainstem and descending towards the spinal cord, which was distinct from the pyramidal, the vestibuluar and the reticulospinal tract, was first reported by von Monakow in 1883 (Massion, 1967). Von Monakow's discovery aroused much interest and in 1890 Held,

who was working on newly born rats, reported that this tract projects from the contralateral RN (Massion, 1967). This new tract was termed the rubrospinal tract.

The course of the rubrospinal tract has been described by many authors in different species. The rubrospinal tract originates in the magnocellular domain of the RN within the ventral mesencephalon and descends into the brain stem, lateral to the lateral lemniscus. At the bulbar level, it lies exterior and dorsal to the olive were it then progresses into the lateral funiculus anterior to the pyramidal tract (Kuypers, 1964; Massion, 1967). The rubrospinal fibers enter the gray matter of the spinal cord at the level of the intermediate zone between anterior and posterior horns and end at the levels of the fifth, sixth and seventh laminae (Massion, 1967).

The structure of the RN has also been studied in great detail. Cajal and von Monakow stated that there were three distinct cell populations present in the RN, characterised by their size; large and small cells (Massion, 1967). The subdivision into a caudal magnocellular region and a rostral parvocellular region is widely accepted, but this subdivision varies between different species (Burman et al., 2000a; Burman et al., 2000b; Massion, 1967; ten Donkelaar, 1988). In lower mammals the magnocellular domain is strongly developed, and much less so in primates (Padel et al., 1981), and is only a rudiment in humans (Nathan and Smith, 1982; ten Donkelaar, 1988). Conversely the parvocellular domain is less developed in lower mammals and considerably increases among primates, and is the largest domain found in humans (Burman et al., 2000a; Burman et al., 2000b; ten Donkelaar, 1988). Topographical arrangements have also been demonstrated for the magnocellular domain of the RN, with zones for posterior limbs and zones for anterior limbs. Fibers from these zones pass down the

rubrospinal tract and terminate in the lumbar and cervical regions of the spinal cord respectively (Massion, 1967). It is also widely accepted that both the neuronal populations in the magnocellular and parvocellular domain also contain local circuit GABAergic neurons (Burman et al., 2000a; Burman et al., 2000b; Massion, 1967; Padel et al., 1981).

The function of the RN has been implicated in the control of limb movement due to the rubrospinal tracts' connection to the spinal cord (Massion, 1967; Massion, 1988; Muir and Whishaw, 2000; ten Donkelaar, 1988). Another descending tract which is implicated in the control of locomotion is the corticospinal tract, which originates in the cerebral cortex and forms connections to similar locations to the rubrospinal tract in the spinal cord (Kennedy, 1990).

Lesions of the corticospinal tract in primates are associated with paresis that is severe, but eventually disappears (Lawrence and Kuypers, 1968a). Lesions of the rubrospinal tract performed by the same group again show a transient deficit similar to the corticospinal tract lesions but are less severe and disappear more rapidly (Lawrence and Kuypers, 1968b). Lesions to both descending tracts results in a severe deficit which never recovers (Lawrence and Kuypers, 1968b). These studies suggest that the functions of these two tracts are interrelated, leading many scientists to believe that the rubrospinal tract was functioning in a redundant system for the control of locomotion with the corticospinal tract (Kennedy, 1990).

In order to distinguish between the functions of the corticospinal tract and the rubrospinal tract, more detailed studies in primates were carried out. Recordings from

the RN of conscious primates have now demonstrated that rubrospinal tract activity precedes movement and that parameters of movement such as force (Cheney et al., 1988), velocity (Gibson et al., 1985) and direction (Kennedy, 1987) are related to its activity (Kennedy, 1990). Another interesting finding was that the activity of the rubrospinal tract is related to the movement of individual digits, and not solely to the grouped movements of the digits, as implicated for the corticospinal tract (Houk et al., 1988; Kennedy, 1987; Kennedy, 1990). Again these findings do not offer any major differences between the two tracts. It was proposed that one difference between these two tracts is that the corticospinal tract was predominately active during the learning of new movements, while the rubrospinal tract was predominately active during the execution of automated (learnt) movements (Massion, 1988; Paillard, 1978).

Another projection from the RN, the rubro-olivary projection, has now also been implicated in working together with the corticospinal and rubrospinal tracts, projecting to the inferior olivary nucleus and then to the cerebellum (Strominger et al., 1979). It has been demonstrated that the rubro-olivary projection is not involved in the control of ongoing movements, but it has been found to play a role in compensating for lesions of the rubrospinal tract.

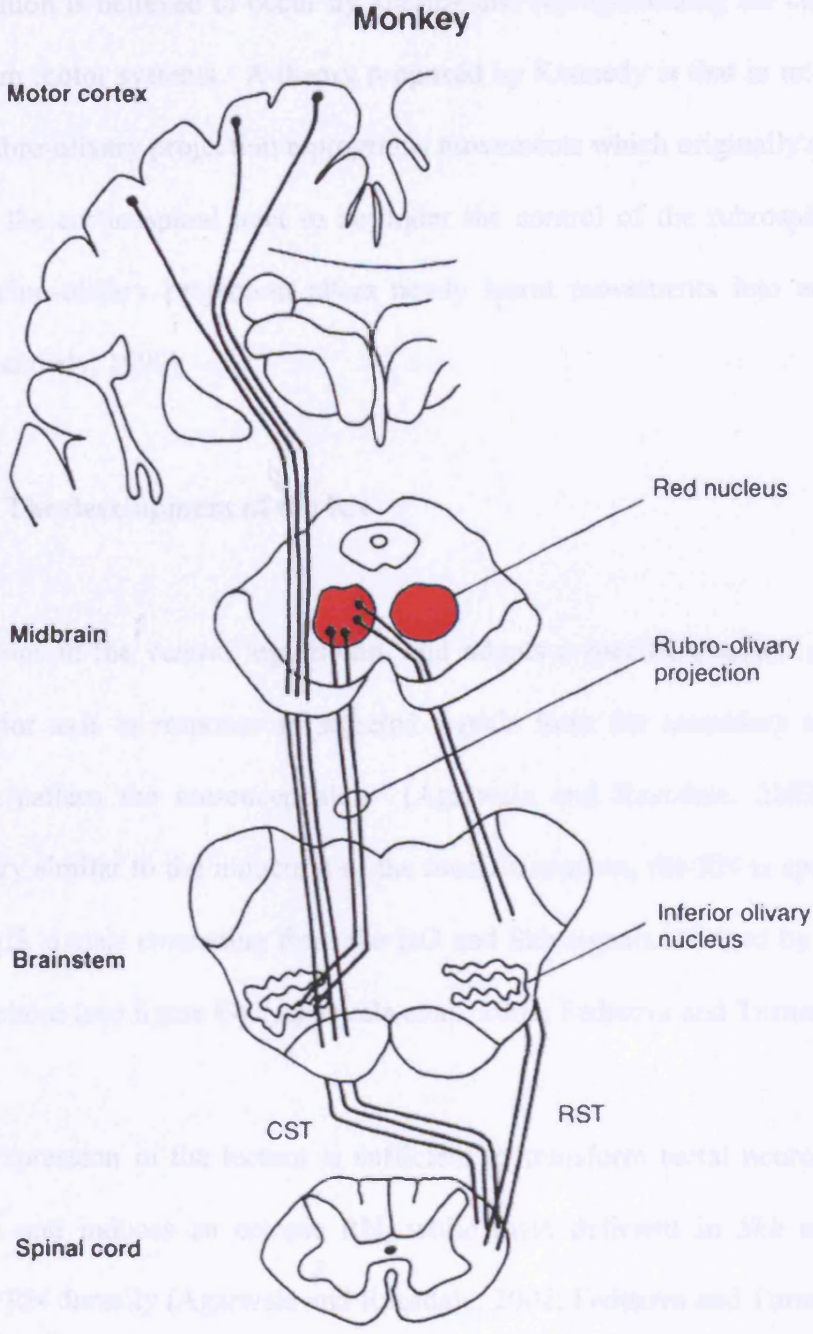

Figure K: The projections of the red nucleus: Shows the projections from the RN and their route towards the spinal cord. The rubrospinal tract (RST) originates in the magnocellular domain of the RN and descends into the brain stem. At the bulbar level, it lies exterior and dorsal to the olive. It then progresses into the lateral funiculus where it lies just anterior to the pyramidal tract. The rubrospinal fibers enter the gray matter of the spinal cord at the level of the intermediate zone between anterior and posterior horns. The diagram also shows the Rubro-olivary projection and the corticospinal tract (CST). Figure adapted from Kennedy, 1990.

This compensation is believed to occur by altering and reprogramming the cerebellum and downstream motor systems. A theory proposed by Kennedy is that in un-lesioned animals, the rubro-olivary projection reprograms movements which originally are under the control of the corticospinal tract to be under the control of the rubrospinal tract. Simply, the rubro-olivary projection alters newly learnt movements into automated movements (Kennedy, 1990).

18.2. The development of the RN

The RN develops in the ventral tegmentum, and adopts a specific position along the anterior-posterior axis in response to secreted signals from the secondary signalling centres which pattern the mesencephalon (Agarwala and Ragsdale, 2002). In a mechanism very similar to the induction of the mesDA neurons, the RN is specified in response to Fgf8 signals emanating from the IsO and Shh signals secreted by the floor plate and notochord (see figure G) (Agarwala et al., 2001; Fedtsova and Turner, 2001).

Ectopic *Shh* expression in the tectum is sufficient to transform tectal neurons into a tegmental fate and induces an ectopic RN, while mice deficient in *Shh* exhibit an absence of the RN dorsally (Agarwala and Ragsdale, 2002; Fedtsova and Turner, 2001). Furthermore, ectopically expressing *Fgf8* or taking neural tissue from the MHB and transplanting it ectopically within the anterior regions of the mesencephalon induces the expression of genes characteristic of posterior regions of the mesencephalon at the expense of anterior mesencephalic genes, and results in the absence of the RN (Agarwala and Ragsdale, 2002; Fedtsova and Turner, 2001). These results suggest that the RN is specified at a specific location within the ventral mesencephalon where the

concentration of Fgf8 signal is low. However it is still unclear whether the Fgf8 signal inhibits the development of the RN or whether it is essential for its specification but at low concentrations.

Two other genes have been implicated with the development of the RN. A class IV Pou-domain transcription factor *Brn3a* (also known as *Brn3.0* and *Pou4f1*), and the homeobox gene *Emx2*. Mice with a homozygous null mutation for *Brn3a* are born and appear grossly normal compared to their wild type littermates (McEvilly et al., 1996; Xiang et al., 1996). However they did display some behavioural and physiological problems, which include the inability to swallow and an inability to right themselves due to a lack of coordinated limb and trunk movements. The *Brn3a* knockout mice do not survive more than 24 hours after birth and lack any RN neurons (Eng et al., 2001; McEvilly et al., 1996; Xiang et al., 1996). Analysis of prenatal *Brn3a* knockout embryos suggests that the neurons of the RN are specified, migrate to their correct positions along the tegmentum, but fail to survive between E16.5 and P0 (McEvilly et al., 1996).

Emx2 is expressed in the developing RN neurons in a partially overlapping fashion with *Brn3a*. In homozygous *Emx2* mutant mice, *Brn3a* expression is retained in the region of the prospective RN between E12.5 and E16.5 but by E18.5 cannot be detected any more (Agarwala and Ragsdale, 2002). The *Emx2* mutant mice also die perinatally, however this is not believed to be a direct consequence from the loss of the RN but caused by the failure of the embryos to develop kidneys (Mallamaci et al., 2000).

Both *Brn3a* and *Emx2* are essential for the survival of the RN, but are not required for its initial specification (Agarwala and Ragsdale, 2002; McEvilly et al., 1996; Xiang et

al., 1996). Whether a specific population of progenitor cells which give rise to the RN exist or whether the red nucleus arises from a common tegmental progenitor cell, which later differentiates into the neurons expressing *Brn3a* or *Emx2* has yet to be discovered.

19. The Oculomotor Complex (OMC)

The OCM is located in the ventral mesencephalon close to the MHB and contains visceral motor neurons corresponding to the third cranial nerve (Cranial Nerve III) (see figure G) which primarily utilise GABA as their neurotransmitter but there is some evidence that the neurotransmitter Gylcine is also used (Spencer et al., 1989).

19.1. Function of the OMC

The OMC neurons are involved in controlling the movement of the eye by innervating the extraocular muscles (medial rectus, inferior rectus, superior rectus). The remaining extraocular muscles, the superior oblique and the lateral rectus muscle are innervated by the Abducens nerve (Cranial Nerve VI) and the Troclear nerve (Cranial Nerve IV) respectively. The OMC is also involved in innervating the striated muscle of the eyelid, and the parasympathetic innervation responsible for the constriction of the pupil in response to light and the accommodation of the lens for near vision (see figure L) (Evinger, 1988; Kandel et al., 2000b)

Medical symptoms displayed due to disorders of the cranial nerves described above include diplopia (double vision), ptosis (drooping eyelid), uneven dilation of the pupils and a deviation of the eye pointing outwards (Kandel et al., 2000b).

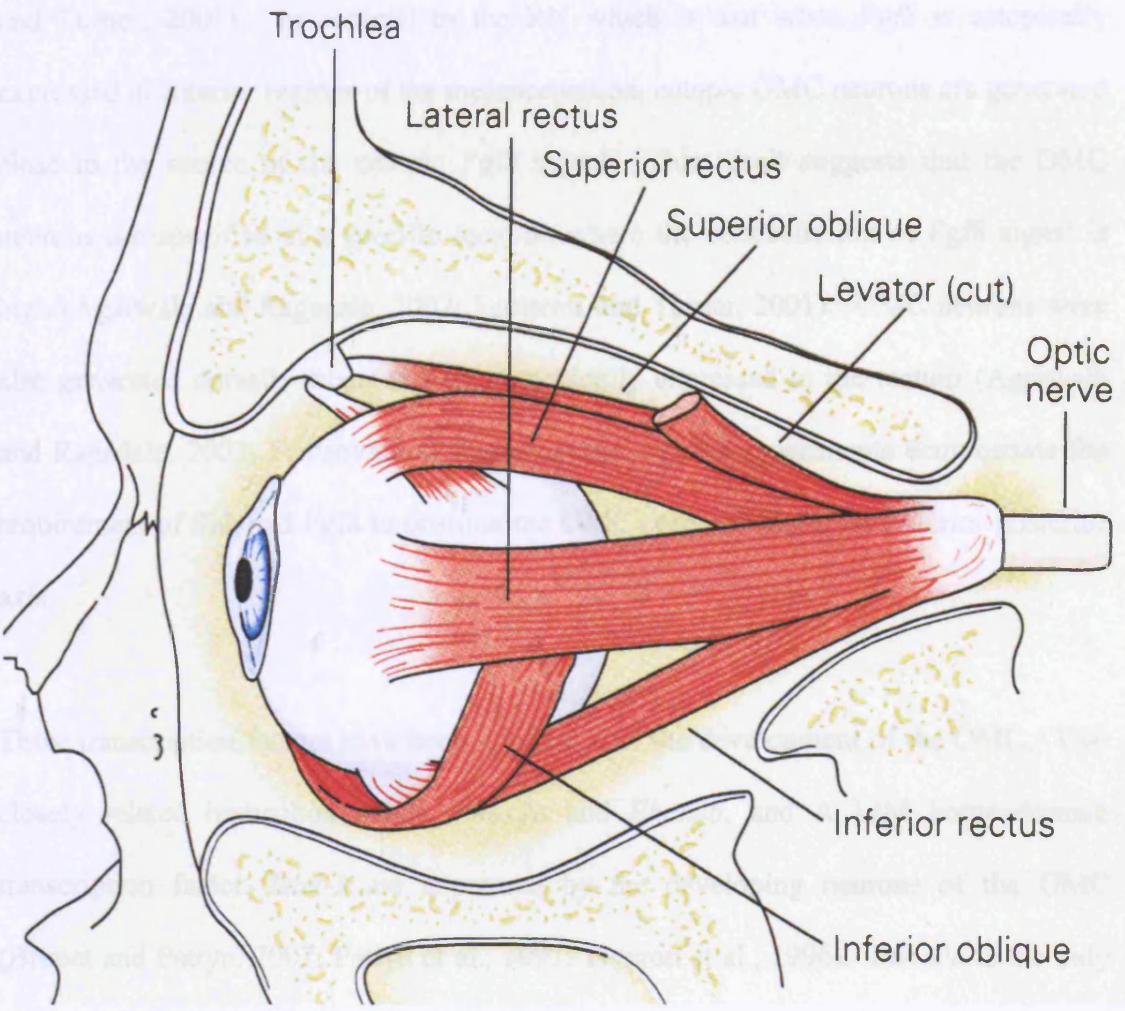

Figure L: Extra ocular muscles are innervated by the OMC neurons: Shows the extraocular muscles which are innervated by the motor neurons from the OMC. The OMC specifically innervates the inferior rectus, superior rectus and the medial rectus (not visible in diagram). It also innervates the striated muscle of the eyelid (not shown on diagram). The Abducens and Troclear nerves innervate the lateral rectus muscle and the lateral rectus respectively. Figure taken from Kandel et al., 2000

19.2. The development of the OMC

The development of the OMC, similar to the development of the red nucleus and mesDA, is governed by signals emanating from the ventral midline and from the MHB boundary (see figure G) (Agarwala and Ragsdale, 2002; Agarwala et al., 2001; Fedtsova

and Turner, 2001). In contrast to the RN which is lost when *Fgf8* is ectopically expressed in anterior regions of the mesencephalon, ectopic OMC neurons are generated close to the source of the ectopic Fgf8 signal. This result suggests that the OMC neurons are specified at a specific location where the concentration of Fgf8 signal is high (Agarwala and Ragsdale, 2002; Fedtsova and Turner, 2001). OMC neurons were also generated dorsally when *Shh* was ectopically expressed in the tectum (Agarwala and Ragsdale, 2002; Fedtsova and Turner, 2001). These experiments demonstrate the requirement of Shh and Fgf8 to position the OMC correctly along the anterior-posterior axis.

Three transcription factors have been implicated in the development of the OMC. Two closely related homeobox genes, *Phox2a* and *Phox2b*, and A LIM homeodomain transcription factor, *Islet-1* are expressed by the developing neurons of the OMC (Brunet and Pattyn, 2002; Pattyn et al., 1997; Tiveron et al., 1996). *Phox2a* is the only gene to be expressed in the progenitor cells of the OMC occupying the ventricular zone, whilst they are all expressed in the post mitotic neurons of the OMC in the mantle layer (Brunet and Pattyn, 2002; Pattyn et al., 1997).

Phox2a knockout mice display an absence of the OMC and the Trochlear nuclei, as seen by the lack of *Islet-1* positive neurons (Pattyn et al., 1997), while *Phox2b* knockout mice, although lacking all noradrenergic neurons and not being able to survive embryonic development past mid gestation, specify the OMC neurons (Brunet and Pattyn, 2002; Pattyn et al., 2000; Pattyn et al., 1997). These results suggest that *Phox2a* plays a critical role in the specification of the OMC neurons. *Islet-1* gene expression is detected in post mitotic neurons of the OMC from E9.5 onwards, and is considered to

be the first marker expressed by future motor neurons, shortly after their exit from the cell cycle (Ericson et al., 1992). Unfortunately the specific role of *Islet-1* in the development of the OMC cannot be addressed directly, as the *Islet-1* knockout mice lack all motor neurons and their development arrests at E9.5 (Pfaff et al., 1996). It is possible that the OMC progenitor cells are born correctly in the *Islet1* deficient mice but cannot be maintained in an environment lacking *Islet-1*, but no evidence has been generated yet.

Aims of Project

Foxa2 is known to be expressed by the mesencephalic dopaminergic neurons (mesDA) (Hynes et al., 1995a), but an investigation into the role of *Foxa2* within this cell group *in-vivo* has not been carried out due the embryonic lethality caused by the deletion of *Foxa2* in mice (Ang and Rossant, 1994; Weinstein et al., 1994). The primary aim of this project is to investigate the possible role for *Foxa2* in the specification of the mesDA and other neuronal populations of the ventral mesencephalon through the generation of conditional knockout mice which lack *Foxa2* in the mesencephalon.

A secondary aim for this project is to determine the relationship between *Foxa2*, *Foxa1* and *Shh*, through the generation of chimaeras, using wild type cells aggregated with *Foxa2* deficient cells, and other mouse models.

Materials & Methods

1. Production and genotyping of *Foxa2* conditional knockout embryos

To obtain conditional *Foxa2* mutants, we crossed *Wnt1-Cre* transgenic mice (provided generously by Andrew McMahon) to mice homozygous for the $Foxa2^{flox}$ allele (Sund et al., 2000). *Wnt1-Cre*/+; $Foxa2^{flox/+}$ male offspring were mated with $Foxa2^{flox/flox}$ females. The *Foxa2* allele was detected by PCR analysis using primers SE166 (5' TTG CTC ACG GAA GAG TAG CC 3') and UP207 (5' CCC CCT GAG TTG GCG GTG GT 3'), using the following PCR program: 95°C for 45 seconds, 60°C for 45 seconds, 72°C for 90 seconds repeated for 34 cycles. The *Cre* allele was detected using primers TK140 (5' ATC CGA AAA GAA AAC GTT GA 3') and TK142 (5' ATC CAG GTT ACG GAT ATA GT 3') using the following PCR program: 94°C for 30 seconds, 55°C for 30 seconds, 72°C for 30 seconds repeated for 34 cycles.

2. Production and genotyping of *Shh* conditional knockout mice

To obtain conditional *Shh* mutants, we crossed *Wnt1-Cre* transgenic mice to mice homozygous for the Shh^{flox} allele (129-Shh^{tm2Amc}/J), which were purchased from the Jackoson Laboratory and created by Paula Lewis (Dassule et al., 2000; Lewis et al., 2001). *Wnt1-Cre*/+; $Shh2^{flox/+}$ male offspring were mated with $Shh^{flox/flox}$ females. The *Shh* allele was detected by PCR analysis using primers Shh1930 (ATG CTG GCT CGC CTG GCT GTG GAA) and Shh1931 (GAA GAG ATC AAG GCA AGC TCT GGC), using the following PCR program: 94°C for 30 seconds, 65°C for 60 seconds, 72°C for 60 seconds repeated for 35 cycles. The *Cre* allele was detected as described above.

3. Production and generation of *Gli3 XT ; Foxa2* conditional knockout mice

To obtain *Wnt1-Cre*/+; $Foxa2^{flox/flox}$; $Gli3^{xt/xt}$ embryos we crossed *Wnt1-Cre*/+; $Foxa2^{flox/+}$; $Gli3^{xt/+}$ males with $Foxa2^{flox/flox}$; $Gli3^{xt/+}$ females. The $Gli3^{xt/+}$ males were generously donated by James Briscoe (Schimmang et al., 1992). The *Gli3* allele was detected by PCR analysis using primers wt1 (GTT GGC TGC TGC ATG AAG ACT GAC) and wt2 (GGC CCA AAC ATC TAC CAA CAC ATA G) for the wild type allele. The mutant allele was detected using XT1 (TAC CCC AGC AGG AGA CTC AGA TTA G) and XT2 (AAA CCC GTG GCT CAG GAC AAG). The PCR program was: 94°C for 30 seconds, 55°C for 30 seconds, 72°C for 30 seconds repeated for 34 cycles.

4. Production of CKO Foxa2 χ embryos

Chimaeric embryos were obtained by aggregating Morula stage embryos generated by crossing $Foxa2^{floxed/+}$; *Wnt1-Cre* males with $Foxa2^{floxed/floxed}$ females into Morula stage embryos generated by crossing heterozygous B5/EGFP males (Hadjantonakis et al., 1998) with Parkes females. Presence of *Wnt1-Cre* gene was detected by PCR analysis previously described. Presence of GFP was detected visually using UV light. Embryos which possessed both GFP and Wnt1-Cre were selected for analysis.

5. Whole-mount *in- situ* hybridization

Embryos were dissected and fixed in 4% paraformaldehyde in 1M phosphate buffered saline (PBS) at 4°C for 2 hours, washed in PBS, and stored at -20° in 100% methanol.

Whole-mount in situ hybridization was performed as previously described (Rosen and Beddington, 1994; Rosen and Beddington, 1993), and certain embryos were selected for antibody staining against *Foxa2*. Embryos were then analysed by embedding in paraffin and sectioned at a thickness of 10μm.

6. *In-situ* hybridization on brain sections

Embryos were dissected and fixed in 4% paraformaldehyde in 1M PBS overnight, washed in PBS and cryo-protected in 30% sucrose in PBS and sectioned on a *Leica Jung* cryostat at a thickness of 12μm. The *in-situ* hybridization procedure has been described previously (Conlon and Herrmann, 1993).

6.1. List of mouse antisense RNA probes that were used:

Foxa2 (Ang et al., 1993), *Foxa1* (Ang et al., 1993), *Otx2* (Rhinn et al., 1998), *Shh* (Echelard et al., 1993), *Ptc* (Goodrich et al., 1996; Platt et al., 1997), *Gli1* (Hynes et al., 1997; Lee et al., 1997; Platt et al., 1997), *Gli2* (Hui et al., 1994; Hynes et al., 1997), *Gli3* (Hui et al., 1994; Hynes et al., 1997), *Pax3* (Goulding et al., 1991), *Pax7* (Jostes et al., 1990), *Dbx1* (Shoji et al., 1996), *Msx1* (Catron et al., 1996; Hill et al., 1989), *Lmx1b* (Chen et al., 1998b), *Nurr1* (Zetterstrom et al., 1997), *Ptx3* (Puelles et al., 2003; Smidt et al., 1997), *AADC* (Smidt et al., 2004a), *TH* (Grima et al., 1985), *Brn3a* (Eng et al., 2001; McEvilly et al., 1996), *Islet1* (Qiu et al., 1998), *Scg10* (Wuenschell et al., 1990), *Phox2a* (Morin et al., 1997; Pattyn et al., 1997), *Gad67* (Asada et al., 1996; Asada et al., 1997), *Nkx2.2* (Kitamura et al., 1997), *Nkx2.9* (Pabst et al., 1998), *Nkx6.1* (Qiu et al., 1998; Sander et al., 2000), *Ngn1* (Ma et al., 1999), *Ngn2* (Fode et al., 1998; Ma et al.,

1999), *Mash1* (Guillemot and Joyner, 1993; Lo et al., 1991), *Irx3* (Cohen et al., 2000), *Olig2* (Richardson et al., 2000; Zhou et al., 2000), *Sim1* (Fan et al., 1996), *Emx2* (Simeone et al., 1992), *Pax6* (Osumi et al., 1997), *Wnt1* (McMahon and Bradley, 1990), *En1* (Danielian and McMahon, 1996).

7. Immunohistochemistry

Embryos were dissected and fixed in 4% paraformaldehyde in 1M PBS overnight, washed in PBS and cryo-protected in 30% sucrose in PBS and sectioned on a *Leica Jung* cryostat at a thickness of 12μm. Antigen retrieval with Citrate Buffer at pH 8.0 was performed as described in the literature (Montero, 2003; Shi et al., 1997).

7.1. List of antibodies used:

Rabbit anti-Foxa2 (1: 500, Gift from Hiroshi Sasaki), Goat anit-Foxa2 (1: 100, Santa Cruz), Mouse anti-Foxa2 (1:2, IgG1, DSHB), Guinea Pig anti-Foxa1 (1:500), Rabbit anti-Shh (1:100, Santa Cruz), Mouse anti-Shh (1:1, DSHB), Rabbit anti-Nkx6.1 (1:1500, Gift from James Briscoe), Mouse anti-Nkx2.2 (1:5, IgG2b, DSHB), Rabbit anti-Nkx2.2 (1:4000, Gift from James Briscoe), Mouse anti-Islet1 (2D6 1:5, IgG2b, DSHB), Mouse anti-Islet1 (4D5 1:100, IgG1, DSHB), Rabbit anti-TH (1:200, Calbiochem), Sheep anti-TH (1:200, Calbiochem), Rabbit anti-Sox2 (1:500, Chemicon) (Ferri et al., 2004; Wood and Episkopou, 1999), Mouse anti-β-tubulin (1:1000, IgG2a) (Menezes and Luskin, 1994), Mouse anti-Huc/HuD (1:100, IgG2b, Molecular Probes) (Marusich et al., 1994; Wakamatsu and Weston, 1997), Rabbit anti-activated Caspase-3 (1:500) (Condorelli et al., 2001), Mouse anti-Brn3a (1:100, IgG2b, Santa Cruz), Mouse

anti-Pax3 (1:50, IgG2a, DSHB), Mouse anti-Pax7 (1:10, IgG1, DSHB), Rabbit anti-Irx3 (1:1000, Gift from James Briscoe), Rabbit anti-5-HT (1:1000, Calbiochem) (Schambra et al., 1990), Rat anti-BrdU (1:20, ImmunologicalsDirect), Mouse anti-Mash1 (1:2, IgG1, Gift from David Anderson), Mouse anti-Ngn2 (1:5, IgG2b, Gift from David Anderson), Toto-3-iodide (1:1000, Molecular Probes) (Martin et al., 2005; Suzuki et al., 1997).

For detection of monoclonal antibodies, side-chain specific secondary antibodies; Goat anti-mouse Alexa 488 or Goat anti-mouse Alexa 594 were used at 1:500 dilutions (Molecular Probes). For detection of polyclonal antibodies secondary antibodies raised in donkey were conjugated with Alexa 488, Alex 594 or CY5 (Jackson ImmunoResearch Laboratories, Inc.) Toto-3-iodide (1:1000, Molecular Probes) was used to detect cell nuclei.

Slides were incubated in 1% BSA diluted in 1X PBS, 0.1% Triton X-100 (PBT) for five minutes. Antibodies were diluted in PBT and slides incubated overnight at 4°C. Slides were washed in 1X PBS and incubated with conjugated secondary antibodies diluted in PBT for 2 hours at room temperature. Slides were washed in PBS and mounted using Vectashield Fluorescent mounting medium (H-1000, VectorLabs). If cell nuclei were to be detected, Toto-3-iodide was applied for 10 minutes at room temperature prior to mounting slides. Images were collected on a Leica TCS SP2 confocal microscope.

8. **Brd-U assays**

Pregnant females were injected intra-peritonealy with a solution of Brd-U (SIGMA B-5002 at 10mg/ml in physiological serum) at 100 µg for 1 g body weight. Embryos were harvested one hour later. Proliferating cells were revealed by immunohistochemistry on frozen sections, using a rat anti-Brd-U antibody, and an Alexa 594 conjugated anti-rat secondary antibody (molecular probes) as described in (Ferri et al., 2004).

9. **TUNEL analysis**

Apoptotic cell death was assayed with TdT-mediated dUTP nick end labelled (TUNEL). Mouse embryos were fixed overnight in 4% paraformaldehyde, washed in PBS and cryoprotected in 30% sucrose overnight. Embryos were embedded in OCT compound and cryosectioned at 12µm, and sectioned were analysed using TUNEL reagents (Q-BIOgene) according to the manufacturer's protocol, and detected using a CY3 conjugated donkey anti rabbit IgG secondary antibody (Jackson ImmunoResearch Laboratories, Inc.) using the protocol described above.

Results

1. Basic characterisation of the nuclei located within the ventral mesencephalon

There are three main nuclei located within the ventral mesencephalon which are involved in neuronal systems controlling movement, and have been described in detail in the introduction. Birth-dating studies on these three nuclei in the rat (Altman and Bayer, 1981) and in the mouse (performed within our laboratory, data not published) have shown that by E14.5 in the mouse the neurogenesis involved in the generation of these nuclei has ceased. E12.5 is a useful stage of embryonic development to analyse these three nuclei as they can be easily detected using molecular markers.

The dopaminergic neurons (mesDA) are easily identified using antibodies or RNA probes which recognise tyrosine hydroxylase (TH), the rate limiting enzyme in the biosynthesis of the dopamine neurotransmitter (Hynes et al., 1995b; Zhou and Palmiter, 1995). The red nucleus (RN) was identified using an antibody against Brn3a which is essential for its development (Eng et al., 2001; McEvilly et al., 1996; Xiang et al., 1996). The motor neurons of the oculomotor complex (OMC) can be identified using the earliest marker for motor neurons, Islet-1(Ericson et al., 1992; Pfaff et al., 1996).

In order to characterise the spatial relationship between these three neuronal populations of the ventral mesencephalon, I performed immunohistochemistry on both coronal and sagittal sections of the E12.5 mouse brain. These three nuclei reside in distinct non-overlapping domains ventral to the alar-basal boundary (ABB) (figure 1A).

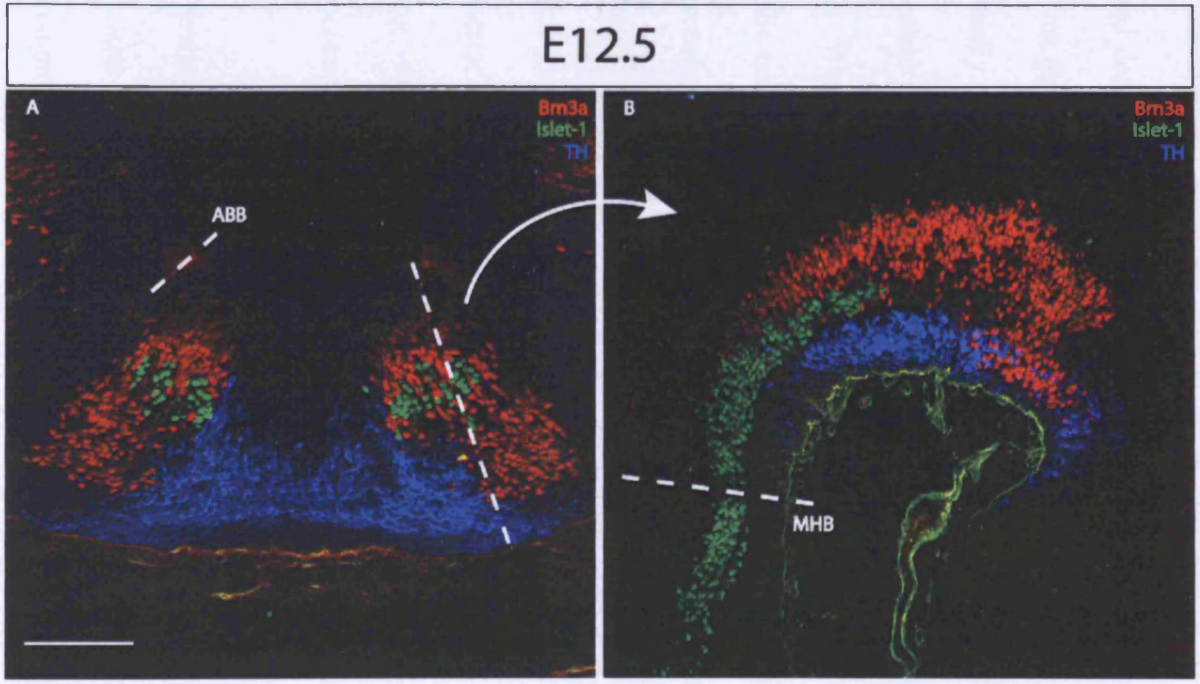

Figure 1: Spatial relationship between the three neuronal populations of the ventral mesencephalon at E12.5. ***A:*** *Coronal section to demonstrate that the mesDA neuronal population is located underneath the ventricular zone of the ventral midline and is labelled using α-TH antibody (blue). Located laterally to the mesDA neurons are the neurons of the RN and OMC labelled with α-Brn3a (red) and α-Islet-1 (green) respectively. Short dotted line represents the boundary between the alar plate dorsally and the basal plate ventrally (ABB). The long dotted line corresponds to the angle of the sagittal section displayed in photograph B.* ***B:*** *Photograph to show the spatial relationship between the three neuronal populations of the ventral mesencephalon along the anterior-posterior axis. The OMC neurons are located at the posterior regions of the mesencephalon, while the RN and mesDA neurons are located more anterior regions. Dotted line represents the boundary between the posterior mesencephalon and the anterior hindbrain (MHB). Scale bar represents 100μm.*

The most ventrally located neuronal population is that of the mesDA. When the mesencephalon is sectioned coronally, the mesDA lies immediately below the ventricular zone of the ventral midline and floor plate (figure 1A) (Hynes et al., 1995a; Hynes et al., 1995b) and stretches across the midline to form a symmetrical shape. When observed along the sagittal plane the mesDA can be clearly seen to occupy a broad domain stretching along the majority of the ventral mesencephalon, terminating before the diencephalon (figure 1B). Coronal sections reveal that the RN is located medially to the mesDA and is the most dorsally located nucleus. It consists of two identical nuclei either side of the midline and resembles the shape of a kidney (figure 1A). When analysed along the sagittal plane, the RN stretches along the dorsal domain of the basal plate and has similar dimensions to the mesDA, and terminates near the mesencephalic-diencephalic boundary (figure 1B). The OMC, like the RN, has two identical neuronal populations located either side of the midline which are located within the grove of the RN (figure 1A). The location of the OMC along anterior-posterior axis differs to that of the RN and mesDA. The OMC stretches from the MHB along the ventral mesencephalon and terminates near the midpoint of the mesencephalon (figure 1B).

Following this basic characterisation I compared the expression pattern of TH, Brn3a and Islet-1 with that of Foxa2 to determine whether Foxa2 could play a role in their development (figure 2A-I). These experiments revealed that approximately 100% of the mesDA neurons are co-expressing Foxa2 (figure 2C), approximately 92% of the RN neurons are co-expressing Foxa2 (figure 2F) and 0% of the OMC neurons are co-expressing Foxa2 (figure 2I).

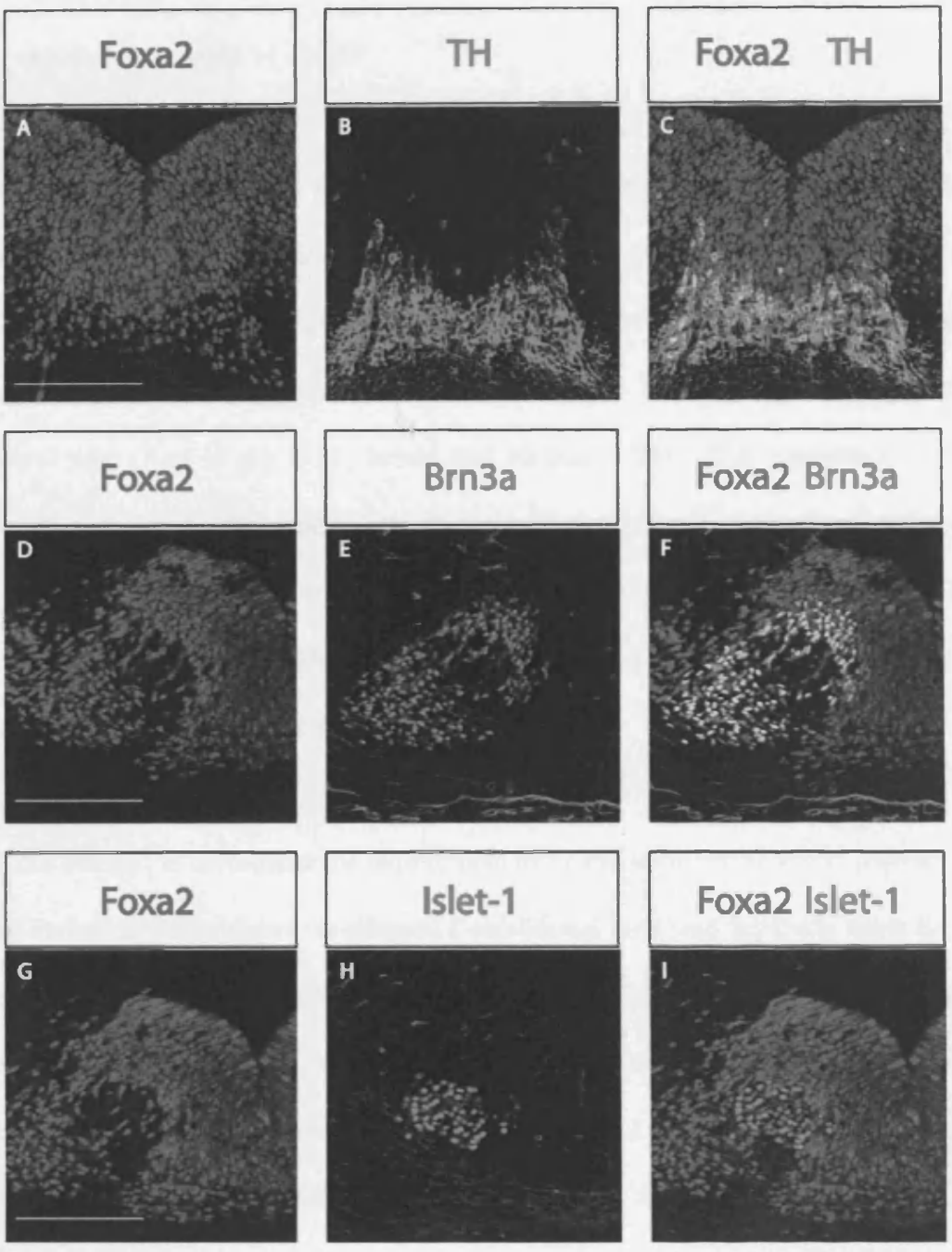

Figure 2: Relationship between Foxa2 and the neuronal populations of the ventral mesencephalon at E12.5. ***A-C:*** *All of the mesDA neurons labelled by α-TH (green) within the mantle layer co-express Foxa2 labelled by α-Foxa2 (red).* ***D-F:*** *Approximately 92% of the post-mitotic RN neurons labelled by α-Brn3a (green) co-express Foxa2 (red).* ***G-I:*** *There is no co-expression between the post-mitotic Islet-1 positive OMC neurons labelled by α-Islet-1 (green) and Foxa2 (red) at E12.5. Scale bar represents 100μm.*

2. Generation of *Foxa2 floxed/floxed; Wnt1-Cre* mice (*Foxa2 CKO*) & the *Cre* mediated deletion of *Foxa2*

Foxa2 is a member of the Forkhead box transcription factor family and is expressed within both mesodermal and endodermal structures during embryonic development. *Foxa2* is expressed within the primitive streak and later the node (mouse equivalent to organiser), followed by expression in the notochord and the ventral midline of the neural tube (Ang et al., 1993; Sasaki and Hogan, 1993). The importance of *Foxa2* during embryonic development was shown with the analysis of the classical knockout mouse, which induced embryonic lethality due to the shortening of the primitive streak, absence of an organised node, absence of the notochord and loss of the floor plate (Ang and Rossant, 1994; Weinstein et al., 1994).

In our attempt to investigate the requirement of *Foxa2* upon the neuronal populations of the ventral mesencephalon we adopted a conditional knockout approach using the *Cre - loxP* recombination system to by-pass the embryonic lethality. In our system, the third exon of the *Foxa2* gene was flanked by *loxP* sites and in the presence of *Cre* recombinase activity is excised producing the effects of a null allele (Sund et al., 2000). *Wnt1* was judged to be the most appropriate promoter for driving the expression of the *Cre* recombinase due to *Wnt1* being expressed within a broad domain of the presumptive mesencephalon at the head fold stages (McMahon and Bradley, 1990; McMahon et al., 1992; Wilkinson et al., 1987). The *Wnt1-Cre* mouse line has been described previously (Brault et al., 2001), thus no reporter analysis has been carried out in this investigation.

The ability of the *Cre* to recombine the *Foxa2* floxed allele was tested by crossing $Foxa2^{floxed}$ hemizygous; *Wnt1-Cre* hemizygous mice ($Foxa2^{floxed/+}$; *Wnt1-Cre* $^{+}$) with $Foxa2^{floxed/floxed}$ homozygous mice. The recombination event was examined using PCR analysis in combination with immunohistochemistry using a polyclonal Foxa2 antibody. The recombination event and the subsequent deletion of *Foxa2* were evident by E8.5 and only occurred in embryos positive for the *Wnt1-Cre* gene (figure 3A, E), which demonstrate that the *Wnt1-Cre* is capable of recombining the *loxP* sites surrounding exon 3 of the *Foxa2* gene.

Foxa2 CKO embryos are recovered in 25% of the total embryos harvested, following the predicted ratio of Mendelian genetics. Throughout this thesis the *Foxa2 CKO* embryos were analysed and compared to $Foxa2^{floxed/floxed}$ (*Foxa2* WT) embryos due to a heterozygous phenotype evident when one allele of *Foxa2* is removed. These embryos displayed a slight reduction in Shh signalling and also slight reductions in the neuronal populations of the ventral mesencephalon, with the lateral population of the mesDA being most affected (data not shown). These issues have been addressed by a colleague in the laboratory and will not be addressed further in this thesis.

The *Foxa2 CKO* embryos do not display any gross external abnormalities and possess a similar size and shape to wild type embryos of similar embryonic development. The *Foxa2 CKO* mice survive embryonic development and once born they are indistinguishable from their littermates. They are fertile once they have reached sexual maturity and there is no evidence that the *Foxa2 CKO* mice die earlier than their wild type littermates.

As stated above, the recombination event is evident by E8.5 in all of the *Foxa2 CKO* embryos analysed. Using a polyclonal antibody raised against Foxa2, the number of Foxa2 expressing cells was quantified in the *Foxa2 CKO* and compared to wild type embryos. There is approximately a 92% (92.37% ± 1.00) reduction in the number of Foxa2 expressing cells within the ventral mesencephalon of the *Foxa2 CKO* embryos upon Cre mediated recombination throughout all the stages analysed

The expression pattern of *Foxa2* in the early embryo has been well documented (Ang et al., 1993; Sasaki and Hogan, 1993). Prior to complete neural tube closure, *Foxa2* expression can be detected within a broad domain of the ventral mesencephalon (figure 3A). This domain encompasses the entire ventral midline, including the floor plate structure, and forms a very sharp boundary of expression at the ABB. This pattern of expression is maintained once the neural tube has completely closed by E9.5 (figure 3B). By E10.5, *Foxa2* positive cells can be detected outside of the ventricular zone indicating that certain cells which exit the ventricular zone maintain the expression of *Foxa2* (figure 3C). At E12.5 there is a substantial increase in the number of *Foxa2* positive cells which are located outside of the ventricular zone (figure 3D). The *Foxa2* positive cells located within the ventricular zone, especially the cells located near the midline display a very tight arrangement, compared to the cells located in the mantle zone which are not densely packed (figure 3B-D).

In the *Foxa2 CKO* embryos the remaining *Foxa2* positive cells are located within the most ventral cells of the midline throughout all the stages that were analysed (figure 3E-H). Additionally, the remaining *Foxa2* expressing cells in the *Foxa2 CKO* are not as closely packed together in comparison to the wild type embryos (figure 3F-H).

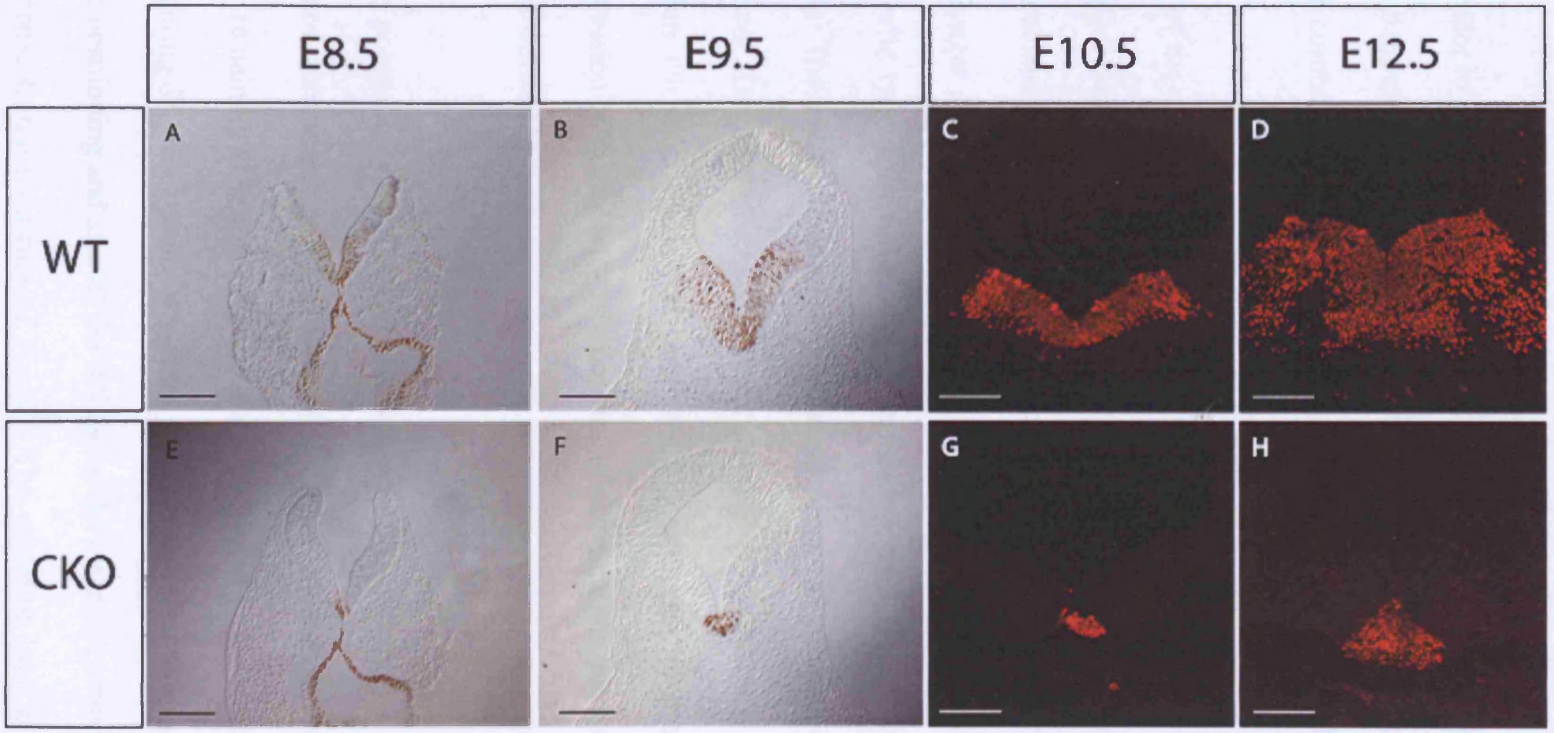

Figure 3: Deletion of Foxa2 gene from the majority of the ventral mesencephalon using Wnt1-Cre mediated recombination of Foxa2 Floxed allele. *The recombination event can be detected by E8.5 in the ventral mesencephalon providing a 92% reduction in the levels of Foxa2 protein at all the stages analysed. The remaining Foxa2 protein is detectable within a small population of cells at the ventral midline which continue to express Foxa2 protein throughout all the stages analysed. Foxa2 protein was detected using DAB-HRP immunohistochemistry (E8.5-E9.5) and fluorescent immunohistochemistry (E10.5-E12.5) using a polyclonal α-Foxa2 antibody. Scale bar corresponds to 100μm.*

3. The neuronal populations of the ventral mesencephalon are severely affected in the *Foxa2 CKO*

In order to investigate the effect of deleting *Foxa2* on the development of the neuronal populations within the ventral mesencephalon, I performed immunohistochemistry on both coronal and sagittal E12.5 brain sections of the *Foxa2 CKO* embryos (figure 4I-T).

All of the neuronal populations are affected by the dramatic reduction of *Foxa2*. The mesDA population is severely reduced in size and shape, and is restricted to a domain immediately underneath the ventral midline while the lateral domains of the mesDA are no longer detectable (figure 4K-L). Cell counting has provided evidence that 82% of the wild type neuronal population is missing, as detected by counting the *TH* positive cells. The size of the mesDA population along the anterior-posterior axis has also been altered. The mesDA spans a shorter distance along this axis terminating some distance before the diencephalon (figure 4S-T). Additionally, there is no longer any co-expression of *Foxa2* with any neurons of the mesDA; the remaining *Foxa2* expressing cells situated immediately above the remaining mesDA neurons (figure 20C).

The population of the RN is also severely affected by the reduction of *Foxa2*. The ventral domain of the RN is completely absent in the *Foxa2 CKO* at E12.5, with only a few remaining cells located immediately adjacent to the ventricular zone (figure 4I, L). Counting of *Brn3a* positive neurons revealed a loss of 65% of the wild type population. The positioning and size of the RN along the anterior-posterior axis has been altered in response to the reduction of *Foxa2*. The posterior limit of the RN has been shifted towards the midpoint of the mesencephalon to the region where the OMC terminates

(figure 4M, P), which is in contrast to the wild type mesencephalon where the RN and OMC form interlocking domains (figure 4H, P). There is an increase in the amount of *Brn3a* positive staining at the ABB in the *Foxa2 CKO* (figure 4I, M) as compared to the wild type brain (figure 4A, E). However unlike all other Brn3a immunoreactivity, this staining is not localised within the nucleus of the cells bodies, as confirmed by having no co-expression with the nuclear marker Toto-3-iodide (data not shown), thus this staining cannot be explained. Similarly to the mesDA, there is no longer any RN neuron which co-expresses *Foxa2* (figure 6D-E).

There is a substantial loss of the neuronal population of the OMC in the *Foxa2 CKO* embryos. Cell counting of *Islet-1* positive neurons revealed a 72% reduction in the neuronal population at E12.5. This reduction is not striking when the *Foxa2 CKO* embryos are analysed along the coronal plane (figure 4B, J). However, it is very clear that there is a severe alteration in the size and location of the OMC along the anterior-posterior axis which can be visualised using the sagittal sections (figure 4N, P). The posterior boundary of the OMC has shifted to a more anterior location, leaving a large gap between the OMC and the MHB, while the anterior limit of the OMC has also receded slightly (figure 4N, P).

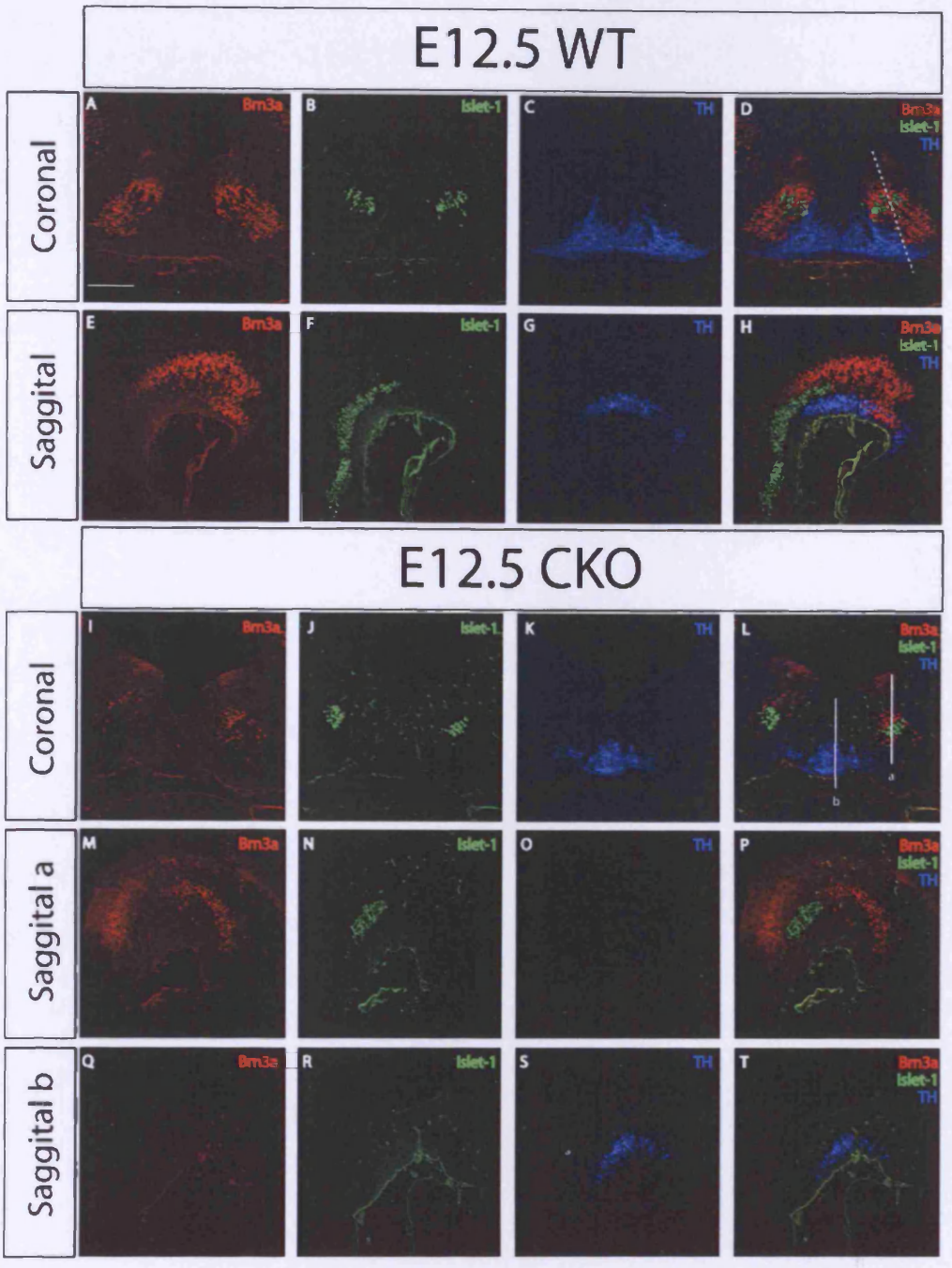

Figure 4: Comparison between the spatial relationships of the neuronal populations situated in the ventral mesencephalon in the wild type and Foxa2 CKO embryos at E12.5. A-H: *Photographs of the wild type embryos at E12.5 in both coronal and sagittal sections which were previously described in figure 2.* ***I-L:*** *Coronal section of an E12.5 Foxa2 CKO embryo reveals a dramatic reduction in the neuronal populations of the ventral mesencephalon. There is an 82% reduction of the mesDA neurons (blue), a 65% reduction in the RN neurons (red) and a 72% reduction of the OMC neurons (green).* ***M-P:*** *Sagittal section of the Foxa2 CKO at E12.5 corresponding to line "a" in photo L, demonstrating that the neuronal populations of the OMC and RN have been reduced along the anterior-posterior axis.*

Figure 4 Continued: ***Q-T:*** *Sagittal section of the Foxa2 CKO embryo at the ventral midline (corresponding to line "b" in photograph L). The mesDA neuronal population is also reduced in similar fashion to the OMC and RN along the anterior-posterior axis. Scale bar corresponds to 100μm. All the photographs were taken using a 20X lens. For cell counting photographs were taken using a X40 lens (data not shown).*

4. There is an 82% reduction of the mesDA neurons at E12.5 despite the mesDA progenitors being correctly specified in the *Foxa2 CKO*

Birth-dating studies in the mouse (Bayer et al., 1995) (Laboratory data not published) have revealed that the first mesDA neurons are born between E10.0 and E10.5 and cease to be born after E12.5. Accordingly, to determine whether the reduction of *Foxa2* affected the progenitor cells of the mesDA, I analysed the expression of genes expressed by mesDA progenitors using *in-situ* hybridization at E10.5 in the *Foxa2 CKO.*

Raldh1, which is a marker for the proliferating mesDA progenitor cells (Wallen et al., 1999), is expressed in a small domain spanning the ventral midline (figure 5A). In the *Foxa2 CKO* there is no clear evidence of a down-regulation of *Raldh1* and no clear alteration in the size of the expression domain (figure 5B). The LIM homeodomain transcription factor *Lmx1b*, which plays a crucial role in the maintenance of the mesDA neurons (Smidt et al., 2000), is also expressed in the same mesDA progenitor cells (figure 5C). In the *Foxa2 CKO* there is no clear reduction in the expression domain of *Lmx1b* (figure 5D).

Lmx1a expression overlaps with *Lmx1b*, but is expressed at higher levels as detected by the intensity of the RNA signal (figure 5E). There is no alteration in signal intensity or size of expression domain of *Lmx1a* in the *Foxa2 CKO* (figure 5F). *Msx1* gene expression can be detected overlapping with both *Lmx1* genes (figure 5G). The expression domain of *Msx1* is unaltered in the *Foxa2 CKO* (figure 5H). *En1* which is expressed in a broad domain of the ventral mesencephalon from E9.5, is also considered to play a role in specifying the mesDA progenitors (Simon et al., 2001). There is an

over-expression of *En1* within the ventral mesencephalon of the *Foxa2 CKO* at E10.5 (figure 5J), as determined from the intensity of the RNA signal. In combination, these data suggest that the numbers of mesDA progenitors are not significantly reduced and are specified correctly in the *Foxa2 CKO*. Additionally it can be proposed that the phenotype described at E12.5 must be caused by defects involved in later aspects of the dopaminergic developmental cascade.

To address whether the reduction of *Foxa2* could cause defects in later aspects of the mesDA differentiation process, I analysed the expression patterns of genes involved in the dopaminergic lineage and which have been demonstrated to be essential for correct mesDA development. Consistent with the data generated using the *TH* antibody; there is a substantial decrease in the mesDA population at E12.5 in the *Foxa2 CKO* (figure 5L). The expression of *AADC*, which is the enzyme required to convert $_{L}$-DOPA into dopamine and is expressed within the mesDA neurons from E11.5 (Smidt et al., 2004a), has been reduced in similar fashion to the *TH* (figure 5N). Additionally there is a clear loss of *AADC* expression within the ventricular zone near the ABB in the *Foxa2 CKO* (figure 5N*).

At E12.5 there are two distinct domains of *Lmx1b* expression. There is a domain of low gene expression within the ventricular zone near the ventral midline, and a domain of high gene expression corresponding to the mesDA neurons (figure 5O). In the *Foxa2 CKO* the domain of low *Lmx1b* gene expression is unchanged, whilst the *Lmx1b* in the differentiating mesDA neurons has been dramatically reduced corresponding to the remaining *TH* positive neurons (figure 5P). The paired-like homeodomain transcription factor *Ptx3* is induced by *Lmx1b* and is expressed within the mesDA (Smidt et al., 2000;

Smidt et al., 1997) and is essential for the generation of nascent mesDA neurons (Maxwell et al., 2005). At E12.5, the expression pattern of *Ptx3* in the *Foxa2 CKO* has been reduced and resembles the size and shape of the remaining mesDA population characterised by *TH* expression (figure 5R). The orphan nuclear receptor *Nurr1*, which is expressed in the mesDA (Saucedo-Cardenas et al., 1998; Zetterstrom et al., 1997), is also reduced in a similar fashion to the other mesDA markers at E12.5 (figure 5T).

At E12.5 there is differential expression of *En1* similar to that of *Lmx1b*. It is expressed in low levels in the ventricular zone of the ventral mesencephalon from the ABB to the ventral midline and in the mantle layer cells lateral to the ventral midline. There is a region of high *En1* expression which corresponds to the mesDA (figure 5U). In the *Foxa2 CKO* there is no alteration in the size of the *En1* expression within the ventricular zone, and in the domains situated laterally to the ventral midline. The remaining *En1* positive cells in the mantle layer correspond to the remaining *TH* positive cells (figure 5V).

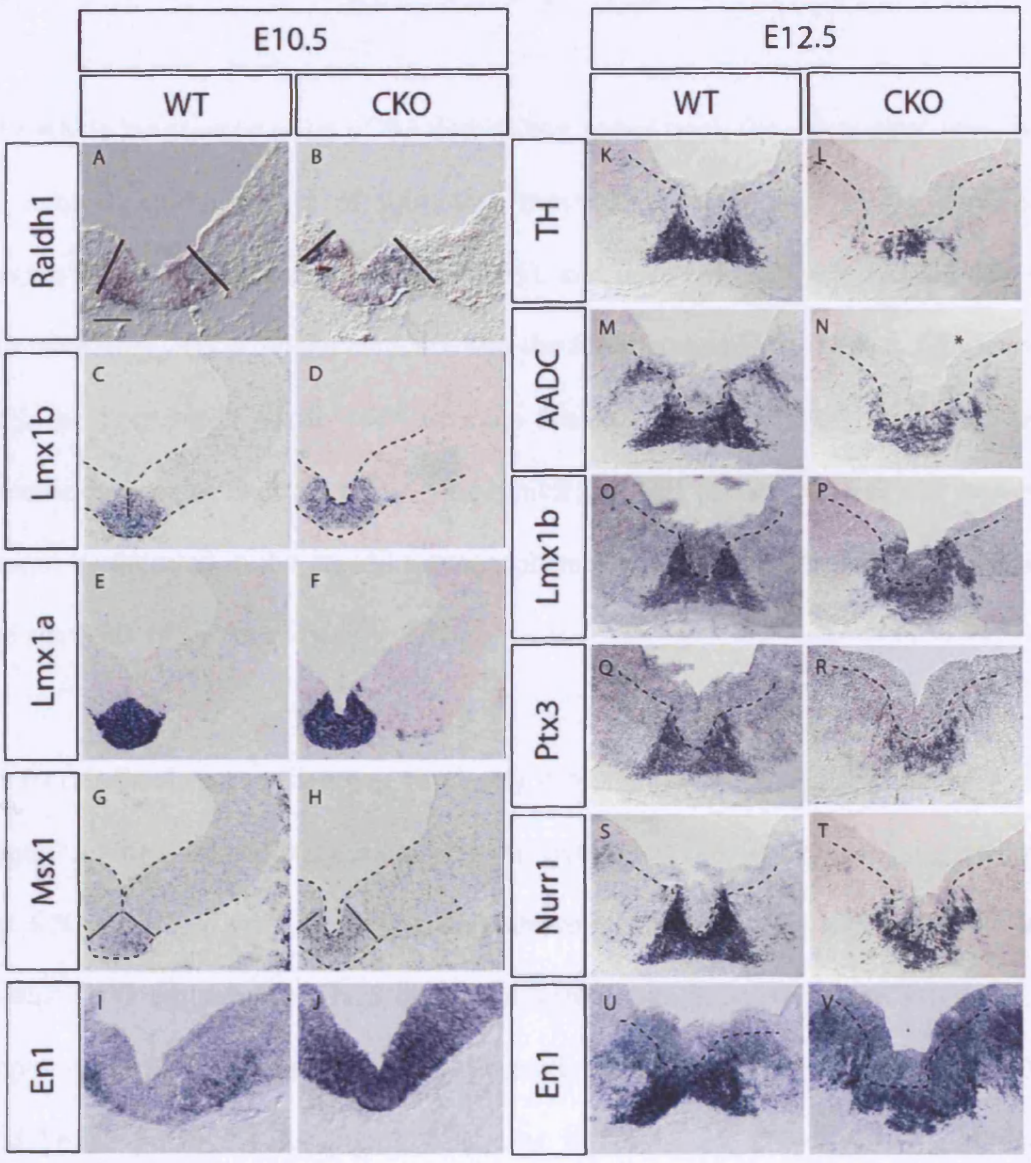

Figure 5: Analysis of genes involved in the development of the mesDA neurons. ***A-J:*** *Coronal sections of both wild type and Foxa2 CKO embryos at E10.5. The gene expression patterns reveal that the mesDA progenitor cells at E10.5 are not dramatically affected by the reduction in the levels of Foxa2. These results suggest that Foxa2 does not play a role in the early specification of the mesDA neurons. The dotted lines in C-D, G-H are to facilitate visualisation of mesencephalon. Solid lines in A-B, G-H demarcate lateral extent of gene expression.* ***K-V:*** *Coronal sections of both wild type and Foxa2 CKO embryos at E12.5. The gene expression patterns of the genes involved in the later development of the mesDA neurons are all affected in similar fashion. The remaining gene expression can be detected near the ventral midline, corresponding to the remaining TH protein. Asterisk in N represents the loss of AADC gene expression from the ventricular zone. The dotted lines in photographs K-V represent the position of the ventricular zone in the ventral mesencephalon at E12.5. Scale bars represent 100μm.*

5. There is a 65% reduction of the RN population at E12.5 in the *Foxa2 CKO*

The RN is the starting point of the descending spinal tract, the rubrospinal tract, which is involved in the control of automated movements (Kennedy, 1990). Birth-dating studies in the rat (Altman and Bayer, 1981), and in the mouse (unpublished data from our laboratory) has provided evidence that the first neurons of the RN are born at ~E11, with the first *Brn3a* positive RN neurons detected at E11.5. Currently there are no specific molecular markers for the progenitor cells of the RN and *Brn3a* expression cannot be detected in the ventral mesencephalon at this time, although it is detected in the alar plate (data not shown).

At E11.5, *Brn3a* expression can be clearly detected in two domains either side of the ventral midline, immediately underlying the ventricular zone (figure 6A) suggesting that the RN progenitor cells lie immediately above the *Brn3a* positive population. In the *Foxa2 CKO* embryos at E11.5 there is a substantial decrease in the *Brn3a* positive population within the mantle layer and there is no longer any co-localisation of Brn3a and Foxa2 positive cells (figure 6D). At E12.5 in the *Foxa2 CKO* embryos, as described above, there is a 65% reduction in the population of the RN. The most ventral domain of the RN is absent and there is no co-expression between Foxa2 and Brn3a (figure 6E).

To be confident that *Brn3a* was marking the location of the RN, I analysed the gene expression pattern of the transcription factor *Emx2*. Loss-of-function analyses have revealed an essential role for *Emx2* in the development of the RN (Agarwala and Ragsdale, 2002; Mallamaci et al., 2000). At E12.5 there are two distinct domains of

Emx2 expression. The dorsal domain which lies above the ABB and the domain which is located at the dorsal limit of the basal plate (figure 6C). The ventral domain of *Emx2* expression does not label exactly the same population of cells as *Brn3a* gene expression, instead demarcating a region much closer to the ABB and further away from the ventral midline than the *Brn3a* positive neuronal population (figure 6C). In the *Foxa2 CKO* embryos at E12.5, *Emx2* expression is unaffected dorsal to the ABB, but there is a large reduction in the number of neurons which still express *Emx2* in the basal plate. The remaining *Emx2* positive cells are located ventral to the ventricular zone and are located in the same domain as the remaining *Brn3a* RN cells (figure 6F). To confirm that these two populations are indeed the same population, analysis was conducted on adjacent sections using both *Brn3a* and *Emx2* RNA (data not shown). The results at E12.5 indicate that there is a severe reduction in the neuronal population of the RN, and that there is no co-expression between the remaining Brn3a/*Emx2* positive RN neurons and Foxa2 (figure 6E). Interestingly, although it is thought that *Emx2* gene expression should outline the domain of the RN; in this study it would seem that *Emx2* gene expression does not encompass the entire RN but merely a subset of its neurons (figure 6F).

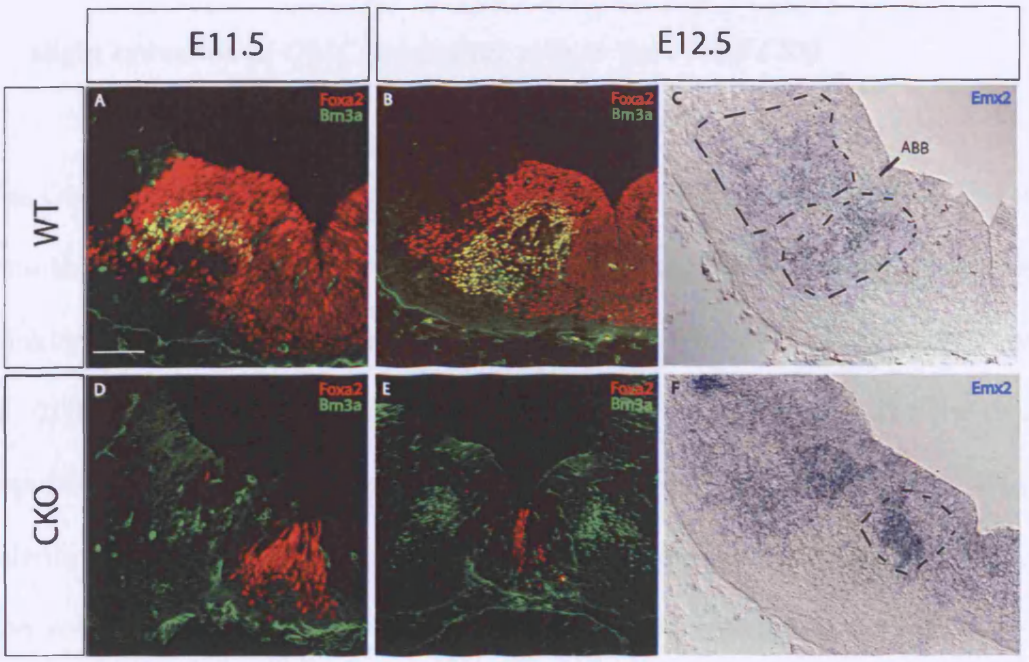

Figure 6: Consequences of reduced levels of Foxa2 on the RN neuronal population. ***A, D:*** *Coronal section of mesencephalon at E11.5 reveals an absence of differentiated neurons expressing Brn3a (green).* ***B, E:*** *Coronal section of mesencephalon at E12.5 reveals some differentiated Brn3a positive RN neurons (green) underlying the ventricular zone. There is no longer any co-expression between Foxa2 and the differentiated RN neurons.* ***C, F:*** *Emx2 is a gene which has been implicated in the development of the RN. Emx2 gene expression can be detected in two distinct domains at E12.5; one domain dorsal to the ABB, and one domain located overlapping with the Brn3a expression in the RN. The two domains are circled in photograph C. The remaining Emx2 gene expression in the Foxa2 CKO resembles the remaining RN neurons as labelled by Brn3a protein expression. Scale bar corresponds to 100μm..*

6. There is a 72% reduction in the OMC neuronal population coupled with a slight reduction in OMC progenitor cells in the *Foxa2 CKO*

The OMC, which is also known as the third cranial nerve, innervates the extra ocular muscles controlling eye movements, the striated muscles of the eyelid controlling blinking and is also involved in the constriction of the pupil (Evinger, 1988; Kandel et al., 2000b). In the *Foxa2 CKO* embryos at E12.5 it was shown that the neuronal population of the OMC was reduced by 72% and that the location of the OMC along the anterior-posterior axis was altered (figure 4L, P). The initial results described above also reveal that at E12.5 the OMC neurons do not express *Foxa2*. To determine whether the OMC neurons transiently express *Foxa2* throughout their early development, I analysed the expression of Foxa2 and Islet-1 from stages E9.5-E12.5, which were shown to be the stages when the OMC neurons are born.

At E9.5, when the first OMC neurons are born, Islet-1 expression can be detected immediately underlying the ventricular zone tightly confined next to Foxa2 positive cells (figure 7A). In some E9.5 wild type embryos there are a few OMC cells which co-express Foxa2 and Islet-1 (figure 7A arrows), but this phenomenon is not evident in the majority of embryos analysed at this stage. This can be explained by the asynchronous development of embryos within the same litter. At E10.5 there is no longer any OMC neuron which expresses Foxa2. The OMC neuronal population is now located immediately adjacent and underlying the Foxa2 positive cells of the ventricular zone. This spatial relationship is maintained throughout the remaining stages analysed (figure 7B-D).

In the *Foxa2 CKO* at E9.5 there is a complete absence of Islet-1 positive OMC cells along the entire anterior-posterior axis. This result was confirmed by analysing coronal sections of the entire mesencephalon (figure 7E). At E10.5 there are some Islet-1 positive OMC neurons present, but their numbers are severely decreased compared to the wild type population (figure 7F). At E11.5 there are many Islet-1 positive OMC neurons present, but the population's numbers are still lower than in the wild type embryos (figure 7G). At E11.5 and E12.5, the quantities of Islet-1 positive OMC neurons present in the *Foxa2 CKO* embryos does not appear to correspond to the 72% reduction of OMC neurons at E12.5 described previously (figure 7G-H). However, as stated previously, the dimensions of the OMC nucleus along the anterior-posterior axis have been altered and the length of the OMC has been shortened, and therefore the 72% reduction described at E12.5 is valid. Another observation is that the remaining OMC neurons are situated in their correct locations in the *Foxa2 CKO* embryos.

To investigate whether *Foxa2* has an early role in the development of the OMC, I analysed E9.5 and E10.5 stage *Foxa2 CKO* embryos to identify whether the reduction of *Foxa2* affected the OMC progenitor cells. The transcription factor *Phox2a* is essential for the development of the OMC and is the only known marker for the OMC progenitor cells (Brunet and Pattyn, 2002; Pattyn et al., 2000; Pattyn et al., 1997). To determine whether the initial absence of OMC neurons at E9.5 and the subsequent 72% reduction of the OMC at E12.5 is due to the decrease in Foxa2 I performed *in-situ* hybridization on adjacent brain sections at E9.5 and E10.5 using *Phox2a* and *Islet-1*. At E9.5, the expression of *Phox2a* is restricted to a narrow band spanning the ventricular zone immediately above the OMC neurons and is also co-expressed with the *Islet-1* positive OMC neurons in the mantle layer (figure 7J). The size of the Phox2a domain

along the medial-lateral axis (~130μm) is identical to that of the *Islet-1* positive OMC cells. In the *Foxa2 CKO* embryos at E9.5 there is no *Islet-1* expression detectable (figure 7K) even though the OMC progenitor cells are still present (figure 7L). However the number of OMC progenitor cells is slightly reduced. This reduction is evident from the weaker staining intensity of the *Phox2a* RNA probe, and also due to the width of the *Phox2a* domain being reduced from 130μm to 100μm (figures 7L).

At E10.5 there are a few *Islet-1* positive OMC neurons present in the mantle layer (figure 7O), which confirms the data acquired using the Islet-1 antibody. The progenitor cells of the OMC maintain the spatial organisation described for the E9.5 embryos (figure 7N). In the *Foxa2 CKO* embryos, the *Phox2a* positive OMC progenitor cells are still present within the ventricular zone and in the mantle layer, but their number has been reduced and the total size of the *Phox2a* domain has been reduced along the medial-lateral axis (figure 7P).

These results indicate that *Foxa2* is not essential for the maintenance of the OMC neurons, as these neurons never express *Foxa2* in the mantle layer. However, there is some evidence at E9.5 to suggest that *Foxa2* could be involved in the regulation of the *Phox2a* positive OMC progenitor cells. *Phox2a* expressing cells within the ventricular zone are located within the *Foxa2* expression domain, and in the *Foxa2 CKO* embryos there is a slight reduction in the population of *Phox2a* expressing cells.

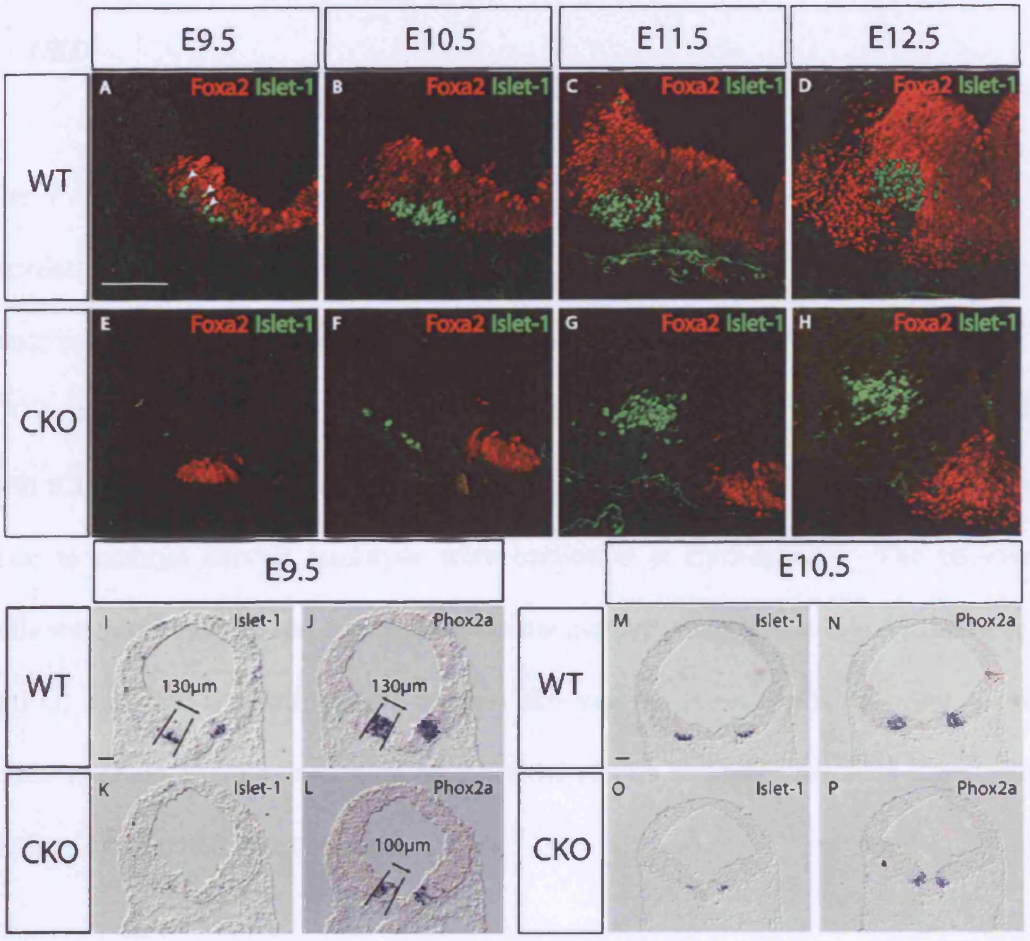

Figure 7: Analysis of the development of the OMC neurons in the Foxa2 CKO. A-H: *The newly differentiated OMC neurons labelled with α-Islet-1 antibody (green) come from a domain of the ventricular zone which expresses Foxa2 (red). In younger E9.5 embryos there is some co-expression between these newly differentiated OMC neurons and Foxa2 (arrows in A). In older E9.5 embryos there is no longer any co-expression between Islet-1 and Foxa2 proteins, suggesting a period of transition between OMC progenitor cells expression Foxa2 and differentiated OMC neurons which no longer express Foxa2. This relationship continues throughout the remainder of OMC development.* ***I-P:*** *The OMC progenitor cells are identified by Phox2a gene expression. In the Foxa2 CKO there is a slight reduction in the size of the OMC progenitor domain. Solid lines represent the domain of the OMC progenitor cells and the domain where the differentiated OMC reside in the ventral mesencephalon. Scale bars represent 100µm.*

7. No statistically significant alteration in the rate of proliferation in the *Foxa2 CKO*

The *Foxa2 CKO* embryos at E12.5 show a dramatic reduction in the neuronal populations of the ventral mesencephalon. To investigate whether the phenotype described above is due to a reduction in the rate of cell proliferation within the *Foxa2 CKO* embryos, I performed short pulse Brd-U assays. Pregnant females were injected with a 100mg/1g body weight solution of Brd-U solution intra-peritonealy 30 minutes prior to embryo harvest (embryos were harvested at E9.5-E12.5). The proliferating cells were revealed by standard immunohistochemistry using an antibody raised against Brd-U, and Brd-U positive cells within the ventral mesencephalon were quantified (table 1, graph 1). To determine whether the results were of statistical significance, a student's one-tailed T-test was carried out.

	# of Cases	% Brd-U Positive Cells	Standard Deviation	95% Confidence	Significance (T-test)
E9.5 WT	n=6	45.367	6.521	5.218	**0.212**
E9.5 CKO	n=5	39.723	7.413	6.497	
E10.5 WT	n=4	37.324	3.640	3.566	**0.507**
E10.5 CKO	n=4	35.771	2.479	2.429	
E11.5 WT	n=3	19.784	0.848	1.175	**0.159**
E11.5 CKO	n=3	21.136	0.200	0.278	
E12.5 WT	n=3	22.777	2.656	3.681	**0.965**
E12.5 CKO	n=3	21.680	0.721	0.816	

Table 1: *Table to show the quantity of proliferating cells within the ventral mesencephalon in wild type and Foxa2 CKO embryos, and the results of the statistical analyses performed.*

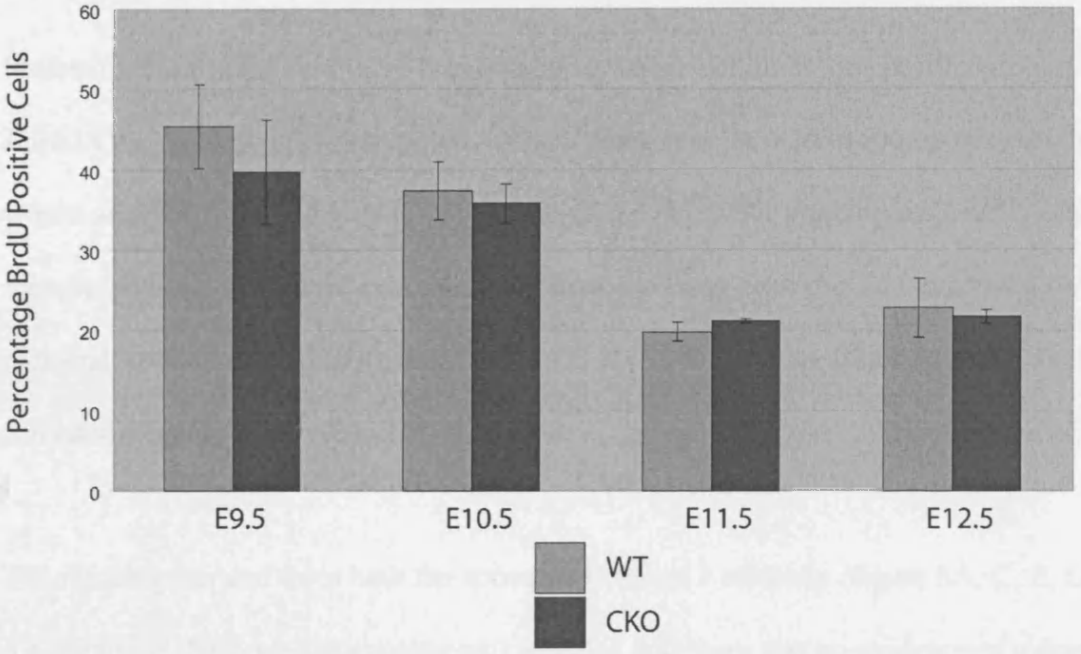

Graph 1: *Graphical representation of the results presented in Table 1. Error bars were calculated using the value of the 95% confidence.*

There was a slight decrease in the percentage of Brd-U positive cells in the *Foxa2 CKO* embryos at E9.5, E10.5 and E12.5, while at E11.5, where there was a slight increase in the rate of proliferation. However, the Student's one-tailed T-Test revealed that these results were not of statistical significance. Therefore there is no significant defect in the rate of proliferation in the *Foxa2 CKO* embryos, and the phenotype described above cannot be attributed to defects in cell proliferation.

8. No evidence of apoptosis within the mesencephalon of the *Foxa2 CKO*

Following the finding that there was no significant defect in the cell proliferation in the *Foxa2 CKO* embryos, I investigated whether there was an increase in apoptosis which would account for the dramatic reductions of the neuronal populations of the ventral mesencephalon. Apoptotic cell death was assayed using both the TdT-mediated dUTP nick end labelled (TUNEL) system (Vernay et al., 2005), and an antibody raised against activated Caspase 3 (Condorelli et al., 2001).

The results generated from both the activated Caspase 3 antibody (figure 8A, C, E, G, I, K) and the TUNEL kit (data not shown) revealed that there was no evidence of pyknotic cells throughout the mesencephalon indicating that there is no apoptosis present in the *Foxa2 CKO* embryos from E9.5-E12.5. To provide a positive control for both the apoptosis detection methods, photographs were taken of pyknotic cells present within the mandibular region of both the wild type and *Foxa2 CKO* embryos (figure 8B, D, F, H, J, L) which were on the same slide. The trigeminal ganglion of both the wild type and *Foxa2 CKO* embryos was also used as a positive control for apoptosis (data not shown).

Therefore, the phenotype described in the *Foxa2 CKO* embryos cannot be attributed to an increase in apoptosis in the ventral mesencephalon.

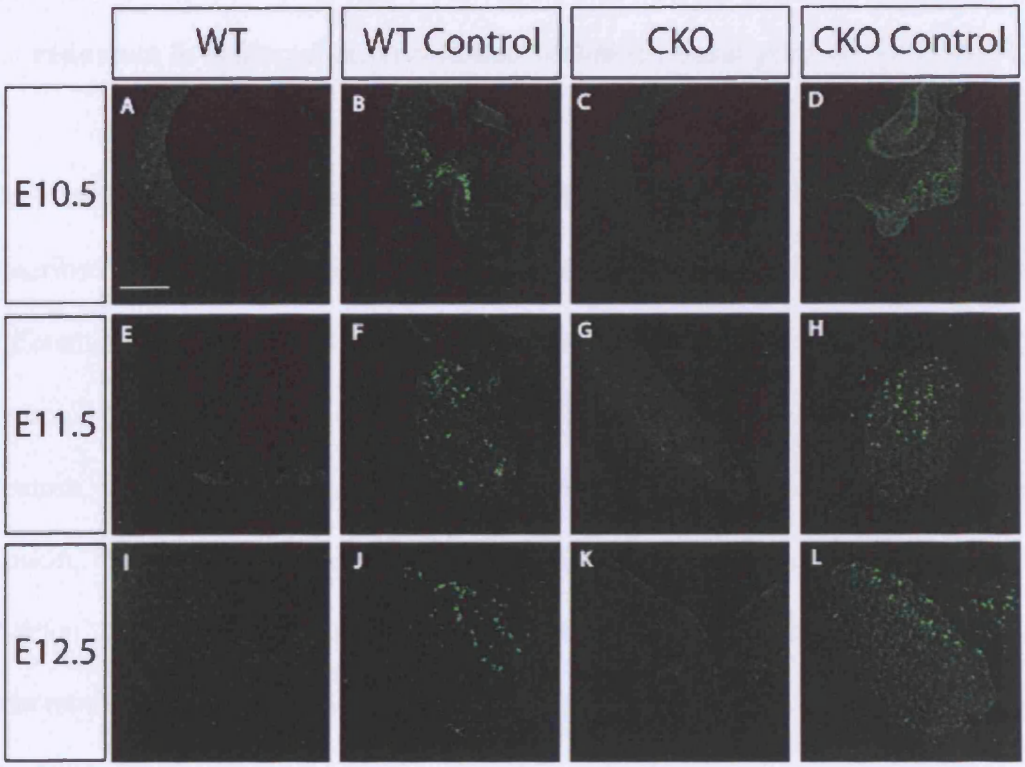

Figure 8: Identification of apoptosis in the Foxa2 CKO. A-L: *Using an antibody raised against activated Caspase3 (α-Caspase3), a gene which is involved in the apoptotic pathway, it is evident that there is no apoptosis present within the developing mesencephalon of both the wild type or Foxa2 CKO embryos, indicating that the phenotype described previously cannot be attributed to an increase in cell death. As a positive control for the efficacy of the α-Caspase3 antibody, either the trigeminal ganglion or the mandibular region from the same section was photographed. Apoptosis is known to occur during development in these two regions, and can be easily seen by pyknotic round cells (green). Scale bar represents 100mm.*

9. Slight temporal alteration in the pattern of neurogenesis coupled with a reduction in neuronal differentiation within the basal plate of the *Foxa2 CKO*

The dramatic reductions in the neuronal populations of the ventral mesencephalon described at E12.5 raised the possibility that there could be a defect in neurogenesis or differentiation. I addressed whether there was a defect in the differentiation process of neuronal progenitor cells becoming post-mitotic neurons. To visualise the differentiated neurons at E10.5 and E12.5, I used the neuronal markers *β-Tubulin* (Menezes and Luskin, 1994; Vernay et al., 2005), *HuC/HuD* (Marusich et al., 1994; Wakamatsu and Weston, 1997) and *Scg10* (Wuenschell et al., 1990). *Sox2*, which identifies uncommitted dividing stem cells or progenitor cells within the developing CNS (Li et al., 1998; Zappone et al., 2000) and has been shown to maintain neuronal progenitor identity (Graham et al., 2003) was used to label the progenitor cells within the ependymal zone (ventricular zone) of the mesencephalon.

At E10.5 β-Tubulin is expressed by the neuronal cells which have exited the ventricular zone and are located within the mantle layer (figure 9A). In the *Foxa2 CKO* at E10.5 there is a slight reduction in the number of differentiated neurons, especially in the region adjacent to the ventral midline and floor plate (figure 9F). HuC/HuD, which labels the neurons immediately after the cessation of proliferation, can be detected in neurons immediately outside of the ventricular zone which are not yet expressing β-Tubulin (figure 9B, D). The young OMC nucleus can be easily detected using HuC/HuD (figure 9U). At E10.5 in the *Foxa2 CKO*, there is a great reduction in the number of differentiated neurons, especially in ventral region of the mesencephalon (figure 9G). The remaining OMC neurons can be easily detected by the HuC/HuD

antibody (figure 9V). To confirm the results generated using β-Tubulin and HuC/HuD, I used the pan neuronal marker *Scg10* to label the differentiated neurons (figure 9E). In the *Foxa2 CKO* embryos the reduction in the number of *Scg10* positive cells within the mesencephalon is not as evident as the results generated using the β-Tubulin and HuC/HuD antibodies, but there is a slight reduction in number of *Scg10* expressing cells in the region where the OMC is located (figure 9J).

Sox2 labels all the cells which are undergoing proliferation within the ventricular zone of the mesencephalon in both the alar and basal plates (figure 9C). There seems to be a slight increase in the size of the Sox2 positive domain at E10.5 in the *Foxa2 CKO*. To confirm this observation I measured the thickness of the ventricular zone at two locations (marked "a & b" in the wild type and "x & y" in the *Foxa2 CKO*) (figure 9C, H). In the conditional knockout embryo the thickness of the Sox2 positive domain at position "x" has increased by 9.09μm, while the thickness at the ventral midline has remained constant.

In the wild type embryos at E12.5, β-Tubulin, HuC/HuD and *Scg10* can be detected throughout the entire mantle layer, and can be observed in tight clusters which correspond to the location of the ventral mesencephalic nuclei (figure 9K-L, N, W). In the *Foxa2 CKO* the quantity of differentiated neurons is severely reduced in the basal plate, especially at the ventral midline (figure 9P-Q, T, X). The remaining β-Tubulin, HuC/HuD and *Scg10* positive neurons correspond to the remaining neurons of the mesDA, RN and the OMC (figure 9X).

The ventricular zone of the *Foxa2 CKO* embryos has also thickened in comparison to the wild type embryos (figure 9M, R). As described at E10.5, position "x" has increased in thickness by approximately 18.18μm, indicating that this region of the ventricular zone has doubled in thickness during two days of development. Interestingly, the thickness of the ventricular zone at the ventral midline in the *Foxa2 CKO* has increased by approximately 4.55μm (figure 9R "b").

When analysing the E10.5 and E12.5 *Foxa2 CKO* embryos, it became apparent that the reduction in neuronal differentiation is only evident in the basal plate, as neurons located in the mantle layer of the alar plate all co-express β-Tubulin, HuC/HuD and *Scg10* and maintain similar levels to the wild type embryos. At E12.5 there is also an apparent reduction in the size of the mantle layer directly underlying the floor plate. The distance from the ventral tip of the floor plate to the neuroepithelium surrounding the ventral mesencephalon is reduced by approximately 18μm in the *Foxa2 CKO*. These results suggest a possible defect of neurogenesis within this region of the ventral mesencephalon which could cause the decrease in the neuronal populations described previously.

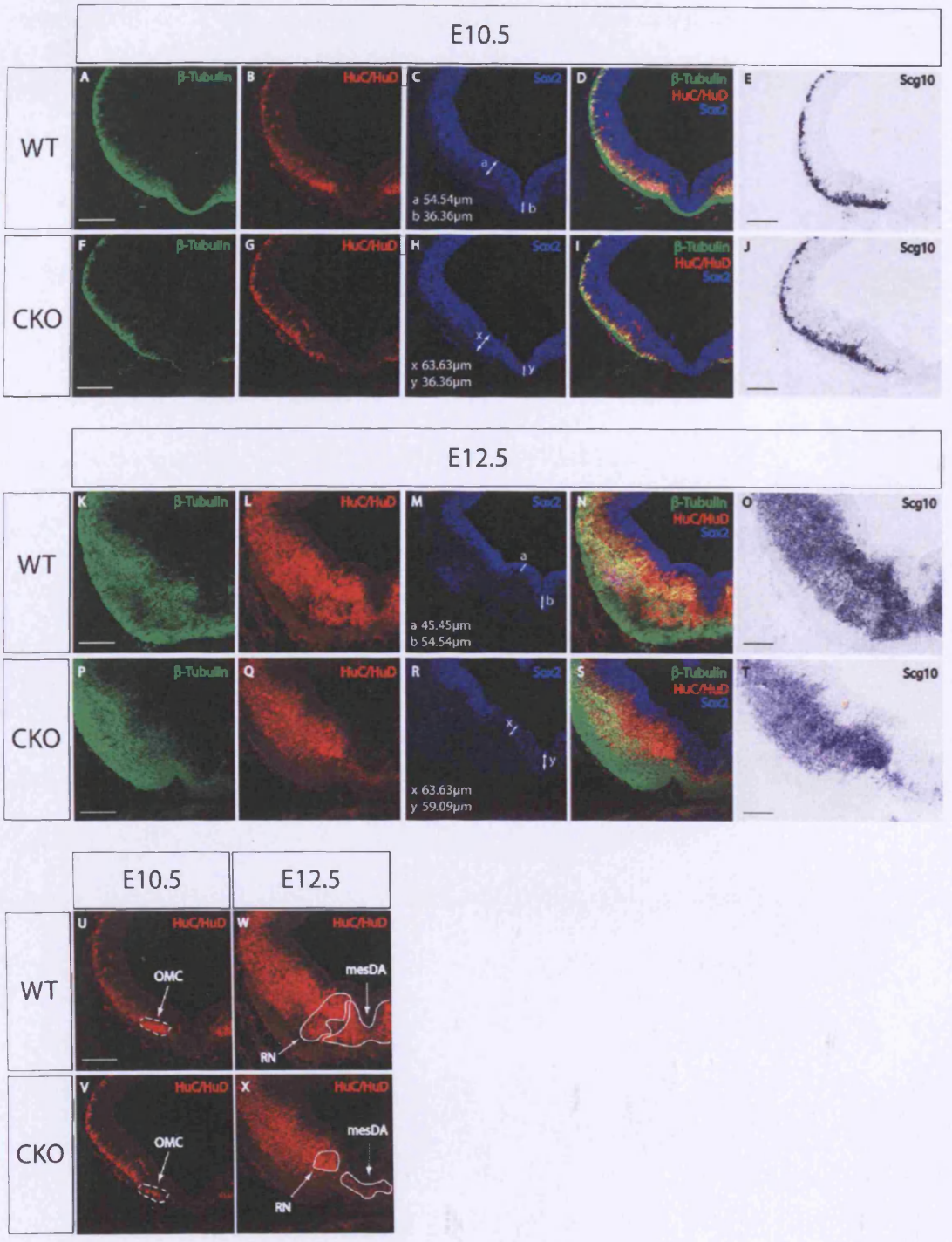

Figure 9: Analysis of neuronal differentiation in Foxa2 CKO. A-T: *Coronal sections of E10.5 and E12.5 wild type and Foxa2 CKO embryos stained with markers neuronal differentiation; β-tubulin (green), HuC/HuD (red). Sox2 identifies the proliferation progenitor cells within the ventricular zone (blue). Scg10 gene expression is produced by newly differentiated neurons. The thickness of the ventricular zone was measured in two locations; a & b in the wild type embryos and at x & y in the Foxa2 CKO.*

Figure 9 continued: *At E10.5 in the Foxa2 CKO the level of differentiation is reduced specifically near the ventral midline where the OMC neurons reside. At E12.5 the level of neuronal differentiation is clearly reduced within the basal plate of the Foxa2 CKO mesencephalon, combined with an increase in the thickness of the ventricular zone. Neuronal differentiation within the alar plate is not affected by the reduction in the levels of Foxa2 protein. The differentiated neuronal populations of the OMC (**U-V**), RN and mesDA (**W-X**) can be easily detected in both the wild type and Foxa2 CKO. These results indicate that there is a severe reduction in neuronal differentiation within the basal plate of the Foxa2 CKO. Scale bar represents 100μm.*

To address this possible defect in neurogenesis in the *Foxa2 CKO*, the expression patterns of markers for neurogenesis were assayed. A group of b-HLH transcription factors, the proneural genes, have been implicated in the regulation of neurogenesis within the CNS and PNS (Bertrand et al., 2002). Two proneural genes, mouse *achaete-scute* homologue (*Mash1*) and the *atonal*-related family member *neurogenin 2* (*Ngn2*) are known to be expressed within the ventral mesencephalon (Kele et al., 2006; Vernay et al., 2005), and were analysed in the *Foxa2 CKO* embryos at E9.5, E10.5 and E12.5.

At E9.5 *Mash1* gene expression cannot be detected within the mesencephalon (data not shown). *Ngn2* gene expression can be detected in a broad domain within the ventricular zone flanking the ventral midline (figure 10A). Superimposition of the *Ngn2* expression domain with that of *Foxa2* reveals a small overlap of expression domains near the ABB (data not shown). There is no considerable alteration in the quantity of *Ngn2* transcript detected in the *Foxa2 CKO* embryos at E9.5 (figure 10B).

In wild type embryos at E10.5, both *Ngn2* and *Mash1* are expressed by neuronal progenitor cells located within the ventricular zone (figure 10C-D). *Ngn2* is expressed in a domain spanning the ventral midline, overlapping with *Foxa2*. The dorsal limit of *Ngn2* forms a sharp boundary with the ventral limit of *Mash1* expression (figure 10D). There are two distinct domains of *Mash1* expression at E10.5; the weakly expressing *Mash1* domain spanning the majority of the dorsal mesencephalon, and two domains of high expression levels located either side of the midline. In the *Foxa2 CKO* at E10.5 there is a substantial decrease in the number of cells expressing *Ngn2*, and the size of the *Ngn2* domain, measured from the ventral midline to the dorsal limit of expression, has been reduced by approximately 44μm (figure 10E). The two *Mash1* domains either

side of the midline have expanded ventrally by the same value, and form a sharp boundary with the remaining *Ngn2* expressing domain, whilst retaining their dorsal limit of expression (figure 10F).

In the E12.5 wild type embryos, there are now three distinct domains of *Ngn2* expression. There is the salt and pepper expression of *Ngn2* within the ventricular zone of the alar plate, the *Ngn2* expressing cells of the basal plate spanning the ventral midline and terminating before the ABB within the ventricular zone, and a small population of *Ngn2* expressing cells in the intermediated zone immediately outside of the ventricular zone (figure 10G). At E12.5 *Mash1* is uniformly expressed throughout the ventricular zone of both the alar and basal plates (figure 10H). In the *Foxa2 CKO* embryos at E12.5 *Ngn2* expression in the ventricular zone of the ventral mesencephalon is less intense while the overall size of the *Ngn2* domain is not evidently reduced in size, as was described at E10.5 (figure 10I). There is a reduction in the intensity of the *Ngn2* expressing cells located in the intermediate zone (figure 10I). Interestingly *Mash1* expression has been eradicated from the cells of the ventricular zone at the ventral midline of the mesencephalon, whist seemingly remaining unaltered dorsally (figure 10J).

These results indicate that a reduction of *Foxa2* in the ventral mesencephalon can lead to the specific alteration of proneural gene function in the region surrounding the ventral midline of the basal plate. This could account for the decrease in the number of differentiated neurons present in the mantle layer immediately adjacent to this domain. Additionally, it has recently been demonstrated that the mesDA progenitor cells express *Ngn2* and that *Ngn2* is required for mesDA development (Kele et al., 2006). The

reduction of the *Ngn2* domain at E10.5 could account for the reduction in the mesDA population described at E12.5 in the *Foxa2 CKO*.

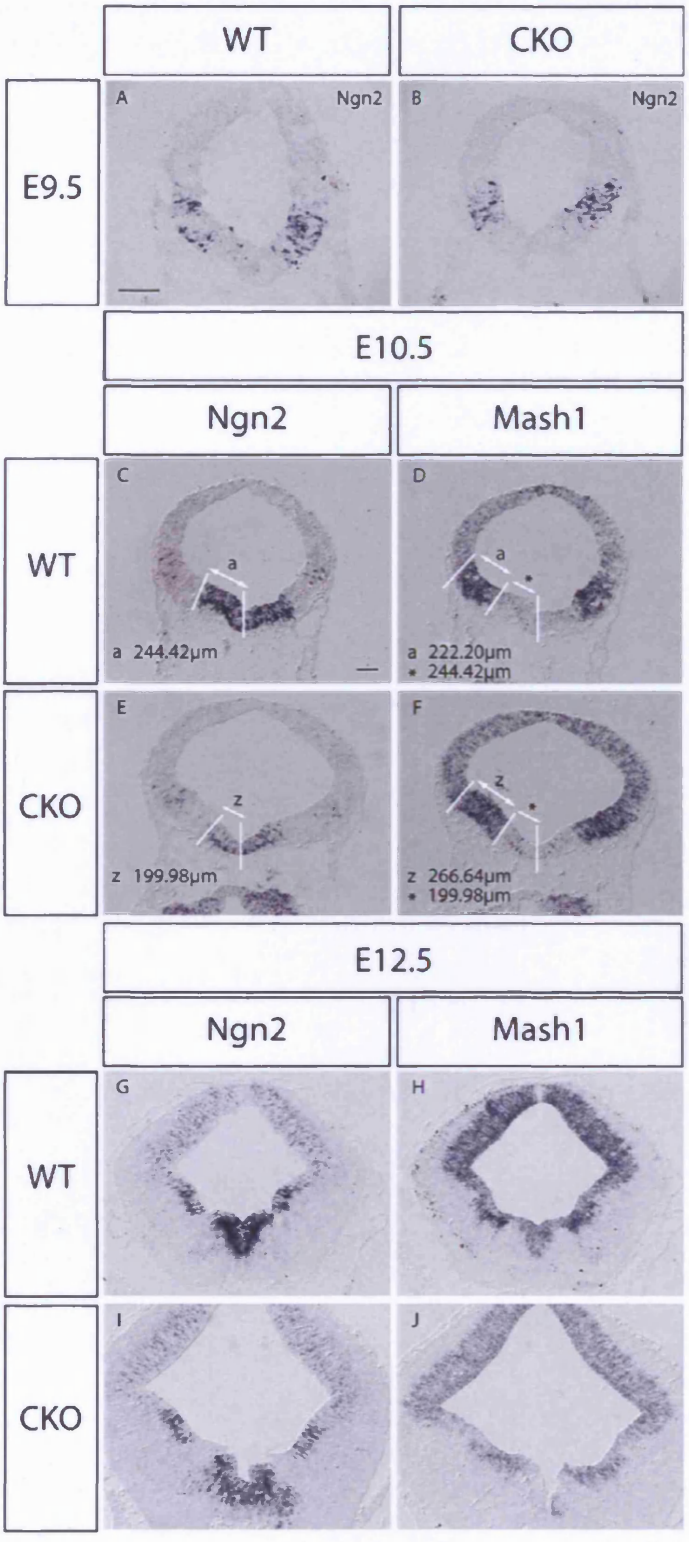

Figure 10: Analysis of neurogenesis in the Foxa2 CKO: A-J: *Ngn2 and Mash1 gene expression was used to identify any possible defects in neurogenesis within the Foxa2 CKO from E9.5-E12.5. There is no significant alteration in ngn2 gene expression at E9.5.*

Figure 10 continued: *At E10.5 Ngn2 and Mash1 gene expression domains abut each other in the ventricular zone near the ABB. In the Foxa2 CKO there is a slight reduction in the gene expression domain of Ngn2 combined with a ventral expansion of Mash1 into the domain relinquished by Ngn2. The extent of the ventral expansion of Mash1 and reduction in the Ngn2 domain were measured on adjacent mesencephalic sections (**C-F**). At E12.5 there is an absence of Mash1 gene expression from the ventral midline in the Foxa2 CKO, whereas Ngn2 gene expression resembles that of the wild type embryo. Scale bar represents 100mm.*

10. Evidence of a tight regulatory mechanism between *Shh*, *Foxa1* and *Foxa2*

Foxa2 has been proposed to be an upstream activator of *Shh* due to the observations that *Foxa2* is expressed in the same cells at the axial mesoderm and ventral midline prior to the onset of *Shh* expression (Ang et al., 1993; Echelard et al., 1993; Marti et al., 1995b; Sasaki and Hogan, 1993), and that the removal of *Foxa2* leads to a loss of *Shh* expression (Ang and Rossant, 1994; Weinstein et al., 1994). Studies where *Foxa2* is ectopically expressed in the neural tube provid evidence that *Foxa2* is able to induce the expression of *Shh* (Sasaki and Hogan, 1994), whilst similar ectopic expression studies using *Shh* have revealed that *Shh* has the ability to induce *Foxa2* (Echelard et al., 1993) via the activity of *Gli1* (Hynes et al., 1997; Sasaki et al., 1997). Thus a positive cross-regulatory loop is created between *Foxa2* and *Shh* maintaining their expression in the ventral midline. Another member of the Forkhead box transcription factors, *Foxa1* has been shown to be expressed at the same time as *Shh* expression within the ventral midline of the mesencephalon and spinal cord (Ang et al., 1993). Even though genetic analyses demonstrated that *Foxa1* is not essential for the transcription of *Shh*, recent *in-vitro* studies provided evidence that *Foxa1* can activate *Shh* but with less potency than *Foxa2* (Duncan et al., 1998).

To address whether *Shh* expression and subsequently Shh signalling was affected due to the reduction of *Foxa2* from E8.5 I used immunohistochemical co-expression studies to analyse the *Foxa2 CKO* embryos from E8.75 to E12.5 with antibodies raised against Foxa1, Foxa2 and Shh. Where triple-label immunohistochemistry was not possible, adjacent mesencephalic sections were used.

At E8.75 Shh expression can be detected at the ventral midline of the mesencephalon (figure 11A), and is restricted within the same cells which express Foxa2 (figure 11C). It is also evident that all cells which express Foxa1 co-express Foxa2, and that the expression domain of Foxa2 is broader than that of Foxa1 (figure 11C). In the *Foxa2 CKO* there is a dramatic reduction of Shh (figure 11B) combined with a reduction in the expression of Foxa1 (figure 11D). The remaining Shh and Foxa1 proteins are restricted to cells which still express Foxa2 at the ventral midline of the mesencephalon. The relationship between Shh, Foxa2 and Foxa1 at E9.5 is very similar to the relationship described above. In the wild type embryos the expression of Shh can be detected spanning the ventral midline in a broad domain (figure 11E), restricted within the expression domain of Foxa2. Foxa1 is expressed in a broad domain, but unlike Foxa2 does not reach the ABB (figure 11G). In the *Foxa2 CKO* the phenotype is consistent with the losses described at E8.75. Shh and Foxa1 expression are reduced to the remaining Foxa2 positive cells in the ventral midline (figure 11F, H).

In the wild type embryos at E10.5, Shh expression is detected in a broad domain spanning the ventral midline with a dorsal limit within the Foxa2 expression domain, a few cell diameters away from the ABB (figure 11I, K, M, O). Shh protein can also be detected in the mantle layer immediately adjacent to the Foxa2 expressing cells of the ventricular zone (figure 11I, M). The Foxa1 expressing cells are restricted within the Foxa2 domain but do not reach the ABB by several cell diameters. In the *Foxa2 CKO* embryos at E10.5 the apparently consistent phenotype described for stages E8.75 and E9.5 does not remain constant along the anterior-posterior axis. In the posterior regions of the mesencephalon both Shh and Foxa1 are reduced dramatically and resemble the phenotype described above, only being detected within the remaining Foxa2 positive

cell population (figure 11J, L). However, in the anterior regions of the mesencephalon there is a restoration of the expression patterns of both Shh and Foxa1 to near wild type levels (figure 11N, P). Interestingly the remaining Foxa2 positive cells express Foxa1 at weaker levels than the other Foxa1 positive cells (figure 11P).

At E11.5 and E12.5 in the wild type embryos there are two clear domains of Shh expression determined by the intensity of the antibody staining. Either side of the ventral midline there is a domain within the ventricular zone lateral to the midline which displays high levels of Shh protein (figure 11Q, U). The region of the Shh domain which spans the ventral midline displays low levels of Shh protein (Figure 11Q, U), consistent with the idea that the floor plate cells in the ventral mesencephalon at E10.5 have switched from being non-neurogenic (not expressing *Ngn2*) to neurogenic (expressing *Ngn2* and *Sox2*) (Andersson et al., 2006; Kele et al., 2006). Consistent will all stages analysed, Shh protein is only detected within the Foxa2 domain (Figure 11Q, S, U, W). The Foxa1 domain at E11.5 and E12.5 is as described for all previous embryonic stages being expressed across the ventral midline, with a lateral limit within the Foxa2 domain (figure 11S, W). Additionally at E12.5, Foxa1 expression can be now detected in some cells located within the mantle layer strongly co-expressing Foxa2. The most notable being the cells underlying the ventral midline which correspond to the mesDA (figure 11W). In the *Foxa2 CKO* embryos at E11.5 and E12.5, with the exception of the most posterior regions of the mesencephalon, the phenotype is consistent with that described in the anterior regions of the E10.5 mesencephalon. Both Shh and Foxa1 appear to be restored to nearly the wild type levels of expression (figure 11R, T, V, X).

Additionally, from the analyses on the *Foxa2 CKO* embryos from E10.5 – E12.5, it appears that the sensitivity of the Foxa1 antibody was increased in the *Foxa2 CKO* compared to the wild type embryos, suggesting that Foxa1 is over-expressed in response to the reduction in Foxa2. Interestingly, Foxa1 protein levels were as normal in the regions of the ventral midline of the *Foxa2 CKO* embryos which maintained the expression of Foxa2 (figure 11P, T, X). This result would suggest that Foxa1 is not over-expressed in this small region as Foxa2 is still present and no compensation is required.

Overall these results indicate that *Foxa2* is a strong positive regulator of both *Shh* and *Foxa1* within the ventral mesencephalon, as demonstrated previously in other regions of the nervous system (Duncan et al., 1998; Epstein et al., 1999). This tight regulation is evident at early stages where in response to the reduction of *Foxa2*, the expression domains of both *Foxa1* and *Shh* are reduced and restricted within the remaining *Foxa2* domain. This would suggest that in the mouse, Shh signalling at these early stages would be greatly reduced and could possibly lead to patterning defects along the dorsal-ventral axis. At later stages, by a currently unknown mechanism, *Foxa1* and *Shh* expression domains are restored to resemble their wild type patterns. Unfortunately, due to the complex positive regulatory mechanism present between *Foxa2* and *Shh* in the ventral neural tube it is not clear whether *Foxa2* is regulating *Shh* via a direct or indirect mechanism.

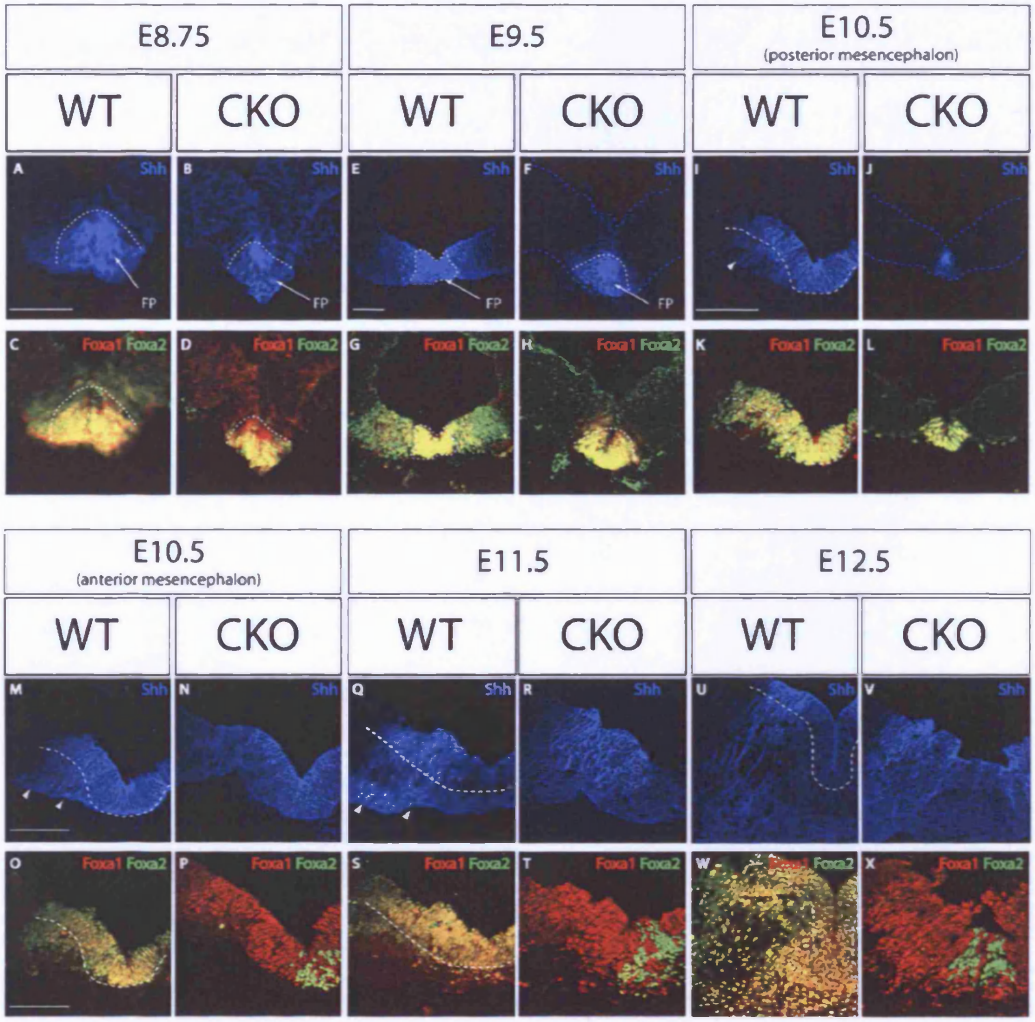

Figure 11: Relationship between Foxa2, Foxa1 and Shh. ***A-X:*** *Many recent studies revealed a positive regulatory mechanism between Foxa2 and Shh within the developing neural tube. In the Foxa2 CKO this relationship between Foxa2 and Shh is evident by the sharp reduction and restriction of Shh within the remaining Foxa2 domain at the ventral midline during the early stages of embryonic development. Interestingly the reduction in Foxa2 also revealed a positive regulatory role of Foxa2 upon Foxa1. At E10.5 in the anterior regions of the mesencephalon both Foxa1 and Shh are restored to resemble their wild type expression domains, even though Foxa2 protein is restricted at the ventral midline. The factor which causes the restoration of both Foxa1 and Shh is still being investigated, but these results could indicate a regulatory role for Foxa1 over Shh.* ***A-H:*** *Secreted proteins (Shh and Netrin) emanating from the floor plate structure have been shown to be important in the specification of neuronal subtypes and axonal guidance in the neural tube. Foxa2 has also been identified as a key regulator in floor plate development. Using Shh (blue), Foxa1 (red) and Foxa2 (green) at E8.75 and E9.5 it is evident that the floor plate structure persists in the Foxa2 CKO, although the dimensions of the floor plate has been reduced (dotted lines and arrows).*

Figure 11 continued. ***I-X:*** *Dotted lines represent the ventricular zone of the basal plate. Arrowheads indicate the presence of diffusible Shh protein within the basal plate. Scale bar represents 100μm.*

11. Floor Plate structure is maintained in the *Foxa2 CKO* embryos

The floor plate is a specialised structure which runs along the anterior posterior axis of the embryo from the spinal cord to the diencephalon, and is involved in patterning the neural tube along the dorsal-ventral axis by secreting the morphogen Shh, and in guiding axons to their targets (Placzek and Briscoe, 2005). *Foxa2* has been shown to be a regulator of floor plate development. When *Foxa2* is ectopically expressed in the mouse, an ectopic floor plate is induced (Sasaki and Hogan, 1994), while the floor plate fails to develop in the *Foxa2 -/-* mice (Ang and Rossant, 1994; Weinstein et al., 1994). It has been demonstrated that both motor neurons (Ericson et al., 1996; Ericson et al., 1995b) and mesDA neurons (Hynes et al., 1995b) are generated in a contact dependent fashion to the floor plate cells.

To determine whether this important structure was affected by the dramatic reduction of *Foxa2*, the analysis of floor plate specific markers was carried out. Unfortunately, the antibodies used to demarcate the floor plate region in previous studies recognised rat proteins for FP3 and FP4 (Hynes et al., 1995a). These antibodies did not detect the mouse equivalents of these genes, so the floor plate region was characterised solely based on the expression domains of *Shh*, *Foxa1* and *Foxa2* at the ventral midline. At E8.75 and E9.5 the floor plate cells can be distinguished by expressing high levels of all three markers (figure 11A, C, E, G). The floor plate in the *Foxa2 CKO* embryos at these stages is still present but the dimensions have been reduced, clearly indicated by the reduction in the expression domains of Foxa1, Foxa2 and Shh (figure 11B, D, F, H).

The presence of the floor plate within the mesencephalon at later stages is a contentious issue. Elsewhere in the developing neural tube, there is no evidence that neurogenesis occurs within the floor plate cells. However, in the mesencephalon recent studies have provided evidence that the mesDA progenitor cells are derived from cells located in the ventral midline (Andersson et al., 2006) and that these cells express both *Ngn2* and *Sox2* indicating that neurogenesis is occurring (Kele et al., 2006). These results suggest that around E10.5 the cells occupying the ventral midline switch from being characteristic floor plate cells to neuronal progenitor cells, thus the floor plate structure is no longer required to perform its known functions.

In the *Foxa2 CKO* embryos it is clear that the floor plate structure is still present at early stages, though it has been clearly reduced in size. At later stages, despite the hypothesis stated above, there is always a domain within the ventricular zone which expresses high levels of Foxa1, Foxa2 and Shh, which correspond to the floor plate structure (figure 11J, L, N, P, R, T, V, X).

12. Immediate downstream targets of Shh signalling are restored to wild type levels in the *Foxa2 CKO* after E10.5

In the *Foxa2 CKO* embryos there is a dramatic reduction of *Shh* expression at E8.75 and E9.5, but appears to be gradually restored by E12.5. To investigate the consequences of the initial reduction in Shh signalling I analysed the expression patterns of downstream targets and transducers of the Shh signalling cascade using *in-situ* hybridisation.

The Shh-Np ligand is bound by the 12-transmembrane receptor Ptc (Fuse et al., 1999; Marigo et al., 1996a; Marigo and Tabin, 1996; Stone et al., 1996). In the ventral mesencephalon at E9.5 *Ptc* gene expression is detected at high levels either side of the ventral midline partially overlapping with the domain of expression domain of *Shh* (figure 12A). In the *Foxa2 CKO Ptc* gene expression is shifted ventrally and is expressed at high levels in a domain spanning the ventral midline and overlying the remaining *Shh* gene expression (figure 12B). In the wild type mesencephalon at E10.5 *Ptc* expression can be detected in the ventricular zone either side of the midline bordering and partially overlapping the *Shh* domain (figure 12C). In the *Foxa2 CKO* there is an alteration in the expression of *Shh* along the anterior-posterior axis as described above. In the posterior regions of the mesencephalon *Ptc* expression is shifted ventrally to surround the remaining *Shh* expression in the ventral midline (figure 12D). At E12.5 the expression domain of *Ptc* in both the wild type and *Foxa2 CKO* embryos is unaltered as expected due to the restoration of Shh signalling. The medial limit of *Ptc* expression within the ventricular zone corresponds to the domain of high *Shh* expression (figure 12E-F).

In vertebrates the Shh signal is transduced by the actions of the zinc finger transcription factors *Gli1*, *Gli2* and *Gli3*, which are homologues of the *Drosophila* Ci (Hui et al., 1994; Jacob and Briscoe, 2003; Lee et al., 1997). To further characterise Shh signalling in the *Foxa2 CKO* I analysed the expression of the three vertebrate Ci homologues using *in-situ* hybridisation. The expression pattern of *Gli1* in the ventral mesencephalon of wild type embryos is located immediately adjacent to the expression domain of *Shh* within the ventricular zone (figure 12G, I, K), consistent with descriptions of *Gli1* expression in other regions of the neural tube (Bai et al., 2002; Platt et al., 1997).

In the *Foxa2 CKO* at E9.5 and E10.5 *Gli1* expands ventrally creating a new ventral boundary with the remaining *Shh* expressing cells in the ventral midline, consistent with the finding that *Gli1* expression is dependent on Shh signalling (Bai and Joyner, 2001). The dorsal limit of the *Gli1* expression domain is unaltered (figure 12H, J). Interestingly at E12.5 *Gli1* expression remains up-regulated in the basal plate, overlapping with the restored *Shh* domain, while the dorsal limit of the *Gli1* expression domain remains unaltered, consistent with the phenotype described at E9.5 and E10.5 (figure 12L).

In vertebrates the primary transducer of the Shh signal is believed to be *Gli2*. In the developing spinal cord, *Gli2* is expressed throughout this tissue in a uniform manner (Hui et al., 1994; Lee et al., 1997). *Gli2* is not expressed uniformly throughout the mesencephalon, but is expressed throughout the ventricular zone of the alar plate with a ventral limit bordering the ABB (figure 12M, O, Q). In the *Foxa2 CKO* at E9.5 there is a ventral expansion of the *Gli2* domain reaching the remaining *Shh* expressing cells (figure 12N). This phenomenon is persistent in the posterior regions of the E10.5

mesencephalon (figure 12P), while in the anterior mesencephalon the expression of *Gli2* regresses dorsally and resembles the wild type pattern (figure 13O-P). At E12.5 the ventral limit of *Gli2* has been restored to the ABB (figure 12R).

The primary repressor of Shh signalling in vertebrates is *Gli3* (Hui et al., 1994; Jacob and Briscoe, 2003; Lee et al., 1997). At E9.5 in the mesencephalon, *Gli3* is expressed throughout the ventricular zone of the alar plate with a ventral border a few cell diameters away from the ABB (figure 12S). *Gli3* is not affected by the reduction of Shh signalling in the *Foxa2 CKO* at E9.5, and maintains the ventral limit of gene expression (figure 12T). At E10.5 the expression of *Gli3* overlaps that of *Gli2* in wild type embryos, sharing a ventral border at the ABB (figure 12U). In the *Foxa2 CKO* at E10.5 there is no alteration to the expression pattern of *Gli3* along the entire anterior-posterior axis (figure 12V). The expression domain of *Gli3* at E12.5 in the wild type overlaps with *Gli2* (figure 12W) and is not affected by the reduction of *Foxa2* (figure 12X).

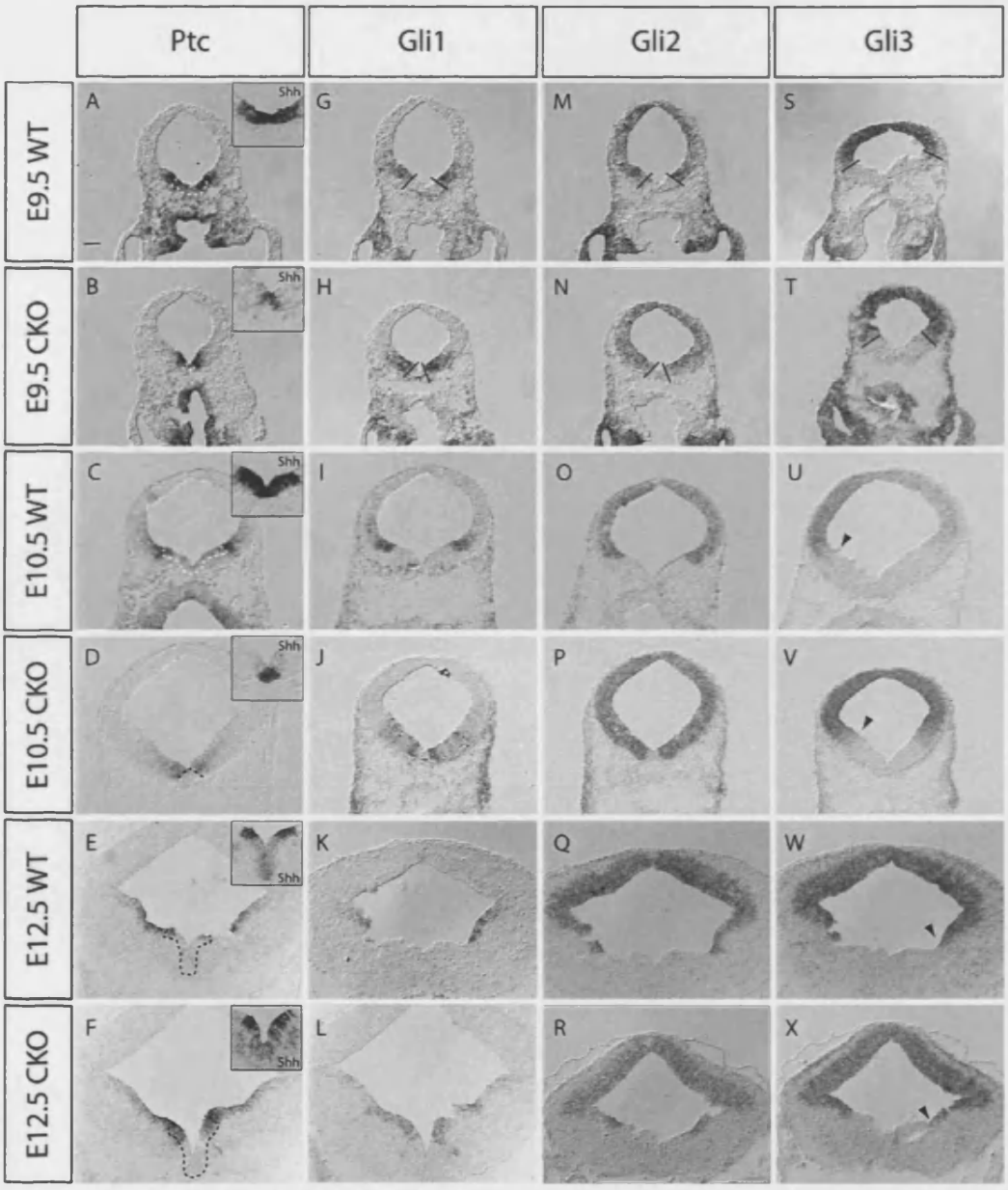

Figure 12: Analysis of downstream targets of Shh signalling in the Foxa2 CKO. ***A-X:*** *In response to the alteration in Shh gene expression and ultimately Shh signalling in the Foxa2 CKO the genes which are involved in the transduction of the Shh signal respond accordingly. Ptc, Gli1 and Gli2 gene expression shift ventrally towards the remaining source of Shh protein at E9.5 and in the posterior regions of the mesencephalon at E10.5, and are restored to their wild type positions in the anterior regions of the mesencephalon at E10.5 and throughout the remaining stages analysed. Interestingly there is no alteration in the gene expression pattern of Gli3 at any time point analysed.* ***A-F:*** *The dotted lines represent the Shh gene expression domain in both the wild type and Foxa2 CKO embryos (also displayed on the adjacent mesencephalic sections as inset photographs).*

Figure 12 continued. *Solid lines in photographs of E9.5 embryos, and arrowheads in Gli3 gene expression photographs represent the ventral limit of the gene expression domains. Scale bar represents 100μm.*

At E10.5 in the *Foxa2 CKO* I have demonstrated that *Shh* and *Foxa1* are restored to their wild type expression domains in the anterior regions of the mesencephalon, whereas they are clearly down-regulated in the posterior regions of the mesencephalon.

The same pattern is evident for the downstream targets of Shh signalling. In the posterior regions of the mesencephalon the downstream targets of Shh signalling are shifted ventrally towards the remaining Shh signal, whereas in the anterior regions they are restored to their wild type expression domains, consistent with the restoration of Shh signalling within this region.

Shh gene expression is clearly restored to wild type levels in the anterior mesencephalon (figure 13A-D) supporting the data of Shh protein expression (figure 11N). The expression domain of *Ptc* in the anterior mesencephalon is no longer shifted ventrally and resembles the wild type gene expression (figure 13E-H). In the posterior mesencephalon, both *Gli1* and *Gli2* expanded ventrally surrounding the remaining *Shh* expressing cells (figure 13I-J, M-N). In the *Foxa2 CKO* both these genes are no longer ectopically expressed near the ventral midline, and have be restored to their wild type positions bordering the restored expression domain of *Shh* (figure 13K-L, O-P).The expression of *Gli3* is not affected by the reduction of *Shh* signalling at any location along the anterior-posterior axis (data not shown).

To complement the data obtained using the Foxa1 antibody (figure 11) I analysed the expression domain of *Foxa1* using *in-situ* hybridisation which is clearly reduced within the posterior regions of the mesencephalon (figure 13Q-R) but is restored to wild type levels in the *Foxa2 CKO*, overlapping with the *Shh* domain (figure 13S-T).

These data suggest that Shh signalling is progressively restored in the *Foxa2 CKO* and this restoration begins at E10.5 within the anterior mesencephalon and by E12.5 is gradually restored within the posterior regions, with the exception of *Gli1*.

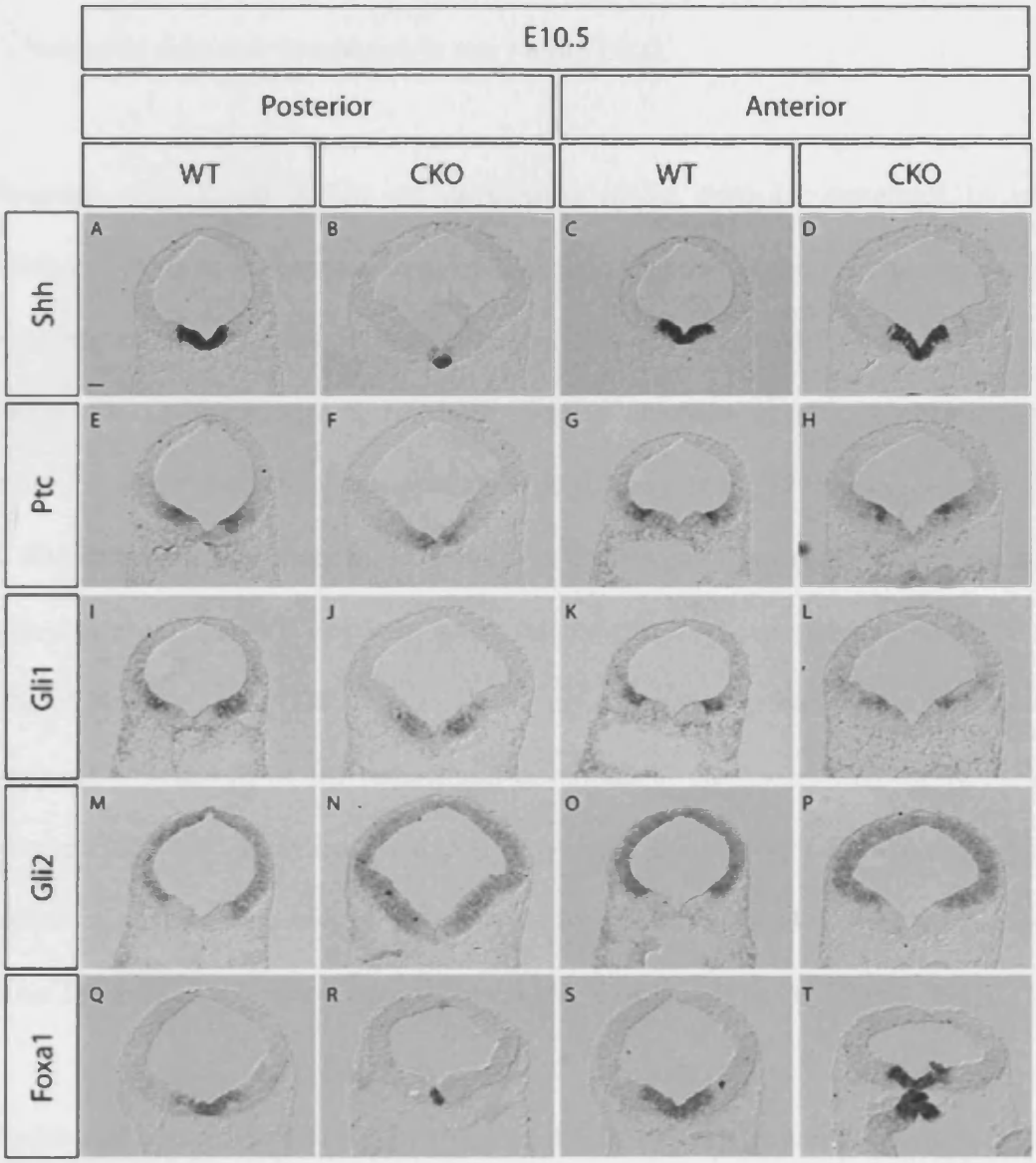

Figure 13: Detailed analysis of downstream targets of Shh signalling at E10.5 in the Foxa2 CKO along the entire anterior-posterior axis of the mesencephalon. A-T: *Coronal sections of E10.5 wild type and Foxa2 CKO embryos. Analysis of the downstream targets of Shh signalling revealed that at E10.5 there was a transition in the phenotype described previously at E9.5. In the posterior regions of the Foxa2 CKO mesencephalon the gene expression patterns of all the downstream targets of Shh signalling are all shifted ventrally to meet the reduced Shh gene expression at the ventral midline. However, in the anterior regions of the mesencephalon in combination with a restoration of both Foxa1 and Shh gene expression to their wild type levels, the downstream targets of Shh signalling are all shifted dorsally to their original positions. Scale bar represents 100μm.*

13. Class I genes are unaffected while several Class II genes expand ventrally towards the ventral midline in the *Foxa2 CKO*

Neuronal populations within the developing neural tube are generated in spatially restricted domains in response to morphogenetic signals. In the ventral neural tube this phenomenon is attributed to the actions of Shh (Briscoe and Ericson, 2001; Jessell, 2000). When Shh signalling has been blocked either by genetic or chemical means, ventral neuronal patterning has been affected (Chiang et al., 1996; Ericson et al., 1996). In *Shh* deficient mice there is complete loss of all ventral neuronal subtypes combined with a ventral expansion of transcription factors normally expressed in the dorsal neural tube (Chiang et al., 1996). Therefore I investigated whether the reductions in the neuronal populations of the tegmentum described in the *Foxa2 CKO* were caused by incorrect neuronal specification due to the initial reduction of Shh signalling. Both double-immunohistochemistry and *in-situ* hybridisation analysis using markers for Class I and Class II genes were used to analyse embryos from E8.75 to E12.5.

To determine whether the initial reduction in Shh signalling caused a ventral expansion of dorsal progenitor domains, I analysed the expression patterns of *Pax3* and *Pax7* from E9.5 to E12.5 (Chiang et al., 1996; Ericson et al., 1996; Goulding et al., 1993; Yamada et al., 1991). At E9.5 in the wild type embryos, *Pax3* and *Pax7* are co-expressed in the ventricular zone of the dorsal regions of the alar plate, with the exception of the roof plate where only *Pax3* is expressed (figure 14A). In the *Foxa2 CKO* the relationship between *Pax3* and *Pax7* is identical to the wild type and there is no ventral expansion of these two genes in response to the reduced levels of Shh at this time point (figure 14B). Analysis of *Pax3* and *Pax7* in the *Foxa2 CKO* embryos at E10.5 to E12.5 revealed that

they are indistinguishable from the wild type embryos. The ventral limit of the expression domains remains constant in all the embryos analysed along the entire anterior-posterior axis (figure 14C-H arrowheads). Qualitative analysis of the *Pax7* positive neurons present in the mantle layer at E12.5 suggest that the early reduction of Shh signalling did not affect dorsal neuronal populations (figure 14G-H).

To supplement the co-expression studies using the paralogous genes, *Pax3* and *Pax7*, I analysed the expression patterns of three other Class I homeodomain transcription factors; *Dbx1*, *Irx3* and *Pax6*. In the developing spinal cord, *Dbx1* expression is restricted to the V1 and V0 domains which are located in the intermediate region of the neural tube (see introduction figure F) (Pierani et al., 1999), but in the mesencephalon it is expressed throughout the ventricular zone of the alar plate but not in the roof plate, and in a small population of cells lying in the mantle layer dorsal to the ABB (figure 14I, M). In the *Foxa2 CKO* embryos there is no ventral expansion of the *Dbx1* domain at either E10.5 or E12.5 (figure 14I-J, M-N).

In the developing spinal cord *Irx3* is expressed in a broad domain spanning the V2 – V0 progenitor domains (see introduction figure 6) (Cohen et al., 2000). At E9.5 the expression of *Irx3* is restricted to a dorsal-lateral domain within the ventricular zone (Cohen et al., 2000) and is unchanged within the *Foxa2 CKO* (data not shown). At E10.5 there are two distinct domains of *Irx3* expression. Within the alar plate *Irx3* is expressed throughout the ventricular zone with the exception of the roof plate, resembling *Dbx1* gene expression, forming a ventral limit prior to the ABB (figure 14K). There is also an *Irx3* domain within the ventricular zone of the basal plate, immediately overlying the region where the OMC neurons are located (figure 14K).

There is no alteration in any of the expression domains of *Irx3* in the *Foxa2 CKO* at E10.5 (figure 14L). In the wild type embryos at E12.5 the pattern of gene expression within the ventricular zone of both the alar and basal plates remains as described for E10.5. However, there are some *Irx3* positive cells located in the mantle layer of the ventral mesencephalon, which are located directly within the OMC domain (figure 14O). There is no alteration in the pattern of *Irx3* gene expression at E12.5 in the *Foxa2 CKO* embryos as compared to the wild type (figure 14P).

In the ventral half of the developing spinal cord *Pax6* is expressed in a broad domain ranging from the MN progenitors to the V0 domain. In the mesencephalon I could not detect *Pax6* expression at E10.5 (data not shown) and at E12.5 it is only expressed by a small population of cells in the mantle layer located immediately dorsal to the ABB (figure 14Q) (Stoykova and Gruss, 1994). In the *Foxa2 CKO* at E12.5 there is a dramatic expansion of *Pax6* gene expression within the basal plate within the region where the remaining OMC and RN neuronal populations are situated, whilst maintaining the dorsal limit of *Pax6* gene expression at the ABB (figure 14R).

These data indicate that the reduction in Shh signalling evident at E8.75 to E10.5 is insufficient to cause a ventral expansion of dorsal cell fates and that the reduction of Shh occurs after a critical time point when dorsal progenitor cells are no longer competent to the Shh signal. Alternatively, genes requiring low levels of Shh signalling are not affected in the *Foxa2 CKO* embryos. The ventral expansion of *Pax6* is consistent with the current theory that Class I genes are inhibited by Shh signalling, but it still remains unclear to why only the *Pax6* domain shows a ventral expansion and not the other Class I genes.

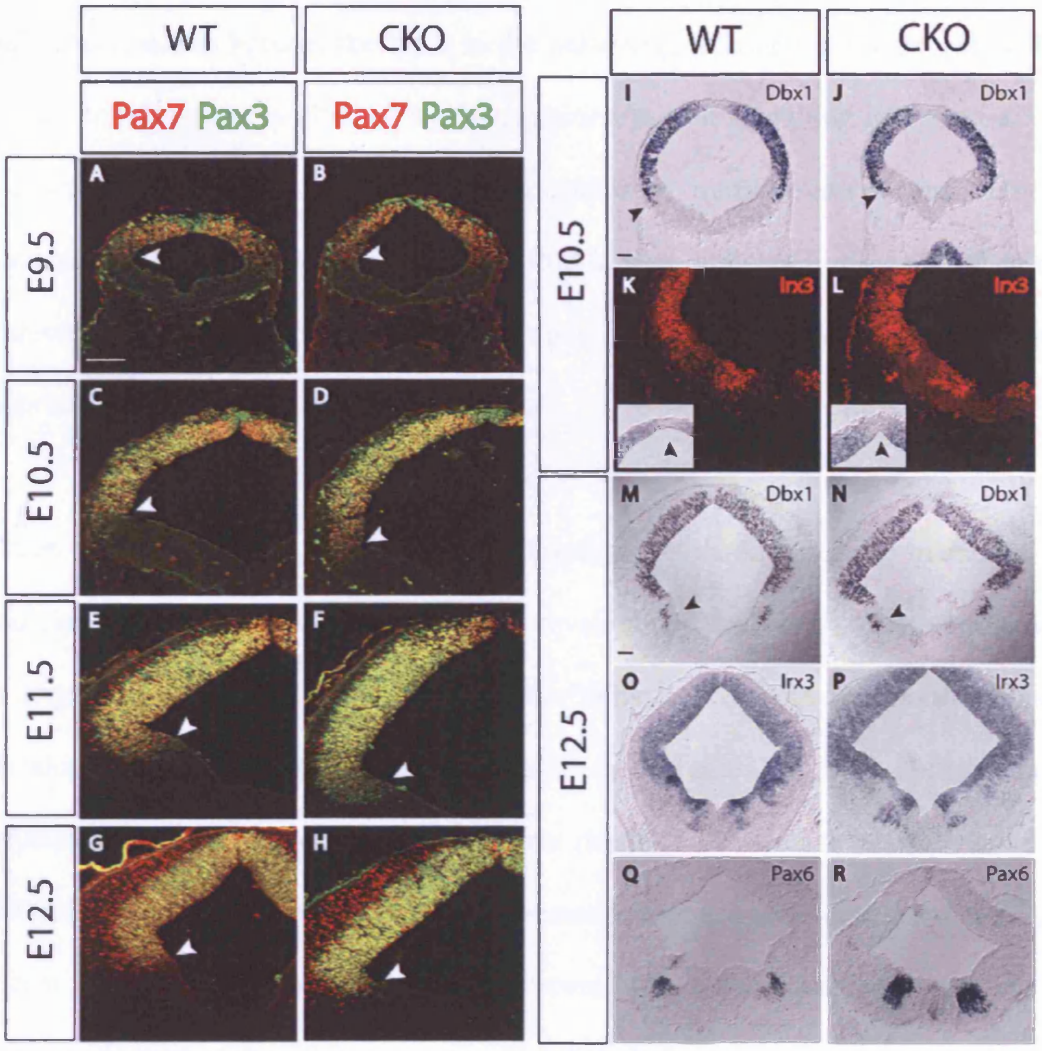

Figure 14: Analysis of Class I genes in the mesencephalon. ***A-R:*** *Due to the reduction in Shh signalling described above, it was expected that there would be an alteration in the progenitor domains of both Class I and Class II genes at the earlier stages of embryonic development. The analysis of the Class I genes with the exception of Pax6 (Pax3, Pax7, Dbx1, and Irx3) revealed that the reduction in Shh signalling did not cause a ventral expansion of the progenitor domains of the alar plate as described in the Shh -/- mice. Pax6, which borders the ABB within the mantle layer, shows a dramatic increase within the mantle layer. Arrowheads in photographs A-J and M-N indicate the ventral limit of the Class I genes within the ventricular zone.* ***K-L inset:*** *Indicates that the dorsal expression of Irx3 flanking the roof plate is not altered by the reduction in Shh signalling in the Foxa2 CKO. Scale bars represent 100μm.*

From the analysis of the Class I homeodomain transcription factors it is evident that only *Pax6*, which borders the ABB in the mesencephalon and is not expressed within the ventricular zone, is affected by the reduction in Shh signalling in the *Foxa2 CKO*. To investigate whether the Class II homeodomain transcription factors, which are induced by Shh signalling (Briscoe et al., 2000), were affected in the basal plate by the reduction of Shh signalling a combination of immunohistochemistry and *in-situ* hybridisation analysis was performed.

Three of the Class II homeodomain transcription factors analysed are members of the *Nkx* family of transcription factors. In the developing spinal cord and hindbrain, *Nkx6.1* is expressed in ventral neuronal progenitor cells and is essential for motor neuron development (Sander et al., 2000). *Nkx2.2* is expressed in the progenitor domain adjacent to the floor plate structure and gives rise to the V3 interneurons (Briscoe et al., 2000; Briscoe et al., 1999). *Nkx2.9* is expressed within the same domain as *Nkx2.2*, and recent genetic analysis has revealed that it could play a redundant role with *Nkx2.2* in the specification of the V3 interneurons (Pabst et al., 2003).

At E8.75 Nkx6.1 protein is detected in a broad domain within the ventral mesencephalon, forming a ventral limit at the floor plate structure (figure 15A). In the *Foxa2 CKO* there is a ventral expansion of Nkx6.1 protein occupying the entire ventral midline (figure 15B). Nkx2.2 protein can be detected within the progenitor domain adjacent to the floor plate as described in the spinal cord (figure 15C). In the *Foxa2 CKO* there is a reduction in the Nkx2.2 domain dorsally, whilst maintaining its ventral limit to the remaining floor plate cells (figure 15D). Co-expression studies revealed that the number of progenitor cells co-expressing Nkx2.2 and Nkx6.1 is reduced in the

Foxa2 CKO (figure 15E-F). Interestingly, unlike the reduction in Nkx2.2, there is an up-regulation of *Nkx2.9* gene expression, as detected by the intensity of the RNA signal. The ventral limit of the *Nkx2.9* domain is maintained adjacent to the remaining floor plate cells, but it is unclear whether the dorsal limit of the expression domain has regressed ventrally (figure 15G-H).

At E9.5 Nkx6.1 protein can be detected in the ventricular zone of the ventral mesencephalon forming a ventral boundary near the floor plate cells. The dorsal limit of Nkx6.1 expression is located a few cell diameters dorsal to the ABB (figure 15I). There is almost a complete loss of Nkx6.1 protein in the *Foxa2 CKO* at E9.5, with the remaining Nkx6.1 positive cells lying above the ABB (figure 15J). *In-situ* hybridisation studies have confirmed the down-regulation of Nkx6.1 at this stage (data not shown). Nkx2.2 protein is detected within the ventricular zone from the ABB and terminating adjacent to the floor plate (figure 15K). There is a ventral expansion of Nkx2.2 protein in the *Foxa2 CKO*, creating a new ventral limit adjacent to the remaining floor plate cells (figure 15L). The dorsal limit of Nkx2.2 protein detection is unchanged. Co-expression studies reveal that the small domain of progenitor cells which co-express Nkx2.2 and Nkx6.1 is missing at E9.5 in the *Foxa2 CKO* (figure 15M-N). *Nkx2.9* gene expression can be detected in overlapping domains with Nkx2.2 in both the wild type and *Foxa2 CKO*, which is consistent with the hypothesis that these two genes function in a redundant system (figure 15O-P).

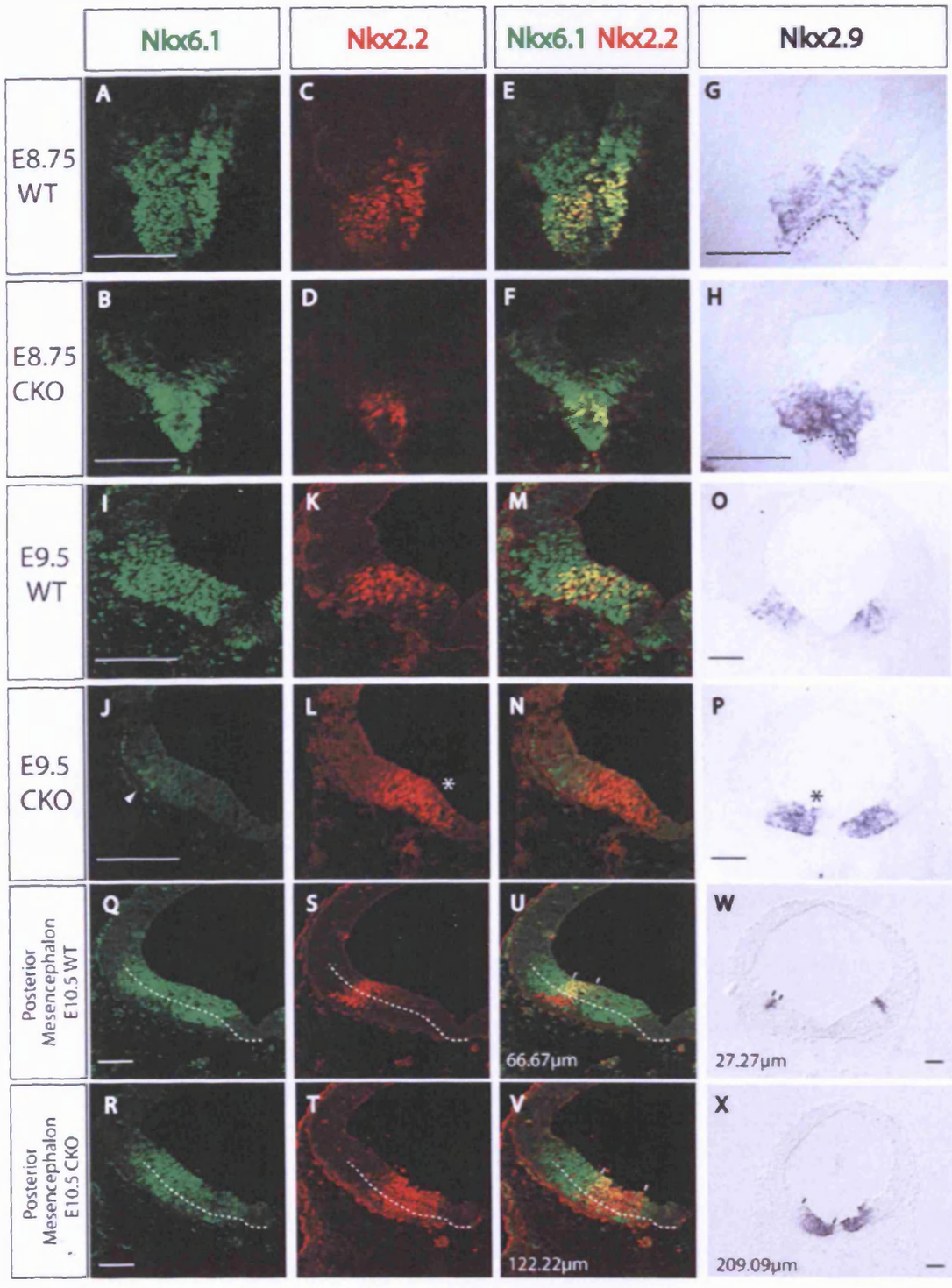

Figure 15: Analysis of Class II genes in the mesencephalon of the Foxa2 CKO (part a). *Coronal sections of both wild type and Foxa2 CKO embryos. Due to the reduced levels of Shh signalling described at E8.75 and E9.5 it would be expected that there would be an alteration in the patterning of the ventral mesencephalon, especially in the positioning of the ventral neuronal progenitor domains which require Shh signalling to be specified correctly. Therefore, analysis was carried out on three Class II genes; Nkx2.2 (red), Nkx6.1 (red) and Nkx2.9 (blue). Initially there is a reduction in the levels of Nkx6.1 protein, leading to a complete loss of Nkx6.1 protein at E9.5.*

Figure 15 continued. *Eventually at E10.5 Nkx6.1 protein can be easily detected throughout the ventricular zone and mantle layer of the mesencephalon at its wild type position. Nkx2.2 and Nkx2.9 expression domains expand ventrally towards the ventral midline, with Nkx2.9 displaying the largest increase in the size of its expression domain.* ***G-H:*** *Dotted lines at E8.75 represent the location of the Foxa2/Foxa1/Shh domain at the ventral midline in the wild type and Foxa2 CKO embryos.* ***Q-U, R-V:*** *Dotted lines used to aid visualisation of the ventricular zone within the basal plate. L, P, X: Asterisk used to point out the expanded progenitor domain of Nkx2.2 or Nkx2.9. Short solid lines in photographs U-X correspond to domain measured for the expansion of either Nkx2.2 or Nkx2.9 expression domain. Scale bars represent 100μm.*

At E10.5 Nkx6.1 protein can be detected at high levels in the ventricular zone of the ventral half of the mesencephalon creating a ventral limit prior to the floor plate (figure 15Q, 16A). Nkx6.1 expression is also detected in post-mitotic neurons present in the mantle layer, which have been described in the hindbrain (figure 15Q, 16A) (Muller et al., 2003). These neurons lie in very close proximity to the OMC neurons, but co-expression studies must be conducted to determine whether they are the same cells.

In the *Foxa2 CKO* there is a variation in the affects of Shh signalling along the anterior-posterior axis as described previously. In the posterior mesencephalon the phenotype is more pronounced than in the anterior regions. The ventral domains of Nkx6.1 expression within the ventricular zone are absent from the posterior regions of the mesencephalon, and only a few post mitotic neurons are detected (figure 15R). The dorsal domain of Nkx.1 expression is unaltered. There is a ventral expansion of the Nkx2.2 domain towards the ventral midline whilst the dorsal limit of the Nkx2.2 domain is not affected (figure 15S-T). Measurements revealed that the length of the expression domain of Nkx2.2 is increased by 1.82X in the Foxa2 CKO. The ventral expansion of *Nkx2.9* is more dramatic than Nkx2.2, with the size of the *Nkx2.9* expression domain increasing by 7.67X that of the wild type (figure 15W-X).

In anterior regions of the mesencephalon the expression domain of Nkx6.1 appears to be restored to wild type levels, but there is a slight reduction in the level of Nkx6.1 protein within the ventricular zone close to the ventral midline (figure 16A-B). There is also a reduction in the number of Nkx6.1 positive post-mitotic neurons (figure 16B). The ventral limit of the Nkx2.2 domain is reduced in the anterior regions of the mesencephalon in comparison to the posterior regions (figure 16C-D) but creates a large

progenitor domain co-expressing Nkx2.2 and Nkx6.1 (figure 16E-F). This domain has increased in the *Foxa2 CKO* by 1.67X. Similar to Nkx2.2, there is an expansion of *Nkx2.9* gene expression in the anterior regions of the mesencephalon, but the range of the ventral expansion is not as great as in the posterior mesencephalon (figure 16G-H).

At E11.5 Nkx6.1 is expressed in a broad domain within the ventricular zone spanning the ABB, with a ventral limit prior to the ventral midline (figure 16I). There is a large population of Nkx6.1 positive post-mitotic neurons underlying immediately the ventricular zone of the basal plate. In the *Foxa2 CKO* the most ventral region of the Nkx6.1 expression domain within the ventricular zone shows a slight reduction in quantity of protein detected (figure 16J). In the wild type embryos, the domain of Nkx2.2 expression within the ventricular zone becomes restricted to a narrow strip of cells bordering the ABB (figure 16K). There is a narrow strip of post-mitotic neurons which express Nkx2.2 which are located in the ventral regions of the alar plate (figure 16K). In the *Foxa2 CKO* the ventral expansion of Nkx2.2 is persistent, and there is a five fold increase in the size of the Nkx2.2 domain within the ventricular zone as compared to wild type embryos (figure 16L) creating a larger Nkx2.2/Nkx6.1 co-expressing progenitor domain (figure 16M-N). Consistent with my previous findings, the effect on *Nkx2.9* is more dramatic than Nkx2.2. The *Nkx2.9* gene expression domain is increased by a factor of 6 in the *Foxa2 CKO* (figure 16O-P).

At E12.5 the expression of Nkx6.1 within the ventricular zone is restricted to two domains either side of the ABB (figure 16Q). The only post-mitotic neurons expressing Nkx6.1 are located in the region of the OMC, adjacent to the ventricular zone of the ventral midline. Within the ventricular zone, Nkx2.2 protein is detected in a narrow

domain adjacent to the ABB. There are two distinct populations of post-mitotic neurons expressing Nkx2.2, one lying dorsal to the ABB, and a thin line of neurons bordering the ABB (figure 16S). The vast expansion of the Nkx2.2 domain within the ventricular zone in the *Foxa2 CKO* persists, and is 11X larger than the wild type expression domain. There is no alteration in the size or location of the post-mitotic neurons within the alar plate, but in the basal plate a novel stream of neurons are exiting the ventricular zone at the ventral limit of the expanded domain (figure 16T). Interestingly, at E12.5 in the *Foxa2 CKO Nkx2.9* is less affected than Nkx2.2, and only displays an overall 2.5X expansion of the expression domain within the ventricular zone (figure 16W-X). To complement these data I performed *in-situ* hybridisation using RNA probes for all the antibodies used above, and the results are consistent with the above data (data not shown).

These data suggest that the progenitor domains within the ventral mesencephalon are altered in the *Foxa2 CKO* embryos from the onset of the recombination event and subsequent alteration in Shh signalling. The dorsal limits of every marker analysed remain constant, and only the ventral regions of the expression domains expand ventrally. Therefore the reduction in Foxa2 protein levels could cause an alteration in the mechanisms (via Shh) which maintain the ventral limits of the progenitor domains within the basal plate.

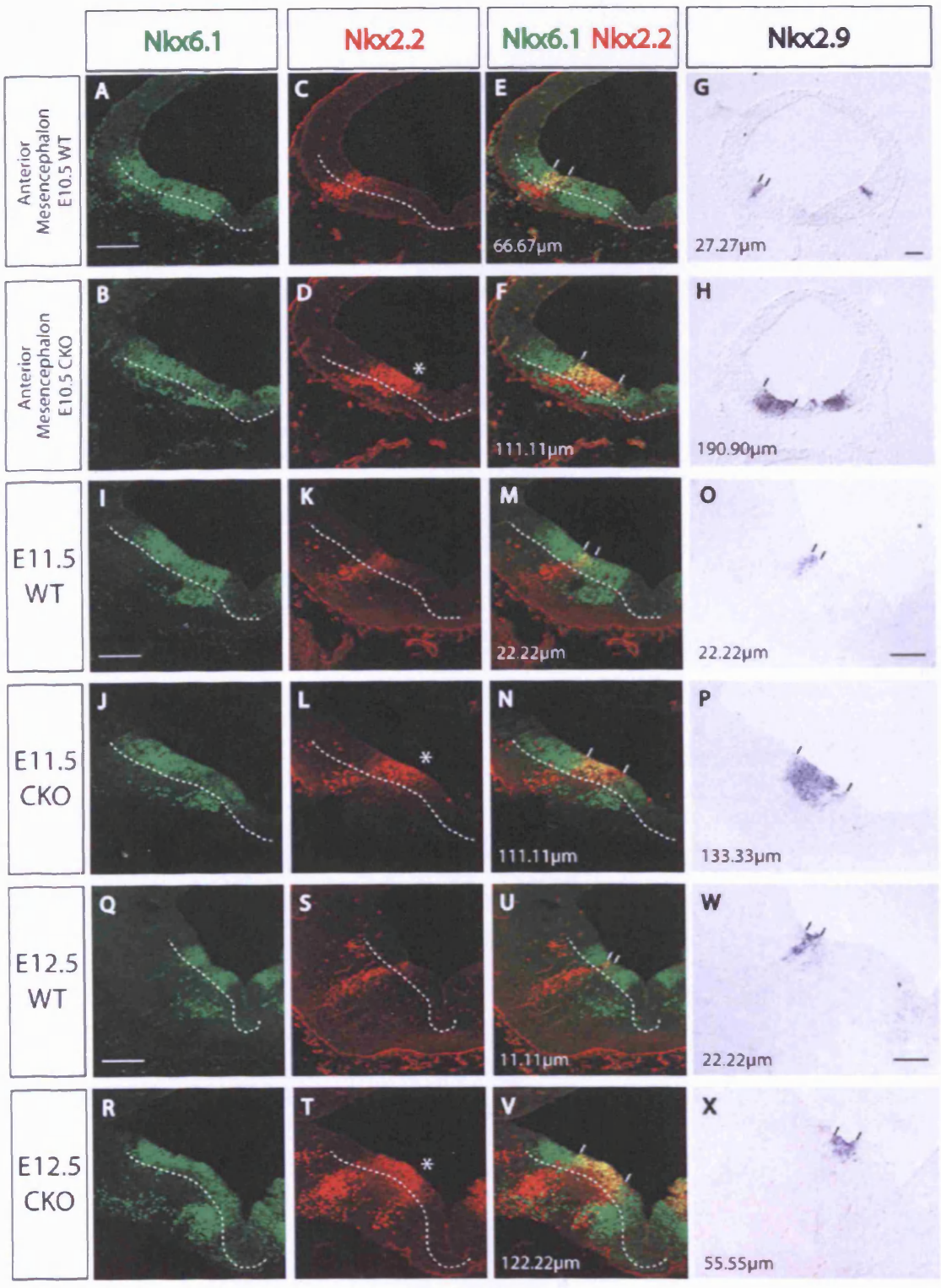

Figure 16: Analysis of Class II genes in the mesencephalon of the Foxa2 CKO (part b). *Coronal sections of both wild type and Foxa2 CKO embryos. Continuing the analysis of the Class II genes within the Foxa2 CKO at later stages revealed that the expression domain of Nkx6.1 (green) is virtually restored to the wild type levels from E10.5. Both Nkx2.2 (red) and Nkx2.9 (blue) display an expansion of their domains ventrally towards the ventral midline. Solid lines in E-H, M-P & U-X represent the domains of Nkx2.2 and Nkx2.9 in the wild type and Foxa2 CKO embryos.*

***Figure 16 continued**. However, whereas Nkx2.9 gene expression is clearly seen to gradually regress towards the ABB, the expanded domain of Nkx2.2 is persistent, maintaining the creation of a larger Nkx2.2/Nkx6.1 progenitor domain within the basal plate. Dotted lines illustrate the division between the ventricular zone and the mantle layer in the basal plate. D, L, T: Asterisk draws attention to the ventral expansion of the Nkx2.2 domain towards the ventral midline. Scale bars represent 100μm.*

In order to visualise the extent of the ventral expansion of Nkx2.2 and *Nkx2.9* I performed co-localisation studies using Foxa2 as a marker for the basal plate in the wild type, and for the remaining cells of the floor plate structure in the *Foxa2 CKO.*

At all the stages analysed the dorsal-lateral limit of the Foxa2 domain is the ABB. Thus it is possible to state with confidence that the Nkx2.2 domain spans the ABB with the majority of cells expressing Nkx2.2 situated dorsal to this boundary. At E9.5 80% of the Nkx2.2 positive progenitor cells co-express Foxa2 within the basal plate, and only a small population are located dorsal to the ABB (figure 17A). In the *Foxa2 CKO* there is clearly no co-expression between Foxa2 and Nkx2.2, and the ventral limit of the Nkx2.2 domain terminates some distance before the remaining floor plate cells (figure 17B).

At E10.5 in the posterior regions of the mesencephalon 44% of the Nkx2.2 expressing cells within the ventricular zone co-express Foxa2 (figure 17C). In the anterior regions of the mesencephalon this relationship is further reduced to 38.2% (figure 17E). In the anterior regions of the mesencephalon it is also evident that the only Nkx2.2 positive cells which co-express Foxa2 reside in the ventricular zone of the basal plate. The newly differentiated neurons in the mantle layer do not co-express Foxa2 (figure 17E). It is also clear that in the anterior regions of the *Foxa2 CKO* mesencephalon the extent of the ventral expansion of Nkx2.2 is reduced compared to the posterior regions (figure 17D, F).

At E11.5 and E12.5, the only cells which co-express Nkx2.2 and Foxa2 reside in the ventricular zone adjacent to the ABB (figure 17G, I). There is no co-expression between these two genes in any of the post-mitotic neurons which are located in the

mantle layer (figure 17G, I). In the *Foxa2 CKO* it is clear that the ventral limit of Nkx2.2 expansion terminates well before the remaining Foxa2 positive cells of the ventral midline (figure 17H, I).

From these data it is possible to characterise the ventral limit of the expanded *Nkx2.9* domain. Even though the expansion of *Nkx2.9* ventrally is greater than that of Nkx2.2 between E8.75 and E11.5, at no point does *Nkx2.9* reach the remaining floor plate cells.

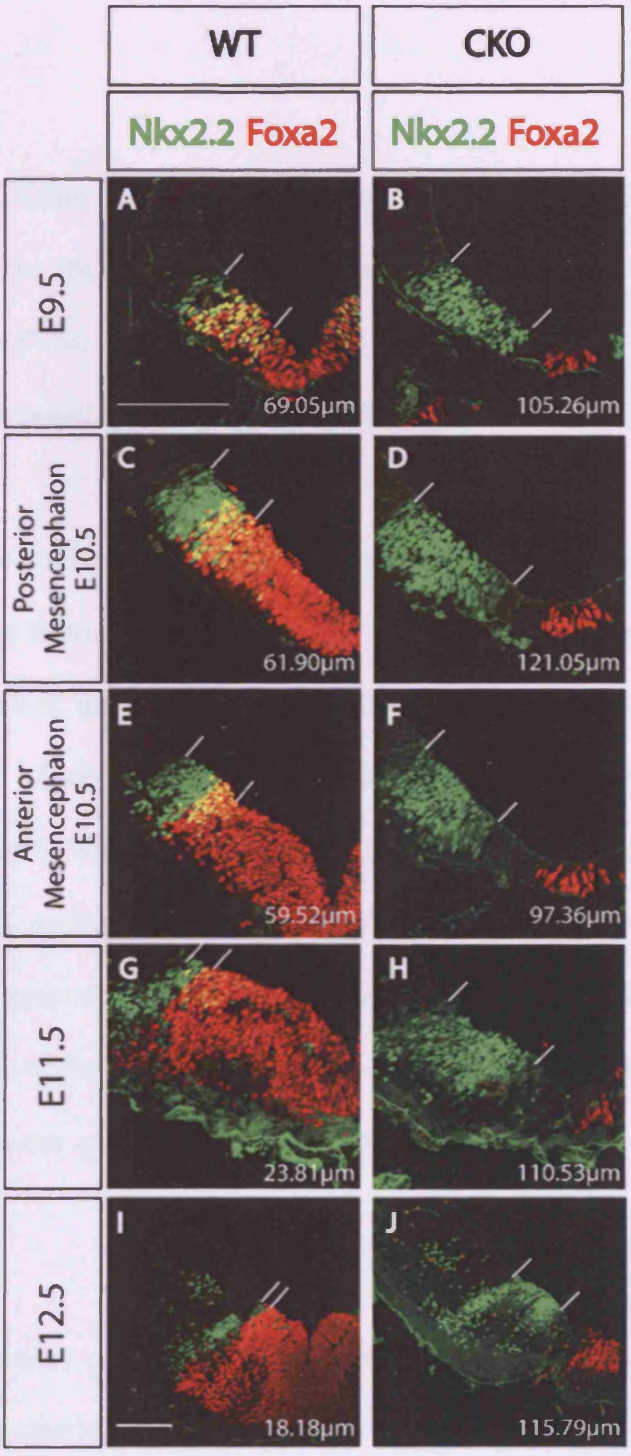

Figure 17: Relationship between Foxa2 and Nkx2.2. ***A-J:*** *To appreciate the extent of the ventral expansion of Nkx2.2 (green) in the Foxa2 CKO, Foxa2 was used as a marker for the ventral midline (red). The expansion of Nkx2.2 is consistent at all stages analysed, but there sharp boundary of expression between Foxa2 and Nkx2.2 is no longer present. Scale bar represents 100µm. Solid lines represent the domains of Nkx2.2 protein which were measured.*

14. Ventral expansion of *Nkx2.2* and *Nkx2.9* affects the generation of the OMC and RN

To determine whether the ventral expansion of the *Nkx2* family members (*Nkx2.2* & *Nkx2.9*) within the ventricular zone of the basal plate caused a possible alteration in the "progenitor code" for the OMC and RN, I performed double-immunohistochemistry using antibodies raised against Nkx2.2, Brn3a and Islet1.

In the wild type embryos the OMC progenitor cells are identified by the expression of the transcription factor *Phox2a* (Brunet and Pattyn, 2002; Pattyn et al., 1997). If we piece together all of the data generated from the co-expression studies it is possible to create an image of progenitor domains within the ventral mesencephalon. At E9.5 the OMC progenitor cells express a combination of *Foxa2*, *Phox2a* and *Nkx6.1* and are flanked by the expression domain of *Nkx2.2* and *Nkx2.9*. At later stages the combinatorial expression of *Foxa2*, *Phox2a* and *Nkx6.1* is maintained within the OMC progenitor cells, while the expression domain of *Nkx2.2* recedes dorsally bordering the ABB. Thus we can assume that *Nkx2.2* and *Nkx2.9* are never expressed by the OMC progenitor cells.

The OMC progenitor cells lie directly above the *Islet-1* expressing neurons (figure 7M-N), and there is clearly no overlap between them and the *Nkx2.2* domain (figure 18A). In the *Foxa2 CKO* the majority of the *Phox2a* expressing OMC progenitor cells now co-express *Nkx2.2* (figure 18B). This alteration coupled with the reduced levels of *Nkx6.1* expression (OMC reside in posterior mesencephalon) and the loss of *Foxa2*

from these progenitor cells suggests that the progenitor code for the OMC has been altered thus leading to the reduction of the neuronal population described previously.

At present there is no specific marker for the progenitor cells of the RN. Birth-dating studies have revealed that the RN neurons are first born at E11.5 (Altman and Bayer, 1981). At E11.5 the newly differentiated RN neurons are located immediately underlying the ventricular zone, suggesting that the RN progenitor cells must reside above the *Brn3a* positive neurons, in a similar domain to the OMC progenitor cells (figure 18C). At this stage the expression of *Phox2a* has been extinguished within this region of the ventricular zone, corresponding to the termination of OMC neuronal birth (Altman and Bayer, 1981). In the *Foxa2 CKO* at E11.5 there is a ventral expansion of *Nkx2.2* and *Nkx2.9* (figure 16K-P). This ventral expansion of both genes causes the majority of progenitor cells located in the hypothesised "RN progenitor domain" to ectopically express *Nkx2.2* and *Nkx2.9* (figure 18D). Thus the "progenitor code" of the RN progenitors is also altered in the *Foxa2 CKO*, which again could be linked to the reduction in the population of *Brn3a* positive RN neurons.

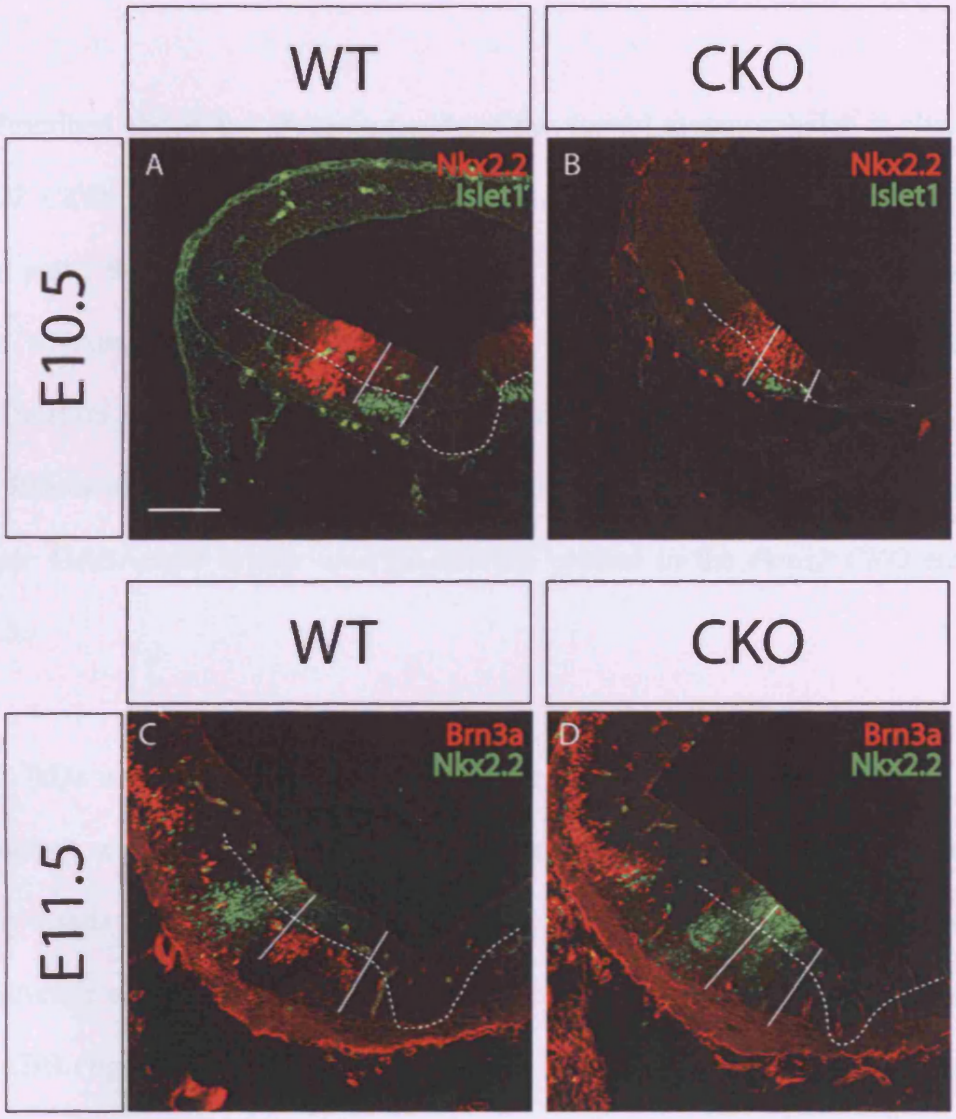

Figure 18: Does ventral expansion of Nkx2.2 interfere with correct specification of OMC or RN neuronal populations in the Foxa2 CKO? ***A-B:*** *In the wild type embryos, Nkx2.2 is not involved in the development of the OMC neurons. In the Foxa2 CKO there is a ventral expansion of Nkx2.2 into the region of the ventricular zone where the OMC progenitor cells are located (domain within solid lines), coinciding with the reduction in the OMC neuronal population.* ***C-D:*** *Markers labelling the progenitor cells of the RN are not currently known, but it is evident that Nkx2.2 is not expressed by these progenitor cells (domain within solid lines). In the Foxa2 CKO the ventral expansion of Nkx2.2 within this progenitor domain persists coinciding with the absence of Brn3a positive RN neurons at E11.5. Scale bar represents 100μm. Dotted lines represent the ventricular zone within the basal plate.*

15. No change in cell fate specification within the basal plate of the *Foxa2 CKO*

As described above, the progenitor code of the ventral mesencephalon is altered in the *Foxa2 CKO* embryos between E8.75 and E12.5. Within the ventricular zone of the basal plate, there is a dramatic expansion of *Nkx2.2* and *Nkx2.9* which creates a new large co-expression domain with *Nkx6.1*. To rule out a possible change of cell specification and the generation of alternate cell fates at the expense of the neuronal populations of the ventral mesencephalon, I investigated whether there were either any ectopic GABAergic or Serotonergic neurons present in the *Foxa2 CKO* embryos at E12.5.

The 67kDa isoform of glutamic acid decarboxylase *Gad67* is expressed by the majority of neurons which use the neurotransmitter γ-aminobutyric acid (GABA) (Asada et al., 1996; Asada et al., 1997). *Gad67* staining reveals that in the wild type embryos, GABAergic neurons are located in the dorsal mesencephalon, with a ventral limit along the ABB (figure 19A). In the *Foxa2 CKO* there is no ventral expansion or ectopic expression of *Gad67* within the basal plate indicating that no ectopic GABAergic neurons are generated in this region (figure 19D).

The Serotonergic neurons, identified using an antibody raised against 5-Hydroxy Tyrosine (5-HT), are not located in the ventral mesencephalon of wild type embryos (figure 19B), but reside in r1 of the hindbrain (figure 19G) (Schambra et al., 1990; Vernay et al., 2005).

There was some 5-HT immunoreactivity in both the wild type and *Foxa2 CKO* embryos in the most ventral regions of the mesencephalon (figure 19B, E). When this immunoreactivity was compared to that of the hindbrain positive control slide, it was evident that the staining in the mesencephalon did not represent neuronal cell bodies, but rather fibres from the serotonergic neurons of r1 (figure 19G). This was confirmed by performing co-localisation assays using the nuclear marker toto-3-iodide (figure 19C, F). It has recently been reported that some fibres from the 5-HT positive neuronal population are known to cross the MHB and reach the mesencephalon (Zervas et al., 2004). These results indicate that there are no ectopic serotonergic neurons generated in the *Foxa2 CKO* embryos.

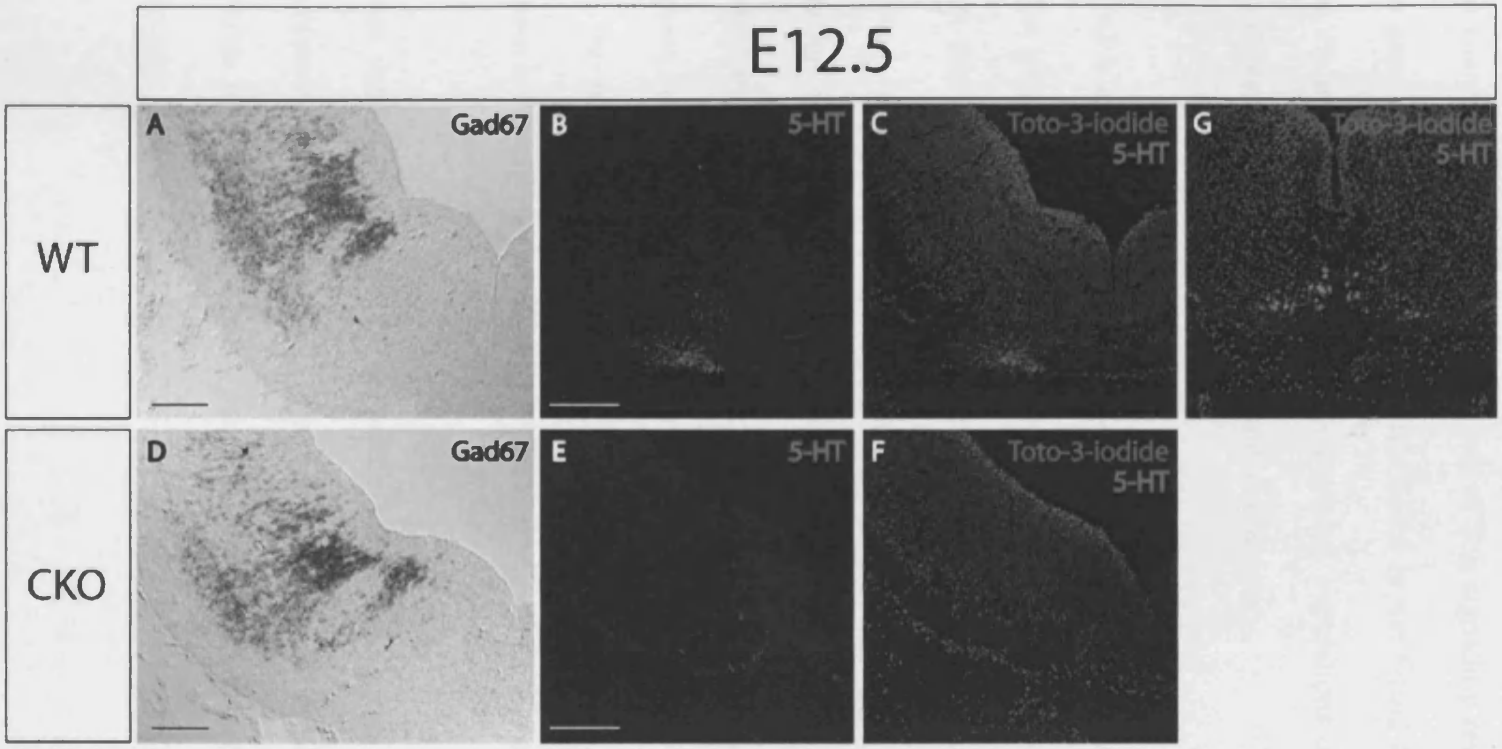

Figure 19: No re-specification of neuronal subtypes in the basal plate of the Foxa2 CKO. A-F: *Coronal sections of mesencephalon. In the Foxa2 CKO there is an alteration in the ventral progenitor domains of the basal plate with a new broader Nkx2.2/Nkx2.9/Nkx6.1 domain, which could possibly cause a re-specification of the ventral neuronal populations, leading to the losses of the mesDA, RN and OMC neurons described previously. Following analyses of markers for GABAergic and Serotonergic neurons, it was evident that no re-specification occurred in the basal plate in response to the alteration in the ventral progenitor domains. Some Serotonergic neuronal fibres (note that there is no nuclear staining) from r1 cross the MHB and reach the posterior regions of the mesencephalon.* ***G:*** *Coronal section of anterior hindbrain to demonstrate the Serotonergic neuronal population located in r1. Scale bar represents 100μm.*

16. Foxa1 is maintained in the remaining mesDA and RN neurons of the *Foxa2 CKO*

The analysis of the downstream targets of Shh signalling revealed that both *Foxa1* and *Shh* gene expression are restored after E10.5 in the *Foxa2 CKO*. Analysis to confirm that the remaining mesDA and RN neuronal populations of the *Foxa2 CKO* express *Foxa1* was carried out using immunohistochemistry.

Foxa2 is expressed by all the mesDA neuronal population and 92% of the RN neurons in the wild type embryos (figure 20A-B, E). Foxa1 protein can also be detected within these neuronal populations, but at reduced levels to Foxa2 based on the sensitivity of the antibody staining (data not shown). In the *Foxa2 CKO* there is no co-expression between mesDA neuronal population and the remaining Foxa2 protein detected in the ventral midline (figure 20C). In contrast all of the remaining mesDA population express Foxa1 protein (figure 20D). Equally there is no co-expression between Foxa2 and the remaining RN population in the *Foxa2 CKO* (figure 20F) whereas Foxa1 protein is detected in the majority of the remaining Brn3a positive neurons (figure 20G).

These data indicate that the remaining mesDA and the RN neurons maintain the expression of Foxa1 protein in the absence of Foxa2 protein. This could suggest a possible intrinsic compensatory role for *Foxa1* in the mesencephalon when *Foxa2* is reduced

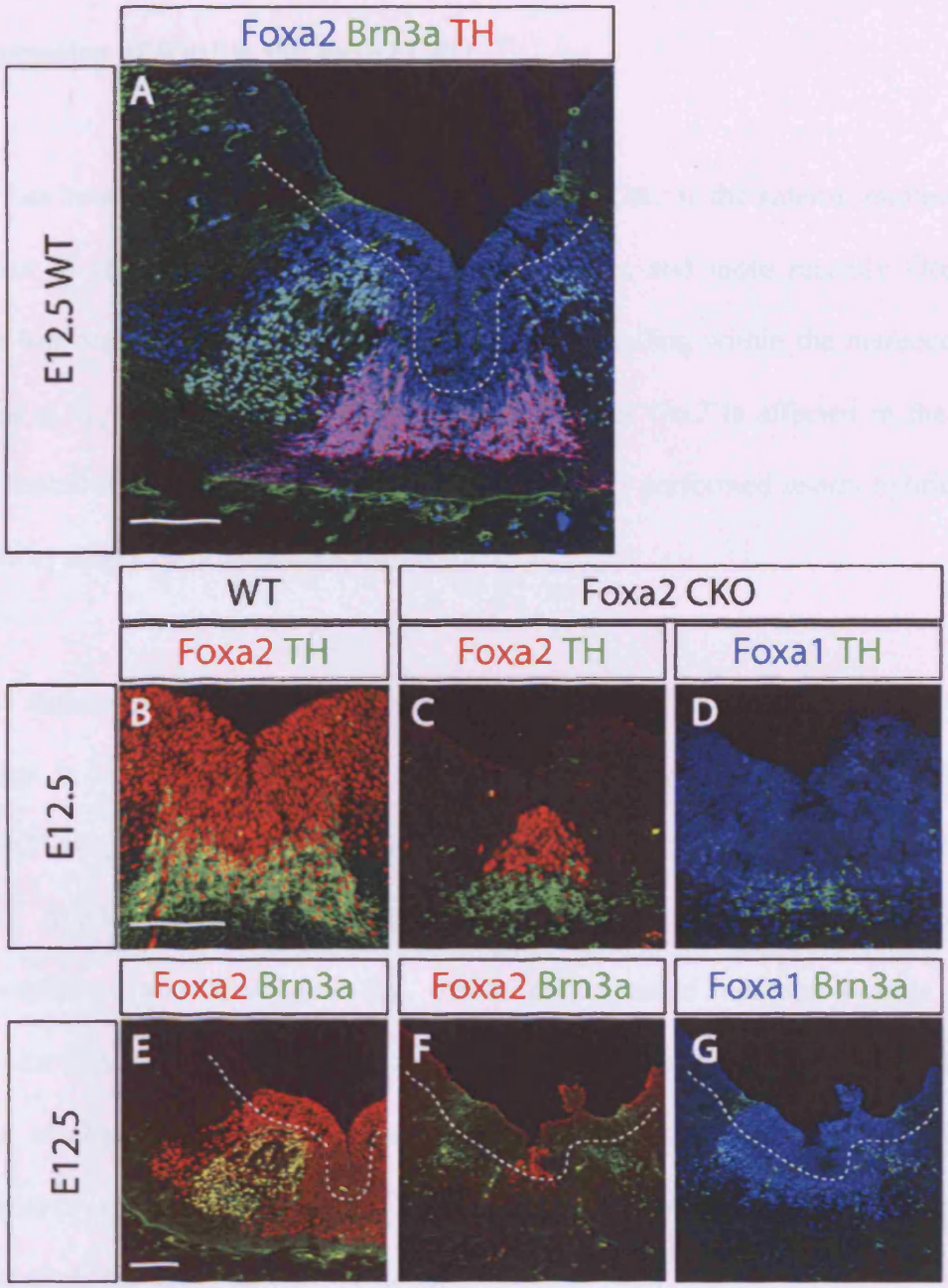

Figure 20: Foxa1 protein found within the RN and mesDA neuronal populations at E12.5 in the Foxa2 CKO. ***A:*** *The neurons of the RN (green) and mesDA (red) at E12.5 co-express Foxa2 (blue).* ***B-G:*** *In the Foxa2 CKO there is a 92% reduction of cells expressing the Foxa2 protein within the ventral mesencephalon and none of the neuronal populations of the basal plate express Foxa2. When Foxa1 gene expression is restored after E10.5 the mesDA and RN neurons maintain the expression of Foxa1, which suggests a role in the maintenance of these neuronal populations by proteins of the Foxa family. Scale bars represent 100μm. Dotted lines represent the ventricular zone of the basal plate.*

17. The mesencephalon is correctly specified and there is a dramatic over-expression of *Wnt1* in the *Foxa2 CKO*

Foxa2 has been demonstrated to work in tandem with *Otx2* in the anterior midline of the forebrain to control Shh signalling (Jin et al., 2001), and more recently *Otx2* gene dosage has been implicated in the control of Shh signalling within the mesencephalon (Puelles et al., 2003). In order to investigate whether *Otx2* is affected in the *Foxa2 CKO*, contributing to the reduction of Shh signalling, I performed *in-situ* hybridisation analysis of stages E9.5 to E12.5.

Otx2 is expressed by all progenitor cells of the mesencephalon. At E9.5 there is no alteration in the expression pattern of *Otx2* along the entire anterior-posterior axis (figure 21A-B). This observation holds true for stages E10.5 and E11.5 (data not shown). At E12.5 *Otx2* can be clearly detected within the ventricular zone of the entire mesencephalon, and also in a few newly differentiated neurons outside of the ventricular zone (figure 21C). In the *Foxa2 CKO* there is no alteration in the expression domain of *Otx2* within the ventricular zone, but there are fewer neurons within the mantle layer expressing *Otx2* (figure 21D). *Otx2* expression within the ventricular zone is intact along the entire anterior-posterior axis.

These data coupled with the finding that there is no ectopic *Fgf8* expression within the mesencephalon (data not shown) suggests that the mesencephalon is correctly specified throughout development, and that the reduction in Shh signalling is not due to an alteration in *Otx2* gene expression.

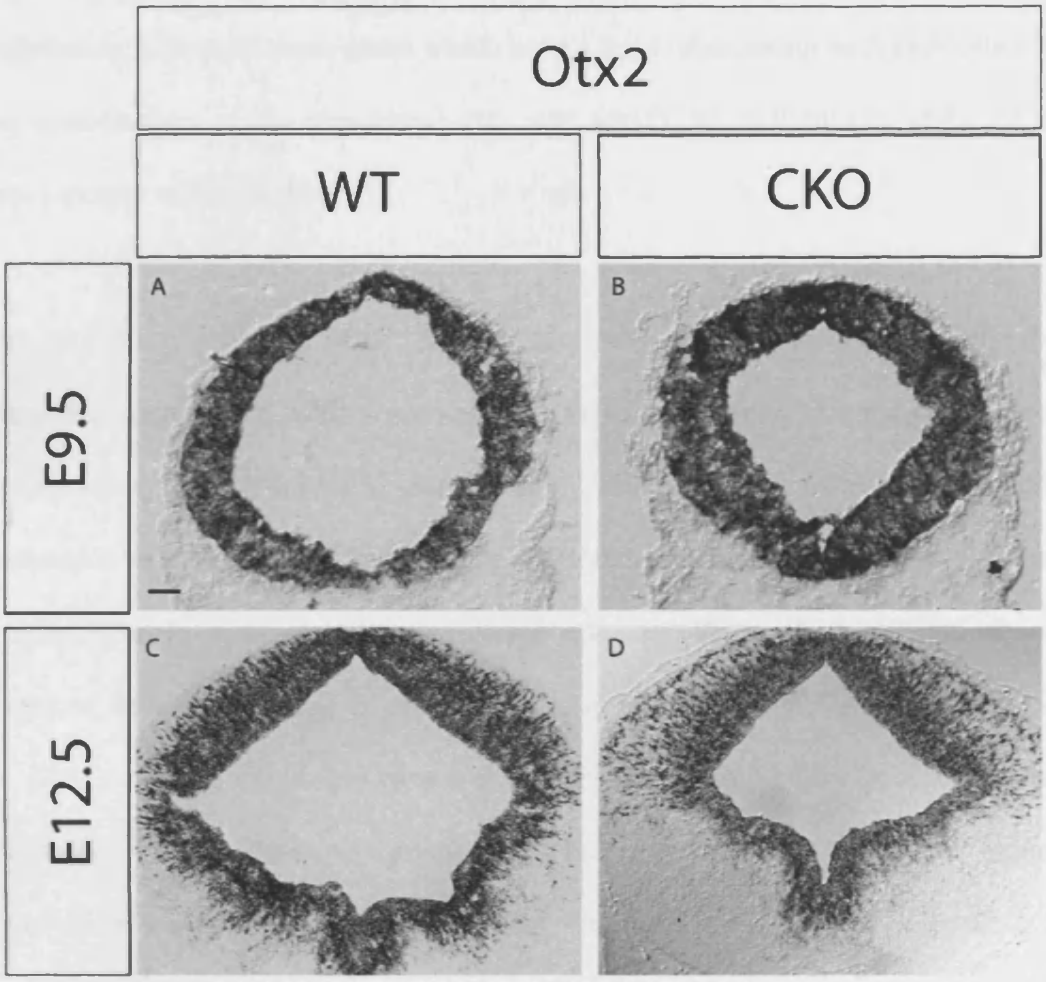

Figure 21: Mesencephalon of Foxa2 CKO is correctly specified. *Gene expression of Otx2, a mesencephalic determinant, at all stages analysed in the Foxa2 CKO reveal that there is no mis-specification of the mesencephalic regions during embryonic development. (Although the ventricular zone of embryo B seems much thicker than its wild type counterpart (A) analysis of all the embryos at this stage do not support an over-expression of Otx2. This phenomenon can be attributed to differential development of the embryos within the same litter) Scale bar represents 100μm.*

Following the finding that *Otx2* is unchanged in the *Foxa2 CKO*, I analysed the expression patterns of three genes which have a tight relationship with each other during the specification of the mesencephalon, and which are individually involved in the development of the mesDA.

The signalling molecule *Wnt1* is an important factor in the specification of the mesencephalon. Mice with a homozygous deletion of *Wnt1* lose the entire forebrain and mesencephalon (McMahon and Bradley, 1990) due to the inability to maintain the expression of the transcription factor *En1* (McMahon et al., 1992). *En1* is expressed in a broad domain in the presumptive mesencephalon (Wurst et al., 1994) and in later stages of development *En1* is expressed in the developing mesDA neurons (Simon et al., 2001) and has the ability to rescue the *Wnt1* knockout phenotype (Danielian and McMahon, 1996). These two genes, in combination with *Lmx1b* and other factors are involved in the early specification of the mesencephalon (Wurst and Bally-Cuif, 2001) and the development of the mesDA (Maxwell and Li, 2005).

The wild type expression pattern of *Wnt1* at E9.5 is identical to the expression pattern at E10.5 (data not shown). At E10.5 there are two stripes of *Wnt1* expression flanking the ventral midline within the ventricular zone (figure 22A). There are also some differentiated neurons within the mantle layer immediately underlying the *Wnt1* expression in the ventricular zone (figure 22A). In the *Foxa2 CKO* there is a dramatic over-expression of *Wnt1*, and *Wnt1* gene expression can be detected within the cells of the ventral midline (figure 22B). This over-expression is maintained throughout the anterior-posterior axis of the ventral mesencephalon. *Wnt1* gene expression is also detected ectopically dorsal to the ABB (figure 22B arrowhead). At E11.5 the over-

expression of *Wnt1* is persistent within the ventral mesencephalon, while the domain of ectopic *Wnt1* expression dorsal to the ABB has also expanded dorsally (figure 22C-D). This pattern of over-expression is un-altered in the *Foxa2 CKO* at E12.5 (figure 22E-F). There is no change in the expression of *Wnt1* in the roof plate at any embryonic stage analysed (figure 22A-F).

At E10.5 *En1* gene expression is detected in a broad domain along the ventral mesencephalon similar to *Foxa2* gene expression (figure 22G). *En1* gene expression is detected at higher levels in the post-mitotic neurons within the mantle layer either side of the ventral midline (figure 22G). In the *Foxa2 CKO* the size of the *En1* expression domain is unaltered, but there is uniform expression of *En1* throughout the ventricular zone and the differentiated neurons of the mantle layer (figure 22H). At E11.5 the wild type expression pattern of *En1* clearly resembles that of *Foxa2* within the ventricular zone. *En1* gene expression is detected spanning the ABB to the ventral midline, and is detectable in the newly differentiated mesDA neurons located immediately ventral to the midline (figure 22I). There is no alteration in the gene expression pattern within the *Foxa2 CKO* at E11.5 (figure 22J). At E12.5, *En1* gene expression within the ventricular zone is detected at lower levels than in the post-mitotic mesDA neurons (figure 22K). In the *Foxa2 CKO* there is no alteration of *En1* gene expression within the ventricular zone, and is detected within the remaining mesDA neuronal population (figure 22L).

Lmx1b gene expression in the *Foxa2 CKO* is unaltered at E10.5 as previously described (figure 5C-D, figure 22M-N). At E11.5 *Lmx1b* gene expression is detectable within the newly differentiated mesDA neurons at higher levels to the gene expression within the ventricular zone (figure 22O). In the *Foxa2 CKO* there is no alteration in this pattern of

gene expression (figure 22P). At E12.5, as previously described (figure 5O-P) there is no alteration in the gene expression within the ventricular zone of the ventral midline, and is detected throughout the remaining mesDA neurons within the mantle layer (figure 22R). *Lmx1b* gene expression within the roof plate, as *Wnt1*, is unaffected by the reduction in *Foxa2* (figure 22M-R).

These results indicate that *Lmx1b* and *En1* gene expression are not affected by the 92% reduction in Foxa2 protein levels at any embryonic stage analysed. *Wnt1* gene expression is dramatically over-expressed within the ventral midline from E9.5, indicating a possible role for *Foxa2* in the down-regulation of *Wnt1* in the ventral midline of the wild type mesencephalon. Unfortunately there is no functional antibody raised against Wnt1 protein, so it was not possible to quantify the over-expression of *Wnt1* in this project.

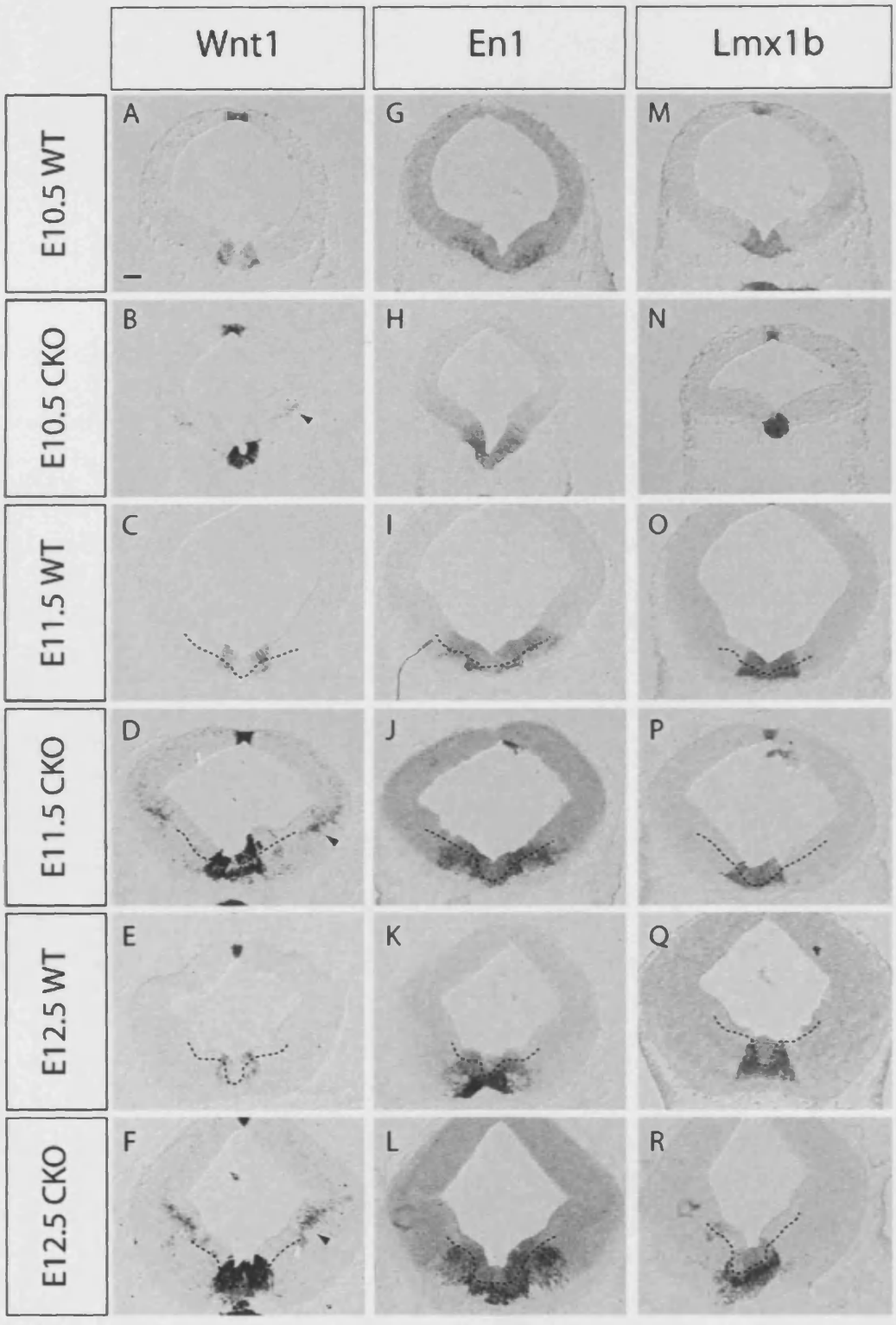

Figure 22: Analysis of genes involved in the early specification of the mesencephalon and which play a role in the development of the mesDA neuronal population. *A-R: Coronal sections of both wild type and Foxa2 CKO embryos. Wnt1, En1 and Lmx1b are expressed by the mesDA progenitor cells during the early stages of their development.*

Figure 22 continued: *In the Foxa2 CKO the gene expression patterns of En1 and Lmx1b are unchanged within the ventricular zone , and at later stages when the differentiated mesDA neurons also express these genes, the gene expression patterns resemble the remaining mesDA neuronal population. However, throughout all the stages analysed there is a dramatic over-expression of Wnt1 expression at the ventral midline of the mesencephalon, combined with ectopic Wnt1 expression within the lateral regions of the alar plate (arrowheads). The Wnt1 expression in the roof plate at the dorsal midline is unaltered throughout the embryonic development of the Foxa2 CKO. Scale bar represents 100μm. Dotted lines aid visualisation of ventricular zone within basal plate.*

18. Expression patterns of *Nkx6.1* and *Irx3* partially overlap with OMC neurons and *Irx3* expression in the ventricular zone suggests a candidate for RN progenitor cell marker

While analysing the Class I and Class II homeodomain transcription factors, it became apparent some post mitotic neurons express *Nkx2.2*, *Nkx6.1* or *Irx3*. In particular, the post mitotic neurons within the basal plate which express *Nkx6.1* and *Irx3* are situated in similar domains to the OMC and the RN. To confirm these speculations, co-localisation studies were performed using markers for the OMC and RN.

These studies revealed that post mitotic neurons expressing Irx3 are located within the OMC neurons. At E10.5 there is no co-expression between the Islet-1 positive OMC neurons and Irx3 in both the wild type and *Foxa2 CKO* (figure 23A-B). At E11.5 in the wild type embryos, the majority of OMC neurons express Irx3 (figure 23C), while in the *Foxa2 CKO* there is no co-expression of these two transcription factors (figure 23D). In the wild type embryos at E12.5 this co-expression is persistent (figure 23E), while some of the OMC neurons in the *Foxa2 CKO* co-express Irx3. However, due to the low sensitivity of the Irx3 antibody within the mesencephalon I am not able to provide confident data on the co-expression of Irx3 and the OMC. *In-situ* hybridisation analysis (figure 14) indicated that there were more post-mitotic neurons expressing *Irx3*.

Further studies revealed that at E10.5 the differentiated OMC neurons co-express Nkx6.1, and this relationship was maintained in the *Foxa2 CKO* (figure 23G-H). At E11.5 the amount of co-expression between these two transcription factors is reduced in the wild type embryos (figure 23I) whereas in the *Foxa2 CKO* all the remaining OMC

neurons are co-expressing Nkx6.1 (figure 23J). At E12.5 the level of co-expression in the wild type embryos is dramatically reduced, with only a few OMC neurons also expressing Nkx6.1 (figure 23K), while there is a higher proportion of the remaining OMC neurons in the *Foxa2 CKO* co-expressing Nkx6.1 (figure 23L).

Studies on the RN neurons revealed that at E12.5 there is no co-expression between the Brn3a positive population and Irx3 (figure 23M). This study provided further evidence that the OMC neurons co-express Irx3 (OMC reside within a pocket of RN neurons at E12.5, figure 1A). At E12.5 there is a salt and pepper like relationship between Brn3a and Nkx6.1, with some co-expression detected in the newly differentiated RN neurons located closest to the ventricular zone (figure 23N). In the *Foxa2 CKO* the remaining Brn3a positive RN neurons lie immediately above the post-mitotic neurons expressing Nkx6.1, and there is minimal co-expression (data not shown). There is no co-expression between Nkx2.2 and any of the neuronal populations of the ventral mesencephalon. The post-mitotic neurons expressing Nkx2.2 are located at the ABB (figure 23O).

These studies indicate that both Irx3 and Nkx6.1 are co-expressed with the OMC neurons, and could possible play a role in their development or maintenance. In the *Foxa2 CKO* the relationship between the OMC and these two transcription factors is maintained. The majority of the RN neurons do not co-express any of these two transcription factors.

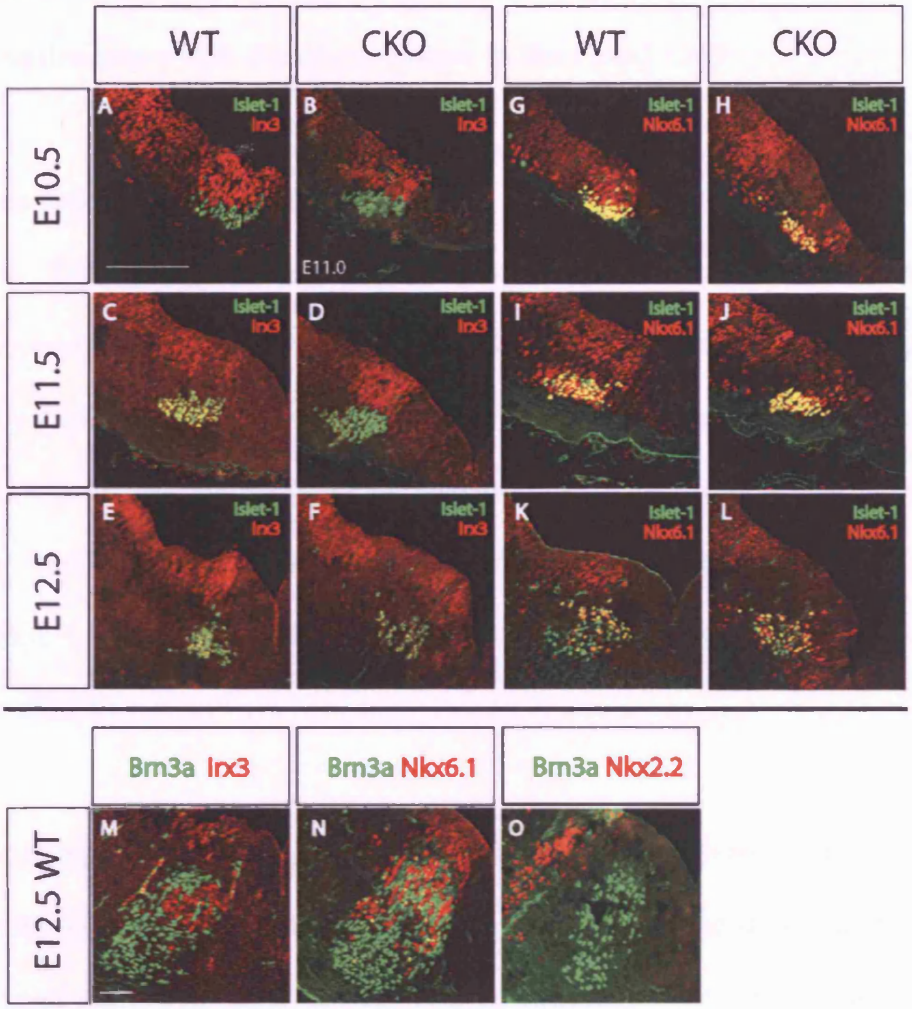

Figure 23: ***Co-expression studies to identify genes expressed by the differentiated OMC and RN neuronal populations.*** ***A-F:*** *previous experimental data suggested that Irx3 could be co-localised with either the RN or OMC neurons. Using the α-Irx3 antibody (red) and α-Islet-1 antibody (green) it was evident that co-expression of these two genes is transient. Irx3 protein is detected within the ventricular zone dorsal to the OMC neurons at all stages analysed, while at E11.5 and E12.5 the majority of OMC neurons co-express Islet-1. In the Foxa2 CKO there is no co-expression of Irx3 and Islet-1 at E11.5, but the wild type relationship is partially restored at E12.5.* ***G-L:*** *The post-mitotic neurons expressing Nkx6.1 were also located within an area resembling the location of the OMC or RN neurons. The OMC neurons co-express Nkx6.1 completely at E10.5 in the wild type embryos, and only partially at E11.5 and E12.5. In the Foxa2 CKO all the remaining OMC neurons express Nkx6.1 at E10.5 and E11.5, while at E12.5 the wild type situation is partially restored.* ***M-O:*** *Analysis of wild type embryos at E12.5 revealed that there is no co-expression between Irx3 and the RN neurons (Brn3a positive). The post-mitotic Nkx6.1 neurons are intermingled with the RN neurons, but there is very little co-expression. None of the post-mitotic Nkx2.2 neurons are co-expressed with any of the ventral neuronal populations. Scale bar represent 100μm.*

19. The ventral boundary of *Gli2* in the mesencephalon abuts *Foxa2* at the ABB. A relationship which *Foxa1* can mimic in the *Foxa2 CKO*

Whilst analysing the targets of Shh signalling, I described the ventral limit of *Gli2* to be the ABB. This border corresponds to the dorsal-lateral limit of *Foxa2* expression. This was surprising as *Gli2* is believed to be the primary transducer of Shh signalling, thus it would be expected that *Gli2* form a boundary with the dorsal-lateral limit of the *Shh* expression domain. To investigate the hypothesis that a possible role of *Foxa* (*HNF3*) proteins within the mesencephalon is to repress the ventral limit of *Gli2* gene expression, I performed double *in-situ* hybridisation experiments on *Foxa2 CKO* from E10.5 to E12.5.

In the wild type embryos along the anterior-posterior axis, the ventral limit of *Gli2* gene expression within the ventricular zone abuts the ABB and the dorsal-lateral extent of *Foxa2* gene expression (figure 24**"X"** A-C arrowheads). The ventral limit of the *Gli2* expression domain does not reach the *Shh* expression domain, and a region of several cell diameters separates the two expression domains (figure 24**"X"** D-E).

The ventral extent of the *Gli2* expression domain forms a sharp boundary with *Foxa2* at the ABB at all the stages analysed in the wild type embryos (figure 24**"Y"** A, E, I). In the *Foxa2 CKO* at E10.5 the ventral limit of the *Gli2* domain depends upon the location of the mesencephalon along the anterior-posterior axis. In the posterior regions of the mesencephalon the ventral limit of *Gli2* reaches the *Foxa2/Foxa1/Shh* domain (data not shown) while in the anterior regions of the mesencephalon the ventral extent of the *Gli2* domain is repressed ventrally and resembles the wild type gene expression pattern

(figure 24**"Y"** B). At later stages the expression domain of *Gli2* is identical to the wild type pattern (figure 24**"Y"** F-G). In the wild type embryos, the relationship between *Foxa1* and *Gli2* resembles the relationship between *Shh* and *Gli2* (figure 24**"Y"** C, G, K). However, in the *Foxa2 CKO* embryos, the ventral limit of *Gli2* gene expression forms a sharp boundary with the dorsal-lateral limit of the restored *Foxa1* gene expression domain (figure 24**"Y"** D, H, L).

These results suggest that the restoration of *Gli2* to its wild type expression domain in the *Foxa2 CKO* could be caused by the restored function of *Foxa1*, compensating the loss of *Foxa2*.

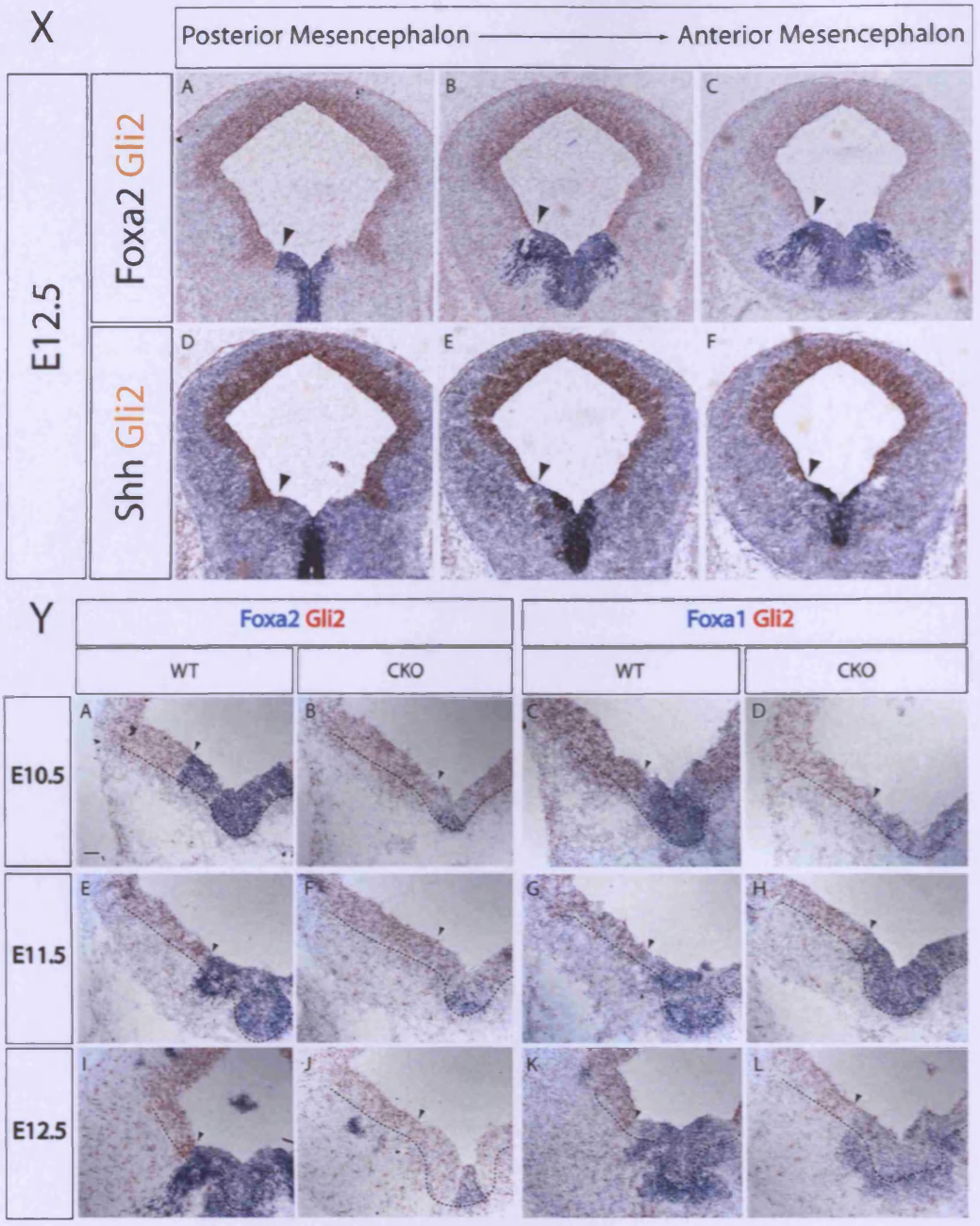

Figure 24: Relationship between Foxa2, Foxa1 and Gli2 in the mesencephalon. X: A-F: *In the wild type embryo at E12.5, Gli2 gene expression is detected within the ventricular zone of the entire alar plate, with the ventral limit of expression located at the ABB abutting the Foxa2 gene expression domain. Shh gene expression never reaches the ABB and thus never forms a boundary with Gli2. Foxa1 gene expression generally overlaps with Shh gene expression, thus in the wild type embryos there is no boundary created between Foxa1 and Gli2 gene expression. Arrowheads correspond to ventral limit of Gli2 gene expression.*

Figure 24 continued: ***Y:A-L:*** *Analysis of the Foxa2 CKO embryos using double in-situ hybridisation allowed the visualisation of the dynamic ventral expansion of Gli2 in response to the reduction of Foxa2. At all stages analysed in the wild type embryos, Gli2 gene expression abuts the Foxa2 expression domain. In the Foxa2 CKO, the ventral limit of Gli2 gene expression expands ventrally initially but is restored at later stages. This restoration is most evident in the anterior regions of the mesencephalon at E10.5. In the Foxa2 CKO the ventral limit of Gli2 expression forms a sharp boundary with Foxa1 gene expression, suggesting that Foxa1 has taken the role of Foxa2 in maintaining the ventral limit of Gli2 gene expression. Arrowheads indicate ventral limit of Gli2 expression domain. Dotted lines depict the ventricular zone of the basal plate. Scale bars represent 100μm.*

20. *Wnt1-Cre* mouse strain not responsible for *Foxa2 CKO* phenotype

It has been shown that in some cases the presence of the Cre recombinase protein can cause cell toxicity (Loonstra et al., 2001; Silver and Livingston, 2001). Although previous studies have used the *Wnt1-Cre* mouse line to drive recombination (Brault et al., 2001), I thought it prudent to perform *in-situ* hybridisation analysis on *Wnt1-Cre* embryos to determine whether the phenotype described in the *Foxa2 CKO* was attributed to the *Wnt1-Cre*.

I firstly analysed the gene expression patterns of *Foxa2*, *Foxa1* and *Shh* in both wild type and *Wnt1-Cre* embryos. There was no alteration in the expression patterns of these genes, indicating that there is no phenotype caused by the activity of the Cre recombinase (figure 25A-F). To complete this analysis I check the expression domains of the genes which mark the specific neuronal populations of the ventral mesencephalon. *Brn3a*, *Islet1*, and *TH* gene expression are not altered in the *Wnt1-Cre* embryos further suggesting that the phenotype described at E12.5 in the *Foxa2 CKO* is not due to the activity of the Cre recombinase (figure 25G-L).

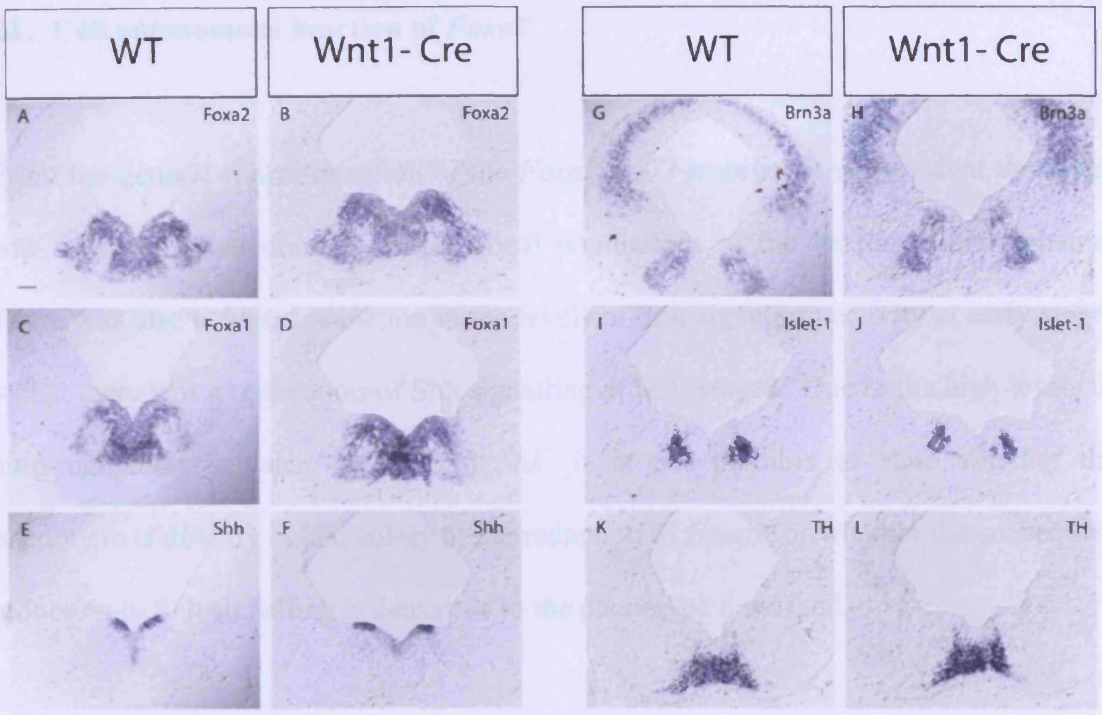

Figure 25: Wnt1-Cre mouse strain not responsible for Foxa2 CKO phenotype. *To ensure that the toxicity of the Cre recombinase protein was not inducing the phenotype described for the Foxa2 CKO, the expression domains of six genes which were affected at E12.5 were analysed on Wnt1-Cre + embryos. There was no alteration in gene expression patterns of any gene analysed, indicating that the Cre recombinase was causing the phenotype described. Scale bar represents 100μm.*

21. Cell autonomous function of *Foxa2*

From the general characterisation of the *Foxa2 CKO* embryos it was evident that there was a dramatic reduction in the neuronal populations of the ventral mesencephalon. There was also a severe reduction in the levels of Shh signalling activity at early stages whilst there was a restoration of Shh signalling at later stages. Due to the high levels of auto-regulation between *Foxa2* and *Shh*, it is not possible to state whether the phenotype is directly linked solely to the reduction of *Foxa2*, or whether the subsequent reduction in Shh signalling is causative to the phenotype described.

To address this issue and to investigate the possible cell autonomous role of *Foxa2* within the ventral mesencephalon, chimaeric embryos composed of wild type cells and *Foxa2 CKO* cells were created (*Foxa2* χ). The *Foxa2* χ were generated by aggregating Morula stage embryos generated by crossing $Foxa2^{floxed/+}$; *Wnt1-Cre* males with $Foxa2^{floxed/floxed}$ females into Morula stage embryos generated by crossing heterozygous B5/EGFP males (Hadjantonakis et al., 1998) with Parkes females. EGFP is expressed in all cells derived from the B5/EGFP males and was used to distinguish between wild type cells (EGFP positive) and *Foxa2 CKO* cells (GFP negative. Following the aggregation, embryos were implanted into pseudo-pregnant transfer mice and were allowed to develop naturally until they were harvested at E10.5 and E12.5. The control *Foxa2* χ (WT *Foxa2* χ) embryos used in the following analysis were $Foxa2^{floxed/floxed}$; GFP^{+} whilst the mutant *Foxa2* χ (CKO *Foxa2* χ) embryos were $Foxa2^{floxed/floxed}$; *Wnt1-Cre* $^{+}$; GFP^{+}. Newly dissected embryos were viewed under a dissecting microscope with ultra violet (UV) light, and embryos positive for GFP expression were selected for genotyping by PCR analysis to identify the presence of the *Wnt1-Cre*, and prepared for

immunohistochemical analysis. Following PCR analysis, selected embryos were fixed, cryosectioned and analysed under UV light to find ones suitable for further analysis which displayed a mixture of both wild type and *Foxa2 CKO* cells within the basal plate. Furthermore, the chimaeric embryos were sorted as strong or weak, depending upon qualitatively estimating the amount of CKO *Foxa2* χ cells present within the basal plate.

In the WT *Foxa2* χ there was no difference between the strong or weak chimaeric embryos (data not shown), while in the CKO *Foxa2* χ the phenotype was more severe in the strongly chimaeric embryos as compared to the weaker chimaeric embryos (data not shown). At E12.5 in the WT *Foxa2* χ all of the GFP negative cells (figure 26A arrowheads) do not possess the *Wnt1-Cre* and are equivalent to wild type cells, as seen by the detection of Foxa2 protein (figure 26A-C). In the *Foxa2 CKO* embryos there is a restoration of *Foxa1* and *Shh* from E10.5 onwards. In the WT *Foxa2* χ embryos both Foxa1 and Shh proteins are detected in the basal plate in the expected locations (figure 26D-F, Shh data not shown). To complete the analysis of the WT *Foxa2* χ I confirmed that both markers for the mesDA and RN were as described in the wild type embryos. Both TH and Brn3a proteins were as described for wild type embryos (figure 26G-I).

These results indicate that the WT *Foxa2* χ were comparable to the wild type embryos used in all previous analyses.

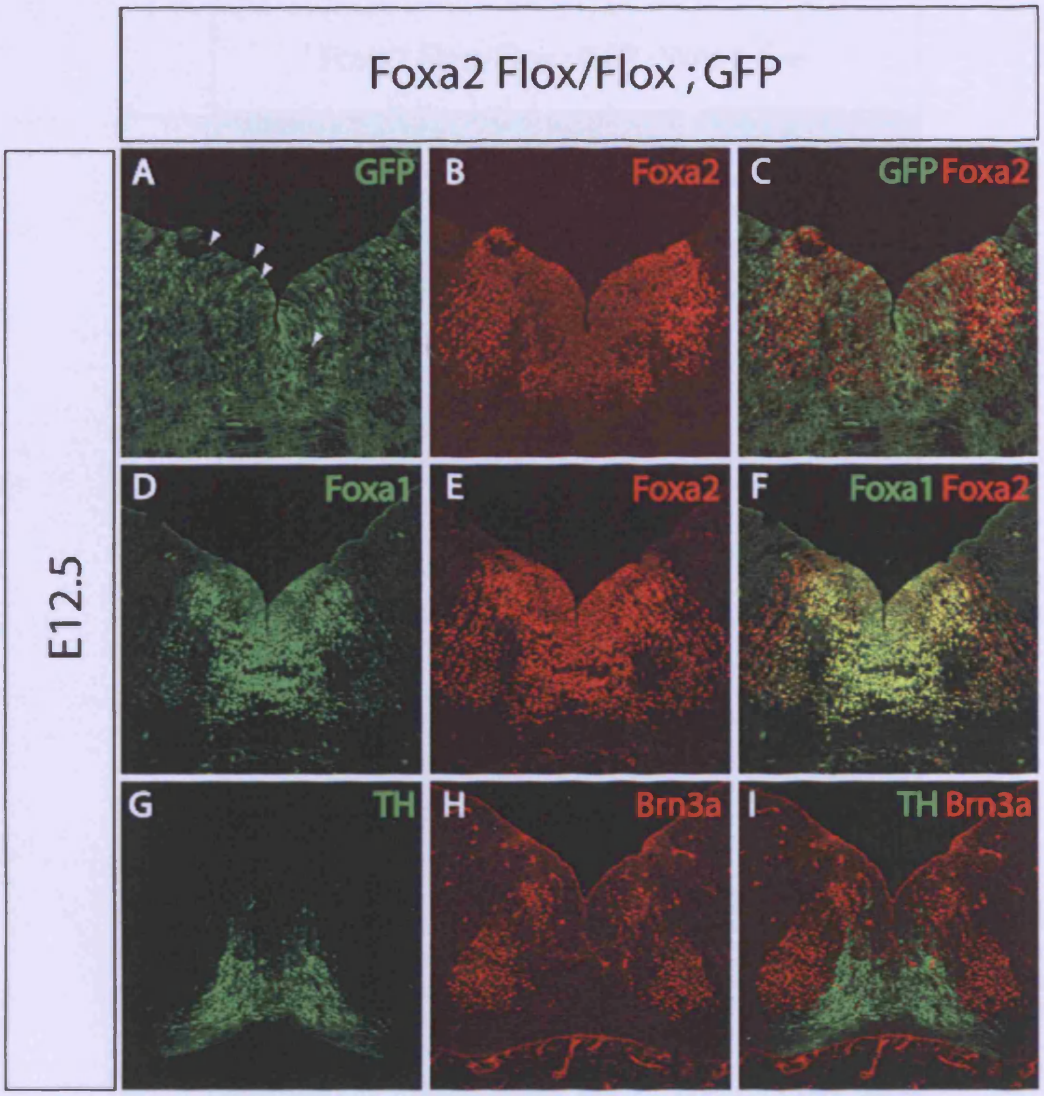

Figure 26: ***Characterisation of wild type chimaeric embryos at E12.5.*** ***A-I:*** *Coronal sections through the mesencephalon of E12.5 embryos. To generate chimaeric embryos, Morula stage embryos derived from crosses of* $Foxa2^{floxed/+}$*; Wnt1-Cre males with* $Foxa2^{floxed/floxed}$ *females were injected into Morula stage embryos generated by crossing heterozygous B5/EGFP males.* ***A-C:*** *GFP (green) antibody reveals the amount of chimaerism present in the ventral mesencephalon, with GFP negative cells are derived from the* $Foxa2^{floxed/floxed}$ *embryo (arrowheads).* ***D-F:*** *Foxa1 and Foxa2 protein are expressed as in the wild type embryos.* ***G-I:*** *The differentiated mesDA and RN neurons were shown to co-express Foxa2. Therefore their expression patterns in the chimaeric embryos were analysed and revealed no alteration from the wild type embryos. Scale bar represent 100μm.*

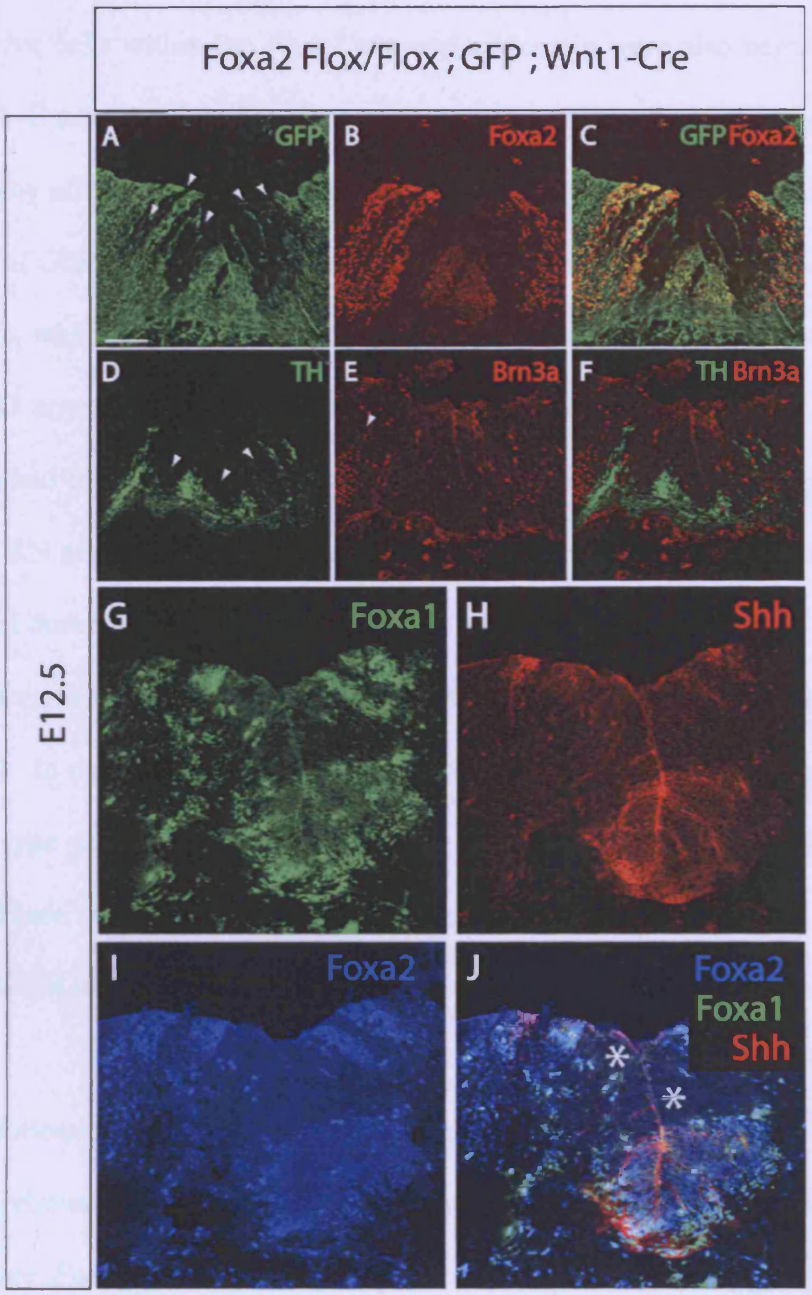

Figure 27: Analysis of CKO Foxa2 χ at E12.5. ***A-C:*** *In the presence of the Cre recombinase, all the GFP negative cells located within the normal Foxa2 expression domain are devoid of Foxa2 protein (arrowheads).* ***D-F:*** *Foxa2 CKO cells located in the basal plate do not express TH nor Brn3a (arrowheads), suggesting that there is a cell autonomous role for Foxa2 in the development of the mesDA and RN respectively.* ***G-J:*** *There is no Foxa1 (green) or Shh (red) protein detected in the Foxa2 CKO cells in the basal plate, whereas in the wild type cells all three proteins can be detected. Regions where all three proteins are absent are labelled with the asterisk (J). Scale bar represent 100μm.*

Analysis of the CKO *Foxa2* χ at E12.5 revealed that in the presence of *Wnt1-Cre*, all the GFP negative cells within the *Foxa2* expression domain were also negative for Foxa2 (figure 27A-C arrowheads). On adjacent mesencephalic sections I investigated whether there was any affect on the mesDA and RN neurons which were partially located within the region of GFP negative cells. TH protein was absent in *Foxa2* negative cells within this domain, while the TH protein was detectable in mesDA cells still expressing Foxa2 (figure 27D arrowheads). There is only a slight overlap between the RN neuronal population and the domain of GFP negative cells near the ventral midline. The only part of the RN neuronal population which was inside the GFP negative domain was the small dorsal domain immediately underlying the ventricular zone. There is an absence of Brn3a protein in the cells which overlap with the *Foxa2* negative cells (figure 27E arrowhead). In cells which express *Foxa2*, both TH and Brn3a proteins are detected in their wild type patterns, and in the absence of *Foxa2*, these two proteins cannot be detected. These two results suggest that *Foxa2* is directly required for the generation of mesDA and RN neurons.

However, following this initial result, I analysed the expression patterns of both *Foxa1* and *Shh* in relation to *Foxa2*. These results reveal that in all *Foxa2* negative cells within the wild type *Foxa2* domain, both Shh and Foxa1 protein are absent (figure 27G-J asterisk). Conversely, in *Foxa2* positive cells, both Shh and Foxa1 proteins are detected (figure 27G-J).

These initial experiments were designed to examine the cell autonomous role of *Foxa2* upon the mesDA and RN. At E12.5 these nuclei have already been specified and the phenotype described could be due to an alteration of progenitor domains at an earlier

stage. To investigate this hypothesis I analysed CKO *Foxa2* χ embryos at E10.5. As described above for the CKO *Foxa2* χ at E12.5, all GFP negative cells, were *Foxa2* negative cells, as seen by the overlapping expression patterns of GFP and Foxa2 (figure 28A-C arrowheads). In the *Foxa2 CKO* I described that *Nkx2.2* and *Nkx2.9* displayed the most pronounced reaction to the reduction in *Foxa2* and Shh signalling by expanding ventrally towards the midline. In the CKO *Foxa2* χ the endogenous Nkx2.2 protein is detected at the ABB (figure 28D dotted line) and is static. In all the GFP negative cells within the *Foxa2* domain, there is ectopic Nkx2.2 protein detected (figure 28D-F arrowheads). This result could indicate that *Foxa2* controls the ventral limit of *Nkx2.2*. However, as Shh is not detectable in *Foxa2* negative cells in the CKO *Foxa2* χ it is not possible to attribute the ectopic Nkx2.2 protein detected to a direct role of *Foxa2*.

Further analysis of chimaeric embryos was abandoned due to difficulties in obtaining suitable chimaeras and due to our inability to distinguish between a cell autonomous role of *Foxa2* and an indirect mechanism via the Shh signalling pathway.

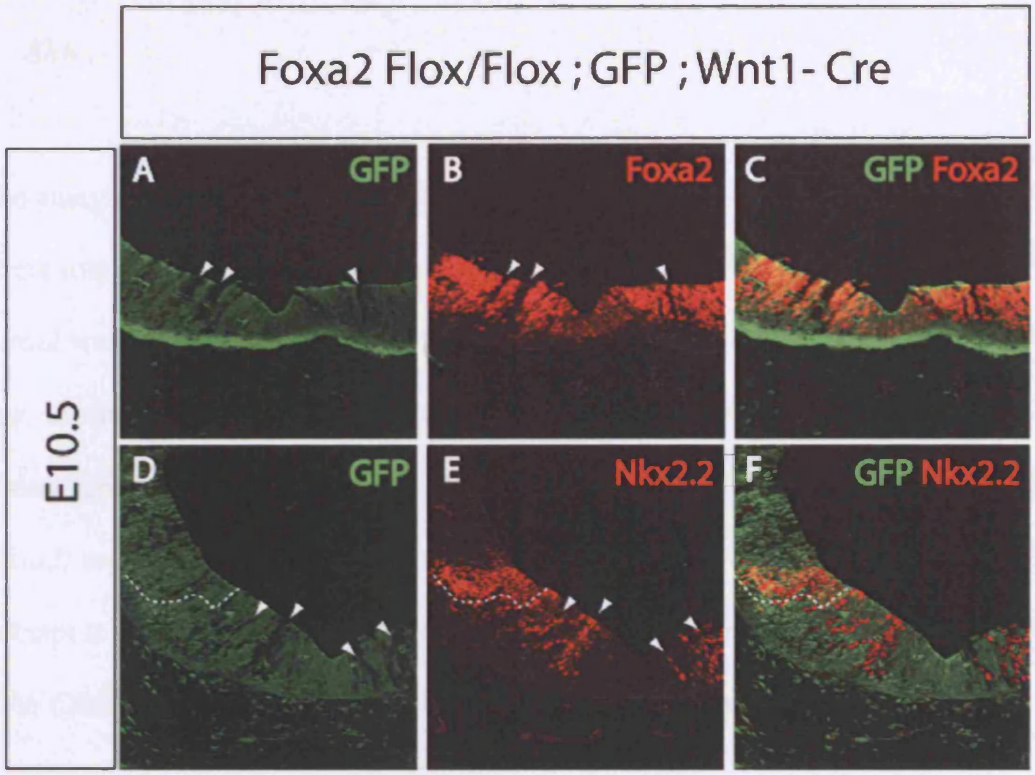

Figure 28: Analysis of E10.5 chimaeric embryos. ***A-C:*** *Coronal section through E10.5 chimaeric embryo. GFP negative cells, in the presence of Wnt1 driven Cre recombinase activity do not possess a functional Foxa2 protein (arrowheads).* ***D-F:*** *In the GFP negative cells within the basal plate, there is ectopic expression of Nkx2.2 protein (arrowheads), while the normal endogenous expression domain of Nkx2.2 at the ABB (dotted line) is not altered. These data could suggest that Foxa2 regulated the ventral limit of Nkx2.2 protein expression in the mesencephalon, but as shown at E12.5, cells which lack Foxa2 also lack Shh, which could contribute to the ectopic expression of Nkx2.2. Scale bar represent 100μm.*

22. Generation of *Shh*$^{flox/flox}$; *Wnt1-Cre* animals and the *Cre* mediated deletion of *Shh*

The analyses of the *Foxa2 CKO* and the chimaeric embryos were not able to elucidate a direct role for *Foxa2* in the neuronal specification of the ventral mesencephalon. When *Foxa2* was reduced initially, there was a sharp reduction in the levels of Shh signalling, due to the cross-regulatory mechanism present between these two genes. This phenomenon makes it difficult to assign a specific aspect of the phenotype directly to *Foxa2*, as it could be caused in response to the reduction in Shh signalling. In an attempt to clarify this issue, I analysed the phenotype of the conditional knockout of *Shh* (*Shh CKO*) to determine if there are similarities between the two phenotypes.

The ability of the Cre to recombine the *Shh* floxed allele was tested by crossing *Shh*^{floxed} heterozygous; *Wnt1-Cre* heterozygous mice (*Shh*$^{floxed/+}$; *Wnt1-Cre* $^{+}$) with *Shh*$^{floxed/floxed}$ homozygous mice. The recombination event was examined using PCR analysis in combination with immunohistochemistry using a polyclonal Shh antibody. The recombination event is evident by E8.5 as described for the Foxa2 CKO, and only occurred in embryos positive for the *Wnt1-Cre* gene, which demonstrates that the *Wnt1-Cre* is capable of recombining the *loxP* sites surrounding the Shh gene.

Shh CKO (*Shh*$^{floxed/floxed}$; *Wnt1-Cre* $^{+}$) embryos are recovered in 25% of the total embryos harvested, following the predicted ratio of Mendelian genetics. The *Shh CKO* embryos were analysed and compared to *Shh*$^{floxed/floxed}$ (*Shh WT*) embryos. The *Shh CKO* embryos do not display any gross external abnormalities and possess a similar size and shape to wild type embryos of similar embryonic development.

A previous study where the notochord was surgically removed reported that the mesencephalic ventricle was completely collapsed (Britto et al., 2002), which is consistent with the phenotype described for the *Shh* -/- (Chiang et al., 1996). Subsequent sectioning of the *Shh CKO* embryos identified a partial collapse of the mesencephalon to be evident at E12.5. While the mesencephalon of the *Shh CKO* at E10.5 is indistinguishable from wild type embryos, at E12.5 the shape of the ventricle is converted from a "pentagon" shape seen in the wild type embryos to the "triangular" shape of the *Shh CKO*, and the dorsal mesencephalon appears to have collapsed onto the ventral mesencephalon. The collapsed ventricle is not as severe as described in the two studies mentioned above. Unlike the Foxa2 CKO mice, the *Shh CKO* mice do not survive embryonic development.

To detect the levels of remaining Shh protein within the *Shh CKO* I used a polyclonal antibody raised against Shh-Np. At E10.5 the Shh protein is easily detected in the wild type embryos spanning the ventral midline (figure 29A). There is no detectable Shh protein throughout the ventral mesencephalon in the *Shh CKO* at E10.5 (figure 29D). At E12.5 Shh protein is detected at high levels within the ventricular zone flanking the ventral midline, and at low levels within the ventral midline, complementing the gene expression pattern described previously (figure 29G). When one copy of the *Shh* gene is removed (*Shh HET*), the lateral extent of Shh protein expression has been greatly reduced and the Shh protein is detected at high levels within a restricted domain at the ventral midline (figure 29J). Consistent with the data generated at E10.5, there is no detectable Shh protein in the *Shh CKO* at E12.5 (figure 29M), even though *Shh* gene expression is still detectable in a small region of the ventricular zone at the ventral midline (figure 35E).

Even though there is no Shh protein detected at either E10.5 or E12.5, the presence of *Shh* RNA transcripts suggest that Shh protein is still produced but at levels lower than the sensitivity of the Shh antibody. These results indicate that the recombination event successfully reduces the levels of Shh protein in the *Shh CKO* embryos, and these levels are sufficient to prevent the complete collapse of the mesencephalic ventricle.

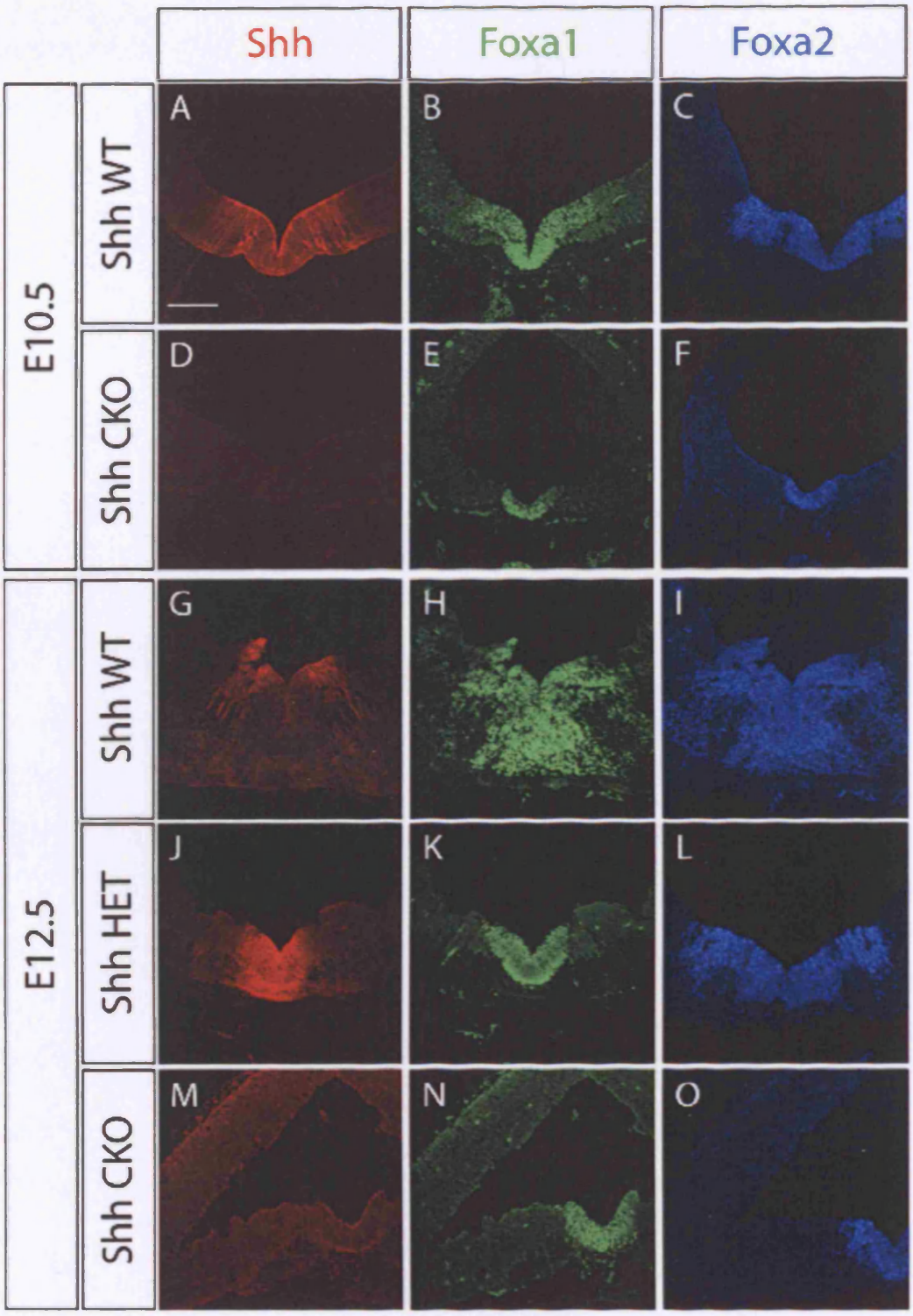

Figure 29: Deletion of Shh gene from the majority of the ventral mesencephalon using Wnt1-Cre mediated recombination of Shh Floxed allele. ***A, D, G, M:*** *Analysis of the Shh CKO revealed that there is no detectable Shh protein (red) remaining in the ventral mesencephalon at either E10.5 or E12.5.*

Figure 29 continued. ***J:*** *The removal of one allele of the Shh gene causes the restriction of the Shh protein at the ventral midline, but it is detected at very high levels. The dramatic reduction in the levels of Shh protein in the Shh CKO also cause an alteration in the morphology of the mesencephalon, which becomes clearly evident at E12.5 by the partial collapse of the ventricle and alar plate onto the basal plate.*

The effect of reduction in levels of Shh protein upon Foxa1 and Foxa2. ***B, E, H, N:*** *In the Foxa2 CKO the relationship between Shh, Foxa1 and Foxa2 have been previously described. In the Shh CKO the reduced levels of Shh protein causes a reduction in the size of the Foxa1 (green) and Foxa2 (blue) domains. In the Shh CKO at E10.5 and E12.5 both Foxa1 and Foxa2 protein domains have been truncated laterally, and are restricted to a narrow domain spanning the ventral midline. Although the Shh protein is not detectable, the remaining Foxa1 and Foxa2 proteins are located in the domain where Shh RNA transcript is still detectable (see figure 35).* ***K:*** *Interestingly, when one allele of Shh is removed at E12.5, the Foxa1 protein domain is restricted to a narrow domain similar to the Shh CKO, whereas the Foxa2 domain resembles the wild type expression pattern. These results provide further evidence of the auto-regulatory mechanisms present between these three genes within the developing ventral neural tube. Scale bar represent 100μm.*

23. Further evidence of a tight relationship between *Foxa2*, *Foxa1* and *Shh*

In the wild type embryos at E10.5, superimposition of *Foxa1*, *Foxa2* and *Shh* expression revealed overlapping *Shh* and *Foxa1* expression in a broad domain spanning the ventral midline with a dorsal limit within the *Foxa2* expression domain, a few cell diameters away from the ABB (figure 29A-C) as previously described (figure 11). In the *Shh CKO* both the expression domains of *Foxa1* and *Foxa2* are dramatically truncated laterally and are restricted to a small domain of the ventricular zone at the ventral midline (figure 29E-F).

Analysis of the *Shh HET* at E12.5 revealed that Shh protein is detected at high levels within a smaller domain than in the wild type embryos (figure 29G, J). There is also a reduction in the size of the *Foxa1* domain within the ventricular zone laterally, overlapping entirely with the remaining Shh protein, while there is also a complete loss of neurons within the mantle layer expressing Foxa1 (figure 29H, K). Interestingly there is no alteration in the expression pattern of *Foxa2* within the ventricular zone, with Foxa2 protein detected in a broad domain spanning the ventral midline until the ABB. However, there are fewer post-mitotic neurons in the mantle layer which express Foxa2, which could be due to the embryo being younger caused by a slightly asynchronous development of the *Shh HET* embryo used for these experiments compared to the *Shh CKO* (figure 29L).

In the *Shh CKO* embryos at E12.5, the Foxa1 expression domain is restricted to the ventral midline as described at E10.5 (figure 29N). Foxa2 protein is reduced dramatically and restricted to the same region of the ventricular zone spanning the

ventral midline as Foxa1 (figure 29O). There is no Foxa1 or Foxa2 protein expressed by any cell outside of the ventricular zone. Although the remaining Foxa1 and Foxa2 protein is detected in a region where no Shh protein is detected (figure 29M), this region overlaps completely with the remaining *Shh* transcript which was detected by *in-situ* hybridisation (figure 35E).

These results provide further evidence that there is a tight relationship between *Foxa2* and *Shh*. Similar to the *Foxa2 CKO*, where a reduction in *Foxa2* caused a reduction in Shh signalling there is a reduction of Foxa2 protein levels in the *Shh CKO*. It is interesting to note that only a slight reduction in the levels of Shh protein was needed to reduce the expression domain of *Foxa1*, while *Foxa2* was largely unaffected in the *Shh HET*.

24.RN and OMC neuronal populations are absent coupled with severe reduction in mesDA neuronal population in *Shh CKO*

In order to examine the effect of reducing the levels of the Shh protein within the ventral mesencephalon upon the neuronal populations which are located there and comparing the phenotype to the *Foxa2 CKO*, I performed immunohistochemistry on coronal E12.5 brain sections of the *Shh CKO* embryos (figure 30A-L).

Compared to the *Foxa2 CKO* where there is an 82%, 65%, 72% reduction in the mesDA, RN and OMC respectively, the phenotype of the *Shh CKO* at E12.5 is much more severe. Analysis along the entire anterior-posterior axis revealed that there is a complete loss of both the OMC and RN neurons from the ventral mesencephalon and a dramatic reduction in the neuronal population of the mesDA (figure 30I-L). The neurons of the RN are absent within the basal plate, and there is a ventral expansion into the basal plate of the Brn3a domain usually located in the alar plate in the wild type (figure 30I). There is no Islet-1 protein detectable in the basal plate at E12.5 indicating a complete loss of the OMC neurons (figure 30J). The mesDA neuronal population is severely reduced in the *Shh CKO* and is located in a restricted domain at the ventral midline (figure 30K). Preliminary cell counting of the remaining TH positive mesDA neurons reveal approximately a 94% reduction in the *Shh CKO*. Interestingly, the analysis of the *Shh HET* along the entire anterior-posterior axis revealed that the neuronal populations of the ventral mesencephalon are largely unaffected by the removal of one allele of the *Shh* gene (figure 30E-H).

Motor neurons expressing the transcription factor Islet-1, are known to be the first neuronal population born in the ventral neural tube and require Shh signalling (Ericson et al., 1996; Ericson et al., 1992). I therefore checked the *Shh CKO* at E10.5 to determine whether the OMC neuronal population was affected by the reduction in Shh signalling. Due to the Shh protein in the *Shh CKO* being to low to detect, I used *Foxa2* as a marker for the ventral mesencephalon. In the wild type embryos, the Islet-1 positive OMC neurons lie immediately underneath the ventricular zone and do not co-express Foxa2 (figure 31A-C). In the *Shh CKO* there is a complete absence of Islet-1 protein indicating that the OMC neurons failed to be specified due to the reduction in Shh signalling (figure 31D-F).

Unfortunately, the phenotype described at E12.5 for the *Shh CKO* cannot be solely attributed to the reduction in Shh levels, as *Foxa2* levels are also reduced. Even though the data supports the concept that motor neurons require constant levels of Shh to differentiate, which would explain the loss of the OMC neurons, the loss of the RN and severe reduction of the mesDA population cannot be solely attributed to the reduction in Shh levels, as there is also a reduction in the levels of Foxa2.

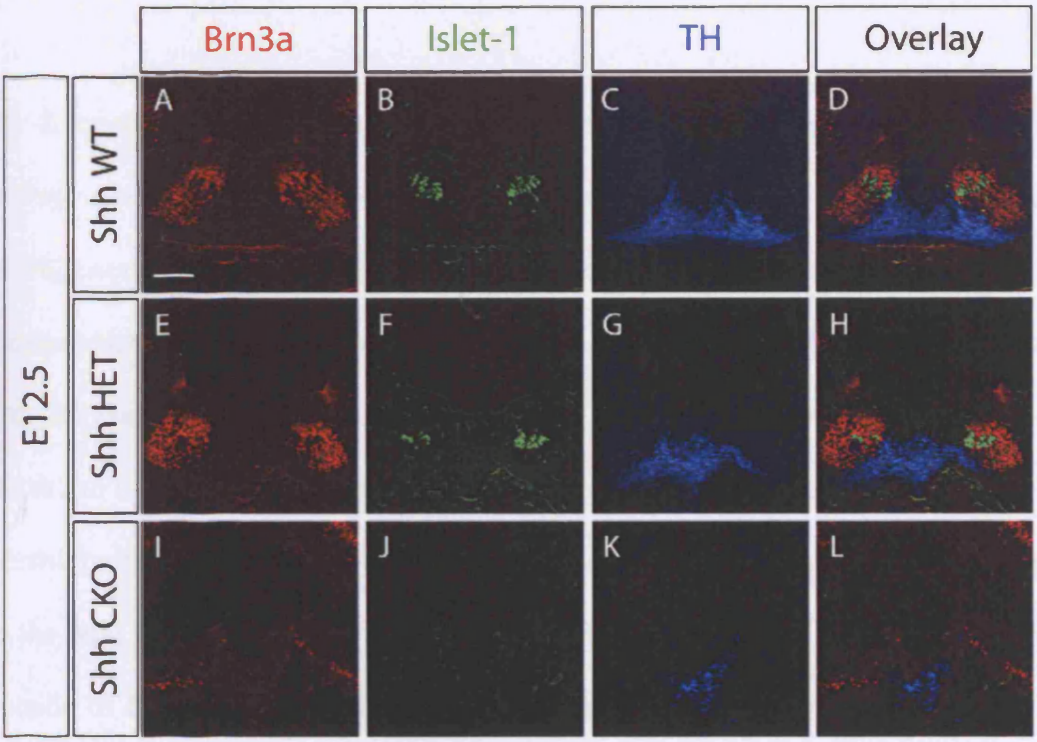

Figure 30: Analysis of neuronal populations within the basal plate of the Shh CKO. A-L: *Coronal sections of E12.5 wild type and Shh CKO embryos. In the wild type embryos there is a distinct spatial relationship of the three neuronal populations in the ventral mesencephalon. In the Shh CKO there is a complete loss of the OMC neurons (Islet-1, green) and RN neurons (Brn3a, red) from the basal plate. The Brn3a positive neurons detected near the ventral midline correspond to the differentiated neurons normally located in the alar plate. There is also a 94% reduction in the mesDA neuronal population (TH, blue), with the remaining differentiated neurons located immediately underlying the ventral midline. When one allele of the Shh gene is removed there is no distinguishable alteration in the spatial organisation of the neuronal populations in the ventral mesencephalon. The neuronal populations seem to be reduced in size compared to the wild type embryos due to the Shh HET embryo being slightly younger than its littermates used in the analysis above. Scale bar represent 100μm.*

25. Neurogenesis is severely affected in the *Shh CKO*

To determine whether the huge losses of the neuronal populations described in the ventral mesencephalon of the *Shh CKO* can be attributed to reduced levels of neurogenesis, I analysed the expression pattern of *Mash1* and *Ngn2* at E12.5 using immunohistochemistry (figure 30G-L). In the *Foxa2 CKO* at E12.5 there is a complete loss of Mash1 protein within the ventricular zone spanning the midline, whilst the Mash1 in the ventricular zone outside of this domain was unaffected. In the *Shh CKO*, Mash1 protein is detected at the ventral midline, but at much reduced levels compared to the wild type (figure 31G, J). The *Mash1* expression domain in the ventricular zone outside of the ventral midline seems to be larger, suggesting that there is a possible increase in the thickness of the ventricular zone. However, due to the alteration in morphology of the mesencephalon in the *Shh CKO* it is not possible to conclude whether this statement is accurate without further analysis.

Recently it was shown that *Ngn2* is required for development of the mesDA neurons (Kele et al., 2006). As previously described, *Ngn2* expression is detected at high levels in the ventricular zone spanning the ventral midline. In the *Foxa2 CKO* there is a transient reduction in the overall levels of *Ngn2*, but the expression domain in not altered at E12.5. In the *Shh CKO* there is a severe reduction in the number of cells expressing *Ngn2* at the ventral midline in addition to a complete loss of Ngn2 protein outside this domain (figure 31H, K), indicating that at E12.5 there is a severe reduction in neurogenesis in the *Shh CKO*, although not a complete absence of neurogenesis.

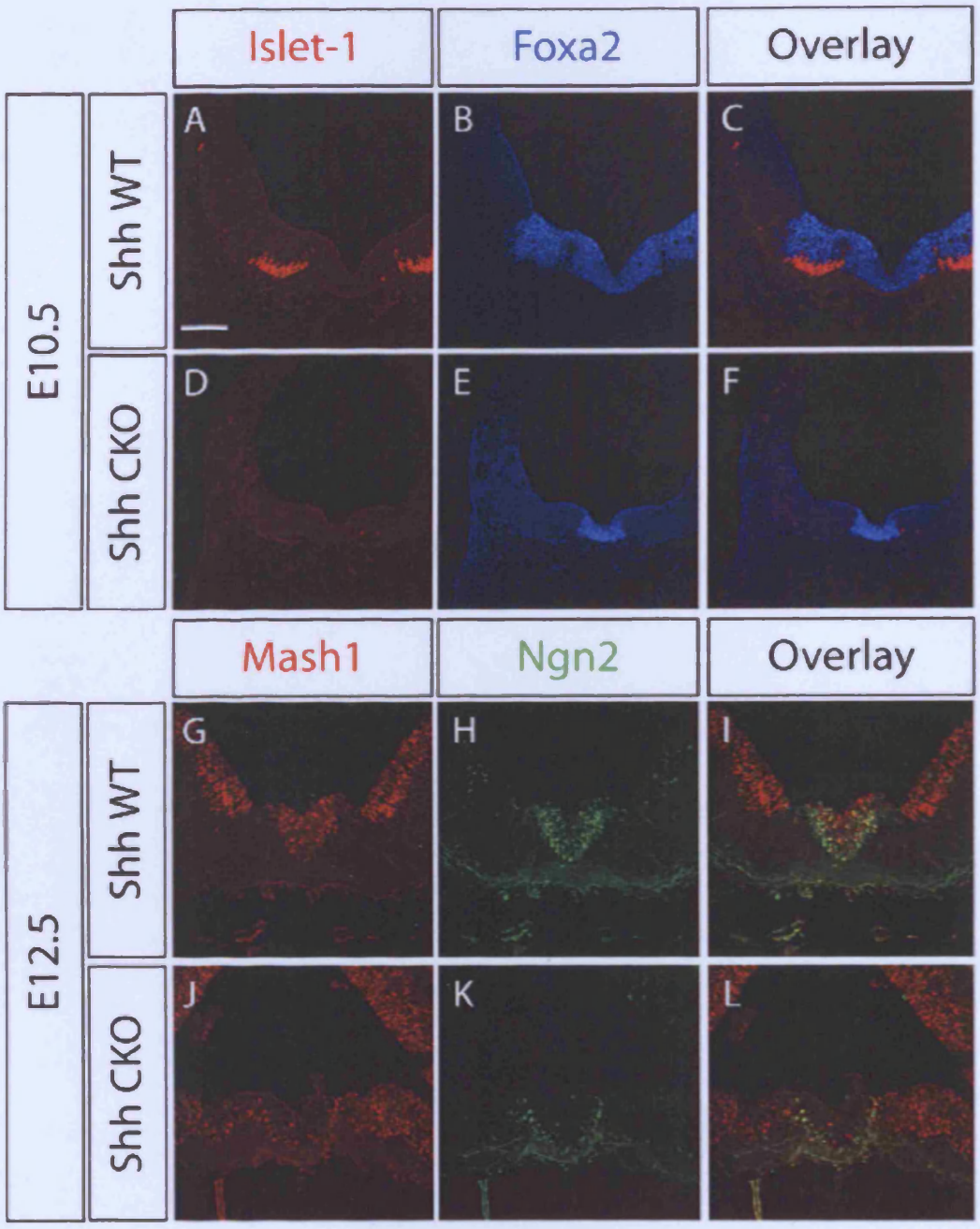

Figure 31: A-F: Analysis of the development of the OMC in the Shh CKO at E10.5. *Previous experiments describe that the motor neurons of developing spinal cord are dependent of high levels of Shh protein. This trend for motor neurons requiring high quantities of Shh protein appears to be consistent in the mesencephalon. The OMC neurons are completely absent in the Shh CKO at E12.5. Closer investigation at E10.5 reveals that the loss of OMC neurons occurs at an earlier developmental stage. These data provide further evidence that motor neurons require high concentrations of Shh protein.*

Figure 31: G-L: Is the phenotype described for the Shh CKO at E12.5 due to a failure of neurogenesis? *The phenotype of the Shh CKO is extremely severe at E12.5, and these embryos do not survive embryonic development. To investigate whether this phenotype is a result of a decrease in neurogenesis in the ventral mesencephalon, the proneural genes Ngn2 and Mash1 were examined in the Shh CKO at E12.5. Although no quantitative data was collected, there is a clear reduction in the number of progenitor cells expressing Ngn2 and Mash1 at the ventral midline. These data indicate that neurogenesis is reduced in the Shh CKO embryos, but is still detectable suggesting that a combination of factors contribute to the Shh CKO phenotype. Scale bar represents 100μm.*

26.Neuronal differentiation is dramatically reduced in the *Shh CKO* at E12.5

As described above, there is a strong reduction in the levels of neurogenesis at the ventral midline of the *Shh CKO* at E12.5 which could account for the loss of the OMC and RN nuclei and the 94% reduction of the mesDA neurons. To investigate any possible differentiation defects in the *Shh CKO* due to the knock on effects of defects in neurogenesis I analysed the expression domains of *Sox2, HuC/HuD and β-Tubulin* using immunohistochemistry.

A previous study in the developing spinal cord revealed that an over-expression of Shh protein induces an increase in cell proliferation and hydromyelia (an increase in thickness of ventricular zone) combined with a loss of differentiated neurons (Rowitch et al., 1999). Another study where the notochord was surgically removed to stop Shh signalling reported a decrease in cell proliferation and an increase in apoptosis (Britto et al., 2002). From these findings it would be expected that in the *Shh CKO*, where there is a severe reduction in the levels of Shh protein, there would be a decrease in the rate of proliferation marked by a decrease in the thickness of the ventricular zone.

However the results I generated from the analysis of the *Shh CKO* are contradictory to previous findings. At E10.5 in the *Shh CKO* there is slight reduction in the levels of β-Tubulin and HuC/HuD proteins indicating a slight reduction in the amount of differentiation (figure 32A-H). These reductions are clearly visible in the ventral regions of the basal plate where the OMC neurons are normally located (figure 32E-F). Measurements of the thickness of the *Sox2* positive ventricular zone reveal that there is a slight increase in the *Shh CKO* in regions lateral to the midline (figure 32C"a", G"a")

while the thickness of the ventricular zone at the ventral midline is decreased (figure 32C"b", G"b"). This phenotype is very similar to the phenotype previously described for the *Foxa2 CKO* at E10.5 (figure 9A-J).

At E12.5 there is a severe reduction in the levels of differentiation throughout the entire mesencephalon of the *Shh CKO* (figure 32I-T). The removal of one allele of the *Shh* gene causes a very slight alteration in the thickness of the *Sox2* positive ventricular zone at the ventral midline (figure 32Kb) while the protein levels of both β-Tubulin and HuC/HuD are not greatly affected (figure 32M-N). In the *Shh CKO* the levels of β-Tubulin and HuC/HuD proteins are dramatically reduced throughout the entire mesencephalon in equal amounts, indicating a global differentiation defect (figure 32Q-R). There are some differentiated neurons expressing HuC/HuD proteins underlying the ventricular zone of the ventral midline, which correspond to the remaining mesDA neurons (figure 32R). Combined with the reduction in the number of differentiated neurons there is serious hydromyelia throughout the entire mesencephalon as determined by the increase in the thickness of the Sox2 protein expression domain (figure 32S).

The *Foxa2 CKO* at E12.5 displays a reduction in the quantity of differentiated neurons within the basal plate, specifically in the mantle layer close to the ventral midline, combined with a ~28% increase in the thickness of the *Sox2* positive ventricular zone at position "x" and ~7% increase at position "y" at the ventral midline (figure 9M, R). In the *Shh CKO* the thickness of the ventricular zone increases by ~33% at position "a" and by ~45% at position "b" (figure 32K, S). These results are suggestive that the progenitor cells of the *Shh CKO* are stuck inside the ventricular zone and do not

differentiate, leading to the complete loss of the OMC and RN nuclei and the severe reduction in the mesDA population. It is worth noting that these results resemble the phenotype described for the over-expression of *Shh* in the dorsal spinal cord (Rowitch et al., 1999).

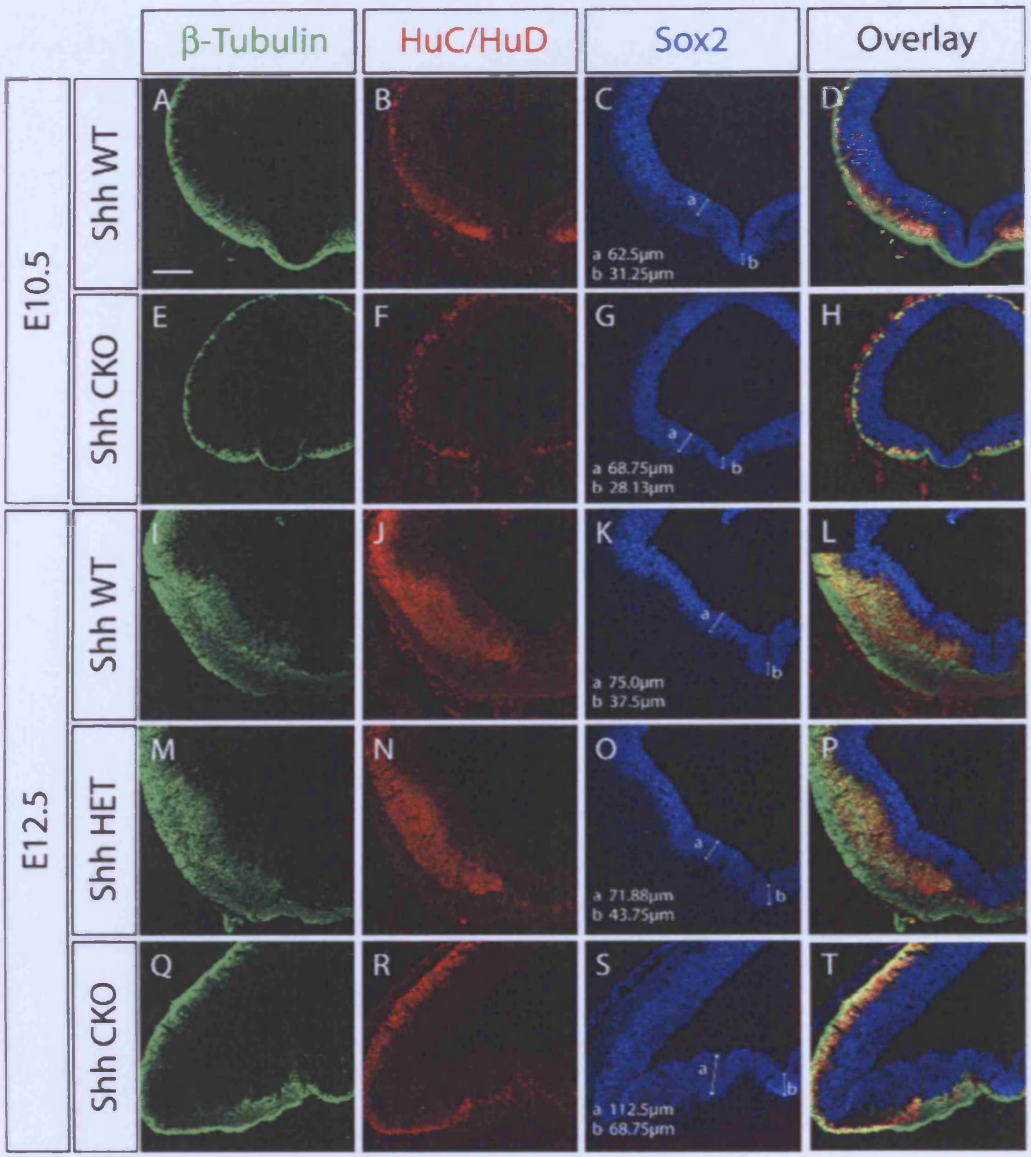

Figure 32: Is neuronal differentiation affected in the Shh CKO embryos? *To explain the loss of the OMC and RN neuronal populations and the 94% reduction in the mesDA population differentiation was analysed in the Shh CKO at E10.5 and E12.5. There is a slight decrease in the number of differentiated neurons at E10.5 labelled with β-tubulin (green) and HuC/HuD (red). At E12.5 these two markers reveal that there is a global reduction in neuronal differentiation throughout the mesencephalon, unlike the Foxa2 CKO where neuronal differentiation was only affected in the basal plate. The remaining differentiated neurons in the basal plate are located underlying the ventral midline corresponding to the remaining mesDA neuronal population. Sox2 protein (blue), labelling the progenitor cells of the ventricular zone, reveals that there is an expansion in the thickness of the ventricular zone (hydromyelia) evident from E10.5. At E12.5 the thickness of the ventricular zone is almost doubled in size, further providing evidence that neuronal differentiation in the Shh CKO is grossly affected.*

Figure 32 continued. *When one allele of the Shh gene is removed from the embryo there is a slight expansion of the ventricular zone, combined with a slight reduction in the quantity of differentiated neurons in the mantle layer. Double headed arrows labelled "a" & "b" represent the locations where the thickness of the ventricular zone were conducted. Scale bar represent 100μm.*

27. Dorsal-ventral patterning and immediate downstream targets of Shh signalling are dramatically affected by the reduced levels of Shh protein

The analysis of the *Shh* -/- revealed that there was a ventral expansion of all transcription factors usually involved in the specification of neuronal populations in the dorsal neural tube in expense of transcription factors involved in the specification of ventral neuronal populations (Chiang et al., 1996). The ventral expansion of the *Brn3a* positive neurons normally located in the alar plate suggested that the specification of neuronal populations along the dorsal-ventral axis was altered in the *Shh CKO* (figure 30I). To investigate whether this ventral expansion was an isolated case, I analysed the expression patterns of both Class I and Class II genes in the *Shh CKO* at E10.5 and E12.5 (figure 33A-O).

Consistent with the analysis of the *Shh* -/- there is a ventral expansion of Class I genes at both E10.5 and E12.5 in the *Shh CKO*. At E10.5 both *Pax7* and *Pax3*, which are normally restricted to the alar plate, have expanded ventrally, seemingly until the ABB (figure 33A-F). At E12.5 the ventral expansion of *Pax7* and *Pax3* are more pronounced. In the *Shh CKO*, both Pax7 and Pax3 protein can be detected in the ventricular zone of the basal plate (figure 33M-O). The ventral limit of their expression domain reaches the remaining *Foxa2/Foxa1/Shh* domain spanning the ventral midline (data not shown). This data also provides further evidence of hydromyelia, evident by the increase in thickness of the *Pax3/Pax7* ventricular zone.

Interestingly, there is no ventral expansion of these two genes in the *Shh HET*, suggesting that one functional allele of *Shh* is sufficient to pattern the dorsal mesencephalon.

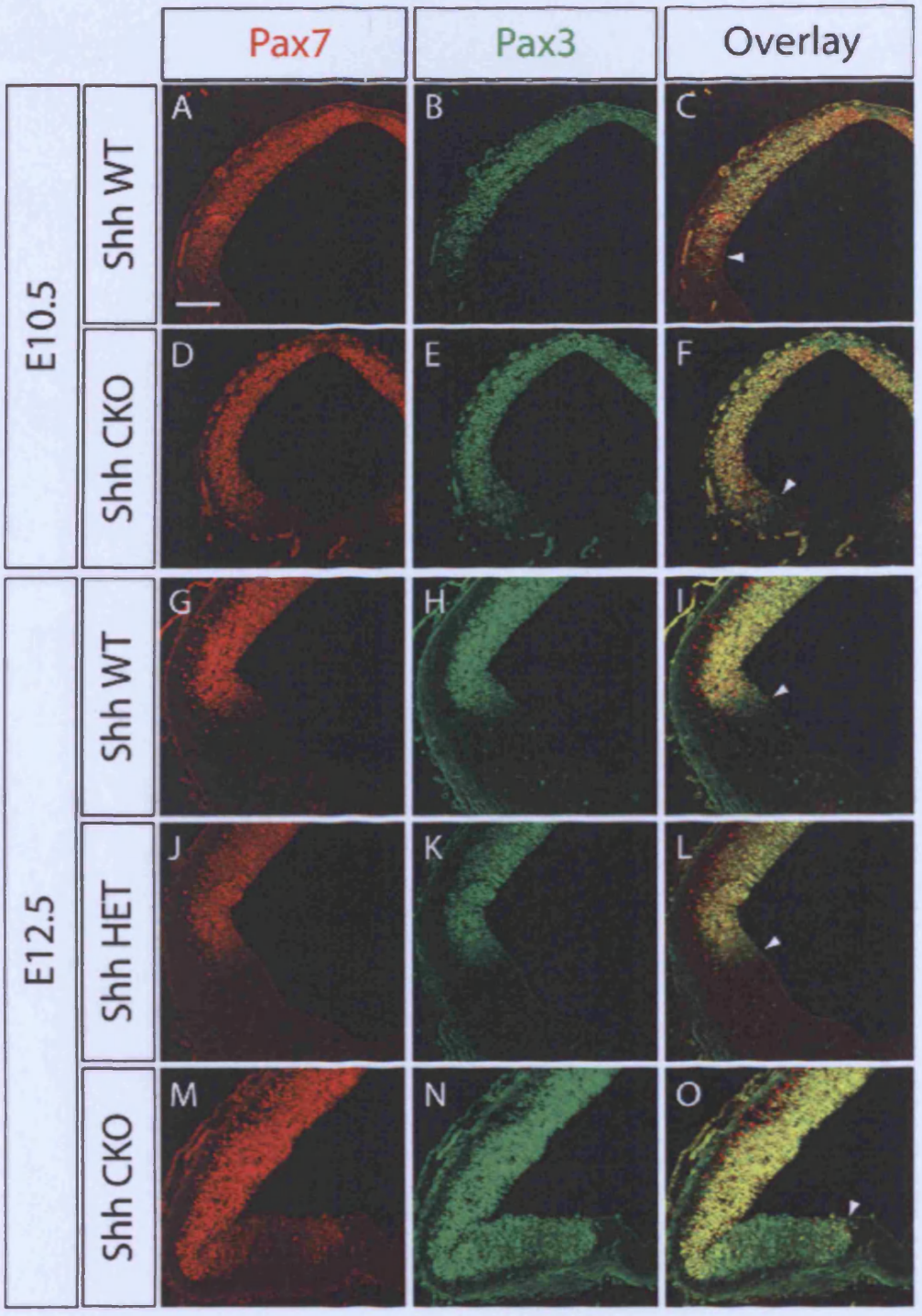

Figure 33: Analysis of Class I genes in the mesencephalon of the Shh CKO. A-O: *Due to the reduction in Shh signalling described above, it was expected that there would be an alteration in the progenitor domains of both Class I and Class II genes. Analysis of two Class I genes (Pax3 & Pax7) at E10.5 and E12.5 revealed that the Shh CKO mesencephalon has been partially "dorsalised." These two markers for dorsal progenitor domains both expand ventrally into the basal plate and form a ventral limit at the border of the Foxa2 domain near the ventral midline.*

Figure 33 continued. *Interestingly, one functional allele of the Shh gene is sufficient to maintain the ventral limits of all the Class I genes analysed. Arrowheads represent the ventral limits of the Pax3/Pax7 progenitor domains. Scale bar represent 100μm.*

The analysis of the Class II transcription factors in the mesencephalon of the *Shh CKO* revealed that at E10.5 there is a complete absence of Nkx2.2 protein (figure 34A, D), and Nkx6.1 protein is not detectable within the ventricular zone, but there are some differentiated neurons which express Nkx6.1 in the mantle later lateral to the midline (figure 34B, E). At E12.5 the absence of Nkx2.2 protein is persistent (figure 34G, M) which is expected due to the ventral expansion of *Pax3/Pax7*. Nkx6.1 protein is detectable within the ventricular zone (figure 34H, N), but due to the gross morphological alteration of the mesencephalon in the *Shh CKO*, it is not possible to determine whether the ventral region of the Nkx6.1 domain is absent whilst maintaining the dorsal domain, or whether the entire domain has been reduced in dimension. Interestingly, there is no loss of *Nkx2.2* or an alteration to the expression domain of *Nkx6.1* in the *Shh HET*, and both proteins are expressed in similar fashion to the wild type embryo (figure 34J-L). These data therefore suggest that one functional allele of *Shh* is sufficient to maintain the progenitor domains of the mesencephalon in the wild type configuration.

The analyses of the Class I and Class II proteins in the mesencephalon of the *Shh CKO* revealed that there is an incomplete "dorsalisation" of the basal plate, with the Class I proteins expanding ventrally, in the expense of *Nkx2.2*, to flank the *Foxa2/Foxa1/Shh* domain at the midline. This phenotype is more severe than that of the *Foxa2 CKO* where only the progenitor domains of the basal plate were affected.

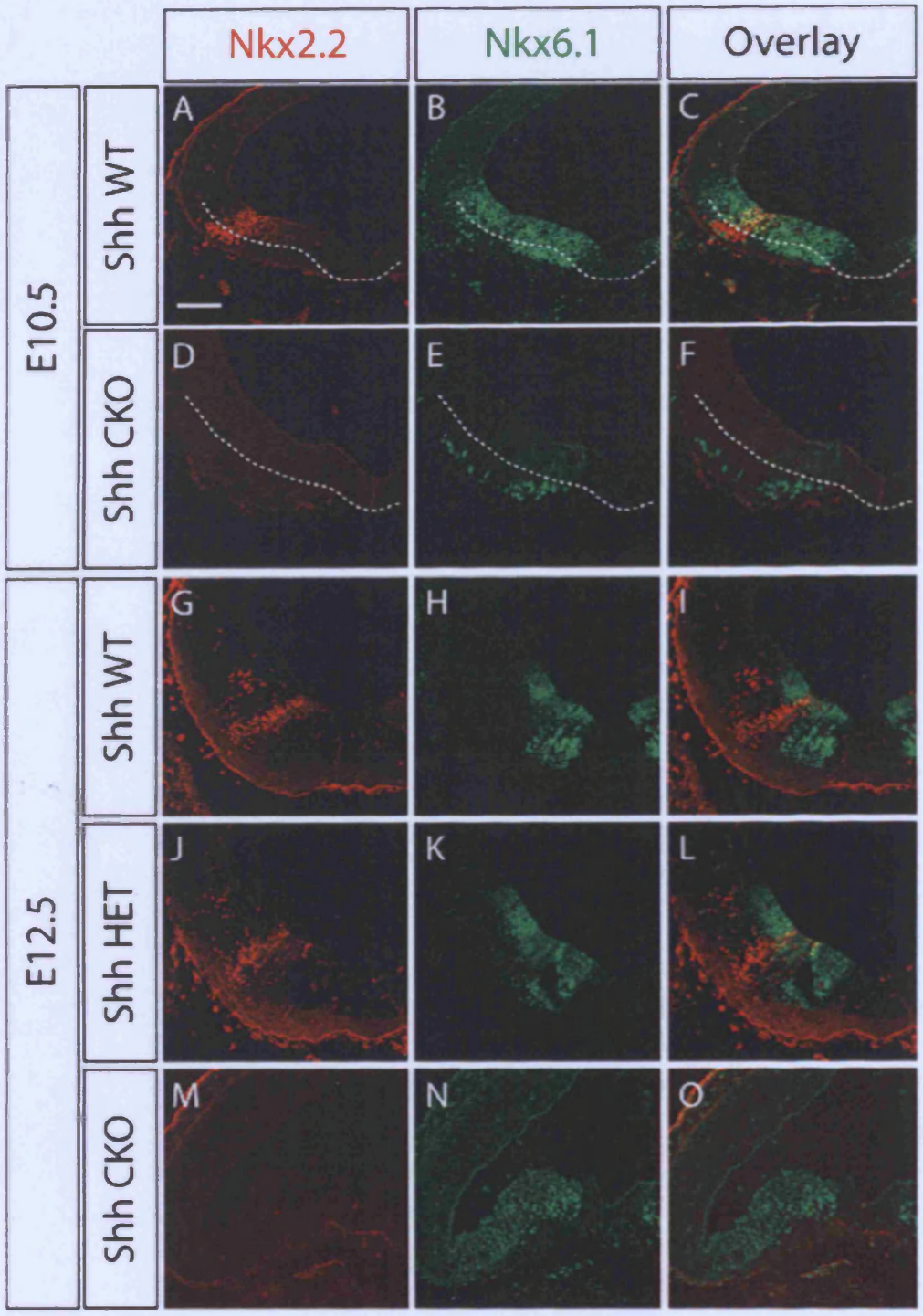

Figure 34: Does the reduction in Shh protein cause an alteration in the patterning of the ventral mesencephalon of Shh CKO embryos? Analysis of Class II genes. *The transcription of the Nkx2.2 gene requires high levels of Shh signalling in the developing neural tube. In the Shh CKO at E10.5 and E12.5, the levels of Shh signalling are dramatically reduced, causing the absence of Nkx2.2 protein (red) as described in the Shh -/- mice.*

Figure 34 continued. *Nkx6.1 protein (green) is absent from the ventricular zone, but a few differentiated neurons maintain Nkx6.1 protein expression at E10.5. At E12.5 there are a few cells within the ventricular zone which express Nkx6.1 protein near the ventral midline, and the differentiated neurons expressing Nkx6.1 protein are no longer detectable. These data, coupled with the analysis of the Class I genes, indicate that the mesencephalon of the Shh CKO embryos is becoming dorsalised, but not to the extent described for the Shh -/-. Interestingly, the removal of one allele of Shh does not cause an alteration in the patterning of the ventral mesencephalic progenitor domains.* ***A-F:*** *Dotted line represents the ventricular zone within the basal plate at E10.5. Scale bar represents 100μm.*

In the *Foxa2 CKO*, the indirect reduction in Shh signalling initially caused a ventral shift of *Ptc* and *Gli1* gene expression towards the remaining *Shh* gene expression at the ventral midline, but was eventually restored. To identify the effects of the direct reduction in Shh signalling has upon the downstream targets or transducers of the Shh signalling cascade I performed *in-situ* hybridisation on the *Shh CKO* at E12.5.

At E12.5 there is a dramatic reduction of *Foxa2* gene expression, with the remaining *Foxa2* gene expression limited to a tight domain at the ventral midline (figure 35A, D). *Shh* gene expression is also reduced in similar fashion to the ventral midline (figure 35B, E). Superimposing the *Foxa2* and *Shh* expression domains reveals complete overlapping within the ventricular zone at the midline, but *Foxa2* gene expression can be detected ventral to the *Shh* gene expression. There is a dramatic reduction in *Ptc* gene expression in the *Shh CKO* (figure 35C, F, inset is *Ptc* gene expression on same section). In similar fashion, the intensity of the RNA signal for *Gli1* is reduced, suggesting a reduction in levels of *Gli1*. There is also a shift of the gene expression domain towards the ventral midline (figure 35G, J). In the *Foxa2 CKO*, *Gli2* gene expression expanded ventrally towards the ventral midline and then subsequently restored to its original position. *Gli3* gene expression however, was unaltered. In contrast to these data, both Gli2 and Gli3 expand ventrally in the *Shh CKO* forming a boundary with the remaining *Foxa2/Foxa1/Shh* domain spanning the midline (figure 35H, K, I, L).

These results indicate that the downstream targets of Shh signalling are affected by the direct loss of *Shh*.

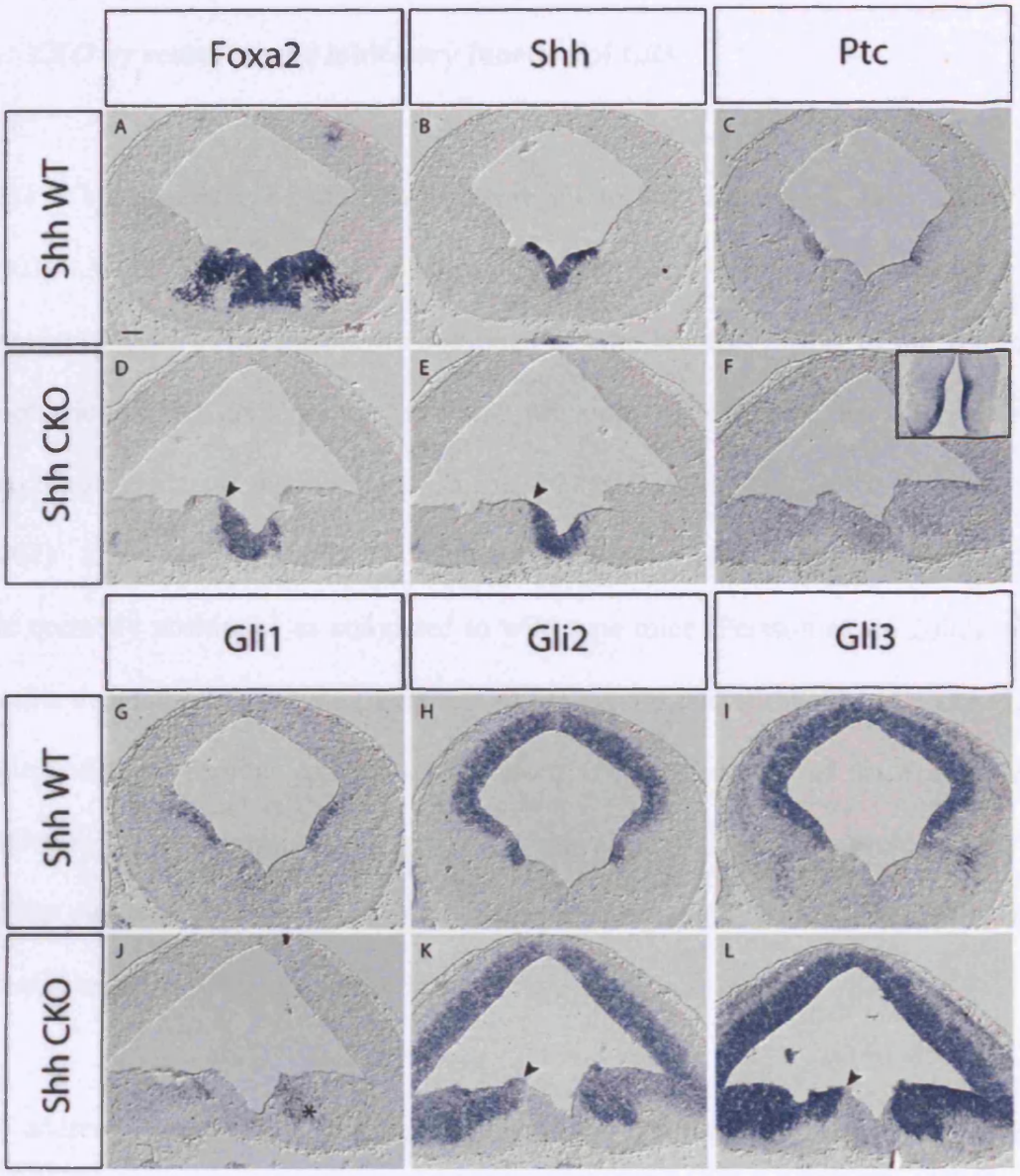

Figure 35: ***Analysis of downstream targets of Shh signalling in the Shh CKO.*** ***A-L:*** *in-situ hybridisation analysis on adjacent coronal mesencephalic sections. Shh and Foxa2 gene expression are reduced in the ventral mesencephalon of the Shh CKO to a narrow domain spanning the midline. There is a dramatic reduction in both Ptc and Gli1 gene expression in the ventral mesencephalon.* ***F:*** *Photograph inset is Ptc gene expression in Shh CKO within the developing diencephalon as a positive control. Both Gli2 and Gli3 gene expression expand ventrally and form new ventral boundaries abutting the Foxa2/Shh/Foxa1 domain in the ventral midline. Arrowheads correspond to the boundary between the Shh/Foxa2 and Gli2/Gli3 gene expression domains.* ***J:*** *Asterisk corresponds to the remaining Gli1 gene expression within the ventricular zone. Scale bar represents 100μm.*

28. Attempt to rescue ventral mesencephalic neuronal populations of the *Foxa2 CKO* by removing the inhibitory function of *Gli3*

Gli3 is considered to be the primary repressor to Shh signalling (Jacob and Briscoe, 2003). When *Gli3* activity is inhibited in either *Shh* -/- or *Smo* -/- mice there is an apparent rescue of the phenotype described in both mutants. Most of the ventral cell populations which are absent in the *Shh* -/- are recovered excluding the V3 interneurons and the floor plate (Litingtung and Chiang, 2000b; Persson et al., 2002; Wijgerde et al., 2002). Upon closer examination of the progenitor domains, it was revealed that they are correctly positioned as compared to wild type mice (Persson et al., 2002). These results demonstrated that the patterning of the ventral neural tube could occur via Shh independent or parallel pathways. Therefore, if the phenotype of the *Foxa2 CKO* is linked to the reduction in Shh signalling, removal of *Gli3* activity should restore some of the neuronal populations in the ventral mesencephalon, with the exception to the mesDA neurons which lie across the ventral midline.

To address whether *Foxa2* has a direct role in the specification of the ventral neuronal populations of the mesencephalon, or whether the phenotype described for the *Foxa2 CKO* was due to the reduction in Shh signalling the activity of *Gli3* in the *Foxa2 CKO* was inhibited. The initial observations revealed that the Islet-1 positive neuronal population lying laterally to the ventral midline were restored (figure37). However, further analysis suggested that the fate of the mesencephalon was compromised as there was no longer any detectable Otx2 protein in the brain region anterior to the isthmus (figure 40), suggesting that the prospective mesencephalon was converted into rhombencephalic tissue. Coupled with this finding, the embryos displayed severe

exencephaly in the region anterior to the otic vesicle resembling the normal structure of the rhombencephalon (figure 36). Although this mouse mutant provided some interesting data, it was not possible to determine whether the phenotype was attributed to the loss of *Foxa2* or to aspects of Shh signalling and coupled with time constraints this project was abandoned. All of the data generated and some preliminary analysis of the phenotype can be seen in Appendix-B.

Discussion

1. Deletion of *Foxa2* in the *Foxa2 CKO* embryos

The main aim of this project was to identify the role of *Foxa2* in the specification of the neuronal populations which are located within the ventral mesencephalon. In order to avoid the embryonic lethality described for the *Foxa2* knockout mice (Ang and Rossant, 1994; Weinstein et al., 1994), we adopted a conditional knockout approach to delete *Foxa2* at a time point when the loss of *Foxa2* function would not lead to the disruption of embryonic development. The *Wnt1* promoter was judged to be the most suitable gene promoter to drive the *Cre* mediated recombination event based on the gene expression domain of *Wnt1*. Previous studies revealed that *Wnt1* gene expression is detected throughout a broad domain of the presumptive mesencephalon from the early head fold stages, with the exception to the most ventral regions at the midline of the basal plate (McMahon and Bradley, 1990; Wilkinson et al., 1987) (our unpublished data).

In order to inactivate *Foxa2* within the region of interest, we used mice in which the third exon of the *Foxa2* gene is flanked by *loxP* sites (Sund et al., 2000). In the presence of the Cre recombinase protein, the third exon is removed, producing a null allele of *Foxa2* (Sund et al., 2000). From our analysis the recombination event was detectable by E8.5, shortly after the onset of *Wnt1* gene expression, as seen by the 92% reduction in cells expressing Foxa2 protein within the basal plate (figure 3). The remaining Foxa2 expressing cells were located at the most ventral region of the midline.

2. Relationship between *Foxa2*, *Foxa1* and Shh signalling in the *Foxa2 CKO*

The regulation of Shh signalling has been an intensely studied area of developmental biology, due to medical implications caused by defects in this pathway. During development, the aberrant function of the Shh signalling pathway can cause an increase in cell proliferation (Echelard et al., 1993), which can ultimately lead to polydactyly in the limb buds and dorsal brain defects, as described for the *Gli3* mutant mice in which Shh signalling is unrestricted (Buscher et al., 1997; Hui and Joyner, 1993). In adults, the inappropriate activation or the aberrant function of the Shh signalling pathway or the downstream components of this pathway contribute to an increase in cell proliferation and ultimately the generation of tumours, such as basal cell carcinoma (Dahmane et al., 1997; Dahmane et al., 2001; Fan et al., 1995; Goodrich et al., 1997; Johnson et al., 1996; Svard et al., 2006; Thayer et al., 2003; Watkins et al., 2003; Xie et al., 1998).

In a bid to identify the key intrinsic regulatory mechanisms present to control the Shh pathway, the detailed analysis of several candidate genes was carried out. Two genes which were implicated in the regulation of the Shh signalling pathway during development were *Foxa1* and *Foxa2*. They were proposed to be potential upstream activators of *Shh* gene transcription based on their overlapping expression domains with *Shh* within the developing neural tissue (Echelard et al., 1993; Ruiz i Altaba et al., 1995a; Ruiz i Altaba et al., 1995b; Sasaki and Hogan, 1994). The ability of *Foxa2* to positively regulate *Shh* transcription in ectopic expression studies also added weight to the argument that *Foxa2* is involved in certain aspects of the regulation of the Shh signalling pathway (Echelard et al., 1993; Sasaki and Hogan, 1994). *Foxa2* was proposed to be the main regulator of *Shh* transcription as its gene expression is detected

12 hours prior to *Shh* gene expression (Echelard et al., 1993), while *Foxa1* gene expression is detected almost simultaneously with that of *Shh* (Ang et al., 1993). Furthermore, genetic evidence does not support an essential role for *Foxa1* in the transcriptional control of *Shh*, based on the observation that *Foxa1* mutant embryos posses a floor plate and maintain *Shh* gene expression (Duncan et al., 1998) (Dr Anna Ferri, unpublished results). The same study also revealed that *Foxa1* was a less potent activator of *Shh* transcription *in-vitro* as compared to *Foxa2* (Duncan et al., 1998). Further studies revealed that there are *Foxa* (*HNF-3*) binding sites present within certain enhancers of the *Shh* promoter, but not all, suggesting that there are both *Foxa*-dependent and *Foxa*-independent mechanisms controlling *Shh* transcription (Epstein et al., 1999). Upon closer inspection of this preliminary data, it was demonstrated that there are homeodomain, *Tbx* and *Foxa* binding sites located within the *Shh* enhancer element, and that a combination of *Foxa* and homeodomain transcription factors are involved in the activation of *Shh* transcription within the floor plate region (Jeong and Epstein, 2003).

The results generated from the analysis of the *Foxa2 CKO* embryos support the above hypotheses. In the *Foxa2 CKO* embryos from as early as E8.75 until E10.5 there is a reduction in both *Foxa1* and *Shh* gene expression in response to the 92% reduction of cells expressing Foxa2 protein. The remaining *Foxa1* and *Shh* gene expression domains are located within a narrow region of the ventral midline, overlapping with the remaining *Foxa2* expressing cells, with no Foxa1 or Shh protein detected outside of the remaining *Foxa2* domain (figure 11) demonstrating that *Foxa2* is a positive regulator of *Shh* transcription in the developing neural tissue. The reduction of *Foxa1* gene

expression is consistent with the observation that *Foxa2* is absolutely required for *Foxa1* gene expression (Duncan et al., 1998).

However, at E10.5 there is a gradual restoration of *Foxa1* gene expression along the anterior-posterior axis, initiated at the most anterior regions of the mesencephalon and gradually progressing towards the posterior end (figure 11, 13). By E11.5, *Foxa1* gene expression can be detected throughout the anterior-posterior axis of the mesencephalon and is maintained throughout the remaining embryonic stages analysed. Immunohistochemical analysis of the Foxa1 protein suggested that Foxa1 appears to be over-expressed, based on the observation that the sensitivity of the Foxa1 antibody was increased in the *Foxa2 CKO* embryos as compared to the wild type embryos. *Shh* gene expression was also restored simultaneously at E10.5 in a similar fashion to *Foxa1*, raising the question as to which gene is restored primarily.

When *Foxa1* gene activity was introduced into the *Foxa2* mutant background, there was a restoration of the expression for various *Foxa2* target genes (Duncan et al., 1998). This result indicates that *Foxa1* has the ability to induce the transcription of *Foxa2* targets. Therefore we could hypothesise that in the *Foxa2 CKO* embryos at E10.5, *Foxa1* is restored by a currently unknown mechanism and *Shh* gene expression is subsequently restored in response to the inducing capabilities of *Foxa1*.

To confirm this hypothesis and to rule out the possibility that residual Shh protein builds up to a level where it is able to induce the transcription of *Foxa1* at later embryonic stages, in collaboration with Miss Carol Yan (Ph.D. student within Ang laboratory) we performed *in-vitro* embryo culture experiments to remove all Shh

signalling activity from the *Foxa2 CKO* embryos by using the teratogenic Veratrum alkaloid; cyclopamine. Cyclopamine, which inhibits the downstream transduction of the Shh signalling pathway by blocking the activity of *Smo* (Chen et al., 2002a; Incardona et al., 1998), can block all Shh signalling, and has been shown to reverse the effects of the oncogenic mutations of both *Ptc* and *Smo* (Taipale et al., 2000).

E9.5 wild type and *Foxa2 CKO* embryos were placed into incubation chambers with either ethanol (control solution) or 20μM of cyclopamine added to their culture medium, and were allowed to develop in culture for 48 hours. Analysis of Foxa1 and Foxa2 proteins in the *Foxa2 CKO* embryos cultured in ethanol revealed an identical phenotype to the *Foxa2 CKO* described previously (Appendix A, figure 36). This consistency was also observed for the Class II transcription factors *Nkx2.2* and *Nkx6.1*, which were utilised as readouts for Shh activity (Appendix A, figure 36). Wild type embryos which were exposed to 20μM cyclopamine revealed no alteration in the expression of both Foxa1 and Foxa2 proteins, but revealed a severe reduction in both Nkx2.2 and Nkx6.1 protein (Appendix A, figure 36). The remaining Nkx2.2 protein was detected in the mantle layer, suggesting that these cells were specified prior to the administration of cyclopamine. Analysis of the *Foxa2 CKO* embryos which were incubated in the presence of 20μM cyclopamine revealed that in the absence of Shh signalling (as determined by the dramatic reduction of Nkx2.2 from the ventricular zone) Foxa1 protein was detected in a domain resembling the wild type expression domain indicating that *Foxa1* gene expression is restored independently from Shh signalling, and that the restoration of *Shh* gene expression is a consequence of the inducing capabilities of *Foxa1* (Appendix A, figure 36).

To complement this data, the analysis of the *Foxa2* chimaeric embryos (*CKO Foxa2* χ *and Foxa2* χ) embryos revealed a cell autonomous regulatory role of *Foxa2* on both *Shh* and *Foxa1*, especially within the ventral midline (figures 25-27). Interestingly, the *CKO Foxa2* χ embryos were analysed at E12.5, a time-point when both *Foxa1* and *Shh* gene expression has been completely restored in the *Foxa2 CKO*, but they still displayed a loss of Shh and Foxa1 proteins within *Foxa2 CKO* cells. This could indicate that there is an intrinsic mechanism within the ventral mesencephalon which can detect whether the levels of Foxa2 protein have reached a critical low point, at which point there is an over-expression of Foxa1 to compensate this loss, as described in the *Foxa2 CKO*. The second observation from the analysis of the *CKO Foxa2* χ is that the diffusible Shh protein from wild type cells does not posses the ability to induce the gene expression of *Foxa1* in neighbouring cells lacking *Foxa2*. Therefore this result clearly indicates that the restoration of *Foxa1* in the *Foxa2 CKO* is independent from Shh activity, and that *Foxa2* positively regulates the expression of both *Foxa1* and *Shh*.

These results, in combination with the observation that there is an over-expression of Foxa1 within the ventral mesencephalon of the *Foxa2 CKO*, suggest that *Foxa1* plays a redundant role in the regulation of *Shh* transcription. This statement is consistent with the previous findings that *Foxa1* has the ability to induce the transcription of *Shh* and other downstream targets of *Foxa2* in the absence of *Foxa2* (Duncan et al., 1998). Interestingly, recent analysis of the *Foxa1* mutant mice within our laboratory has revealed that in the absence of *Foxa1*, the transcription of *Shh* is unaltered as previously described (Duncan et al., 1998), but there is a slight over-expression of *Foxa2* (Dr. Anna Ferri unpublished results).

The results of the *Foxa2 CKO* and the *Foxa1* mutant mice reveal that there is a redundant regulatory system for the induction of *Shh* transcription within the ventral mesencephalon. If either the function of *Foxa1* or *Foxa2* is inhibited, there is a response from the remaining gene, which gradually compensates for the loss of the related gene. However, from our observations and from the *in-vitro* data generated by Duncan et al., *Foxa2* is the more potent activator of *Shh* transcription. When the activity of both genes is inhibited (*Foxa2 CKO; Foxa1 -/-*) there is no induction of *Shh* transcription and the embryos do not survive embryonic development and display severe morphological abnormalities (Dr. Anna Ferri, unpublished results). This functional redundancy between *Foxa1* and *Foxa2* could be an evolutionarily conserved mechanism to ensure that the Shh signalling pathway functions correctly throughout embryonic development, which when disrupted leads to severe developmental defects (Chiang et al., 1996).

2.1. Consequences of fluctuating Shh signalling in the *Foxa2 CKO*

To confirm the activity of the Shh signalling pathway in the *Foxa2 CKO*, the expression patterns of genes which are immediate transcriptional targets of Shh signalling were analysed. *Ptc*, *Gli1* and *Gli2* gene expression followed the transition of the *Shh* gene expression in the *Foxa2 CKO* expanding ventrally to border the remaining Shh signal near the ventral midline at E9.5. Once *Shh* gene expression is restored in the majority of the mesencephalon by E10.5 they are restored to their wild type locations (figure 12, 13, 23). The primary repressor of Shh signalling is *Gli3* (Meyer and Roelink, 2003; Persson et al., 2002), which has also recently been demonstrated to possess a role as an activator in the ventral neural tube in combination with *Gli2* activity (Bai et al., 2004;

Lei et al., 2004). Surprisingly the analysis of the *Foxa2 CKO* revealed that *Gli3* gene expression is restricted to the alar plate and does not expand ventrally in the same fashion as *Gli1* and *Gli2* (figure 12).

The analysis of *Shh* deficient mice revealed that there was a complete loss of the ventral neuronal populations of the neural tube, coupled with the ventral expansion of genes normally expressed in the progenitor domains of the dorsal neural tube (Chiang et al., 1996). Therefore a slight alteration in the specification of the progenitor domains would be expected in the *Foxa2 CKO*, although not as severe as the phenotype described for embryos with a complete loss of *Shh* activity. Interestingly, there was no ventral expansion of any of the genes normally restricted to the dorsal progenitor domains. Both *Pax3* and *Pax7* were restricted to the alar plate and never crossed the ABB, in similar fashion to Gli3. The gene expression patterns of both *Irx3* and *Dbx1* were also unaltered in the *Foxa2 CKO* (figure 14), indicating that the dorsal mesencephalon is correctly specified in the *Foxa2 CKO* embryos.

In contrast, the progenitor domains within the basal plate were all affected by the initial reduction in Shh signalling. Surprisingly the Class II genes analysed were neither simultaneously affected nor affected in similar fashion (figure 15, 16). Firstly at E8.75 there is a reduction in the size of the *Nkx2.2* expression domain, while there is a slight over-expression of the orthologous gene *Nkx2.9*. At E9.5 there is a ventral expansion of *Nkx2.2* and *Nkx2.9* gene expression towards the ventral midline while the *Nkx6.1* expression domain, which was unaltered at E8.75 is completely absent from the basal plate. By E10.5 there is a restoration of the *Nkx6.1* domain resembling the wild type domain, while the ventral expansion of both the *Nkx2.2* and *Nkx2.9* domains is

persistent. By E12.5 in the *Foxa2 CKO*, the extent of the ventral expansion of the *Nkx2.9* domain is reduced, with *Nkx2.9* gene expression regressing towards the ABB, while the ventral limit of the expanded *Nkx2.2* domain is persistent. The analysis of all the Class II genes revealed that the dorsal limits of their expression domains was unaltered by the reduced levels of Shh signalling. Following the result the dorsal limits of the Class II genes were expected to remain constant, maintaining the cross-repressive interactions between the Class I and Class II genes which ultimately create the specific borders between progenitor domains, as demonstrated in the developing spinal cord (Briscoe et al., 2000).

Nkx2.2 and its orthologous gene *Nkx2.9* are considered to play a redundant role in the specification of ventral neuronal populations within the developing spinal cord, based on gene expression patterns and from loss-of-function analyses. Whereas the *Nkx2.2* mutant mice revealed a ventral to dorsal transformation of cell fates (Briscoe et al., 1999), the analysis of the *Nkx2.9* mutant mice revealed no such phenotype in the spinal cord (Pabst et al., 2003). Continued analysis of the *Nkx2.9* mutant mice revealed a novel role in the fate determination of branchial motor neurons within the rhombencephalon, indicating that *Nkx2.9* does play a specific role in converting positional information from Shh signalling into cell fate decisions (Pabst et al., 2003). No such analysis has yet been carried out within the mesencephalon, but the fact that *Nkx2.9* responded to the reduction of the Shh protein in more dramatic fashion than *Nkx2.2* could suggest another functionally divergent role between these two genes. It could be suggested that *Nkx2.9* is more sensitive to fluctuations in Shh signalling within the mesencephalon, as it is the first gene to be over-expressed at E8.75, and from E11.5 the extent of its over-expression is gradually diminished as levels of Shh signalling are

restored. The result of the ventral expansions of *Nkx2.2* and *Nkx2.9* is to create a larger progenitor domain expressing *Nkx2.2*, *Nkx2.9* and *Nkx6.1*, which at E10.5 is almost twice as large as compared to the wild type progenitor domain which expresses these three genes.

From subsequent co-localisation studies between *Foxa2* and *Nkx2.2* (figure 17) and *Shh*, *Foxa1* and *Nkx2.2* (data not shown) it became evident that at E9.5 and E10.5 there is some co-expression between *Foxa2* and *Nkx2.2* within the ventricular zone, while Shh and Foxa1 formed sharp boundaries of expression with *Nkx2.2*. As embryonic development progresses, the differentiated neurons expressing *Nkx2.2* form a boundary with *Foxa2* at the ABB and the extent of co-expression between these two genes within the ventricular zone is diminished. Therefore it could be speculated that the ventral limit of the *Nkx2.2* expression domain is regulated by *Foxa1* or *Shh* initially at E8.75-E10.5, and subsequently by *Foxa2*. This observation raised the question as to whether the ventral expansion of *Nkx2.2* and *Nkx2.9*, was caused directly by the reduction of *Foxa2*, and subsequent reduction of *Foxa1* between E8.75-E10.5 or whether both the *Nkx2* genes were following the fluctuations described in the Shh signalling.

To address this issue the *CKO Foxa2* χ embryos were analysed at E10.5, providing some interesting results (figure 27). In all the *Foxa2* deficient cells within the basal plate, ectopic Nkx2.2 protein was detectable, which draws the conclusion that *Foxa2* cell autonomously controls the ventral limit of the *Nkx2.2* expression domain, and that the cause of the ventral expansion described for *Nkx2.2* in the *Foxa2 CKO* was a response to the reduction of *Foxa2* rather than the reduced levels of Shh signalling. However, closer examination of the results generated from the *Foxa2 CKO* embryos

and *CKO Foxa2* χ embryos do not entirely support this statement. Firstly, in the *CKO Foxa2* χ embryos all the *Foxa2* negative cells are also negative for the expression of Foxa1 and Shh. Therefore it is not possible to simply state that *Foxa2* solely regulates the ventral limit of the *Nkx2.2* expression domain, as both *Foxa1* and *Shh* could still be implicated. Secondly, at E9.5 the ventral expansion of the *Nkx2.2* domain in the *Foxa2 CKO* does not reach the remaining *Foxa2* (*Foxa1 or Shh*) expressing cells at the ventral midline, and therefore cannot create a direct cross-repressive mechanism to limit the ventral extent of the *Nkx2.2* progenitor domain.

However, it is possible to exclude the role of *Shh* in controlling the ventral limit of the *Nkx2.2* expression domain. As Shh is known to function as a diffusible protein (Briscoe et al., 2001), it would be expected that if it played a role in regulating the ventral limit of the progenitor domains, Shh protein produced from wild type cells located adjacent to the *Foxa2* negative cells would be able to maintain the ventral limit of the *Nkx2.2* expression domain. The results from the *CKO Foxa2* χ embryos exclude a possible contribution of Shh signalling in maintaining the location of the most ventral progenitor domain. This process of elimination leaves both *Foxa1* and *Foxa2* as the only remaining candidates for regulating the ventral limit of the *Nkx2.2* (and possibly *Nkx2.9*) gene expression domain within the ventral mesencephalon.

Another observation, lending weight to the speculations that *Foxa1* and *Foxa2* are able to control the ventral limits of the progenitor domains in the basal plate is that the gradual regression of the *Nkx2.9* expression domain from E11.5 onwards corresponds to the gradual restoration of the *Foxa1* expression domain within the basal plate. Later analysis of the *Foxa2 CKO* at E15.5 revealed that both *Nkx2.2* and *Nkx2.9* gene

expression domains are completely restored to their wild type size and location (Dr. Anna Ferri, unpublished results).

Previous studies in the developing spinal cord have revealed that there is a critical period of Shh signalling which is required to specify the progenitor cells. During the neural plate stages, Shh signalling from the notochord causes the down-regulation of genes such as *Pax3* and *Pax7*, which are ultimately expressed in the dorsal neural tube (Ericson et al., 1996; Liem et al., 1995). Early progenitor cells, located ventrally require continuous exposure to the Shh signal to maintain a ventral identity. If the Shh signal was blocked prior to a critical time point, these progenitor cells re-expressed the dorsal markers. However, after a certain period of development, removal of the Shh signal did not alter the specification of the progenitor cells within the neural tube (Ericson et al., 1996). Therefore these studies could explain why the Class I genes do not expand into the basal plate of the *Foxa2 CKO*, and why the dorsal limits of the Class II genes remain constant. The progenitor cells within the basal plate of the *Foxa2 CKO* have already been exposed to the Shh signal for an appropriate period of time and thus are not competent to change fate in response to the alteration in levels of Shh signalling thus maintaining their ventral identity.

From the collective data generated it is possible to speculate that the ventral expansion of the Class II genes towards the ventral midline is due to the initial reductions of both Foxa1 and Foxa2 protein levels, in similar fashion to *Gli1* and *Gli2* gene expression. These two proteins could be involved in cross-repressive mechanisms to maintain the ventral extent and spatial organisation of the progenitor domains in the ventral

mesencephalon, in similar fashion to the mechanisms involved in the cross-repression between Class I and Class II genes outside of the ventral midline.

However, it cannot be excluded that the most ventral progenitor cells require higher levels of Shh signal and therefore are more plastic than their dorsal counterparts to any alterations in the levels of Shh protein to which they are exposed. From this study it is not possible to identify a reason to explain why *Nkx6.1* gene expression is absent from the E9.5 *Foxa2 CKO* embryos, but is subsequently restored.

2.2. A floor plate structure is maintained in the *Foxa2 CKO*

The floor plate structure is known to be a source of the Shh signalling molecule and is an important factor in the specification of neuronal subtypes along the dorsal-ventral axis (Placzek et al., 1993; Yamada et al., 1993). Studies in which this region is ablated describe the loss of specific classes of ventral neuronal populations (Placzek et al., 1991; Yamada et al., 1991). Although the origin of the floor plate within different species is a controversial subject area, it is acknowledged that in the mouse, a Shh signal derived from the notochord is able to induce the floor plate structure in the ventral midline of the overlying neural plate (Hynes et al., 1995a; Roelink et al., 1995). It has also been demonstrated that this specification of ventral midline cells into a floor plate structure is dependent upon early Shh signalling (Ericson et al., 1996).

The floor plate domain in the *Foxa2 CKO* was characterised using the gene expression patterns of *Foxa2* and *Shh*, which have been shown to be essential for floor plate development (Ang and Rossant, 1994; Chiang et al., 1996; Sasaki and Hogan, 1994).

Based upon the statement that the floor plate is dependent upon the early stages of Shh signalling, and the fact that the *Foxa2 CKO* embryos provide evidence that this early phase of Shh signalling remains intact, it was expected that the floor plate would be specified in the *Foxa2 CKO*. From the gene expression studies performed on the *Foxa2 CKO* embryos it was evident that a floor plate structure was maintained at the ventral midline (figure 11). Unfortunately, I was unable to successfully use other molecular markers such as floor plate 3 (FP3) or floor plate 4 (FP4) to demarcate the floor plate region within the wild type or *Foxa2 CKO* embryos. However, a previous study revealed that FP4 protein expression in located in a restricted domain at the ventral midline at E14 in the rat mesencephalon, (equivalent to E12 in the mouse), which closely resembles the remaining *Foxa2* expression domain in the *Foxa2 CKO* (Hynes et al., 1995a).

The floor plate region in the mesencephalon does not entirely share the characteristics of the classic floor plate described within the spinal cord. The classical floor plate is a collection of glial-like cells and is described as being non-neurogenic. Within the mesencephalon, the progenitor cells which eventually give rise to the mesDA are located within the ventral midline, suggesting that this region must become neurogenic. Consistent with this hypothesis, *Ngn2* gene expression can be detected spanning the ventral midline from E10.5 (figure 10) (Andersson et al., 2006; Kele et al., 2006), coupled with the expression of *Msx1* (figure 5), a gene previously inhibited by the early expression of *Shh* (Liem et al., 1995).

Therefore the floor plate structure is maintained within the ventral midline of the *Foxa2 CKO* during the early stages of mesencephalic development (E8.75-E9.5), and is

subsequently transformed into a neurogenic, non-floor plate region, in similar fashion to the wild type embryos at E10.5.

3. Effect of *Foxa2* deletion upon neuronal populations of the ventral mesencephalon

The substantial deletion of *Foxa2* from the ventral mesencephalon caused a dramatic reduction in the neuronal populations located within the basal plate. From the immunohistochemical assays performed on E12.5 embryos, it was determined that there was an 82% reduction of the *TH* positive mesDA neurons, a 65% reduction of the *Brn3a* positive RN neurons and a 72% reduction in the *Islet-1* positive OMC neurons (figures 4-7).

The three main neuronal populations which I analysed in the *Foxa2 CKO* embryos are spatially restricted along both the anterior-posterior and dorsal-ventral axes (figure 4). The regions of the mesencephalon where they are located are determined by the interpretation of the Fgf8 signal emanating from the MHB and Shh from the floor plate (Agarwala and Ragsdale, 2002; Fedtsova and Turner, 2001). Analysis of coronal and sagittal sections at E12.5 revealed that the most posterior neuronal population is the OMC, while the mesDA and RN occupy a similar position along the anterior-posterior axis closer to the diencephalon, but are distributed differently along the dorsal-ventral axis. In the *Foxa2 CKO*, even though there is a dramatic reduction and a subsequent decrease in the three dimensional size of each neuronal population at E12.5, the spatial relationships between these three nuclei remains conserved along the dorsal-ventral axis, while the domains are truncated along the anterior-posterior axis. This would

suggest that the progenitor cells which give rise to each population have been positioned correctly, and that this event occurred prior to the reduction of Shh signalling at E8.75, but possibly fewer progenitor cells were specified, resulting in the reductions in differentiated neurons described at E12.5. To determine whether this suggestion is plausible, I analysed the expression patterns of genes which are specifically expressed by the progenitor cells for each individual population.

From the analysis of genes specifically expressed by the mesDA progenitor cells at E10.5, I did not report any significant alterations in the size of the gene expression domains or intensity of the *in-situ* hybridisation signals, suggesting that the progenitor cells of the mesDA are correctly specified and are not reduced in number (figure 5). The gene expression domains of *Raldh1*, *Msx1* and *Lmx1a/1b* were unaltered within the ventricular zone of the *Foxa2 CKO* as compared to the wild type embryos. Additionally, *Ngn2* which is required for the correct development of the mesDA neurons (Kele et al., 2006) is also present within the ventricular zone spanning the ventral midline, further suggesting that the mesDA progenitor cells are generated correctly. Although Foxa2 protein is still detectable within the ventral midline, the progenitor domain of the mesDA neurons occupies a much broader domain of the ventricular zone, with the majority of the domain remaining *Foxa2* negative. This would suggest that there is no direct role for *Foxa2* in the specification of the mesDA progenitor cells. These data indicate that the reduction in the mesDA population at E12.5 is not a consequence of the incorrect specification or the generation of reduced numbers of progenitor cells within the *Foxa2 CKO*.

Following this observation, the molecular cascade which gives rise to the differentiated mesDA neurons was analysed to determine whether the 92% reduction in Foxa2 protein levels caused the failure of the mesDA progenitor cells to give rise to the *TH* positive differentiated mesDA neurons. Using *in-situ* hybridisation I analysed the expression patterns of several genes which have been demonstrated to be essential for the correct development of the mesDA neurons at E12.5. The newly differentiated mesDA neurons within the mantle layer express the transcription factors *Nurr1*, *Ptx3*, *Lmx1b* and *En1/En2* (Simon et al., 2001; Smidt et al., 2000; Smidt et al., 1997; Zetterstrom et al., 1997). The disruption of any one of these transcription factors (or both in the case of *En1/En2*) leads to the eventual loss of the mesDA neurons. From my analysis at E12.5 it was evident all of the transcription factors listed above were affected in an identical manner, and were all restricted within the remaining *TH* positive mesDA neurons underlying the ventral midline (figure 5), suggesting that the molecular pathway which is required for proper mesDA neuronal development remains intact within the *Foxa2 CKO*, and that *Foxa2* does not influence this molecular cascade directly. However this interpretation does not provide any clues as to why there is an 82% decrease in the *TH* positive mesDA population at E12.5. The fact that the mesDA progenitor cells are correctly specified by E10.5 would suggest that certain events must be occurring between E10.5 and E12.5 which cause the reductions described.

A similar conundrum arose from the analysis of the OMC progenitor cells. To determine whether the OMC progenitor cells were correctly generated in the *Foxa2 CKO*, I analysed the gene expression pattern of the OMC determinant gene *Phox2a*. A targeted disruption of *Phox2a* leads to the loss of the OMC population and other specific neuronal populations of the autonomic nervous system (Pattyn et al., 1997). At

E9.5 and E10.5 there was a slight reduction in the medial-lateral dimensions of the *Phox2a* expression domain within the ventricular zone (figure 7). However this slight reduction cannot possibly account for the 72% reduction in *Islet-1* positive OMC neurons at E12.5.

The progenitor cells which give rise to the RN neuronal population remain elusive. Although *Emx2* and *Brn3a* have been demonstrated to be essential for the correct development of this nucleus, both of these genes are not expressed within the ventricular zone and do not label the progenitor cells (Agarwala and Ragsdale, 2002; McEvilly et al., 1996; Xiang et al., 1996). Therefore it was not possible to determine whether the progenitor cells of the RN were correctly generated in the *Foxa2 CKO*.

The remaining *Brn3a* positive RN neurons, in similar fashion to the remaining *TH* positive mesDA neurons are located in the anterior regions of the mesencephalon. As described previously, there are two distinct domains which create the RN population. The anterior domain of the RN is characterised by the parvocellular cells, while the posterior domain is made from magnocellular cells (Massion, 1967; Massion, 1988). The analysis of the sagittal sections of the *Foxa2 CKO* embryos at E12.5 reveals that the parvocellular domain of the RN population remains, whilst there is a reduction in the size of the posterior magnocellular domain. However, without knowing whether the two neuronal populations which make up the RN are derived from a common group of progenitor cells or possess a different lineage, the significance of the magnocellular domain being affected in response to the deletion of *Foxa2* or the reduction of Shh signalling cannot be addressed.

With the exception of the RN neuronal population, it is possible to state that the neuronal progenitor cells which give rise to each neuronal population are largely intact in the *Foxa2 CKO*. It is also possible to state that the molecular cascade involved in the generation of the mesDA neuronal population is also unaffected by the reduction in Foxa2 protein levels. However, as the phenotype of the *Foxa2 CKO* seems to be related to a temporal defect in neurogenesis and neuronal differentiation, it is not possible to conclude that any subsequent steps in the molecular pathway for the mesDA or OMC development are unaffected by the loss of *Foxa2*.

4. What is causing the phenotype in the *Foxa2 CKO*?

4.1. Is there a decrease in rate of proliferation or an increase in programmed cell death, which causes the reduction in the three neuronal populations at E12.5?

To determine whether the phenotype described at E12.5 for the *Foxa2 CKO* was attributed to a decrease in cell proliferation, Brd-U incorporation assays were conducted from E9.5 until E12.5. The over expression of Shh signalling has been demonstrated to cause an increase in cell proliferation, as witnessed in many tumours (Dahmane et al., 2001; Echelard et al., 1993; Rowitch et al., 1999). It would therefore be expected that proliferation in the *Foxa2 CKO* at E9.5 and E10.5 would be reduced as compared to the wild type embryos, while it would be increased by the restoration of Shh signalling from E10.5 onwards. The data generated from the Brd-U incorporation studies suggested that there was a slight decrease in the rate of proliferation at E9.5 and E10.5, followed by a slight increase in proliferation at E11.5 (table 1, graph 1). However this

data was found to be statistically insignificant (table 1). Without increasing the number of embryos analysed in this study to determine whether the above statement is correct, it must be assumed that there is no significant alteration in the rate of proliferation in the *Foxa2 CKO*.

One explanation for the decreased neuronal populations at E12.5 could be that *Foxa2* is required to maintain the neuronal progenitor cells of the basal plate. Using the mesDA neurons as an example, it can be suggested that the progenitor cells which were correctly specified by E10.5 in the basal plate undergo apoptosis in the absence of Foxa2 protein at subsequent embryonic stages. This suggestion could explain why the remaining *TH* positive mesDA neurons are located immediately underneath the remaining Foxa2 protein domain at the ventral midline. The progenitor cells which give rise to these neurons must lie within the *Foxa2* positive domain at the midline and therefore can be maintained, whereas the progenitor cells located in more lateral regions of the basal plate cannot be maintained, resulting in the phenotype described at E12.5. However there was no evidence of any pyknotic cells present within the mesencephalon at any stage analysed indicating that there is no apoptosis present within mesencephalon of the *Foxa2 CKO* (figure 8).

Therefore, these two series of experiments reveal that the reductions in the neuronal populations of the *Foxa2 CKO* at E12.5 cannot be attributed to an increase in apoptosis or a decrease in the rate of proliferation.

4.2. Does the ventral expansion of *Nkx2.2* and *Nkx2.9* disrupt the development of the OMC or RN neuronal populations or cause an alteration in cell fate?

I previously described that there is a ventral expansion of the homeodomain transcription factors *Nkx2.2* and *Nkx2.9* towards the ventral midline, which results in the creation of a new broader *Nkx2.2*, *Nkx2.9*, and *Nkx6.1* positive progenitor domain. Co-localisation studies revealed that in the wild type embryos, this progenitor domain is relatively narrow and lies dorsally to the *Phox2a* positive OMC progenitor domain, whereas in the *Foxa2 CKO* this progenitor domain partially overlaps with the OMC (and possibly the RN) progenitor domain (figure 18). It is possible that this partial overlap of *Nkx2.2* and *Nkx2.9* gene expression within the OMC progenitor domain could disrupt the normal development of the OMC (and possibly RN) neurons by altering the specific "progenitor code" for these cells types.

To eliminate the possibility that the reduction in the neuronal populations described at E12.5 was caused by a change of cell fate in response to this ventral expansion of *Nkx2.2* and *Nkx2.9*, I analysed the expression patterns of genes which label other neuronal subtypes. At E12.5 there was no evidence of any alternative cell fates generated ectopically in response to the ventral expansion of *Nkx2.2* and *Nkx2.9* (figure 19). GABAergic neurons which are normally located near the ABB were not generated in more ventral locations, while there was no evidence of any ectopic serotonergic neurons generated in the *Foxa2 CKO*. Therefore it can be concluded that there is no alteration in cell fate specification within the ventral mesencephalon of the *Foxa2 CKO*. However, it is not possible to exclude a delay in the generation of the OMC or RN neurons in the *Foxa2 CKO* in response to the ventral expansion of *Nkx2.2* and *Nkx2.9*.

4.3. Is neurogenesis affected by the reduction in *Foxa2* protein levels?

From the analysis of the *Foxa2 CKO* embryos from E9.5 until E12.5 it was apparent that there were some slight alterations in the gene expression patterns of both *Ngn2* and *Mash1*, but generally neurogenesis was occurring at near to normal levels (figure 10). Birth-dating studies have revealed that the OMC neurons are born at E9.5 (Dr. Anna Ferri, unpublished work) (Altman and Bayer, 1981), and the expression of *Phox2a* lies within the broad domain of the *Ngn2* gene expression at this stage within the mesencephalon. At E9.5 *Ngn2* gene expression is unaltered in the *Foxa2 CKO*, suggesting neurogenesis and neuronal differentiation should be intact. However there is a complete absence of *Islet-1* positive post-mitotic OMC neurons at this stage in the *Foxa2 CKO*, suggesting that the phenotype in the *Foxa2 CKO* is related to defects in neuronal differentiation and not neurogenesis.

At E10.5 there is a slight reduction in the medial-lateral extent of the *Ngn2* expression domain, while there is a concomitant ventral expansion of the *Mash1* gene expression domain. It has previously been demonstrated that in the developing telencephalon, *Mash1* has the capability to re-specify the fate of progenitor cells which were previously influenced by *Ngn2* gene activity (Parras et al., 2002). However, no such alteration in cell fate was reported in the *Foxa2 CKO*, as seen by the absence of ectopic GABAergic neurons located ventral to the ABB (figure 19).

In the rhombencephalon, *Mash1* activity is believed to induce the transcription of *Phox2a* and *Phox2b* leading to the generation of specific noradrenergic neuronal populations such as the *locus coeruleus* (Bertrand et al., 2002). The induction of

Phox2a in the mesencephalon and ultimately the specification of the OMC cannot be attributed to *Mash1* activity as I was unable to detect any *Mash1* gene expression or protein at E9.5. Interestingly, a recent study has demonstrated that *Ngn2* activity is not required for the development of the OMC neurons, which were still detectable in the *Ngn2* knockout mice (Kele et al., 2006). How this result ties in with the observation that the OMC progenitor cells arise from within the *Ngn2* expression domain remains to be clarified. One possibility is that *Ngn1* activity is a requirement for the generation of the OMC progenitor cells, but no gene expression studies were performed at E9.5 for *Ngn1* during this study and therefore no conclusion can be made.

Taken together, all these results suggest that although there are some slight alterations in the gene expression patterns of the proneural genes, these small alterations cannot account for the dramatic phenotype described at E12.5. These results suggest that neurogenesis in the *Foxa2 CKO* is largely unaffected and should not be considered the primary source of the phenotype.

4.4. Is the phenotype described for the *Foxa2 CKO* mice attributed to defects in neuronal differentiation?

To explain the dramatic reductions in the neuronal populations within the ventral mesencephalon of the *Foxa2 CKO* embryos at E12.5 many different assays were conducted. It was shown that there was no increase in apoptosis (figure 8) or any statistically significant alteration in the proliferation of the neuronal progenitor cells (table 1, graph 1). Furthermore, the progenitor cells which give rise to the mesDA neuronal population (figure 5) and the OMC neurons (figure 7) were detected in the

Foxa2 CKO at E10.5. Even though it could be suggested that the size of these progenitor domains were slightly reduced, these reduction could not account for the dramatic losses described at E12.5. Moreover the gene expression patterns of the proneural genes revealed that even though there were some alterations in the *Foxa2 CKO* embryos, neurogenesis was largely unaffected by the reduced levels of Foxa2 protein within the ventral mesencephalon (figure 10). Taken together these results indicate that the neuronal progenitor cells are correctly specified, positioned and generated within the *Foxa2 CKO*, suggesting that the defect which causes the dramatic phenotype described at E12.5 is attributed to neuronal differentiation.

To confirm this hypothesis, analysis of the *Foxa2 CKO* at E10.5 and E12.5 was conducted using post-mitotic neuronal markers to detect neuronal differentiation. The results generated are suggestive of a defect in neuronal differentiation in the absence of Foxa2 protein. At E10.5 within the basal plate, the domain where Foxa2 protein would normally be expressed, there was a marked reduction in differentiated neurons as labelled by *β-tubulin* + or *HuC/HuD* + neurons (figure 9). The analysis of another neuronal differentiation marker, *Scg10* confirmed this result suggesting that there is an arrest of neuronal differentiation in the absence of Foxa2 protein in the ventral mesencephalon. This phenomenon was more evident at E12.5 where there was a dramatic reduction in the quantity of differentiated neurons within the basal plate. The remaining differentiated neurons correspond to the remaining neurons of each of the three neuronal populations studied at E12.5.

Furthermore, coupled with the reduced numbers of differentiated neurons observed in the *Foxa2 CKO* embryos, there was also an increase in the quantity of cells remaining

within the ventricular zone. Analysis of Sox2 protein, which is a marker for uncommitted, dividing neuronal progenitor cells (Li et al., 1998; Zappone et al., 2000), within the ventricular zone revealed that there was an increase in the thickness of this domain. Although quantification of the *Sox2* positive cells within the ventricular zone was not conduced, it can be qualitatively demonstrated that there is an increase in the thickness of the ventricular zone. Measurements of the ventricular zone at two specific locations (one where Foxa2 protein is no longer present, and another at the ventral midline where Foxa2 protein is still present) were conducted. At E10.5, there was no indication of any alteration in the thickness of the ventricular zone at the ventral midline, where the remaining Foxa2 protein is located. Conversely, in a more lateral domain of the ventricular zone where Foxa2 protein is no longer present, there was an increase in the thickness of the *Sox2* positive ventricular zone. Although at E12.5, there was also an increase in the thickness of the ventricular zone at the ventral midline, this alteration was less evident than at the lateral regions.

Taken together, all these results suggest that in the absence of Foxa2 protein within the basal plate there is a reduction in the numbers of differentiated neurons generated, and an increase in the number of progenitor cells which remain within the ventricular zone. Therefore these results provide evidence of a novel function of *Foxa2* within the basal plate of the mesencephalon to regulate the neuronal differentiation of the specific neuronal populations generated there, and that the phenotype described for the *Foxa2 CKO* embryos at E12.5 is attributed to a lack of neuronal differentiation.

5. Why do the *Foxa2 CKO* embryos survive embryonic development and why are they indistinguishable from their wild type littermates?

The analysis of the *Foxa2 CKO* embryos at E12.5 revealed that there was a substantial reduction in the three major neuronal populations of the ventral mesencephalon which are individually involved in controlling certain aspects of movement. It would therefore be expected that the ramifications of such dramatic losses at E12.5 would produce a severe phenotype to any *Foxa2 CKO* embryo which survived embryonic development. The observation that the *Foxa2 CKO* embryos survived development and were born according to the expected Mendelian genetical ratios (25% of litter were *Foxa2 CKO*) provided a puzzling paradoxical result. How was it possible that these mice were able to be born and be indistinguishable from their wild type litter mates, when the neuronal populations at E12.5 were nearly decimated by the loss of *Foxa2*?

In humans, the onset of Parkinson's disease is attributed to the gradual loss of the mesDA neurons (Eells, 2003; Simon et al., 2003; Wallen and Perlmann, 2003). When levels of the dopamine neurotransmitter are decreased, the control over voluntary movements is lost. In the analysis of the *Foxa2 CKO* embryos the differentiated mesDA neurons were identified by using *tyrosine hydroxylase* (*TH*). *TH* is the rate limiting enzyme in the synthesis of the dopamine neurotransmitter converting the amino acid tyrosine into $_{L}$-DOPA (Goridis and Rohrer, 2002; Kobayashi et al., 1995; Zhou et al., 1995), and a loss of *TH* function in mice leads to a global loss of all catecholamines, which proves to be lethal (Kobayashi et al., 1995). Although the complete loss of all catecholamines is lethal, it was not known to what effect the loss of only the dopamine neurotransmitter would cause during embryonic development. To address this issue,

mice which were solely deficient in the dopamine neurotransmitter were generated. These mice displayed hypoactivity, adipsia, aphagia and eventually died due to their inability to feed properly (Zhou and Palmiter, 1995).

The analysis of the *Foxa2 CKO* embryos at E12.5 revealed a reduction of 82% in the number of *TH* positive differentiated mesDA neurons (figure 4, 5). It would also be expected that the synthesis and subsequently the levels of the dopamine neurotransmitter would be greatly reduced due to the 82% reduction in TH. This hypothesis is supported by the finding that *AADC*, the enzyme involved in converting L-DOPA into the dopamine neurotransmitter (Goridis and Rohrer, 2002) is reduced at E12.5 in a similar fashion to *TH* (figure 5). These results would suggest that the *Foxa2 CKO* embryos which survive development should have reduced levels of dopamine neurotransmission and would exhibit certain aspects of the phenotype described for the dopamine deficient mice and some aspects of Parkinsonism. Although detailed movement analysis of the *Foxa2 CKO* mice was not conducted, mere observation revealed that none of the above mentioned characteristics were evident.

The red nucleus (RN) is located within the ventral mesencephalon and is believed to control the execution of finely learned movements, such as individual digit movements of the hand, and generally most automated movements (Kennedy, 1987; Kennedy, 1990). Although the function of the RN has been studied extensively during the past Century, little is known about the development of this nucleus within the ventral mesencephalon until recently. Loss of function analyses revealed that two transcription factors, *Brn3a* and *Emx2* play a vital role in the development of the RN. The inhibition of either transcription factor causes the loss of the RN (Eng et al., 2001; McEvilly et al.,

1996; Xiang et al., 1996). In both cases, newly born pups were unable to suckle correctly and eventually died. Generally, pups from the same litter must compete for the mother's milk, with the stronger pups gaining access to the source of milk more frequently than weaker pups. Whether the *Brn3a* or *Emx2* deficient mice were unable to suckle and feed correctly due to their inability to initiate the automated movements involved in suckling (due to the loss of the RN), thus making them less able to compete with their wild type littermates still remains unclear.

In the *Foxa2 CKO* embryos at E12.5, cell counting of *Brn3a* positive differentiated neurons revealed that there was a 65% reduction in the neuronal population of the RN (figure 6). Presuming that the phenotype described at E12.5 is persistent in the *Foxa2 CKO*, it would be expected that there would continue to be a dramatic reduction in the neuronal population of the RN. Although there is not a complete loss of the RN neurons in the *Foxa2 CKO* mice, the dramatic reduction in the RN neuronal population could suggest that the *Foxa2 CKO* mice would display a phenotype similar to the *Brn3a* or *Emx2* deficient mice, although milder. However no such phenotype could be identified from the *Foxa2 CKO*, with the ability of the newly born pups to suckle not being altered.

The Oculomotor complex (OMC), also known as the third cranial nerve, develops within and remains in the ventral mesencephalon. The motor neurons which form the OMC innervate the extraocular muscles surrounding the eye and the striated muscle of the eyelid, and also control the constriction of the pupil in response to changes in light intensity (Evinger, 1988; Kandel et al., 2000b).

Following the similar preconceptions of the results at E12.5, where there was a 72% reduction in the number of differentiated *Islet-1* positive OMC neurons, it would be expected that some mild phenotype should persist in the new-born *Foxa2 CKO* mice or in the adults. Identifying any defects in the innervation of the extraocular muscles or even the striated muscle of the eye lid would be very difficult, without conducting a series of intense physiological experiments. However, based on the previous findings that there was no discernable phenotype described for the new-born or adult *Foxa2 CKO* mice, no physiological tests of these muscles was conducted.

The observation that the adult *Foxa2 CKO* mice do not display any movement related disorders provides a paradoxical situation. If the *Foxa2 CKO* embryos at E12.5 reveal such a dramatic reduction in all three of the ventral neuronal populations which are involved in the control of various movements, why do the *Foxa2 CKO* mice survive embryonic development and why do they not display any of the expected phenotypes, either mild or severe? Could the lack of any obvious phenotype in the adult mice be a result of a compensatory mechanism present within the mesencephalon of the *Foxa2 CKO* mice? Could other neuronal populations compensate for the reductions in the mesDA, RN or the OMC neurons described at E12.5?

To address whether the phenotype described at E12.5 was persistent throughout the remaining stages of embryonic development, and whether there was a compensatory mechanism present within the *Foxa2 CKO* a post doctoral colleague within the laboratory continued the analysis of the *Foxa2 CKO* embryos from E12.5 until birth to determine whether the phenotype described at E12.5 was persistent. The results generated provided an explanation to why there was no apparent phenotype displayed

by the adult *Foxa2 CKO* mice. Detailed cell counting assays revealed that each of the neuronal populations within the ventral mesencephalon is gradually restored to near wild type levels by E18.5 (see Appendix A, figure 37, Table 2). At E12.5 in the *Foxa2 CKO*, there are only 18% differentiated mesDA neurons remaining in the ventral mesencephalon. At E15.5 and E18.5 there were a total of 46% and 83% differentiated mesDA neurons respectively. This gradual pattern of restoration of the mesDA neurons is also observed for the neurons of the RN and OMC.

Embryonic Stage	mesDA (*TH*)	RN (*Brn3a*)	OMC (*Islet-1*)
E12.5	18%	35%	28%
E15.5	46%	61%	45%
E18.5	83%	93%	83%

Table 2: Results of cell counting assays on the neuronal populations of the ventral mesencephalon. Results kindly donated by Dr. A. Ferri.

Concentrating on the molecular cascade involved in the generation of the mesDA neurons, by E15.5 there was also a gradual restoration of the gene expression patterns of *AADC*, *Lmx1b*, *Nurr1* and *Ptx3* (see appendix A, figure 38). These results generally comply with the quantity of *TH* positive mesDA neurons counted at this stage. The gradual restoration of the neuronal populations within the basal plate would explain why there was no phenotype evident in the adult *Foxa2 CKO* mice. Although by E18.5 there was not a complete restoration of the size of each neuronal population within the basal plate, it is suggestive that at later post-natal stages the neuronal populations are fully restored. This phenomenon would explain why there is no evident phenotype present in the adult *Foxa2 CKO* mice.

Continued analysis of the *Foxa2 CKO* embryos after E12.5 revealed that there was also a restoration in the gene expression patterns of the Class II transcription factors within the basal plate. Prior to E12.5 I described that *Nkx2.2* and *Nkx2.9* expression domains expand ventrally towards the ventral midline in response to a reduction in Shh signalling (figure 15, 16). Whereas the majority of downstream targets of Shh signalling were already restored to their wild type locations by E12.5, both *Nkx2.2* and *Nkx2.9* expression domains remained enlarged. By E15.5 they were restored to their wild type locations suggesting that the progenitor domains of the ventral mesencephalon are completely restored in the *Foxa2 CKO* after E12.5. Consistent with these findings, Dr. Ferri also demonstrated that neuronal differentiation was also geadually restored in the *Foxa2 CKO* between E12.5 and E15.5 (data not shown). Analysis of β-tubulin, HuC/HuD proteins and *Scg10* gene expression revealed that the quantities of differentiated neurons within the basal plate were almost similar to the wild type levels. The size of the *Sox2* positive ventricular zone was also restored to normal size by E15.5, providing further evidence to suggest that *Foxa2* plays an important role in the regulation of neuronal differentiation within the basal plate of the mesencephalon.

Throughout the remaining analysis of the late stage *Foxa2 CKO* embryos it was observed that Foxa1 protein levels were always elevated when compared to the wild type embryos. This observation provides further evidence to suggest that *Foxa1* is over-expressed in the basal plate to compensate for the reduced levels of Foxa2 protein, and that these elevated levels of Foxa1 protein are responsible for restoring the phenotype described in the early embryonic stages of the *Foxa2 CKO* embryos. This observation is in keeping with previous studies which demonstrated that *Foxa1* has the ability to restore certain aspects of the *Foxa2* null mice (Duncan et al., 1998).

6. Reduction of *Foxa2* protein levels causes the over-expression of *Wnt1*

Wnt1 is detectable in the developing embryo from the 6-8 somite stage and is expressed within a broad domain of the presumptive mesencephalon (Wilkinson et al., 1987). The gene expression pattern of *Wnt1* is later restricted to the ventral and dorsal midline and also in a ring around the MHB. It has been demonstrated that *Wnt1* is important for the development of the mesencephalon, as mice deficient for *Wnt1* lack the mesencephalon and gradually lose regions of the anterior rhombencephalon (McMahon and Bradley, 1990). It was later determined that *Wnt1* functions to maintain the expression of *En1* within the mesencephalon (Danielian and McMahon, 1996; McMahon et al., 1992). Furthermore it was shown that *Wnt1* possesses a mitogenic effect over neuronal progenitor cells within the developing neural tube (Dickinson et al., 1994). Ectopic expression of *Wnt1* causes an increase in progenitor cell proliferation and expansion of the ventricular zone (Dickinson et al., 1994).

More specifically, *in-vitro* assays provide a role for *Wnt1* in the development of the mesDA neuronal population, by controlling the differentiation of mesDA progenitor cells into mesDA differentiated neurons (Castelo-Branco et al., 2003). Over expression of *Wnt1* in cell culture of mesDA progenitors increases the proliferation of the precursor cells. More recently, a novel role for *Wnt1* in the specification of the mesDA neurons has been proposed (Prakash et al., 2006). *Wnt1* activity is also essential to maintain the expression of *Otx2* in the ventral mesencephalon which in turn downregulates the expression of *Nkx2.2* creating a region of ventricular zone where the mesDA progenitors are located (Prakash et al., 2006)

In the *Foxa2 CKO* there is a 92% reduction in the number of *Foxa2* expressing cells within the basal plate of the mesencephalon. This deletion of *Foxa2* is concomitant with an over-expression of *Wnt1* (figure 21), which is persistent throughout the remainder of embryonic development (Dr. Ferri, unpublished results).

Why is there an over-expression of *Wnt1* in the *Foxa2 CKO*? There are several possibilities which could explain this phenomenon. One such suggestion is that *Foxa2* is involved in the down-regulation of *Wnt1* at the ventral midline. When *Foxa2* levels are reduced, there is an increase in *Wnt1* gene expression as expected for loss of a repressive system. However, this suggestion cannot be true for the entire ventral mesencephalon, as *Wnt1* is over-expressed within the ventral midline and in the same cells as the remaining *Foxa2* gene expression. Another possible suggestion is that *Wnt1* plays a role in an intrinsic regulatory system which monitors the levels of Foxa2 protein in the basal plate of the mesencephalon such that if Foxa2 protein levels reach a critical low (as in the *Foxa2 CKO*) *Wnt1* is over-expressed to induce the over-expression of *Foxa1* to compensate.

To address whether *Wnt1* has the capability to induce the transcription of *Foxa1*, assays are being conducted within the laboratory in which Wnt signalling is blocked in the *Foxa2 CKO* embryos. Very preliminary data reveals that in the absence of *Wnt1* signalling, there is no recovery of *Foxa1* expression suggesting therefore that the over-expression of *Wnt1* in the *Foxa2 CKO* is possibly involved in the restoration of *Foxa1* gene expression and ultimately phenotype described for the *Foxa2 CKO*. However these experiments must be repeated to ensure reproducibility before any conclusions can be drawn. Interestingly, contrasting results have been generated from the analysis of the

Foxa1 -/- and *Nestin::Cre; Foxa2 Floxed* mice. In these embryos there is no over-expression of *Wnt1* while *Foxa2* and *Foxa1* are respectively restored (Dr. Ferri, unpublished results).

The most recent assays conducted within the Wurst laboratory (Prakash et al., 2006) could suggest another possible role for the over-expression of *Wnt1* within the *Foxa2 CKO* embryos. In their model, *Wnt1* indirectly represses the expression of *Nkx2.2* at the ventral midline through the maintenance of *Otx2* (Prakash et al., 2006). When *Otx2* is conditionally deleted from the mesencephalon there is a ventral expansion of *Nkx2.2* towards the ventral midline (Vernay et al., 2005). Therefore, when these data are used to interpret the phenotype of the *Foxa2 CKO* it could be proposed that the *Wnt1* is over-expressed in order to inhibit the ventral expansion of *Nkx2.2* and *Nkx2.9* coming into the mesDA progenitor domain potentially leading to an alteration in the specification of these progenitor cells into 5-HT neurons of the rhombencephalon. Superimposition of the *Wnt1* expression domain in the *Foxa2 CKO* embryo with *Nkx2.2* or *Nkx2.9* gene expression reveals no overlap, supporting this hypothesis. The ventral limit of the *Nkx2.2* or *Nkx2.9* domain reaches the dorsal-later limit of the *Wnt1* expression domain (data not shown). One potential problem with this interpretation is that the expression of *Otx2* is never altered in the *Foxa2 CKO* (figure 21), yet during the time when *Otx2* is supposedly repressing *Nkx2.2* (E9.5 and E10.5) there is a dramatic ventral expansion of the *Nkx2.2* and *Nkx2.9* domain. Therefore, it could be proposed that *Wnt1* is directly inhibiting the ventral expansion of *Nkx2.2* and *Nkx2.9* by currently unidentified methods. Ectopically expressing *Wnt1* within the *Nkx2.2* domain could potentially resolve this hypothesis.

Whether the over-expression of *Wnt1* at the ventral midline is directly linked to *Foxa2* remains unclear. Analysis of the *Foxa2 CKO* at E11.5 and E12.5 reveal ectopic *Wnt1* gene expression within the alar plate (figure 21) which could suggest that *Wnt1* is under the control of a yet unidentified mechanism, independent of *Foxa2*.

Finally, another more speculative explanation for the over-expression of *Wnt1* in the basal plate of the *Foxa2 CKO* embryos could be to control proliferation. Shh signalling is known to induce proliferation of progenitor cells, and hyperactive Shh signalling induces tumours (Dahmane et al., 1997; Dahmane et al., 2001; Echelard et al., 1993; Rowitch et al., 1999). *Wnt1* is also known to induce the proliferation of progenitor cells, and ectopic expression of *Wnt1* in the neural tube can induce the expansion of the ventricular zone (Dickinson et al., 1994). In the *Foxa2 CKO*, there was a marked reduction in differentiated neurons, while the *Sox2* positive progenitor cell domain within the ventricular zone became thicker (figure 9). This expansion of the ventricular zone could therefore be a consequence of increased proliferation induced by the over-expression of *Wnt1*. Therefore *Wnt1* could be over-expressed in the basal plate to ensure that the rate of proliferation is not dramatically altered in an environment where Shh signalling has been reduced. However, this is mere speculation as the rate of proliferation in the *Foxa2 CKO* embryos was not altered in a statistically significant manner, even though there was a marked reduction of Shh signalling from E8.75 until E11.5. The over-expression of *Wnt1* is maintained throughout all the embryonic stages analysed. Why this consistent over-expression does not induce any over-proliferation within the mesencephalon cannot be explained without conducting a more thorough investigation into the rate of proliferation in the *Foxa2 CKO* embryos.

One un-explained phenomenon was observed during the analysis of the *Foxa2 CKO* embryos. In these embryos *Wnt1* gene expression is located in a broad domain within both the ventricular zone and the mantle later at the ventral midline. This domain overlaps with the remaining Foxa2 positive cells at the ventral midline, especially at E10.5 when all the remaining Foxa2 positive cells co-express *Wnt1*. Therefore the question raised is; why do the cells which ectopically over-express *Wnt1* not cause a recombination event to delete *Foxa2*? One possible answer to this question could lie with the specific enhancer used in the *Wnt1-Cre* animals. Maybe the *Wnt1-Cre* construct did not contain a specific enhancer or promoter which is essential for the ventral midline expression of *Wnt1*. Therefore there would be no Cre recombinase protein encoded in the cells located at the ventral midline and therefore *Foxa2* would not be inactivated in these cells, regardless of the over-expression of *Wnt1*. This possibility is currently being investigated within the laboratory.

7. Analysis of the *Shh CKO*

The analysis of the *Shh CKO* embryos was intended to provide evidence as to whether the phenotype described in the *Foxa2 CKO* was caused directly by the deletion of *Foxa2*, or indirectly via the Shh signalling pathway. To reduce Shh protein levels from the ventral mesencephalon, the *Wnt1-Cre* mouse line was used to drive the recombination event, thus ensuring that a fair comparison could be made between the *Foxa2 CKO* and *Shh CKO* embryos. This recombination event was evident by E8.5, as previously described for the *Foxa2 CKO*. Although *Shh* RNA transcript was still detected in a small domain spanning the ventral midline, it was not possible to detect any Shh protein within the ventral mesencephalon (figure 28, 34). It was not possible to

determine whether the loss of Shh protein was due to the specificity of the antibody or whether the recombination event altered the post-translation control of the *Shh* RNA, which resulted in the loss of the Shh protein. Consistent with the idea that Shh protein levels were dramatically reduced, the gene expression of immediate downstream targets of Shh signalling *(Ptc and Gli1)* were also detected at extremely low levels in the mesencephalon, further indicating that Shh signalling was dramatically reduced in the *Shh CKO*. *Shh* expression elsewhere in the embryo was unaffected (data not shown). This observation suggested that Shh signalling would be greatly reduced within the ventral mesencephalon.

From the analysis of the *Foxa2 CKO* and previous studies, it has been well documented that *Foxa2* and *Foxa1* can induce the transcription of *Shh* (Duncan et al., 1998; Echelard et al., 1993; Sasaki and Hogan, 1994). It has also been demonstrated within our laboratory that the ectopic expression of *Shh* is able to induce the expression of *Foxa1* and *Foxa2,* albeit indirectly (Dr Wei Lin, unpublished data). In the *Shh CKO* there was a reduction of the size of the *Foxa1* and *Foxa2* domains at E10.5, which was persistent until E12.5, and the domain was restricted to a narrow domain spanning the ventral midline (figure 28). This was an unsurprising result, as it would be expected that a reduction in Shh signalling, would affect the expression of either *Foxa1* or *Foxa2.* Interestingly, this loss of lateral *Foxa1* and *Foxa2* expression in the *Shh CKO* is reminiscent to the zebrafish *syu* -/- (zebrafish *Shh* homologue) phenotype. These mutant fish maintain the notochord and mFP cells as determined by *Foxa2* expression, whilst losing the lFP cells, marked by the absence of *Foxa2* expression (Schauerte et al., 1998). Therefore it is possible to suggest that in the absence of Shh signalling the usual homeogenetic induction of *Foxa2* and *Shh* within the ventral neural tube is absent in the

Shh CKO embryos. The absence of *Foxa1* and *Foxa2* expression lateral to the ventral midline could also suggest that an earlier signalling event is important to induce both *Foxa1* and *Foxa2* in lateral regions of the ventral neural tube.

The data generated from the cyclopamine experiments using the *Foxa2 CKO* embryos revealed that Foxa1 protein was still detected when there was no Shh signalling present. However, the cyclopamine was administered to the embryos at a time after Shh signalling activity has been functioning for some time, and therefore it is not possible to state that *Shh* is not required for the expression of *Foxa1* or *Foxa2*. Together, the data suggest that there is a transient requirement of *Shh* for the activation of *Foxa1* and *Foxa2*.

Unlike the *Foxa2 CKO* where Shh signalling was affected by E8.75, the recombination of the *Shh* floxed alleles would occur much earlier, thus reducing Shh signalling at an earlier time point. It seems that this short period of time plays a crucial role in the specification of the mesencephalon. It has been previously described that there are two critical periods for Shh signalling to correctly pattern the developing neural tube (Ericson et al., 1996). The first period is involved in repressing the Class I transcription factors which are initially expressed near the ventral midline, and allowing the progenitor cells at the ventral midline to adopt a ventral fate. The second period of Shh signal is intended to induce the diversity of gene expression within the ventral domains which eventually leads to the generation of distinct neuronal populations. However, it has also been documented that high levels of Shh signalling are required to maintain the ventral fate of the progenitor cells for a distinct period of time. If Shh signalling is

blocked during this critical period, the progenitor cells in the ventral domains re-express the Class I transcription factors and revert to a dorsal cell fate (Ericson et al., 1996).

The analysis of both Class I and Class II transcription factors in the *Shh CKO* reveal that the Shh signalling during this critical early period has been affected. By E12.5 it was evident that the majority of the mesencephalon was "dorsalised," marked by the distinct ventral expansion of *Pax3* and *Pax7* expression domains towards the remaining *Shh* gene expression domain at the ventral midline (figure 32), and also the ventral expansion of *Gli2* and *Gli3* to the same ventral location (figure 34). Concomitant with the ventral expansion of the Class I genes, there was a complete absence of *Nkx2.2* in the basal plate from E10.5, and a marked reduction in the expression domain of *Nkx6.1* (figure 33). Therefore it can be concluded from these data that at the time of the recombination event, Shh signalling was in the process of specifying the mesencephalon during the primary critical period. The immediate reduction in Shh protein levels caused the progenitor cells of the ventral mesencephalon to abandon the expression of the Class II genes (*Nkx2.2*) and revert back to their dorsal cell fates. It is interesting to consider that inhibiting Shh signalling only 6 hours earlier would have such dramatic consequences.

These results could explain why the *Foxa1* and *Foxa2* expression domains were restricted to a small region spanning the midline. As Shh signalling from the notochord would not have been inhibited by the recombination event, continued Shh signalling would have specified the floor plate structure and maintained the expression of *Foxa1* and *Foxa2* at the ventral midline. The ventral identity of progenitor cells within the floor plate would be maintained. However, the reduced levels of Shh protein emanating

from the floor plate were inadequate to maintain the expression of the Class II genes and maintain the ventral fate of progenitor cells located in the lateral domains of the basal plate. Alternatively, if we make a comparison with the zebrafish model for floor plate induction, we could suggest that the expression of both *Foxa1* and *Foxa2* at the ventral midline is induced by a signalling pathway other than Shh signalling. In the zebrafish it has been shown that the mFP cells, characterised by the expression of *Foxa1* and *Foxa2*, are induced by *Nodal* signalling from the notochord and that there are *Nodal* related binding sites on the *Foxa2* promoter (Muller et al., 2000; Rastegar et al., 2002; Strahle et al., 2004). However, there is currently no evidence to suggest that this signalling pathway is also active in the mouse.

Comparisons between the *Foxa2 CKO* and *Shh CKO* can already be made. The progenitor cells in the *Foxa2 CKO* maintain their ventral identity and inhibit the expression of the Class I genes in the basal plate, due to the reduction in Shh signalling occurring after its critical period of signalling, whereas the progenitor cells of the *Shh CKO* revert to their original fate, and express the Class I genes. Therefore the phenotype of the *Shh CKO* embryos resembles the phenotype of the *Shh* deficient mice more closely than the *Foxa2 CKO* phenotype.

To determine what affect the reduced levels of Shh signalling, and the subsequent alterations in the specification of the progenitor domains of the ventral mesencephalon, had on the three main neuronal populations. The analysis of the *Shh CKO* at E12.5 revealed that the reductions of the neuronal populations were more severe than in the *Foxa2 CKO* embryos. Consistent with this severe phenotype at E12.5, the development of the *Shh CKO* was arrested, and there was no record of any *Shh CKO* embryo

surviving embryonic development. These embryos displayed a complete absence of the OMC and RN neurons from the basal plate. Cell counting of *TH* positive differentiated mesDA neurons revealed that only 6% were generated at E12.5 (figure 29). Due to time constraints, I did not analyse the *Shh CKO* thoroughly using every molecular marker utilised in the analysis of the *Foxa2 CKO*. To determine whether there were any other factors contributing to the phenotype, I checked to see whether there were any defects in neurogenesis or in neuronal differentiation.

From the analysis, it was evident that neurogenesis was dramatically affected at E12.5 in the ventral region of the mesencephalon. Both Mash1 and Ngn2 protein domains were reduced near the ventral midline, whereas Mash1 protein was maintained in the regions of the alar plate (figure 30). As previously stated, *Ngn2* is essential for the development of the mesDA neurons (Kele et al., 2006). The remaining *TH* positive mesDA neurons would therefore be generated from the remaining *Ngn2* positive cells at the ventral midline, whereas there was no neurogenesis evident in the domain where the RN or OMC neurons originate from. It became evident that there was also a dramatic reduction in the number of differentiated neurons present in the *Shh CKO* (figure 31), especially in the regions where Foxa1 or Foxa2 proteins were no longer present. Concomitant with the reduced number of differentiated neurons, there is a dramatic expansion of the *Sox2* positive ventricular zone, providing further evidence that the progenitor cells in the absence of Foxa2 or Foxa1 protein cannot progress through normal neuronal differentiation in the ventral mesencephalon. This aspect of the *Shh CKO* phenotype is very similar to the *Foxa2 CKO*.

It is well documented that ectopic Shh signalling increases the rate of proliferation in progenitor cells (Echelard et al., 1993; Rowitch et al., 1999). It would therefore be expected that due to the reduced levels of Shh signalling, there would be a decrease in the rate of proliferation. Closer investigation of coronal brain sections revealed that the ventricular zone was dramatically enlarged at E12.5, which would suggest that the proliferation of the progenitor cells was increased. However, due to time constraints I was unable to investigate whether the rate of proliferation was affected in the *Shh CKO*, or whether the phenotype described was due to an increase in apoptosis. These assays are currently being conducted within the laboratory.

Concluding the interpretation of the results generated from the *Shh CKO*, it is possible to suggest three causes to the losses of the OMC and RN and severe reductions in the mesDA neuronal populations. Firstly, the patterning of the ventral mesencephalon was altered to adopt a dorsal mesencephalic fate, and therefore the fate of the progenitor cells which would give rise to the OMC, RN and mesDA would also be altered. Secondly, there was a dramatic reduction in neurogenesis, which could ultimately lead to the losses described. Thirdly, and most similar to the phenotype described in the *Foxa2 CKO* at the same stage, is that neuronal differentiation is affected in the basal plate of the mesencephalon in the absence of *Foxa1* or *Foxa2*.

In the *Shh CKO* the remaining *Foxa1* and *Foxa2* expression domains are located spanning the ventral midline. It is no coincidence that the only differentiated neurons (the remaining 6% of the TH positive mesDA neurons) lie immediately ventral to this domain. Consistent with the third statement above, in the *Shh HET* embryos at E12.5

where there is no alteration in the expression of *Foxa2* within the ventricular zone, there is hardly any reduction in the neuronal populations of the ventral mesencephalon.

More recent work within the laboratory has revealed that the progenitor cells for the mesDA neurons can be detected spanning the ventral midline within the remaining *Foxa2* domain (Dr. A. Ferri, unpublished data). Taken together, the data suggests that the defects described in the *Shh CKO* embryos are likely to be primarily due to a failure of neurogenesis, followed by defective neuronal differentiation. It is unlikely that the defects described for the mesDA neurons are due to the reduction in *Foxa* proteins, since they are expressed within the remaining mesDA progenitor cells near the ventral midline. It is also possible that the dorsalisation of the majority of the basal plate could also contribute to the final phenotype.

It has recently been demonstrated within our laboratory that *Wnt1* is slightly over-expressed in the *Shh CKO* embryos, but not to the same extent as in the *Foxa2 CKO* embryos. Whether this slight over-expression of *Wnt1* is sufficient to cause the hydromyelia described at E10.5 and E12.5, as demonstrated in previous studies (Dickinson et al., 1994) remains to be seen.

Although interesting, the phenotype of the *Shh CKO* cannot be directly compared to that of the *Foxa2 CKO* due to the kinetics of the reduction in Shh signalling. In the *Foxa2 CKO*, Shh signalling is reduced by E8.75, whilst in the *Shh CKO* it is reduced at E8.5. The dramatic phenotype of the *Shh CKO* reveals how important 6 hours of Shh signalling is to the overall development of the embryo.

8. Characterisation of progenitor domains in the mesencephalon

In the developing spinal cord neuronal populations are generated at distinct locations along the dorsal-ventral axis. Neurons which are involved in processing sensory information are located dorsally, whilst neurons involved in the processing of motor output are located ventrally (Briscoe and Ericson, 2001; Jessell, 2000; Price and Briscoe, 2004). The physiology and anatomy of the neuronal populations which inhabit the spinal cord have been well characterised. In combination with multiple studies using either a gain-of-function or loss-of-function approach for genes expressed in the developing spinal cord, it was possible to determine where the progenitor cells for each neuronal population were specified along both the anterior-posterior and dorsal-ventral axes, and which genes contributed to their specification. All this work was combined to create the progenitor code for neuronal specification of the spinal cord (reviewed by Jessell, 2000).

At present there is no such progenitor code for the neuronal populations of the mesencephalon. From all the co-expression studies I performed during my analysis of the wild type or *Foxa2 CKO* embryos, I attempted to create a progenitor code for the ventral mesencephalon, in similar fashion to the spinal cord model. However, unlike the spinal cord where each neuronal population can be easily identified using molecular markers, it is currently impossible to identify each specific population within the mesencephalon. For instance, the three main neuronal populations (mesDA, RN and OMC) can be easily using molecular markers, while other neuronal populations such as the Edinger-Westphal nucleus or the nucleus of Darkschewitsch which are located in the immediate vicinity of the OMC neurons cannot be specifically labelled during

embryogenesis. We know of their presence based on histological analyses of adult mice, and know of their specific generation times based on birth-dating studies (Altman and Bayer, 1981). This situation is also true for the dorsal mesencephalon where specific molecular markers are not known to label specific nuclei such as the inferior and superior colliculi or the parabigaminal nucleus. Regardless of this potential setback, I characterised the ventral mesencephalon into five specific progenitor domains solely based on gene expression studies, and not based upon the neuronal populations generated from each domain as in the spinal cord model. Three domains were assigned to the alar plate, but more intensive studies of the dorsal mesencephalon will no doubt reveal more (see diagram M below).

The progenitor cells which give rise to the mesDA neurons and the OMC neurons have been identified. Progenitor cells expressing *Msx1* and *Lmx1a* at the ventral midline of the mesencephalon give rise to the mesDA neuronal population (Andersson et al., 2006) (Diagram M, red domain). Loss-of-function analysis of the *Phox2a* gene revealed that it is the determinant for OMC neuronal generation in the mesencephalon (Pattyn et al., 1997), and the OMC progenitor cells are located in a domain adjacent to the mesDA progenitor domain (diagram M, yellow domain). The progenitor cells which give rise to the RN neuronal population have not yet been identified. Although it is known that both *Emx2* and *Brn3a* are required for the generation of the RN, it is not known which genes are involved in the specification of the progenitor cells (Agarwala and Ragsdale, 2002; McEvilly et al., 1996; Xiang et al., 1996).

Birth-dating studies in the rat suggest the RN population is born between E12-E14 (equivalent to E10 - E12 in the mouse) (Altman and Bayer, 1981). From my analysis of

Brn3a protein expression at E11.5 it became evident that the newly differentiated RN neurons lie immediately ventral to the progenitor domain from where the OMC neuronal population is generated. Therefore it may be assumed that the RN progenitor cells are located within this same domain. These observations would suggest that the OMC neurons are generated during a specific time point, and once their generation is completed, the progenitor cells within this domain somehow switch to generate RN neurons. Birth-dating studies for the OMC neuronal population support this hypothesis. The OMC neurons are generated from E9.5 until E11.5.

This type of temporal switching of cell fate from a common set of neuronal progenitors is not uncommon. In the developing spinal cord depending upon the stage of embryonic development, motor neurons or oligodendrocytes are generated from within the same restricted progenitor domain within the ventral neural tube (Kessaris et al., 2001). Motor neurons which are the first neuronal population to differentiate (Ericson et al., 1992) cease to be generated, and in response to an alteration in gene expression, oligodendrocytes are generated instead.

I am proposing that such a mechanism is also present within the ventral mesencephalon to generate either OMC or RN neurons from a common pool of progenitor cells. It became apparent that *Phox2a* gene expression was absent from the progenitor domain when the first *Brn3a* positive differentiated neurons were detected (data not shown). Although birth-dating studies conducted within our laboratory have confirmed that a small proportion of OMC neurons are born at E11.5 (~2%), they are most likely to be generated in the more posterior regions, while the RN neurons are detected in more posterior regions first. It also became apparent that *Irx3* gene expression was present

within this progenitor domain from E9.5 (data not shown). Therefore there is a possibility that *Irx3* also plays a key role in the specification of these two neuronal populations, and possibly *Irx3* gene expression could be used to label the RN progenitor cells. *Phox2a* is known to be the determinant for the development of the OMC, thus it is possible that when *Phox2a* gene expression is switched on, it may inhibit the specification of an alternative cell fate. The down-regulation of *Phox2a* gene expression along the anterior-posterior axis of the mesencephalon allows the specification of the RN neurons.

Therefore I propose that the combinatorial expression of *Foxa2*, *Phox2a, Nkx6.1* and *Irx3* between E9.5 and E11.5 is required to generate the OMC neurons. When *Phox2a* gene expression is down-regulated at E11.5, the RN neurons are generated (see table 3).

Neuronal population	**Genes expressed in progenitor domain**	**Time scale of neurogenesis**
OMC	*Foxa2, Phox2a, Irx3, Nkx6.1*	E9.5 – E11.5
RN	*Foxa2, Irx3, Nkx6.1*	E11.5 – E12.5

Table 3: *Table to display genes specifically expressed within the progenitor domains of the OMC and RN. The neurons of the RN are first detected when Phox2a gene expression has been down-regulated.*

In order to test this hypothesis we must re-analyse the *Phox2a* and *Irx3* deficient mice. If *Phox2a* plays a role in inhibiting the generation of RN neurons while it is expressed, it would be expected that RN neurons would be generated at an earlier time-point in the *Phox2a* deficient mice, instead of the OMC neurons (which are absent). If my hypothesis for the possible role of *Irx3* in the specification of these two neuronal

populations is correct, then it would be expected that in the *Irx3* deficient mice, there would be an absence of both populations from the ventral mesencephalon.

The interpretation of the co-expression studies allowed me to propose a potential molecular marker for the RN progenitor cells, and propose that both the OMC and RN neurons originate from a common precursor pool. However, further molecular markers for each specific neuronal population of the mesencephalon must be discovered in order to generate a comprehensive map of the expression patterns of the transcription factors involved in neuronal specification.

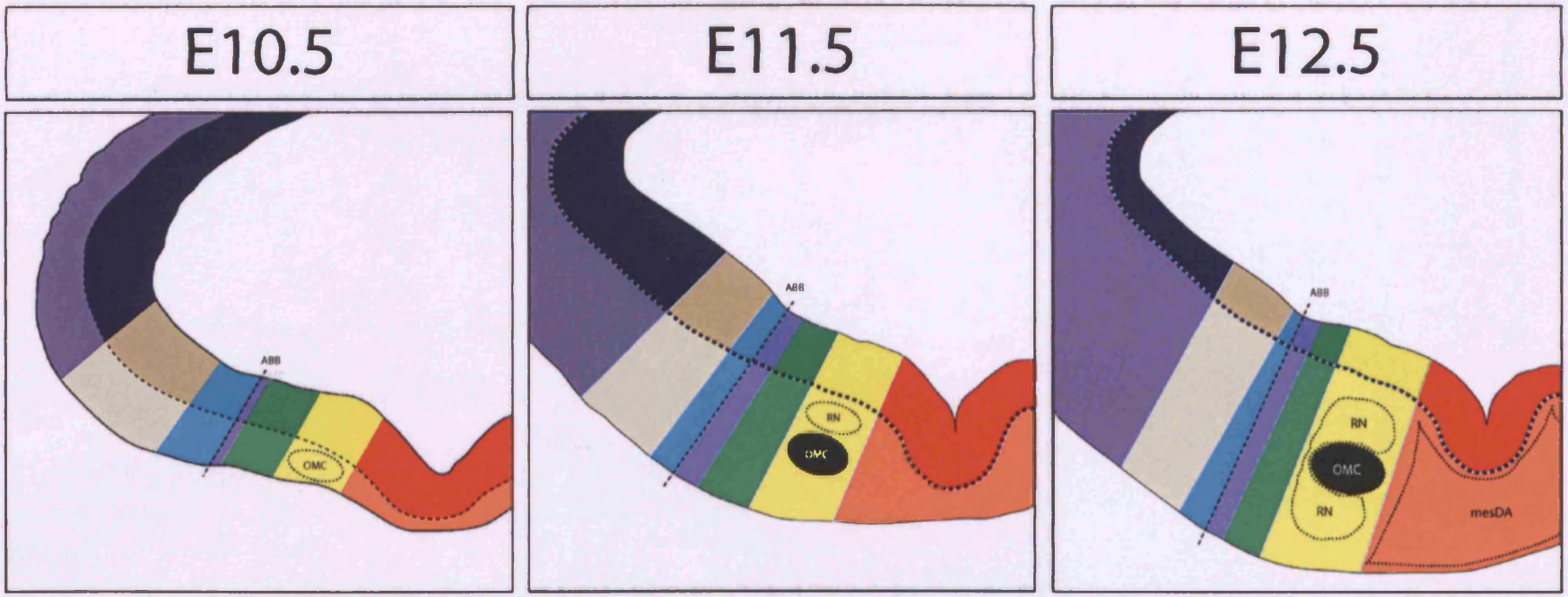

Diagram M: *Schematic representation of gene expression patterns within the ventral mesencephalic progenitor domains along the dorsal-ventral axis. All gene expression patterns were compared to Foxa2. ABB corresponds to the alar-basal boundary. Bold black dotted line corresponds to the boundary between the ventricular zone and the mantle layer. OMC, RN, mesDA represent the oculomotor complex, the red nucleus and the dopaminergic neurons of the ventral mesencephalon respectively.*

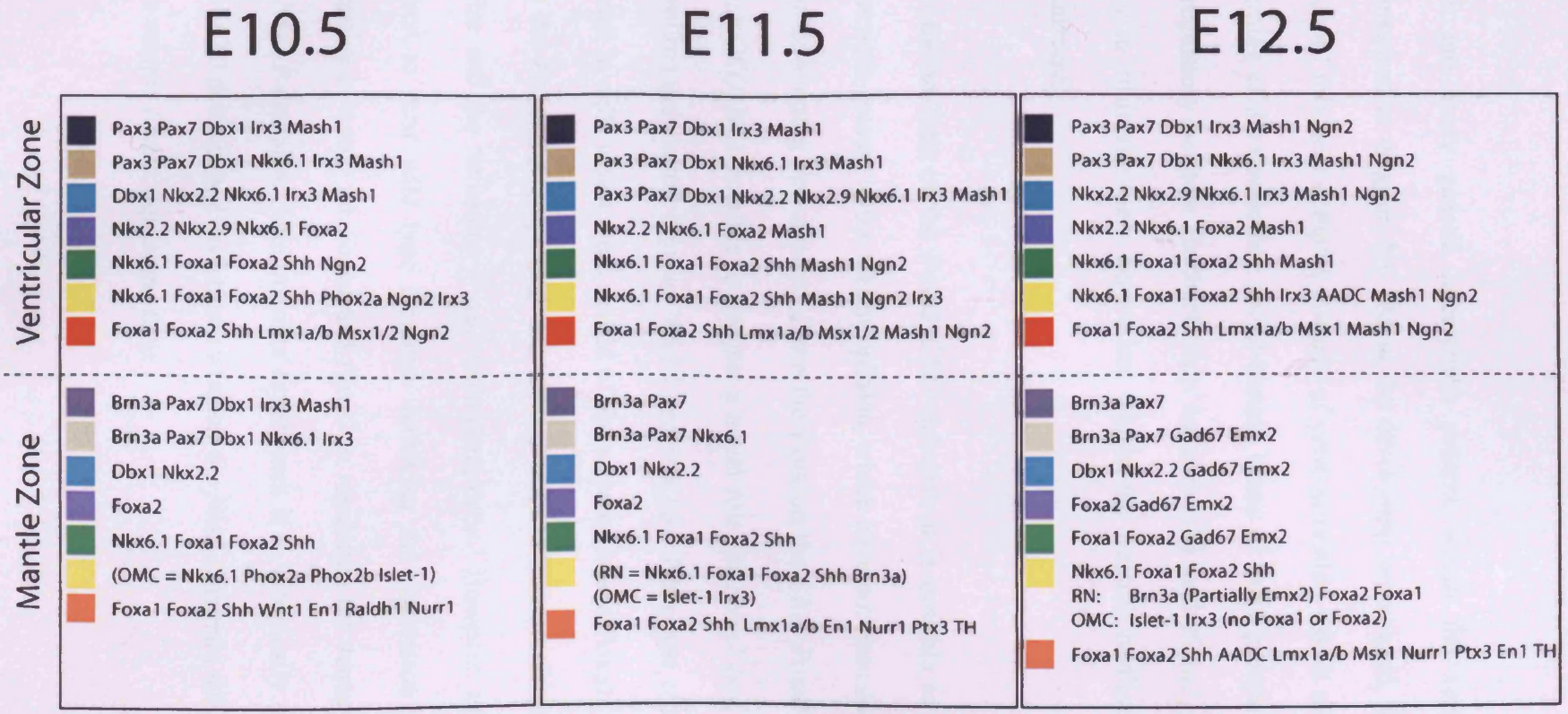

Key to Schematic representation of gene expression patterns within the mesencephalon

9. Novel genetic interactions within the ventral mesencephalon of the mouse

There are many genetic interactions present within the ventral mesencephalon (summarised in diagram N). As in the developing spinal cord, Shh signals from the notochord initiate a complex cascade of gene activation which ultimately leads to the patterning of the developing neural tissue. Many of these genetic interactions such as the regulatory positive feedback loop between *Shh* and *Foxa2*, which enables both genes to maintain their expression within the ventral midline tissue, have been documented.

From the analysis of the *Foxa2 CKO* embryos, it is possible to suggest some novel interactions present in the mesencephalon, which have not been documented elsewhere in the developing neural tube. From the work on the *CKO Foxa2* χ embryos, and the *Foxa2 CKO*, it is possible to suggest a novel role for *Foxa2* (and possibly *Foxa1*) in controlling the ventral limit of *Nkx2.2* and *Nkx2.9*. There was ectopic Nkx2.2 protein detected in cells which were devoid of Foxa2 protein (and Foxa1). However, the data from the *Foxa2 CKO* revealed that either *Nkx2.2* or *Nkx2.9* did not reach the ventral midline and the remaining *Foxa2* expressing cells. However, these two genes were restored to their wild type locations following the restoration of *Foxa1*, which is suggestive of a role for *Foxa1* and *Foxa2* in regulating the ventral limit of the *Nkx2.2* and *Nkx2.9* domains. One possible experiment is to ectopically express *Foxa2* within the *Nkx2.2* domain, and investigate whether the *Nkx2.2* domain shifts dorsally in respect to the ectopic *Foxa2* expressing cells.

It is documented that *Gli2* is the primary transducer of the initial Shh signal during the specification of the floor plate and that it is subsequently down-regulated by *Foxa2* (possibly also *Foxa1*). From the double in-situ hybridisation assays performed, it became evident that the ventral limit of *Gli2* and *Gli3* expression domains form a strict boundary with *Foxa2* (figure 23). In the *Foxa2 CKO*, there is a ventral expansion of *Gli2* (although not *Gli3*) towards the ventral midline, reaching the remaining *Foxa2* expressing cells. By E11.5 when *Foxa1* gene expression is restored throughout the majority of the anterior-posterior axis of the mesencephalon, the *Gli2* expression domain is immediately restored towards the ABB, forming a new ventral border with *Foxa1*. Previous studies have revealed that *Foxa1* can mimic the actions of *Foxa2* in its absence (Duncan et al., 1998), therefore it is possible to suggest that the restoration of *Gli2* to its wild type domain is due to the actions of *Foxa1*. From this interpretation it is also possible to suggest that *Foxa2* and also *Foxa1* (with less efficiency) regulate the ventral limit of *Gli2* gene expression at the ABB.

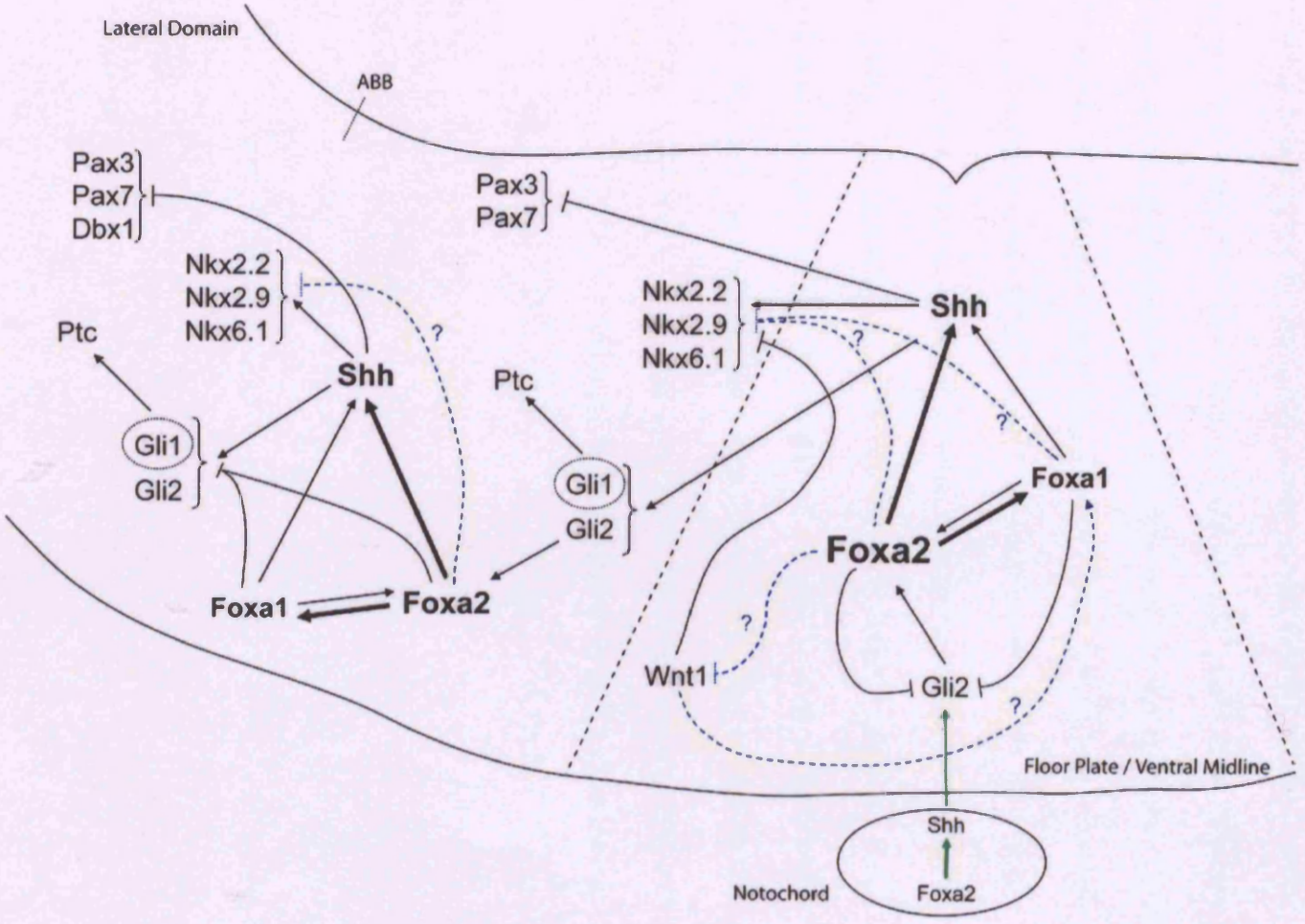

Diagram N: Genetic relationships within the ventral mesencephalon

Genetic relationships within the ventral mesencephalon:

1. *Foxa2 gene activity induces the transcription of Shh within the notochord and subsequent diffusion of the morphogenetic Shh protein induces the expression of genes involved in specifying the floor plate region in the overlying neural plate (green arrows). Gli2, which is known to mediate the primary response of Shh signalling, induces the expression of Foxa2 within the presumptive floor plate region.*
2. *Foxa2 protein induces the transcriptional activation of Shh and Foxa1 in this region. Foxa2 is able to induce both Shh and Foxa1 more efficiently than Foxa1's ability to induce Shh or Foxa2 (hence thicker positive arrows from Foxa2 to target genes than Foxa1's arrows). Shh is unable to induce Foxa1 or Foxa2 directly. Foxa2 and possibly Foxa1 are involved in the down-regulation of Gli2 gene expression from the ventral midline.*
3. *Shh signalling is responsible for specifying the progenitor domains of the neural tube by inducing or repressing the expression of various transcription factors. High levels of Shh signalling are required to repress Class I gene expression such as Pax3 and Pax7, while inducing the expression of Class II transcription factors such as Nkx2.2 and Nkx6.1.*
4. *Shh signalling also induces the transcription of mediators of the Shh signalling cascade including Ptc, the membrane bound Shh receptor. Through this activation of mediators, Foxa2 gene expression is induced, therefore creating a positive feedback loop in which both Foxa2 and Shh maintain their gene expression within this midline tissue.*
5. *In the domains lateral to the floor plate the same mechanisms as described above are utilised to specifically allow the expression of distinct transcription factors along the dorsal-ventral axis of the neural tube. The Shh signal inhibits the expression of any Class I genes within the basal plate, whilst maintaining the expression of several Class II genes.*
6. *A novel role for Wnt1 has recently been described. It is required to maintain the expression of Otx2 which in turn represses Nkx2.2 at the ventral midline during E9.5 and E10.5, thus creating a domain where the mesDA progenitor cells can be generated (Prakash et al., 2006).*
7. *Results from this study suggest that Foxa1 and Foxa2 may regulate the ventral limit of Nkx2.2 and Nkx2.9 (dotted blue repression lines with question marks).*
8. *In the Foxa2 CKO there was a dramatic over-expression of Wnt1, suggesting that Foxa2 may play a role in the down-regulation of Wnt1 in the ventral midline (dotted blue repression line with question mark).*
9. *There is a possibility that Wnt1 over-expression is required to induce the transcription of Foxa1 in the absence of Foxa2 to maintain the balance of Foxa proteins within the ventral mesencephalon. More experiments must be conduced before any conclusions may be drawn.*

Dotted black lines surrounding ventral midline represent the extent of the floor plate region. ABB represents the alar-basal boundary. Schematic diagram is not drawn to scale and certain genes are not located in their physiological positions, in an attempt to simplify the complex pattern of genetic interactions which occur in the ventral mesencephalon.

10. Recent analyses which provide further evidence for a regulatory mechanism of neuronal differentiation in the basal plate of the mesencephalon under the control of *Foxa1* and *Foxa2*

To determine whether *Foxa* (both *Foxa1* and *Foxa2*) proteins have a role in the control of neuronal differentiation, Dr. Ferri proceeded to analyse *Foxa1* null mutant embryos (*Foxa1 -/-)* and *Foxa2 CKO; Foxa1 -/-* embryos. A previous study of the *Foxa1 -/-* mice revealed that they were indistinguishable from their wild type littermates at E8.5 (Duncan et al., 1998). Due to time constraints, the analysis of the *Foxa1 -/-* mice was concentrated upon the mesDA neurons. When Dr. Ferri analysed the E12.5 *Foxa1 -/-* embryos she reported a 50% reduction in the mesDA neuronal population within the basal plate (data not shown). There was a reduction in the number of *TH* positive differentiated mesDA neurons coupled with no decrease in neuronal differentiation as detected using *β-tubulin*. The analysis of the gene expression patterns for *Msx1*, *Lmx1a* and *Lmx1b* at E10.5 revealed that the mesDA progenitor cells were correctly specified in the *Foxa1 -/-* (Dr. Ferri, unpublished results). Therefore, in similar fashion to the *Foxa2 CKO*, the phenotype described at E12.5 was a result of reduced levels of neuronal differentiation in response to the loss of *Foxa1*.

This data not only suggests that *Foxa1* plays a role in the control of neuronal differentiation in the basal plate of the mesencephalon, but is suggestive of a similar compensatory mechanism as describe in the *Foxa2 CKO* functioning to restore the phenotype described at E12.5 to levels indistinguishable from the wild type in the adult mice. Consistent with this hypothesis, Foxa2 protein levels were elevated in the *Foxa1 -/-* mice throughout embryonic development. In line with previous studies which have

determined that *Foxa2* activity is more "potent" than *Foxa1* (Ang and Rossant, 1994; Duncan et al., 1998; Weinstein et al., 1994), the restoration of the neuronal differentiation and subsequently the neuronal populations in the *Foxa1* -/-occurred at a more rapid pace than in the *Foxa2 CKO* embryos.

Taken together, all the data generated from the studies of the *Foxa1* -/- and *Foxa2 CKO* embryos, it is possible to suggest that *Foxa1* and *Foxa2* both play a crucial role in the regulation of neuronal differentiation but function within a redundant system, resembling the redundant system in place for the regulation of Shh signalling described above. When the activity of either *Foxa1* or *Foxa2* is lost, the remaining gene is over-expressed in a bid to compensate the loss of its partner. The analysis of the *Foxa2 CKO, Foxa1* -/- double mutant embryos appear to support this statement. In these embryos there is a complete absence of functional *Foxa1* or *Foxa2* protein, and subsequently there is a complete absence of the neuronal populations of the ventral mesencephalon. Analysis using an antibody raised against β-tubulin revealed that there was no neuronal differentiation within the basal plate, coupled with a complete absence of Shh protein (Dr. Ferri, unpublished results).

However, from the analysis of the *Foxa2 CKO; Foxa1* -/- mice it is not possible to claim with complete confidence that the phenotype described is solely attributed to the 92% reduction in cells expressing Foxa2 protein and the complete loss of Foxa1 protein affecting neuronal differentiation. The mesDA progenitor cells, identified using *Msx1*, *Lmx1a* and *Lmx1b* gene expression patterns, are absent from these double mutant embryos. There is also a complete absence of detectable Shh protein from the ventral mesencephalon (Shh protein is detected within the spinal cord). Therefore it is possible

that the phenotype described could be attributed to the inappropriate patterning of the ventral mesencephalon in the absence of Shh signalling and subsequently the progenitor cells for each neuronal population of the basal plate not becoming specified.

In order to delineate between a *Shh* attributed phenotype or a neuronal differentiation defect caused by the reduction in Foxa proteins, Dr. Ferri proceeded to analyse *Nestin::Cre; Foxa2* $^{Floxed/Floxed}$ mice. The recombination event in these embryos occurs at E10.5 (Vernay et al., 2005), therefore the deletion of *Foxa2* will occur after the patterning of the ventral mesencephalon has been completed. The results generated from this study revealed that even though Shh protein levels were initially reduced in response to the reduction of *Foxa2*, the patterning of the progenitor domains of the basal plate were unaltered in contrast to the *Foxa2 CKO*, suggesting that the competence of the progenitor cells to respond to Shh signalling is lost by E10.5. In keeping with previous results, Foxa1 protein levels were detected at elevated levels in response to the reduction of *Foxa2*. As expected from all the previous studies, the mesDA progenitor cells were correctly specified. However, at E12.5 there was a 48% reduction in the number of *TH* positive differentiated mesDA neurons, coupled with a marked reduction in neuronal differentiation.

Therefore these data provide clear evidence that the there is a role for Foxa proteins within the ventral mesencephalon to control the differentiation of neuronal progenitor cells into differentiated neurons, regardless of Shh activity. It also demonstrates that the phenotype of the *Foxa2 CKO* embryos at E12.5 is due to a delay in neuronal differentiation which is restored once Foxa1 protein levels reach a critical level, compensating for the loss of *Foxa2*.

11. Concluding ideas from analysis of *Foxa2 CKO* and other related mutant mice

Taken together, all the data generated from this study and from another on-going project in collaboration with Dr. A. Ferri, provide evidence of a novel role for *Foxa2* and *Foxa1* within the ventral mesencephalon in controlling neuronal differentiation. It would seem that these two genes work together in a redundant system to control neuronal differentiation. When either one of the genes is removed from the system, there is an over-expression of the remaining gene, and a subsequent compensatory response. In the *Foxa2 CKO*, the restoration of *Foxa1* gene expression throughout the ventral mesencephalon restored the neuronal differentiation and as a result, the dramatic losses described at E12.5 were gradually restored to near wild type levels, and the *Foxa2 CKO* animals are able to survive until adulthood. Furthermore, from the analysis of the *Foxa2 CKO* embryos treated with cyclopamine, it was possible to determine that the restoration of *Foxa1* gene expression occurs independently from Shh signalling. When both *Foxa1* and *Foxa2* are inactivated, there is a complete absence of neuronal differentiation from the basal plate.

It would be interesting to determine whether *Foxa2* (and possibly *Foxa1*) are involved in the control of neuronal differentiation in other regions of the developing neural tube, or whether this role is only present within the basal plate of the mesencephalon.

Another observation made from the studies of the *Foxa2 CKO* and *Shh CKO* is that the correct patterning of the mesencephalon along the dorsal-ventral axis requires Shh signalling to be uninterrupted before E8.75. If levels of Shh signalling are reduced prior to E8.75, some of the ventral progenitor cells revert to a dorsal progenitor fate, as seen

in the *Shh CKO*. If Shh signalling is affected after E8.75, the ventral progenitor cells maintain their ventral identity, as seen in the *Foxa2 CKO* embryos. It would seem that once the patterning of the mesencephalon has been concluded, *Shh* does not play a role in the specification of the neuronal populations, mainly because the progenitor cells are no longer competent to respond to changes in the *Shh* signalling. However it is not possible to rule out the role of the continued expression of Shh in maintaining the proliferation of neurons born after the initial dorsal-ventral patterning even has been concluded.

Despite the functions of *Foxa* proteins in regulating neuronal differentiation, it remains to be seen whether these findings can contribute and ameliorate the current concepts being used to successfully grow mesDA neurons *in-vitro* for use in transplant therapies to combat Parkinson's disease.

Appendix A

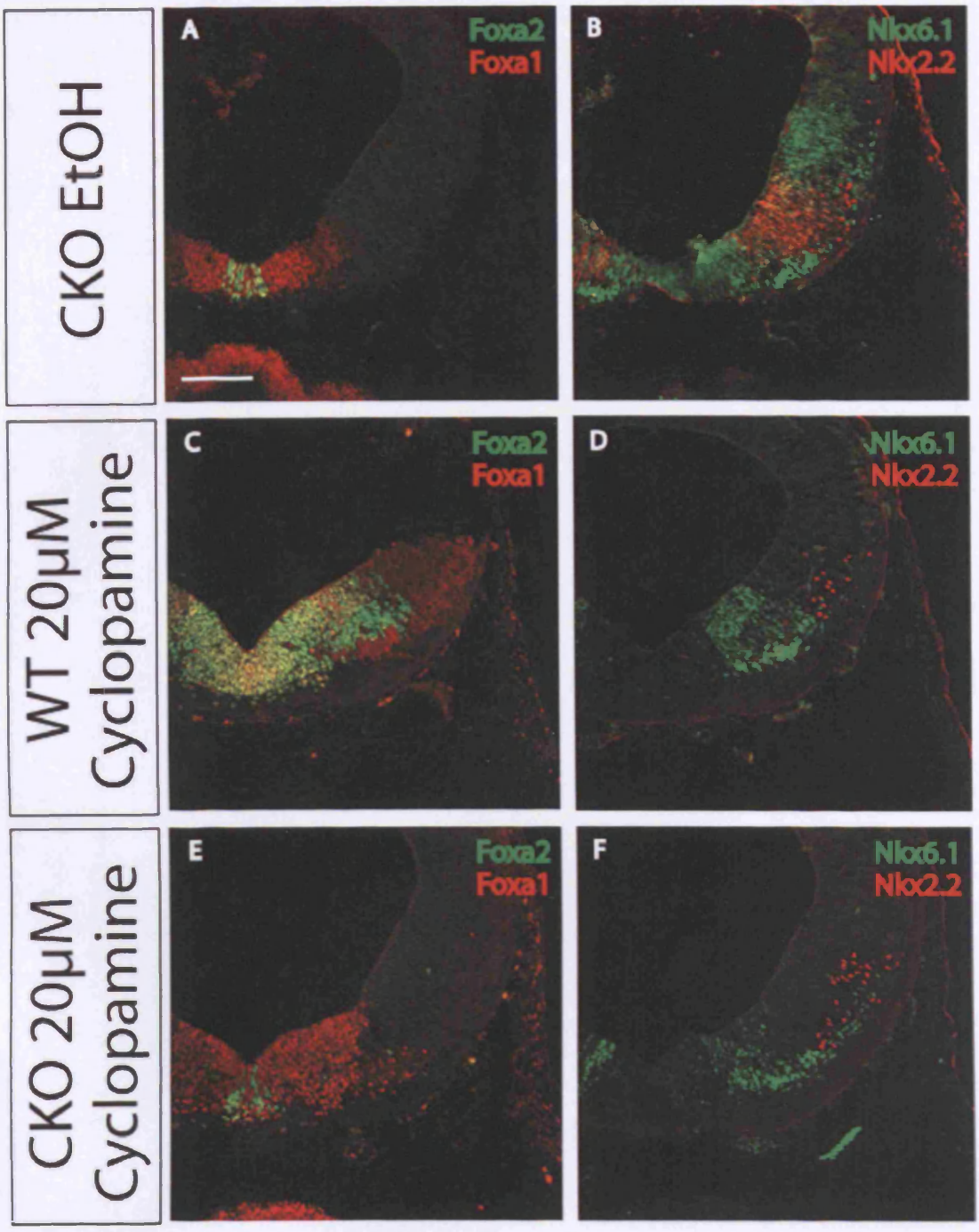

Figure 36: Investigation into whether the restoration of Foxa1 in the Foxa2 CKO is dependent on Shh signalling. *Wild type and Foxa2 CKO were incubated in the presence of cyclopamine to determine if Shh signalling was required for the restoration of Foxa1. (E) Foxa1 protein was detected in Foxa2 CKO embryos cultured in the presence of cyclopamine. (F) Nkx2.2 and Nkx6.1 protein expression revealed that Shh signalling was indeed affected by the blockade of Shh signalling. Therefore from this data it is possible to conclude that Foxa1 gene transcription is activated independently from Shh signalling. In-vitro embryo culture assays were conducted by Miss Carol Yan. Scale bar represents 100μm.*

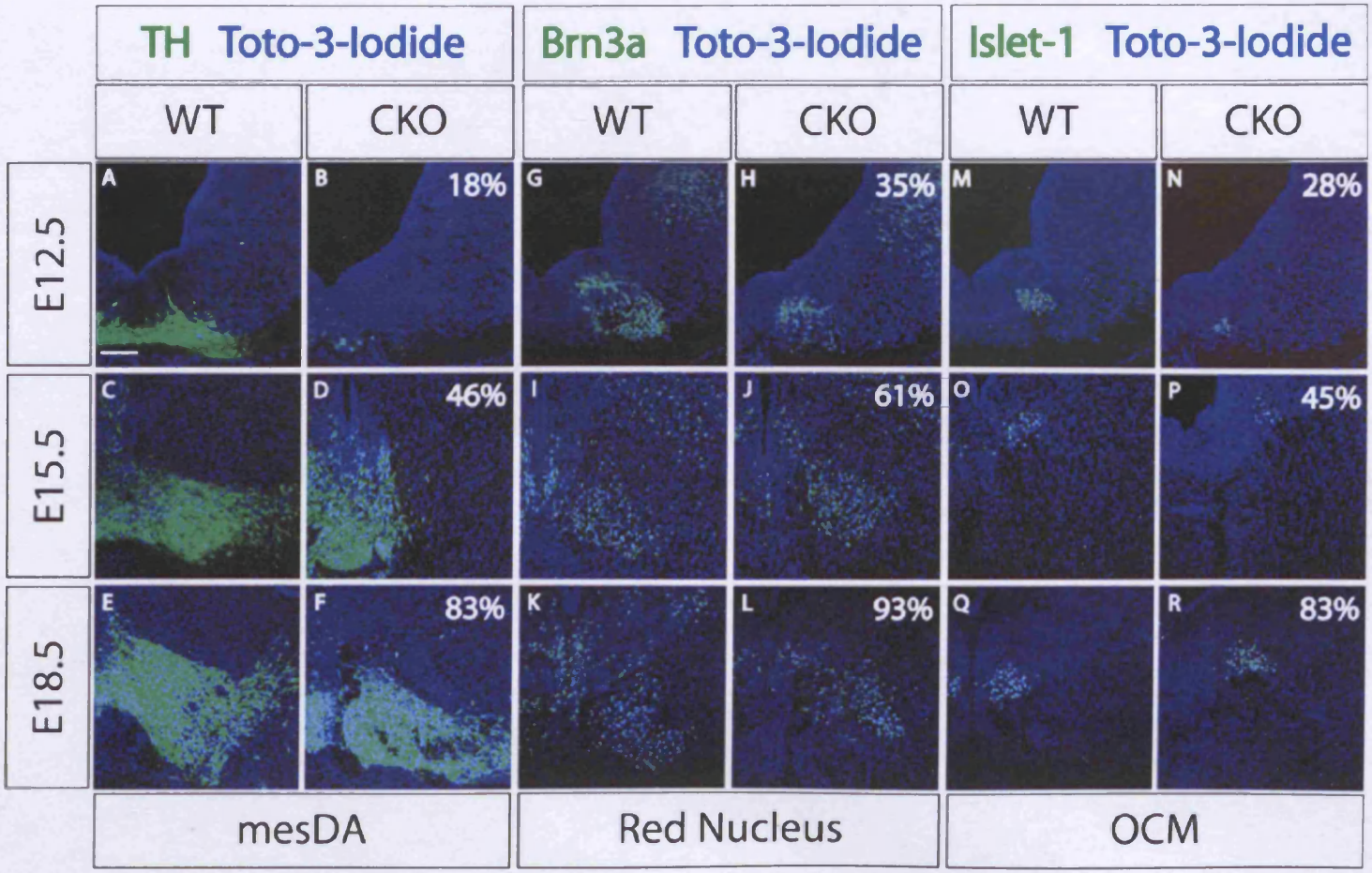

Figure 37: Cell counting assays for the three main neuronal populations of the ventral mesencephalon from E12.5 until E18.5 in both WT and Foxa2 CKO.

Figure 37 continued: *Cell counting assays revealed that each of the neuronal populations which were dramatically reduced at E12.5 in the Foxa2 CKO embryos, are gradually restored to near wild type levels. This gradual restoration in the neuronal populations coincides with the restoration of Foxa1 gene expression and the neuronal differentiation program. Cell counting assays were conducted by Dr. A. Ferri. Scale bar represents 100μm.*

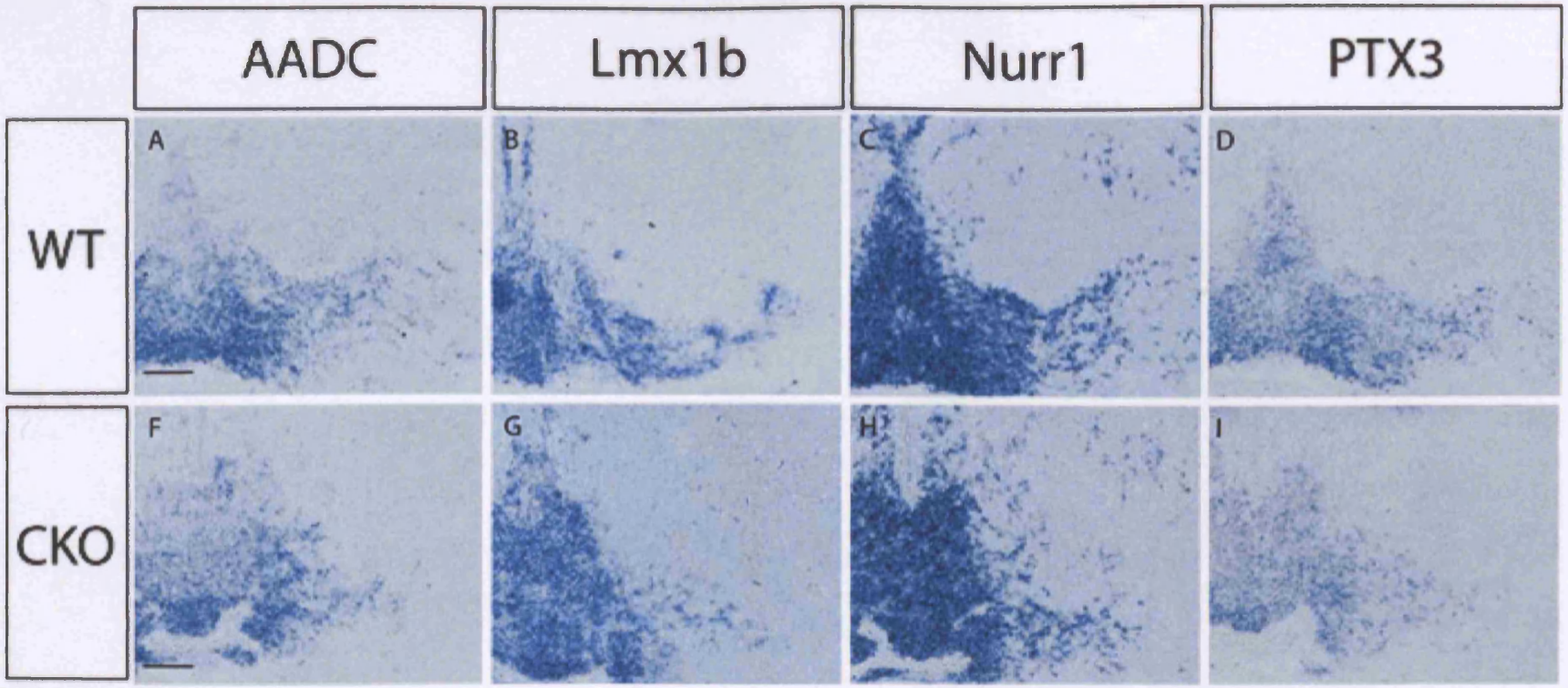

Figure 38: Analysis of genes involved in the development of the mesDA at E15.5: *Gene expression studies of certain transcription factors involved in the development of the mesDA also reveal that there is a gradual restoration of this neuronal population. In-situ hybridisation analysis performed by Dr. A. Ferri. Scale bar represents 100μm.*

Appendix B

29. Generation of *Foxa2 CKO; Gli3 KO* mice

Gli3 is considered to be the primary repressor to Shh signalling (Jacob and Briscoe, 2003). When *Gli3* activity is inhibited in *Shh -/-* or *Smo -/-* mice there is an apparent rescue of the phenotype described in both mutants. The majority of neuronal populations which are absent in the *Shh -/-* or *Smo -/-* mice are restored, with the exception to the floor plate and the V3 interneurons (Jacob and Briscoe, 2003; Litingtung and Chiang, 2000b; Persson et al., 2002; Wijgerde et al., 2002). If the phenotype for the *Foxa2 CKO* is linked to the reduction in Shh signalling, removal of *Gli3* activity should restore some of the neuronal populations in the ventral mesencephalon, with the exception to the mesDA neurons which lie across the ventral midline.

To address whether *Foxa2* has a direct role in the specification of the ventral neuronal populations of the mesencephalon, or whether the phenotype described for the *Foxa2 CKO* was due to the reduction in Shh signalling we inhibited the activity of *Gli3* in the *Foxa2 CKO*. *Gli3 -/-* mice were crossed into the *Foxa2 CKO* mice. *Foxa2*$^{floxed/+}$; *Wnt1-Cre* $^{+}$; *Gli3* $^{+/-}$ mice were crossed with *Foxa2*$^{floxed/+}$; *Gli3*$^{+/-}$ mice to generate *Foxa2*$^{floxed/floxed}$; *Wnt1-Cre* $^{+}$; *Gli3* $^{-/-}$ embryos (*Foxa2 CKO; Gli3 KO*). *Foxa2 CKO; Gli3 KO* embryos were harvested at E9.5 and E12.5 for analysis, and were recovered at a rate of 6.25% from all embryos harvested, as expected by standard Mendelian genetics. The *Foxa2 CKO; Gli3 KO* mice do not survive embryonic development.

At E9.5 the *Foxa2 CKO; Gli3 KO* embryos display a severe defect in neural tube closure in the regions anterior to the otic vesicle, with the entire dorsal region of the

mesencephalon remaining open. The first site of apposition and fusion of the neural folds at the future junction between the mesencephalon and diencephalon remains correctly positioned and the neural folds anterior to this point are correctly fused. The mandibular component of the first branchial arch and the optic eminence are also correctly positioned in the *Foxa2 CKO; Gli3 KO* embryos (figure 36A-C). At E12.5 the *Foxa2 CKO; Gli3 KO* embryos display severe exencephaly within the region of the mesencephalon (figure 36D-F) which is similar to the phenotype described for the over-expression of *Shh* (Rowitch et al., 1999). The *Foxa2 CKO; Gli3 KO* embryos also exhibit polydactyly in the limb buds with the generation of 7 separate digits (figure 36G).

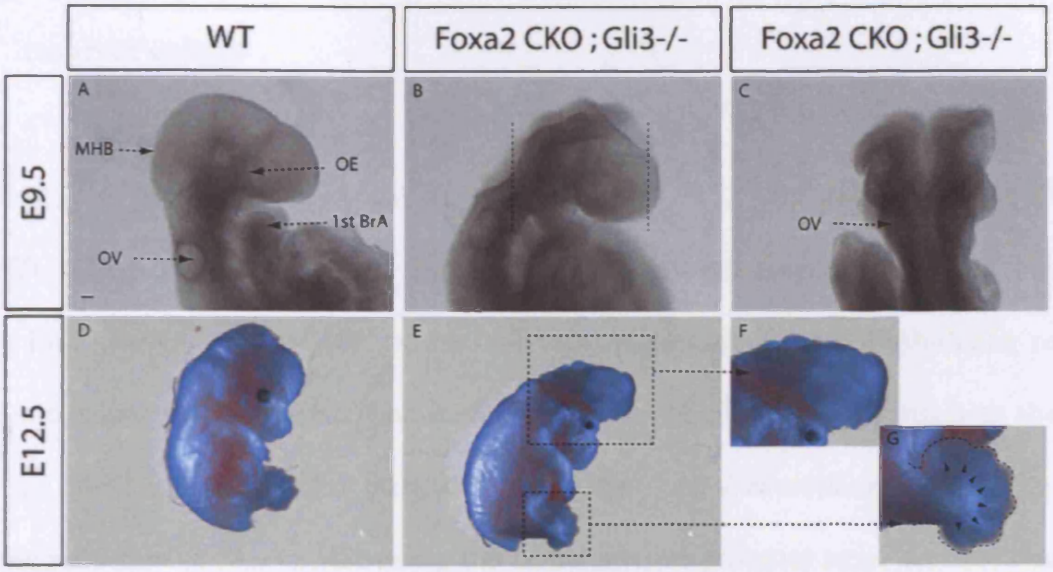

Figure 36: Creation and morphology of the Foxa2 CKO; Gli3 KO embryos. *It has been documented that certain aspects of Shh mutants can be rescue when the repressive actions of Gli3 are inhibited. In a bid to determine whether the phenotype of the Foxa2 CKO was indirectly caused by the reduced levels of Shh signalling described at early stages, Gli3 activity was inhibited in the Foxa2 CKO embryos. Foxa2 CKO; Gli3 KO embryos were harvested at E9.5 and E12.5.* ***A:*** *The morphology of the wild type embryo at E9.5 (MHB: midbrain-hindbrain boundary, OV: otic vesicle, OE: optic eminence, 1st BrA: 1st brancial arch).* ***B:*** *Sagittal view of Foxa2 CKO; Gli3 KO embryo at E9.5 displays a failure of neural tube closure anterior to the OV, while the OE and 1st BrA are specified and formed normally. Analysis of embryo was conducted on tissue within the two dotted lines.* ***C:*** *View of dorsal mesencephalic region of the Foxa2 CKO; Gli3 KO.* ***E-F:*** *E12.5 Foxa2 CKO; Gli3 KO embryos display severe exencephaly in the region where the mesencephalon is normally located.* ***E, G:*** *These embryos also display polydactyl, with the generation of 7 distinct digits at each limb bud (arrowheads). Dotted line in photograph G is to aid the visualisation of the limb bud. Scale bar represent 100μm.*

30. Islet1 positive neuronal population is present in the *Foxa2 CKO; Gli3 KO* embryos at E9.5

Due to the gross morphological defects evident at E12.5, the analysis of the *Foxa2 CKO; Gli3 KO* was confined to the E9.5 embryos. At this stage it is possible to detect the first neurons of the OMC within the basal plate (unpublished birth-dating results from our laboratory) (Altman and Bayer, 1981). In the *Foxa2 CKO* there is an absence of the OMC neurons at E9.5 marked by the loss of *Islet-1* expression, combined with a large reduction of Shh protein along the entire anterior-posterior axis. At later stages it is possible to detect some OMC neurons, combined with the restoration of Shh protein to wild type levels. In the *Shh CKO* there is a complete loss of the OMC at all stages analysed suggesting that, in similar fashion to data generated in the spinal cord, the motor neurons are dependent upon Shh signalling. In order to investigate whether there is a restoration of the OMC neurons in the *Foxa2 CKO; Gli3 KO*, indicating a specific role for *Shh* in the specification of these neurons, I performed immunohistochemistry assays using antibodies raised against Islet-1 and Foxa2.

To gain a better picture of a possible restoration of the OMC neurons, I analysed all possible genotypes of embryos available. Due to the unrecognisable shape of the *Foxa2 CKO; Gli3 KO* embryo, analysis was carried out on all brain sections from the anterior region of the telencephalon until the otic vesicle (figure 36B dotted lines).

The OMC neurons can be detected in the wild type embryos by the presence of Islet-1 protein. The OMC neurons at E9.5 are located underneath the ventricular zone in a domain between the ABB and the ventral midline (figure 37A). When one allele of the

Gli3 gene is removed in the wild type background, there is no alteration in the location of the OMC neurons (figure 37B). The slight reduction in the neuronal population can be attributed to asynchronous development of littermates. Analysis of the *Gli3 -/-* embryo at E9.5 revealed a dramatic alteration in the size of the mesencephalic ventricle, combined with a thickening and elongation of the ventral regions of the mesencephalon (figure 37C). Foxa2 expression is detected in a large domain at the ventral midline, and partially resembles the pattern of Foxa2 expression in the spinal cord. Islet-1 expression is detected in differentiated neurons lateral to the Foxa2 domain (figure 37C). The *Foxa2 CKO* phenotype is identical to the phenotype described previously, with no Islet-1 expression detected in the basal plate, and Foxa2 expression restricted to a small domain at the ventral midline (figure 37D). This indicates that crossing the *Foxa2 CKO* into another mouse strain does not alter the phenotype. It had previously been reported in the spinal cord that if one allele of *Gli3* was removed in the *Shh -/-* background there would be a partial rescue of the phenotype (Litingtung and Chiang, 2000b). However, when one allele of *Gli3* is removed in the *Foxa2 CKO* background, the OMC neuronal population is still absent from the basal plate (figure 37E). When all Gli3 function was inhibited in the *Foxa2 CKO* background, Islet-1 protein was detected throughout the entire anterior-posterior axis of the domain analysed. Foxa2 protein is detected within the expected domain at the ventral midline, and Islet-1 protein is detected in non-overlapping fashion lateral to the *Foxa2* domain (figure 37F).

These results reveal that the Islet-1 positive neuronal population in the basal plate of the mesencephalon is restored in the *Foxa2 CKO; Gli3 KO* embryos, suggesting that the specification of these neurons is dependent on Shh signalling.

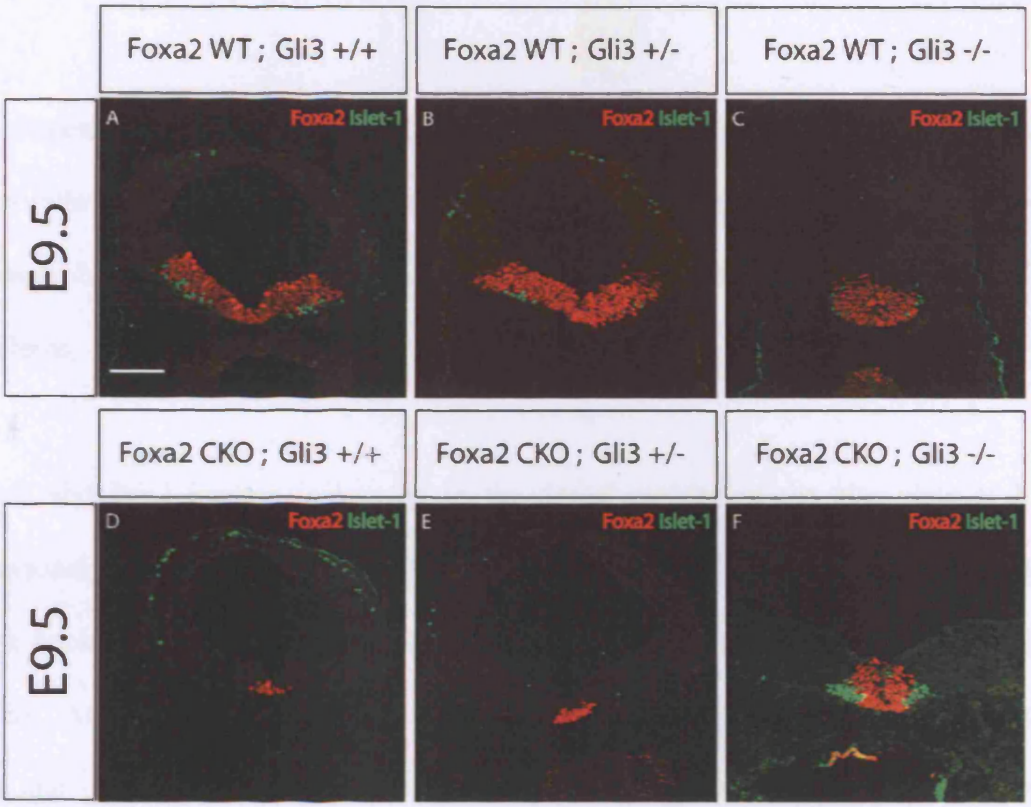

Figure 37: Is there a restoration of the OMC neurons in the Foxa2 CKO; Gli3 KO embryos at E9.5? *In the Shh -/-; Gli3 -/- mice there was a restoration of the ventral neuronal populations with the exception of the floor plate and V3 interneurons. To determine whether there was a rescue of the OMC neurons in the Foxa2 CKO; Gli3 KO embryos at E9.5, Islet-1 which labels the motor neurons of the OMC was analysed (green). Foxa2 protein (red) was used as a marker of the ventral midline. Analysis was carried out on all possible genotypes. When one allele of Gli3 is removed in the Foxa2 CKO there is no restoration of the OMC neuronal population. However, in the Foxa2 CKO; Gli3 KO Islet-1 protein is detected in the differentiated neurons flanking the ventral midline, suggesting that there is a restoration of the OMC neurons in these embryos. Scale bar represents 100μm.*

31. Dorsal-ventral patterning is severely affected in the *Foxa2 CKO; Gli3 KO*

To investigate whether the inhibition of *Gli3* activity in the *Foxa2 CKO* caused a restoration of the progenitor domains along the dorsal-ventral axis, I performed immunohistochemistry assays using antibodies raised against both Class I and Class II proteins.

Pax7 and Pax3 protein is located in the dorsal regions of the alar plate at E9.5 as previously described (figure 38A). When one allele of *Gli3* is removed from the wild type background there is no alteration in the position of the *Pax7/Pax3* domain (figure 38B). Analysis of the *Gli3* -/- embryo at E9.5 revealed that the *Pax7/Pax3* domain in the alar plate is restricted to the most dorsal regions spanning the roof plate, with a sizable reduction in the ventral limit of their domains (figure 38C).

In the *Foxa2 CKO*, both Pax7 and Pax3 protein is detected in the alar plate similar to the wild type pattern. There is no ventral expansion of either Pax7 or Pax3 protein within the ventricular zone as previously described (figure 38D). There is no alteration in the expression domains of both Pax7 and Pax3 proteins when one functional allele of *Gli3* is removed from the *Foxa2 CKO* background (figure 38E).

In the *Foxa2 CKO; Gli3 KO* the change in shape of the mesencephalic region causes an alteration in the expression domains of both Pax7 and Pax3 proteins (figure 38F). Pax3 protein is detected from the dorsal tip of the mesencephalic neural folds (possibly each half of the roof plate) to an intermediate location along the dorsal-ventral axis. Pax7 protein is not detectable at the dorsal tip of the neural folds, further suggesting that this

region represents the remnants of the roof plate, but is co-expressed with Pax3 protein at the intermediate regions of the mesencephalon. Due to the morphological alteration evident in the embryo it is not possible to determine whether the ventral limit of both *Pax7* and *Pax3* is at the ABB. The previous studies which inhibit the activity of *Gli3* in *Shh -/-* backgrounds describe that the progenitor domains are located at wild type positions (Litingtung and Chiang, 2000b; Persson et al., 2002; Wijgerde et al., 2002), which would suggest that the ventral limit of the *Pax7/Pax3* progenitor domain would be located at the ABB.

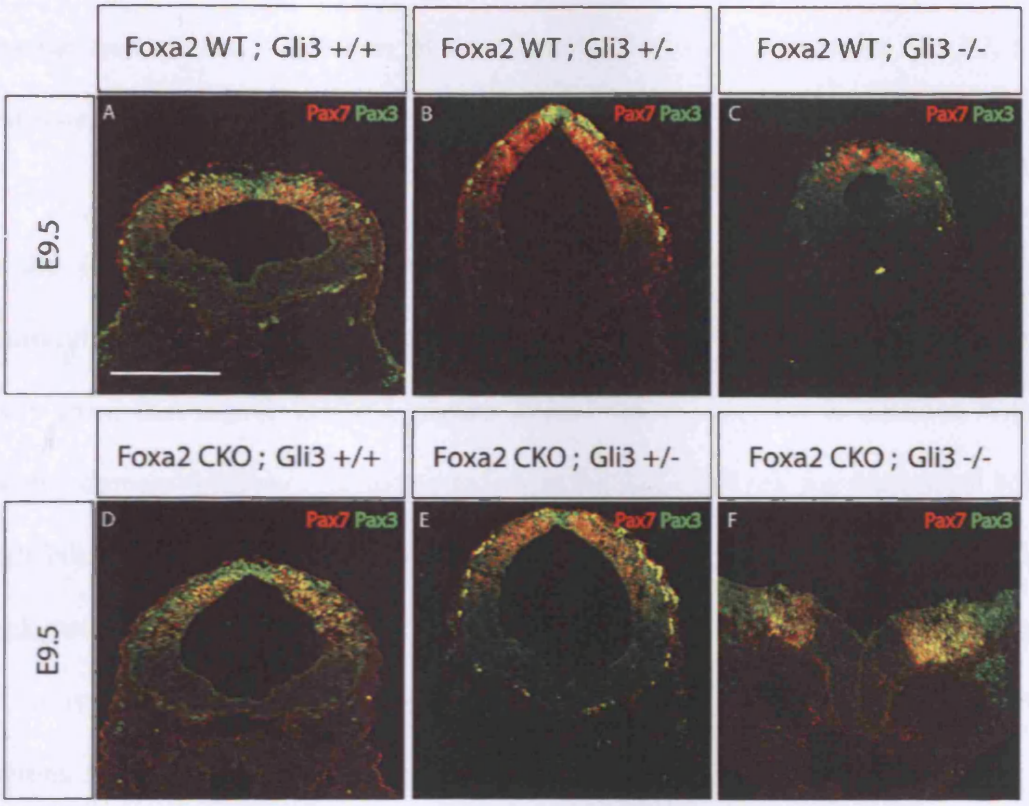

Figure 38: Analysis of Class I genes the mesencephalic region of the Foxa2 CKO; Gli3 KO. *In the previous studies of Shh -/-; Gli3 -/- mice all of the progenitor domains in the dorsal regions of the neural tube were restored to their wild type positions. In the Foxa2 CKO; Gli3 KO embryos, the morphological alteration of the brain tissue does not help the analysis of correct positioning of the progenitor domains along the dorsal-ventral axis. The dorsal tip of each neural fold expresses Pax3 protein, and is devoid of Pax7 protein suggesting that this area corresponds to a segment of the roof plate. It is not possible to specifically state where the ventral limit of the Pax3/Pax7 domain is located. Scale bar represents 200μm.*

Following the analysis of the Class I proteins in the *Foxa2 CKO; Gli3 KO* I investigated whether there was a restoration of the Class II proteins, in particular *Nkx2.2*, in these embryos.

In the wild type embryos, Nkx6.1 protein is detected in a broad domain of the ventricular zone spanning the ABB and forming a ventral limit a few cell diameters away from the ventral midline (figure 39A). Nkx2.2 protein is detected within the Nkx6.1 domain forming a dorsal boundary at the ABB and sharing the ventral boundary with Nkx6.1 (figure 39A). When one allele of *Gli3* is removed from the wild type background there is no alteration in the size and locations of these two progenitor domains (figure 39B). The *Gli3* -/- shows an alteration in morphology of the ventral regions as previously stated, resembling the ventral regions of the developing spinal cord. In keeping with this observation, Nkx2.2 protein is detected in a narrow domain at the ventral midline, flanking the Foxa2 expression domain at the ventral tip (figure 39C). Nkx6.1 protein is detected in a broad domain with the ventral limit of the progenitor domain flanking the Foxa2 positive ventral tip (figure 39C).

Both Nkx2.2 and Nkx6.1 expression domains in the *Foxa2 CKO* are as previously described (figure 39D). The removal of one functional allele of Gli3 in the *Foxa2 CKO* background causes a restoration of the Nkx6.1 progenitor domain as described in the wild type embryos, and the Nkx2.2 domain is unchanged (figure 39E). The analysis of the *Foxa2 CKO; Gli3 KO* embryos revealed a broad domain of Nkx6.1 protein flanking the ventral tip of the mesencephalon where the remaining Foxa2 protein is located (figure 39F). Superimposing the *Pax3/Pax7* and *Nkx6.1* domains reveal that there is a boundary between the Class I and Class II proteins. Whether this boundary lies at the

ABB still remains unclear (data not shown). Although the studies of *Gli3* mutants in *Shh* mutant backgrounds demonstrated that there is no restoration of the floor plate cells or the V3 interneurons (Litingtung and Chiang, 2000b; Persson et al., 2002; Wijgerde et al., 2002), the *Foxa2 CKO; Gli3 KO* embryos displayed both floor plate cells, and also the *Nkx2.2* progenitor domain (in spinal cord corresponds to V3 interneuron progenitor domain). This may be a result of some Shh protein still being present at the ventral midline. Another observation of the *Foxa2 CKO; Gli3 KO* embryos is that the expression domains of the Class II proteins resemble the pattern of the Class II protein expression within the ventral hindbrain.

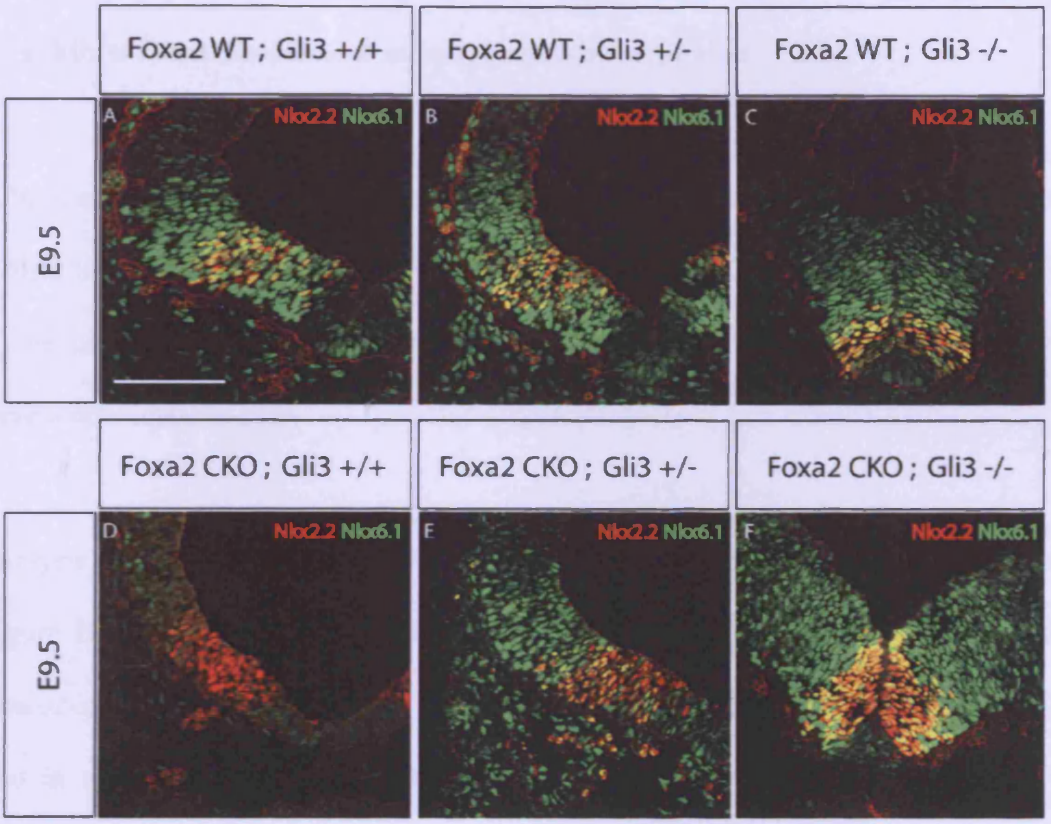

Figure 39: Analysis of Class II genes in the Foxa2 CKO; Gli3 KO embryos at E9.5. *The analysis of Nkx2.2 (red) and Nkx6.1 (green) protein expression at E9.5 on all the possible genotypes revealed that the Class II genes were affected by the reduction of both Shh (via reduction in Foxa2) and Gli3. Removal of one allele of Gli3 is insufficient to cause an alteration in the patterning of the mesencephalon at E9.5, whereas in the Gli3 -/- embryos, the morphology of the ventral region of the mesencephalon has been altered to resemble the spinal cord. Nkx2.2 protein is located in a narrow domain immediately flanking the ventral midline, whereas Nkx6.1 protein is located within a broad domain, resembling the size of the wild type Nkx6.1 protein domain. In the Foxa2 CKO there is a complete absence of Nkx6.1 protein from the ventral mesencephalon combined with an expansion of the Nkx2.2 expression domain. When one allele of Gli3 is removed from the Foxa2 CKO background there is a restoration of the Nkx6.1 protein expression within the ventral mesencephalon, but the expanded Nkx2.2 domain is persistent. In the Foxa2 CKO; Gli3 KO embryos the expression patterns of Nkx2.2 and Nkx6.1 resemble that of the wild type hindbrain, where both Nkx2.2 and Nkx6.1 form a ventral boundary immediately flanking the Foxa2 domain at the ventral midline. These results would suggest that there has been a restoration of the progenitor domains which produce the motor neurons (based on spinal cord model), but also that the "mesencephalic" area in the Foxa2 CKO; Gli3 KO possesses a hindbrain identity. Scale bar represents 100μm.*

32. The mesencephalon of the *Foxa2 CKO; Gli3 KO* is not correctly specified and exhibits characteristics of anterior rhombencephalon

In light of my observation that the expression patterns of the Class II proteins within the ventral half of the mesencephalon in the *Foxa2 CKO; Gli3 KO* embryos resembled that of the hindbrain, I used an antibody raised against Otx2 to determine whether the mesencephalon was correctly specified (figure 40A-D).

Analysis of *Otx2* expression at E9.5 in the *Foxa2 CKO* has been previously described (figure 20A-B). Otx2 protein is detected throughout the entire ventricular zone of the mesencephalon in embryos where one allele of *Gli3* has been removed (figure 40A) and also in embryos where one allele of *Gli3* has been removed from the *Foxa2 CKO* embryos (figure 40C). This indicates that in both cases, the mesencephalon is specified correctly and maintains its identity. The *Gli3 -/-* embryos revealed that there is no Otx2 protein detected within the entire "mesencephalic region" (figure 40B). Otx2 protein is still detected within the diencephalon (figure 40B) suggesting that the mesencephalon in *Gli3* mutants is not correctly specified. The *Foxa2 CKO; Gli3 KO* embryos display a complete absence of Otx2 protein along the anterior-posterior axis of the region analysed (figure 40D). This indicates that this region does not posses mesencephalic identity.

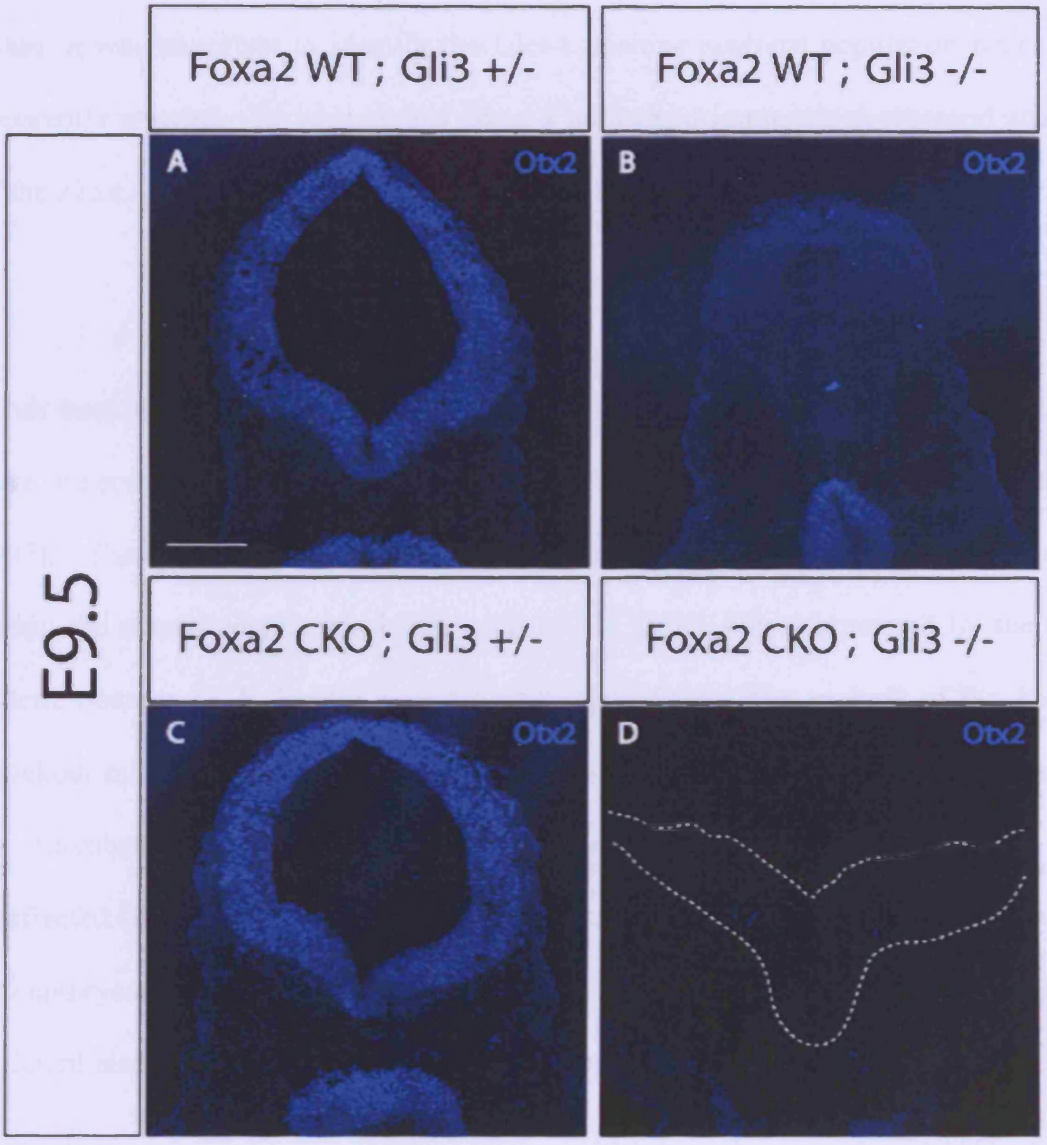

Figure 40: Analysis of mesencephalic identity in the Foxa2 CKO; Gli3 KO embryos at E9.5. *Due to the previous results, which suggest that the Foxa2 CKO; Gli3 KO embryos undergo a transformation from mesencephalic tissue into hindbrain tissue, a marker for mesencephalic identity (Otx2, blue) was analysed.* ***A, C:*** *The removal of one allele of the Gli3 gene does not influence the identity of the mesencephalic tissue at E9.5, as evident by the strong Otx2 protein expression within the entire mesencephalon.* ***B:*** *Interestingly, the Gli3 -/- do not possess any Otx2 protein within the area presumed to be mesencephalon. Otx2 protein is still detectable within the developing diencephalon, thus suggesting that there is no mesencephalic tissue in the Gli3 -/- embryos.* ***D:*** *There is no Otx2 protein detected within the presumed mesencephalic area of the Foxa2 CKO; Gli3 KO embryos, further providing evidence that the mesencephalon has been re-specified into anther brain territory. Dotted lines in D provide outline of brain tissue. Scale bar represents 100μm.*

Following the revelation that the *Foxa2 CKO; Gli3 KO* does not posses mesencephalic tissue, it was important to identify the Islet-1 positive neuronal population which was apparently rescued. To address this issue, I performed immunohistochemical analysis of the *Foxa2 CKO; Gli3 KO* embryos using antibodies raised against Phox2b and Islet-1.

It has been described that *Phox2a* is expressed by all the OMC progenitor cells, and there is a complete absence of the OMC neurons when *Phox2a* is removed (Pattyn et al., 1997). The closely related transcription factor *Phox2b* however is never expressed within the mesencephalic progenitor cells of the OMC, but is expressed by the post-mitotic neurons (J. F. Brunet personal communication). The analysis of the *Phox2b* knockout mice revealed a role for *Phox2b* in the specification of motor neurons within the rhombencephalon, while the OMC neurons within the mesencephalon were unaffected (Pattyn et al., 2000). Therefore for a quick analysis of the *Foxa2 CKO; Gli3 KO* embryos I examined whether the Islet-1 positive neurons expressed Phox2b only as differentiated neurons or prior to neuronal differentiation.

At E9.5 Phox2b protein was detected within the Islet-1 positive neurons either side of the ventral midline (figure 41A-C). Phox2b protein was also detected in the progenitor cells within the ventricular zone at the ventral midline, (figure 41A). This further suggests that the region of brain tissue being analysed in the *Foxa2 CKO; Gli3 KO* being transformed into a non-mesencephalic fate, and possibly into a hindbrain fate. It also suggests that the *Islet-1* neuronal population detected are not members of the OMC, but possibly belong to the Serotonergic neurons of r1.

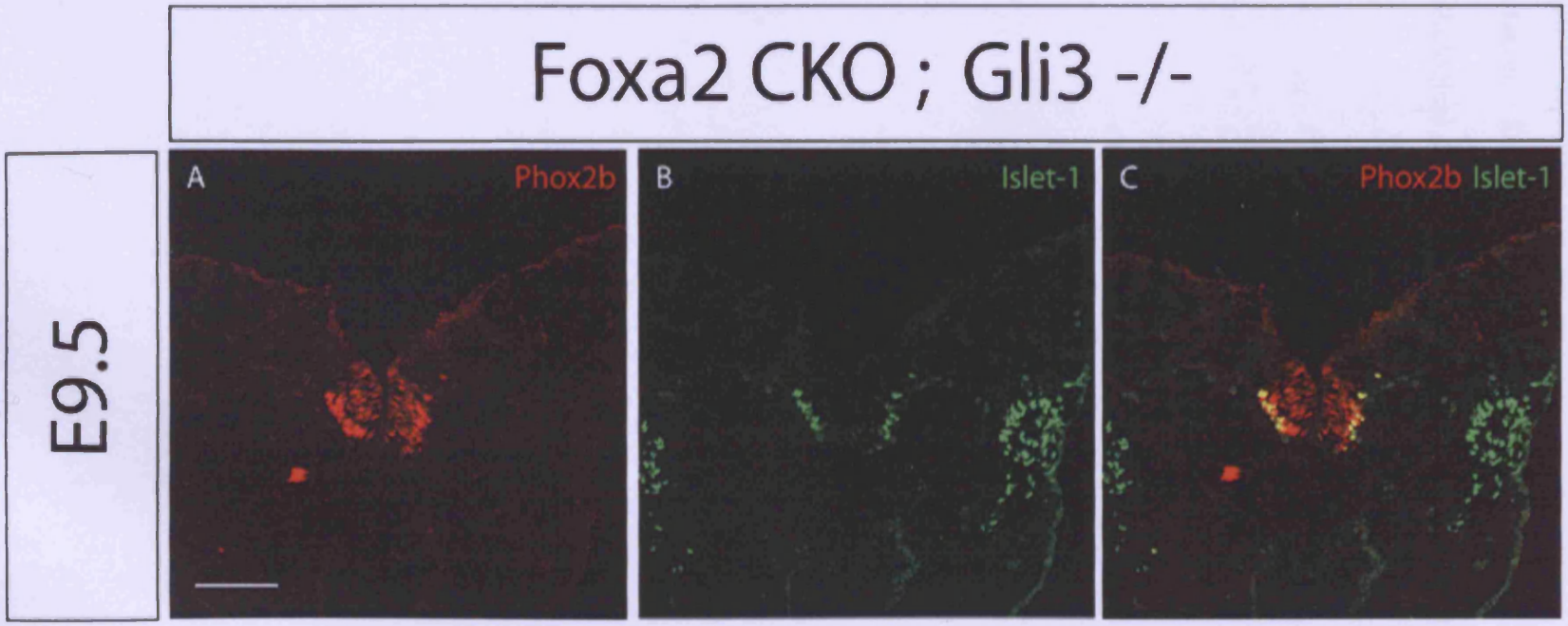

Figure 41: Identification of Islet-1 neuronal population in the Foxa2 CKO; Gli3 KO embryos at E9.5. *Following the revelation that the tissue being analysed in the Foxa2 CKO; Gli3 KO was not mesencephalic tissue, but possibly hindbrain tissue, a marker for the progenitor cells of the serotonergic neurons of r1 (Phox2b, red) was used to reveal the identity of the Iselt-1 (green) positive neurons flanking the ventral midline. Phox2b protein is detectable within the ventricular zone at the ventral midline, and also in the newly differentiated Islet-1 positive neurons. As Phox2b is never expressed by the OMC neurons (Phox2b -/- mice maintain the OMC neurons), but is expressed by the serotonergic neurons of r1, this data provides further evidence that the mesencephalon is transformed into hindbrain tissue in the Foxa2 CKO; Gli3 KO. Scale bar represents 100μm.*

Although the phenotype of these embryos was very interesting, it became apparent that the restored motor neurons described were not members of the OMC neuronal population. Due to this result and combined with time constraints and the gross morphological defects described at E9.5 and E12.5, this project was discontinued.

33. Analysis of *Foxa2 CKO; Gli3 KO* embryos

Shh deficient mice display a complete loss of all ventral neuronal populations within the developing neural tube (Chiang et al., 1996). Many studies have now demonstrated that when *Gli3* repressor activity is inhibited from the *Shh* deficient mice (or mice deficient for *Smo* or *Ptc*) there is a partial restoration of the ventral neuronal populations, excluding the floor plate and the V3 interneurons (Litingtung and Chiang, 2000b; Persson et al., 2002; Wijgerde et al., 2002). The generation of *Foxa2 CKO* embryos deficient in *Gli3* repressor activity was conducted in a bid to delineate aspects of the *Foxa2 CKO* phenotype from being directly caused by the reduced Foxa2 protein levels or being indirectly caused by the subsequent reduction in Shh signalling. It was hoped that if certain aspects of the *Foxa2 CKO* phenotype were directly linked to the reduction in Shh signalling, there would be a restoration of the neuronal populations, specifically the OMC and RN populations. The mesDA neuronal population was not expected to be rescued in these embryos, due to its location directly underlying the floor plate.

Due to time constrains an in depth analysis was not conducted on these embryos for each individual neuronal population, but specifically for the OMC neurons at E9.5, which are identified using the motor neuron marker *Islet-1*. There is no detectable Islet-1 protein expression at E9.5 in the *Foxa2 CKO* embryos, suggesting that a differentiated OMC neuronal population is absent at this stage (OMC progenitor cells are present). In contrast, there was Islet-1 protein expression located flanking the ventral midline of the *Foxa2 CKO; Gli3 KO* embryos suggesting that there was a restoration of the OMC neuronal population within these embryos. This data alone would indicate that the OMC neuronal population develops under the influence of Shh signalling and is only

missing at E9.5 from the *Foxa2 CKO* due to the reduced levels of Shh signalling. However, this statement cannot be made in confidence based on the data I generated. For example the entire region of the mesencephalon is morphologically altered in the *Foxa2 CKO; Gli3 KO* embryos, and there is no expression of Otx2 protein detected within this region, suggesting that the mesencephalon is no longer specified in these embryos, but resembles the gene expression patterns of the anterior rhombencephalon. Consistent with this statement, the arrangement of the *Islet-1* expressing motor neurons flanking the ventral midline resemble the spatial organisation of motor neurons located within the rhombencephalon (Ericson et al., 1995b). Furthermore, the expression patterns of the Class II transcription factors *Nkx2.2* and *Nkx6.1* also resemble the spatial organisation of the anterior rhombencephalon. One further piece of evidence to suggest that the mesencephalon has been re-specified to adopt a rhombencephalic fate is that the progenitor cells giving rise to the Islet-1 positive cells in the *Foxa2 CKO; Gli3 KO* embryos express *Phox2b*, a gene which is not expressed within the ventricular zone of the mesencephalon (figure 41) (J.F. Brunet personal communication). A recent study has now shown that the maintenance of *Fgf8* at the MHB requires the inhibition of *Gli3* repressor activity by *Shh* (Blaess et al., 2006). Therefore this result could explain the phenotype described in the *Foxa2 CKO; Gli3 KO* embryos, as *Fgf8* expression expands anteriorly causing the transformation of the mesencephalon into the rhombencephalon.

In the absence of *Gli3* repressor activity, Shh signalling is over-expressed ectopically. One example of this ectopic over-expression can be seen in the limb buds of the developing embryos which lack *Gli3*, where polydactlyly is reported (Buscher et al., 1997; Hui and Joyner, 1993; Litingtung et al., 2002). It was later shown from further analysis that Shh signalling from the zone of polarising activity (ZPA) controls the

number and identity of the individual digits (Litingtung et al., 2002). Consistent with the resutls from these studies, I reported the presence of polydactlyly in the *Gli3 -/-* and *Foxa2 CKO; Gli3 KO* embryos at E12.5 (figure 35). These data confirmed that in the absence of *Gli3* repressor activity there was an over-expression of Shh signalling in the limb bud. Whether there was an over-expression of Shh signalling in the mesencephalon remains to be identified.

From this observation it was assumed that in regions where endogenous *Gli3* activity was inhibited, there would be an over-expression of Shh signalling. In the *Foxa2 CKO; Gli3 KO* embryos at E12.5 there was severe exencephaly evident (figure35). This phenomenon can be attributed to the over-expression of Shh signalling in the absence of *Gli3* repressor activity. In a previous study it was demonstrated that ectopically inducing Shh signalling in the dorsal neural tube would cause an increase in cell proliferation in this region and result in exencephaly (Rowitch et al., 1999).

As stated previously, there was no comprehensive analysis conducted on these animals, due to the gross morphological defects and due to time constraints. Even though some of the data generated was of huge interest, it did not aid the interpretation of the *Foxa2 CKO* phenotype and therefore any further analysis of these animals was discontinued.

Bibliography

Abi-Dargham, A., Rodenhiser, J., Printz, D., Zea-Ponce, Y., Gil, R., Kegeles, L. S., Weiss, R., Cooper, T. B., Mann, J. J., Van Heertum, R. L. et al. (2000). Increased baseline occupancy of D2 receptors by dopamine in schizophrenia. *Proc Natl Acad Sci U S A* **97**, 8104-9.

Acampora, D., Avantaggiato, V., Tuorto, F. and Simeone, A. (1997). Genetic control of brain morphogenesis through Otx gene dosage requirement. *Development* **124**, 3639-50.

Acampora, D., Mazan, S., Lallemand, Y., Avantaggiato, V., Maury, M., Simeone, A. and Brulet, P. (1995). Forebrain and midbrain regions are deleted in Otx2-/- mutants due to a defective anterior neuroectoderm specification during gastrulation. *Development* **121**, 3279-90.

Adams, K. A., Maida, J. M., Golden, J. A. and Riddle, R. D. (2000). The transcription factor Lmx1b maintains Wnt1 expression within the isthmic organizer. *Development* **127**, 1857-67.

Agarwala, S. and Ragsdale, C. W. (2002). A role for midbrain arcs in nucleogenesis. *Development* **129**, 5779-88.

Agarwala, S., Sanders, T. A. and Ragsdale, C. W. (2001). Sonic hedgehog control of size and shape in midbrain pattern formation. *Science* **291**, 2147-50.

Alberi, L., Sgado, P. and Simon, H. H. (2004). Engrailed genes are cell-autonomously required to prevent apoptosis in mesencephalic dopaminergic neurons. *Development* **131**, 3229-36.

Altman, J. and Bayer, S. A. (1981). Development of the brain stem in the rat. V. Thymidine-radiographic study of the time of origin of neurons in the midbrain tegmentum. *J Comp Neurol* **198**, 677-716.

Amoyel, M., Cheng, Y. C., Jiang, Y. J. and Wilkinson, D. G. (2005). Wnt1 regulates neurogenesis and mediates lateral inhibition of boundary cell specification in the zebrafish hindbrain. *Development* **132**, 775-85.

Andersson, E., Tryggvason, U., Deng, Q., Friling, S., Alekseenko, Z., Robert, B., Perlmann, T. and Ericson, J. (2006). Identification of intrinsic determinants of midbrain dopamine neurons. *Cell* **124**, 393-405.

Ang, S. L., Jin, O., Rhinn, M., Daigle, N., Stevenson, L. and Rossant, J. (1996). A targeted mouse Otx2 mutation leads to severe defects in gastrulation and formation of axial mesoderm and to deletion of rostral brain. *Development* **122**, 243-52.

Ang, S. L. and Rossant, J. (1994). HNF-3 beta is essential for node and notochord formation in mouse development. *Cell* **78**, 561-74.

Ang, S. L., Wierda, A., Wong, D., Stevens, K. A., Cascio, S., Rossant, J. and Zaret, K. S. (1993). The formation and maintenance of the definitive endoderm lineage in the mouse: involvement of HNF3/forkhead proteins. *Development* **119**, 1301-15.

Asada, H., Kawamura, Y., Maruyama, K., Kume, H., Ding, R., Ji, F. Y., Kanbara, N., Kuzume, H., Sanbo, M., Yagi, T. et al. (1996). Mice lacking the 65 kDa isoform of glutamic acid decarboxylase (GAD65) maintain normal levels of GAD67 and GABA in their brains but are susceptible to seizures. *Biochem Biophys Res Commun* **229**, 891-5.

Asada, H., Kawamura, Y., Maruyama, K., Kume, H., Ding, R. G., Kanbara, N., Kuzume, H., Sanbo, M., Yagi, T. and Obata, K. (1997). Cleft palate and decreased brain gamma-aminobutyric acid in mice lacking the 67-kDa isoform of glutamic acid decarboxylase. *Proc Natl Acad Sci U S A* **94**, 6496-9.

Asbreuk, C. H., Vogelaar, C. F., Hellemons, A., Smidt, M. P. and Burbach, J. P. (2002). CNS expression pattern of Lmx1b and coexpression with ptx genes suggest

functional cooperativity in the development of forebrain motor control systems. *Mol Cell Neurosci* **21**, 410-20.
Bai, C. B., Auerbach, W., Lee, J. S., Stephen, D. and Joyner, A. L. (2002). Gli2, but not Gli1, is required for initial Shh signaling and ectopic activation of the Shh pathway. *Development* **129**, 4753-61.
Bai, C. B. and Joyner, A. L. (2001). Gli1 can rescue the in vivo function of Gli2. *Development* **128**, 5161-72.
Bai, C. B., Stephen, D. and Joyner, A. L. (2004). All mouse ventral spinal cord patterning by hedgehog is Gli dependent and involves an activator function of Gli3. *Dev Cell* **6**, 103-15.
Bally-Cuif, L. and Wassef, M. (1995). Determination events in the nervous system of the vertebrate embryo. *Curr Opin Genet Dev* **5**, 450-8.
Bassareo, V. and Di Chiara, G. (1997). Differential influence of associative and nonassociative learning mechanisms on the responsiveness of prefrontal and accumbal dopamine transmission to food stimuli in rats fed ad libitum. *J Neurosci* **17**, 851-61.
Bayer, S. A., Wills, K. V., Triarhou, L. C. and Ghetti, B. (1995). Time of neuron origin and gradients of neurogenesis in midbrain dopaminergic neurons in the mouse. *Exp Brain Res* **105**, 191-9.
Beckstead, R. M., Domesick, V. B. and Nauta, W. J. (1979). Efferent connections of the substantia nigra and ventral tegmental area in the rat. *Brain Res* **175**, 191-217.
Beddington, R. S. and Robertson, E. J. (1999). Axis development and early asymmetry in mammals. *Cell* **96**, 195-209.
Berry, N., Jobanputra, V. and Pal, H. (2003). Molecular genetics of schizophrenia: a critical review. *J Psychiatry Neurosci* **28**, 415-29.
Bertrand, N., Castro, D. S. and Guillemot, F. (2002). Proneural genes and the specification of neural cell types. *Nat Rev Neurosci* **3**, 517-30.
Billard, J. M., Daniel, H. and Pumain, R. (1991). Sensitivity of rubrospinal neurons to excitatory amino acids in the rat red nucleus in vivo. *Neurosci Lett* **134**, 49-52.
Bjorklund, A. and Lindvall, O. (1984). Dopamine-containing systems in the CNS. Handbook of Chemical Neuroanatomy.: Elsevier.
Blaess, S., Corrales, J. D. and Joyner, A. L. (2006). Sonic hedgehog regulates Gli activator and repressor functions with spatial and temporal precision in the mid/hindbrain region. *Development* **133**, 1799-809.
Blum, D., Torch, S., Lambeng, N., Nissou, M., Benabid, A. L., Sadoul, R. and Verna, J. M. (2001). Molecular pathways involved in the neurotoxicity of 6-OHDA, dopamine and MPTP: contribution to the apoptotic theory in Parkinson's disease. *Prog Neurobiol* **65**, 135-72.
Brand, M., Heisenberg, C. P., Warga, R. M., Pelegri, F., Karlstrom, R. O., Beuchle, D., Picker, A., Jiang, Y. J., Furutani-Seiki, M., van Eeden, F. J. et al. (1996). Mutations affecting development of the midline and general body shape during zebrafish embryogenesis. *Development* **123**, 129-42.
Brault, V., Moore, R., Kutsch, S., Ishibashi, M., Rowitch, D. H., McMahon, A. P., Sommer, L., Boussadia, O. and Kemler, R. (2001). Inactivation of the beta-catenin gene by Wnt1-Cre-mediated deletion results in dramatic brain malformation and failure of craniofacial development. *Development* **128**, 1253-64.
Briscoe, J., Chen, Y., Jessell, T. M. and Struhl, G. (2001). A hedgehog-insensitive form of patched provides evidence for direct long-range morphogen activity of sonic hedgehog in the neural tube. *Mol Cell* **7**, 1279-91.
Briscoe, J. and Ericson, J. (1999). The specification of neuronal identity by graded Sonic Hedgehog signalling. *Semin Cell Dev Biol* **10**, 353-62.

Briscoe, J. and Ericson, J. (2001). Specification of neuronal fates in the ventral neural tube. *Curr Opin Neurobiol* **11**, 43-9.
Briscoe, J., Pierani, A., Jessell, T. M. and Ericson, J. (2000). A homeodomain protein code specifies progenitor cell identity and neuronal fate in the ventral neural tube. *Cell* **101**, 435-45.
Briscoe, J., Sussel, L., Serup, P., Hartigan-O'Connor, D., Jessell, T. M., Rubenstein, J. L. and Ericson, J. (1999). Homeobox gene Nkx2.2 and specification of neuronal identity by graded Sonic hedgehog signalling. *Nature* **398**, 622-7.
Briscoe, J. and Therond, P. (2005). Hedgehog signaling: from the Drosophila cuticle to anti-cancer drugs. *Dev Cell* **8**, 143-51.
Britto, J., Tannahill, D. and Keynes, R. (2002). A critical role for sonic hedgehog signaling in the early expansion of the developing brain. *Nat Neurosci* **5**, 103-10.
Broccoli, V., Boncinelli, E. and Wurst, W. (1999). The caudal limit of Otx2 expression positions the isthmic organizer. *Nature* **401**, 164-8.
Brunet, J. F. and Pattyn, A. (2002). Phox2 genes - from patterning to connectivity. *Curr Opin Genet Dev* **12**, 435-40.
Buervenich, S., Carmine, A., Arvidsson, M., Xiang, F., Zhang, Z., Sydow, O., Jonsson, E. G., Sedvall, G. C., Leonard, S., Ross, R. G. et al. (2000). NURR1 mutations in cases of schizophrenia and manic-depressive disorder. *Am J Med Genet* **96**, 808-13.
Bumcrot, D. A., Takada, R. and McMahon, A. P. (1995). Proteolytic processing yields two secreted forms of sonic hedgehog. *Mol Cell Biol* **15**, 2294-303.
Burbach, J. P., Smits, S. and Smidt, M. P. (2003). Transcription factors in the development of midbrain dopamine neurons. *Ann N Y Acad Sci* **991**, 61-8.
Burman, K., Darian-Smith, C. and Darian-Smith, I. (2000a). Geometry of rubrospinal, rubroolivary, and local circuit neurons in the macaque red nucleus. *J Comp Neurol* **423**, 197-219.
Burman, K., Darian-Smith, C. and Darian-Smith, I. (2000b). Macaque red nucleus: origins of spinal and olivary projections and terminations of cortical inputs. *J Comp Neurol* **423**, 179-96.
Buscher, D., Bosse, B., Heymer, J. and Ruther, U. (1997). Evidence for genetic control of Sonic hedgehog by Gli3 in mouse limb development. *Mech Dev* **62**, 175-82.
Castellanos, F. X. (1997). Toward a pathophysiology of attention-deficit/hyperactivity disorder. *Clin Pediatr (Phila)* **36**, 381-93.
Castelo-Branco, G., Wagner, J., Rodriguez, F. J., Kele, J., Sousa, K., Rawal, N., Pasolli, H. A., Fuchs, E., Kitajewski, J. and Arenas, E. (2003). Differential regulation of midbrain dopaminergic neuron development by Wnt-1, Wnt-3a, and Wnt-5a. *Proc Natl Acad Sci U S A* **100**, 12747-52.
Castillo, S. O., Baffi, J. S., Palkovits, M., Goldstein, D. S., Kopin, I. J., Witta, J., Magnuson, M. A. and Nikodem, V. M. (1998). Dopamine biosynthesis is selectively abolished in substantia nigra/ventral tegmental area but not in hypothalamic neurons in mice with targeted disruption of the Nurr1 gene. *Mol Cell Neurosci* **11**, 36-46.
Catron, K. M., Wang, H., Hu, G., Shen, M. M. and Abate-Shen, C. (1996). Comparison of MSX-1 and MSX-2 suggests a molecular basis for functional redundancy. *Mech Dev* **55**, 185-99.
Chang, B. E., Blader, P., Fischer, N., Ingham, P. W. and Strahle, U. (1997). Axial (HNF3beta) and retinoic acid receptors are regulators of the zebrafish sonic hedgehog promoter. *Embo J* **16**, 3955-64.

Chang, D. T., Lopez, A., von Kessler, D. P., Chiang, C., Simandl, B. K., Zhao, R., Seldin, M. F., Fallon, J. F. and Beachy, P. A. (1994). Products, genetic linkage and limb patterning activity of a murine hedgehog gene. *Development* **120**, 3339-53.
Charrier, J. B., Lapointe, F., Le Douarin, N. M. and Teillet, M. A. (2002). Dual origin of the floor plate in the avian embryo. *Development* **129**, 4785-96.
Charron, F., Stein, E., Jeong, J., McMahon, A. P. and Tessier-Lavigne, M. (2003). The morphogen sonic hedgehog is an axonal chemoattractant that collaborates with netrin-1 in midline axon guidance. *Cell* **113**, 11-23.
Chen, H., Lun, Y., Ovchinnikov, D., Kokubo, H., Oberg, K. C., Pepicelli, C. V., Gan, L., Lee, B. and Johnson, R. L. (1998a). Limb and kidney defects in Lmx1b mutant mice suggest an involvement of LMX1B in human nail patella syndrome. *Nat Genet* **19**, 51-5.
Chen, H., Ovchinnikov, D., Pressman, C. L., Aulehla, A., Lun, Y. and Johnson, R. L. (1998b). Multiple calvarial defects in lmx1b mutant mice. *Dev Genet* **22**, 314-20.
Chen, J. K., Taipale, J., Cooper, M. K. and Beachy, P. A. (2002a). Inhibition of Hedgehog signaling by direct binding of cyclopamine to Smoothened. *Genes Dev* **16**, 2743-8.
Chen, J. K., Taipale, J., Young, K. E., Maiti, T. and Beachy, P. A. (2002b). Small molecule modulation of Smoothened activity. *Proc Natl Acad Sci U S A* **99**, 14071-6.
Chen, W., Burgess, S. and Hopkins, N. (2001a). Analysis of the zebrafish smoothened mutant reveals conserved and divergent functions of hedgehog activity. *Development* **128**, 2385-96.
Chen, Y. H., Tsai, M. T., Shaw, C. K. and Chen, C. H. (2001b). Mutation analysis of the human NR4A2 gene, an essential gene for midbrain dopaminergic neurogenesis, in schizophrenic patients. *Am J Med Genet* **105**, 753-7.
Cheney, P. D., Mewes, K. and Fetz, E. E. (1988). Encoding of motor parameters by corticomotoneuronal (CM) and rubromotoneuronal (RM) cells producing postspike facilitation of forelimb muscles in the behaving monkey. *Behav Brain Res* **28**, 181-91.
Chi, C. L., Martinez, S., Wurst, W. and Martin, G. R. (2003). The isthmic organizer signal FGF8 is required for cell survival in the prospective midbrain and cerebellum. *Development* **130**, 2633-44.
Chiang, C., Litingtung, Y., Lee, E., Young, K. E., Corden, J. L., Westphal, H. and Beachy, P. A. (1996). Cyclopia and defective axial patterning in mice lacking Sonic hedgehog gene function. *Nature* **383**, 407-13.
Chinta, S. J. and Andersen, J. K. (2005). Dopaminergic neurons. *Int J Biochem Cell Biol* **37**, 942-6.
Clark, K. L., Halay, E. D., Lai, E. and Burley, S. K. (1993). Co-crystal structure of the HNF-3/fork head DNA-recognition motif resembles histone H5. *Nature* **364**, 412-20.
Cohen, D. R., Cheng, C. W., Cheng, S. H. and Hui, C. C. (2000). Expression of two novel mouse Iroquois homeobox genes during neurogenesis. *Mech Dev* **91**, 317-21.
Collins, R. T. and Cohen, S. M. (2003). The secret life of Smoothened. *Dev Cell* **5**, 823-4.
Condorelli, G., Roncarati, R., Ross, J., Jr., Pisani, A., Stassi, G., Todaro, M., Trocha, S., Drusco, A., Gu, Y., Russo, M. A. et al. (2001). Heart-targeted overexpression of caspase3 in mice increases infarct size and depresses cardiac function. *Proc Natl Acad Sci U S A* **98**, 9977-82.
Conlon, R. A. and Herrmann, B. G. (1993). Detection of messenger RNA by in situ hybridization to postimplantation embryo whole mounts. *Methods Enzymol* **225**, 373-83.

Crossley, P. H. and Martin, G. R. (1995). The mouse Fgf8 gene encodes a family of polypeptides and is expressed in regions that direct outgrowth and patterning in the developing embryo. *Development* **121**, 439-51.
Crossley, P. H., Martinez, S. and Martin, G. R. (1996). Midbrain development induced by FGF8 in the chick embryo. *Nature* **380**, 66-8.
Dahmane, N., Lee, J., Robins, P., Heller, P. and Ruiz i Altaba, A. (1997). Activation of the transcription factor Gli1 and the Sonic hedgehog signalling pathway in skin tumours. *Nature* **389**, 876-81.
Dahmane, N., Sanchez, P., Gitton, Y., Palma, V., Sun, T., Beyna, M., Weiner, H. and Ruiz i Altaba, A. (2001). The Sonic Hedgehog-Gli pathway regulates dorsal brain growth and tumorigenesis. *Development* **128**, 5201-12.
Danielian, P. S. and McMahon, A. P. (1996). Engrailed-1 as a target of the Wnt-1 signalling pathway in vertebrate midbrain development. *Nature* **383**, 332-4.
Dassule, H. R., Lewis, P., Bei, M., Maas, R. and McMahon, A. P. (2000). Sonic hedgehog regulates growth and morphogenesis of the tooth. *Development* **127**, 4775-85.
Davis, C. A. and Joyner, A. L. (1988). Expression patterns of the homeo box-containing genes En-1 and En-2 and the proto-oncogene int-1 diverge during mouse development. *Genes Dev* **2**, 1736-44.
Di Chiara, G. and Imperato, A. (1988). Drugs abused by humans preferentially increase synaptic dopamine concentrations in the mesolimbic system of freely moving rats. *Proc Natl Acad Sci U S A* **85**, 5274-8.
Di Chiara, G., Morelli, M., Acquas, E. and Carboni, E. (1992). Functions of dopamine in the extrapyramidal and limbic systems. Clues for the mechanism of drug actions. *Arzneimittelforschung* **42**, 231-7.
Dickinson, M. E., Krumlauf, R. and McMahon, A. P. (1994). Evidence for a mitogenic effect of Wnt-1 in the developing mammalian central nervous system. *Development* **120**, 1453-71.
Ding, Q., Motoyama, J., Gasca, S., Mo, R., Sasaki, H., Rossant, J. and Hui, C. C. (1998). Diminished Sonic hedgehog signaling and lack of floor plate differentiation in Gli2 mutant mice. *Development* **125**, 2533-43.
Ding, Y. Q., Marklund, U., Yuan, W., Yin, J., Wegman, L., Ericson, J., Deneris, E., Johnson, R. L. and Chen, Z. F. (2003). Lmx1b is essential for the development of serotonergic neurons. *Nat Neurosci* **6**, 933-8.
Dreyer, S. D., Zhou, G., Baldini, A., Winterpacht, A., Zabel, B., Cole, W., Johnson, R. L. and Lee, B. (1998). Mutations in LMX1B cause abnormal skeletal patterning and renal dysplasia in nail patella syndrome. *Nat Genet* **19**, 47-50.
Duncan, S. A., Navas, M. A., Dufort, D., Rossant, J. and Stoffel, M. (1998). Regulation of a transcription factor network required for differentiation and metabolism. *Science* **281**, 692-5.
Echelard, Y., Epstein, D. J., St-Jacques, B., Shen, L., Mohler, J., McMahon, J. A. and McMahon, A. P. (1993). Sonic hedgehog, a member of a family of putative signaling molecules, is implicated in the regulation of CNS polarity. *Cell* **75**, 1417-30.
Echelard, Y., Vassileva, G. and McMahon, A. P. (1994). Cis-acting regulatory sequences governing Wnt-1 expression in the developing mouse CNS. *Development* **120**, 2213-24.
Echevarria, D., Vieira, C., Gimeno, L. and Martinez, S. (2003). Neuroepithelial secondary organizers and cell fate specification in the developing brain. *Brain Res Brain Res Rev* **43**, 179-91.

Eells, J. B. (2003). The control of dopamine neuron development, function and survival: insights from transgenic mice and the relevance to human disease. *Curr Med Chem* **10**, 857-70.
Egan, M. F. and Weinberger, D. R. (1997). Neurobiology of schizophrenia. *Curr Opin Neurobiol* **7**, 701-7.
Eng, S. R., Gratwick, K., Rhee, J. M., Fedtsova, N., Gan, L. and Turner, E. E. (2001). Defects in sensory axon growth precede neuronal death in Brn3a-deficient mice. *J Neurosci* **21**, 541-9.
Epstein, D. J., McMahon, A. P. and Joyner, A. L. (1999). Regionalization of Sonic hedgehog transcription along the anteroposterior axis of the mouse central nervous system is regulated by Hnf3-dependent and -independent mechanisms. *Development* **126**, 281-92.
Ericson, J., Morton, S., Kawakami, A., Roelink, H. and Jessell, T. M. (1996). Two critical periods of Sonic Hedgehog signaling required for the specification of motor neuron identity. *Cell* **87**, 661-73.
Ericson, J., Muhr, J., Jessell, T. M. and Edlund, T. (1995a). Sonic hedgehog: a common signal for ventral patterning along the rostrocaudal axis of the neural tube. *Int J Dev Biol* **39**, 809-16.
Ericson, J., Muhr, J., Placzek, M., Lints, T., Jessell, T. M. and Edlund, T. (1995b). Sonic hedgehog induces the differentiation of ventral forebrain neurons: a common signal for ventral patterning within the neural tube. *Cell* **81**, 747-56.
Ericson, J., Rashbass, P., Schedl, A., Brenner-Morton, S., Kawakami, A., van Heyningen, V., Jessell, T. M. and Briscoe, J. (1997). Pax6 controls progenitor cell identity and neuronal fate in response to graded Shh signaling. *Cell* **90**, 169-80.
Ericson, J., Thor, S., Edlund, T., Jessell, T. M. and Yamada, T. (1992). Early stages of motor neuron differentiation revealed by expression of homeobox gene Islet-1. *Science* **256**, 1555-60.
Etheridge, L. A., Wu, T., Liang, J. O., Ekker, S. C. and Halpern, M. E. (2001). Floor plate develops upon depletion of tiggy-winkle and sonic hedgehog. *Genesis* **30**, 164-9.
Evinger, C. (1988). Extraocular motor nuclei: location, morphology and afferents. *Rev Oculomot Res* **2**, 81-117.
Fan, C. M., Kuwana, E., Bulfone, A., Fletcher, C. F., Copeland, N. G., Jenkins, N. A., Crews, S., Martinez, S., Puelles, L., Rubenstein, J. L. et al. (1996). Expression patterns of two murine homologs of Drosophila single-minded suggest possible roles in embryonic patterning and in the pathogenesis of Down syndrome. *Mol Cell Neurosci* **7**, 1-16.
Fedtsova, N. and Turner, E. E. (2001). Signals from the ventral midline and isthmus regulate the development of Brn3.0-expressing neurons in the midbrain. *Mech Dev* **105**, 129-44.
Ferri, A. L., Cavallaro, M., Braida, D., Di Cristofano, A., Canta, A., Vezzani, A., Ottolenghi, S., Pandolfi, P. P., Sala, M., DeBiasi, S. et al. (2004). Sox2 deficiency causes neurodegeneration and impaired neurogenesis in the adult mouse brain. *Development* **131**, 3805-19.
Fode, C., Gradwohl, G., Morin, X., Dierich, A., LeMeur, M., Goridis, C. and Guillemot, F. (1998). The bHLH protein NEUROGENIN 2 is a determination factor for epibranchial placode-derived sensory neurons. *Neuron* **20**, 483-94.
Fuse, N., Maiti, T., Wang, B., Porter, J. A., Hall, T. M., Leahy, D. J. and Beachy, P. A. (1999). Sonic hedgehog protein signals not as a hydrolytic enzyme but as an apparent ligand for patched. *Proc Natl Acad Sci U S A* **96**, 10992-9.

Gibson, A. R., Houk, J. C. and Kohlerman, N. J. (1985). Relation between red nucleus discharge and movement parameters in trained macaque monkeys. *J Physiol* **358**, 551-70.
Gilbert, S. F. (2003). Developmental Biology: Seventh Edition: Sinauer Associates, Inc.
Giros, B. and Caron, M. G. (1993). Molecular characterization of the dopamine transporter. *Trends Pharmacol Sci* **14**, 43-9.
Goldman, J. E., Yen, S. H., Chiu, F. C. and Peress, N. S. (1983). Lewy bodies of Parkinson's disease contain neurofilament antigens. *Science* **221**, 1082-4.
Goodrich, L. V., Johnson, R. L., Milenkovic, L., McMahon, J. A. and Scott, M. P. (1996). Conservation of the hedgehog/patched signaling pathway from flies to mice: induction of a mouse patched gene by Hedgehog. *Genes Dev* **10**, 301-12.
Goodrich, L. V., Milenkovic, L., Higgins, K. M. and Scott, M. P. (1997). Altered neural cell fates and medulloblastoma in mouse patched mutants. *Science* **277**, 1109-13.
Goridis, C. and Rohrer, H. (2002). Specification of catecholaminergic and serotonergic neurons. *Nat Rev Neurosci* **3**, 531-41.
Goulding, M. D., Chalepakis, G., Deutsch, U., Erselius, J. R. and Gruss, P. (1991). Pax-3, a novel murine DNA binding protein expressed during early neurogenesis. *Embo J* **10**, 1135-47.
Goulding, M. D., Lumsden, A. and Gruss, P. (1993). Signals from the notochord and floor plate regulate the region-specific expression of two Pax genes in the developing spinal cord. *Development* **117**, 1001-16.
Graham, V., Khudyakov, J., Ellis, P. and Pevny, L. (2003). SOX2 functions to maintain neural progenitor identity. *Neuron* **39**, 749-65.
Grima, B., Lamouroux, A., Blanot, F., Biguet, N. F. and Mallet, J. (1985). Complete coding sequence of rat tyrosine hydroxylase mRNA. *Proc Natl Acad Sci U S A* **82**, 617-21.
Guillemot, F. and Joyner, A. L. (1993). Dynamic expression of the murine Achaete-Scute homologue Mash-1 in the developing nervous system. *Mech Dev* **42**, 171-85.
Hadjantonakis, A. K., Gertsenstein, M., Ikawa, M., Okabe, M. and Nagy, A. (1998). Generating green fluorescent mice by germline transmission of green fluorescent ES cells. *Mech Dev* **76**, 79-90.
Hall, T. M., Porter, J. A., Young, K. E., Koonin, E. V., Beachy, P. A. and Leahy, D. J. (1997). Crystal structure of a Hedgehog autoprocessing domain: homology between Hedgehog and self-splicing proteins. *Cell* **91**, 85-97.
Hatta, K. (1992). Role of the floor plate in axonal patterning in the zebrafish CNS. *Neuron* **9**, 629-42.
Hatta, K., Kimmel, C. B., Ho, R. K. and Walker, C. (1991). The cyclops mutation blocks specification of the floor plate of the zebrafish central nervous system. *Nature* **350**, 339-41.
Hill, R. E., Jones, P. F., Rees, A. R., Sime, C. M., Justice, M. J., Copeland, N. G., Jenkins, N. A., Graham, E. and Davidson, D. R. (1989). A new family of mouse homeo box-containing genes: molecular structure, chromosomal location, and developmental expression of Hox-7.1. *Genes Dev* **3**, 26-37.
Hirsch, E., Graybiel, A. M. and Agid, Y. A. (1988). Melanized dopaminergic neurons are differentially susceptible to degeneration in Parkinson's disease. *Nature* **334**, 345-8.
Hirsch, E. C. and Faucheux, B. A. (1998). Iron metabolism and Parkinson's disease. *Mov Disord* **13 Suppl 1**, 39-45.
Horn, A. S. (1990). Dopamine uptake: a review of progress in the last decade. *Prog Neurobiol* **34**, 387-400.

Houk, J. C., Gibson, A. R., Harvey, C. F., Kennedy, P. R. and van Kan, P. L. (1988). Activity of primate magnocellular red nucleus related to hand and finger movements. *Behav Brain Res* **28**, 201-6.
Huangfu, D. and Anderson, K. V. (2006). Signaling from Smo to Ci/Gli: conservation and divergence of Hedgehog pathways from Drosophila to vertebrates. *Development* **133**, 3-14.
Huelsken, J. and Behrens, J. (2002). The Wnt signalling pathway. *J Cell Sci* **115**, 3977-8.
Hui, C. C. and Joyner, A. L. (1993). A mouse model of greig cephalopolysyndactyly syndrome: the extra-toesJ mutation contains an intragenic deletion of the Gli3 gene. *Nat Genet* **3**, 241-6.
Hui, C. C., Slusarski, D., Platt, K. A., Holmgren, R. and Joyner, A. L. (1994). Expression of three mouse homologs of the Drosophila segment polarity gene cubitus interruptus, Gli, Gli-2, and Gli-3, in ectoderm- and mesoderm-derived tissues suggests multiple roles during postimplantation development. *Dev Biol* **162**, 402-13.
Hwang, D. Y., Ardayfio, P., Kang, U. J., Semina, E. V. and Kim, K. S. (2003). Selective loss of dopaminergic neurons in the substantia nigra of Pitx3-deficient aphakia mice. *Brain Res Mol Brain Res* **114**, 123-31.
Hynes, M., Porter, J. A., Chiang, C., Chang, D., Tessier-Lavigne, M., Beachy, P. A. and Rosenthal, A. (1995a). Induction of midbrain dopaminergic neurons by Sonic hedgehog. *Neuron* **15**, 35-44.
Hynes, M., Poulsen, K., Tessier-Lavigne, M. and Rosenthal, A. (1995b). Control of neuronal diversity by the floor plate: contact-mediated induction of midbrain dopaminergic neurons. *Cell* **80**, 95-101.
Hynes, M. and Rosenthal, A. (1999). Specification of dopaminergic and serotonergic neurons in the vertebrate CNS. *Curr Opin Neurobiol* **9**, 26-36.
Hynes, M., Stone, D. M., Dowd, M., Pitts-Meek, S., Goddard, A., Gurney, A. and Rosenthal, A. (1997). Control of cell pattern in the neural tube by the zinc finger transcription factor and oncogene Gli-1. *Neuron* **19**, 15-26.
Hynes, M., Ye, W., Wang, K., Stone, D., Murone, M., Sauvage, F. and Rosenthal, A. (2000). The seven-transmembrane receptor smoothened cell-autonomously induces multiple ventral cell types. *Nat Neurosci* **3**, 41-6.
Ilyas, M. (2005). Wnt signalling and the mechanistic basis of tumour development. *J Pathol* **205**, 130-44.
Incardona, J. P., Gaffield, W., Kapur, R. P. and Roelink, H. (1998). The teratogenic Veratrum alkaloid cyclopamine inhibits sonic hedgehog signal transduction. *Development* **125**, 3553-62.
Ingham, P. W. and McMahon, A. P. (2001). Hedgehog signaling in animal development: paradigms and principles. *Genes Dev* **15**, 3059-87.
Irving, C., Malhas, A., Guthrie, S. and Mason, I. (2002). Establishing the trochlear motor axon trajectory: role of the isthmic organiser and Fgf8. *Development* **129**, 5389-98.
Jacob, J. and Briscoe, J. (2003). Gli proteins and the control of spinal-cord patterning. *EMBO Rep* **4**, 761-5.
Jenner, P. (1998). Oxidative mechanisms in nigral cell death in Parkinson's disease. *Mov Disord* **13 Suppl 1**, 24-34.
Jeong, Y. and Epstein, D. J. (2003). Distinct regulators of Shh transcription in the floor plate and notochord indicate separate origins for these tissues in the mouse node. *Development* **130**, 3891-902.

Jerath, I. (1964). The red nucleus in the mice, monkey and man. *Indian J Physiol Pharmacol* **8**, 143-8.
Jessell, T. M. (2000). Neuronal specification in the spinal cord: inductive signals and transcriptional codes. *Nat Rev Genet* **1**, 20-9.
Jia, J., Tong, C. and Jiang, J. (2003). Smoothened transduces Hedgehog signal by physically interacting with Costal2/Fused complex through its C-terminal tail. *Genes Dev* **17**, 2709-20.
Jia, J., Tong, C., Wang, B., Luo, L. and Jiang, J. (2004). Hedgehog signalling activity of Smoothened requires phosphorylation by protein kinase A and casein kinase I. *Nature* **432**, 1045-50.
Jiang, C., Wan, X., He, Y., Pan, T., Jankovic, J. and Le, W. (2005). Age-dependent dopaminergic dysfunction in Nurr1 knockout mice. *Exp Neurol* **191**, 154-62.
Jin, O., Harpal, K., Ang, S. L. and Rossant, J. (2001). Otx2 and HNF3beta genetically interact in anterior patterning. *Int J Dev Biol* **45**, 357-65.
Jostes, B., Walther, C. and Gruss, P. (1990). The murine paired box gene, Pax7, is expressed specifically during the development of the nervous and muscular system. *Mech Dev* **33**, 27-37.
Joyner, A. L., Herrup, K., Auerbach, B. A., Davis, C. A. and Rossant, J. (1991). Subtle cerebellar phenotype in mice homozygous for a targeted deletion of the En-2 homeobox. *Science* **251**, 1239-43.
Joyner, A. L., Kornberg, T., Coleman, K. G., Cox, D. R. and Martin, G. R. (1985). Expression during embryogenesis of a mouse gene with sequence homology to the Drosophila engrailed gene. *Cell* **43**, 29-37.
Joyner, A. L. and Martin, G. R. (1987). En-1 and En-2, two mouse genes with sequence homology to the Drosophila engrailed gene: expression during embryogenesis. *Genes Dev* **1**, 29-38.
Kaestner, K. H., Knochel, W. and Martinez, D. E. (2000). Unified nomenclature for the winged helix/forkhead transcription factors. *Genes Dev* **14**, 142-6.
Kandel, E. R., Schwartz, J. H. and Jessell, T. M. (2000a). Principles of Neural Science : Chapter 43: The Basal Ganglia: McGraw-Hill.
Kandel, E. R., Schwartz, J. H. and Jessell, T. M. (2000b). Principles of Neural Science : Chapter 44: Brain stem, reflexive behavior, and the cranial nerves. Pages 873-888: McGraw-Hill.
Karlstrom, R. O., Tyurina, O. V., Kawakami, A., Nishioka, N., Talbot, W. S., Sasaki, H. and Schier, A. F. (2003). Genetic analysis of zebrafish gli1 and gli2 reveals divergent requirements for gli genes in vertebrate development. *Development* **130**, 1549-64.
Kaufmann, E. and Knochel, W. (1996). Five years on the wings of fork head. *Mech Dev* **57**, 3-20.
Kele, J., Simplicio, N., Ferri, A. L., Mira, H., Guillemot, F., Arenas, E. and Ang, S. L. (2006). Neurogenin 2 is required for the development of ventral midbrain dopaminergic neurons. *Development* **133**, 495-505.
Kennedy, P. R. (1987). Parametric relationships of individual digit movements to neuronal discharges in primate magnocellular red nucleus. *Brain Res* **417**, 185-9.
Kennedy, P. R. (1990). Corticospinal, rubrospinal and rubro-olivary projections: a unifying hypothesis. *Trends Neurosci* **13**, 474-9.
Kessaris, N., Pringle, N. and Richardson, W. D. (2001). Ventral neurogenesis and the neuron-glial switch. *Neuron* **31**, 677-80.
Kiecker, C. and Lumsden, A. (2004). Hedgehog signaling from the ZLI regulates diencephalic regional identity. *Nat Neurosci* **7**, 1242-9.

Kiecker, C. and Lumsden, A. (2005). Compartments and their boundaries in vertebrate brain development. *Nat Rev Neurosci* **6**, 553-64.
Kingsbury, B. F. (1930). The developmental significance of the floor plate of the brain and spinal cord. *J Comp Neurol* **32**, 177-207.
Kitamura, K., Miura, H., Yanazawa, M., Miyashita, T. and Kato, K. (1997). Expression patterns of Brx1 (Rieg gene), Sonic hedgehog, Nkx2.2, Dlx1 and Arx during zona limitans intrathalamica and embryonic ventral lateral geniculate nuclear formation. *Mech Dev* **67**, 83-96.
Knoers, N. V., Bongers, E. M., van Beersum, S. E., Lommen, E. J., van Bokhoven, H. and Hol, F. A. (2000). Nail-patella syndrome: identification of mutations in the LMX1B gene in Dutch families. *J Am Soc Nephrol* **11**, 1762-6.
Kobayashi, K., Morita, S., Sawada, H., Mizuguchi, T., Yamada, K., Nagatsu, I., Hata, T., Watanabe, Y., Fujita, K. and Nagatsu, T. (1995). Targeted disruption of the tyrosine hydroxylase locus results in severe catecholamine depletion and perinatal lethality in mice. *J Biol Chem* **270**, 27235-43.
Korotkova, T. M., Ponomarenko, A. A., Haas, H. L. and Sergeeva, O. A. (2005). Differential expression of the homeobox gene Pitx3 in midbrain dopaminergic neurons. *Eur J Neurosci* **22**, 1287-93.
Krauss, S., Concordet, J. P. and Ingham, P. W. (1993). A functionally conserved homolog of the Drosophila segment polarity gene hh is expressed in tissues with polarizing activity in zebrafish embryos. *Cell* **75**, 1431-44.
Kuypers, H. G. (1964). The Descending Pathways to the Spinal Cord, Their Anatomy and Function. *Prog Brain Res* **11**, 178-202.
Lai, E., Clark, K. L., Burley, S. K. and Darnell, J. E., Jr. (1993). Hepatocyte nuclear factor 3/fork head or "winged helix" proteins: a family of transcription factors of diverse biologic function. *Proc Natl Acad Sci U S A* **90**, 10421-3.
Lai, E., Prezioso, V. R., Smith, E., Litvin, O., Costa, R. H. and Darnell, J. E., Jr. (1990). HNF-3A, a hepatocyte-enriched transcription factor of novel structure is regulated transcriptionally. *Genes Dev* **4**, 1427-36.
Lai, E., Prezioso, V. R., Tao, W. F., Chen, W. S. and Darnell, J. E., Jr. (1991). Hepatocyte nuclear factor 3 alpha belongs to a gene family in mammals that is homologous to the Drosophila homeotic gene fork head. *Genes Dev* **5**, 416-27.
Law, S. W., Conneely, O. M., DeMayo, F. J. and O'Malley, B. W. (1992). Identification of a new brain-specific transcription factor, NURR1. *Mol Endocrinol* **6**, 2129-35.
Lawrence, D. G. and Kuypers, H. G. (1968a). The functional organization of the motor system in the monkey. I. The effects of bilateral pyramidal lesions. *Brain* **91**, 1-14.
Lawrence, D. G. and Kuypers, H. G. (1968b). The functional organization of the motor system in the monkey. II. The effects of lesions of the descending brain-stem pathways. *Brain* **91**, 15-36.
Le Douarin, N. M. and Halpern, M. E. (2000). Discussion point. Origin and specification of the neural tube floor plate: insights from the chick and zebrafish. *Curr Opin Neurobiol* **10**, 23-30.
Le, W., Conneely, O. M., Zou, L., He, Y., Saucedo-Cardenas, O., Jankovic, J., Mosier, D. R. and Appel, S. H. (1999). Selective agenesis of mesencephalic dopaminergic neurons in Nurr1-deficient mice. *Exp Neurol* **159**, 451-8.
Lebel, M., Gauthier, Y., Moreau, A. and Drouin, J. (2001). Pitx3 activates mouse tyrosine hydroxylase promoter via a high-affinity binding site. *J Neurochem* **77**, 558-67.

Lee, J., Platt, K. A., Censullo, P. and Ruiz i Altaba, A. (1997). Gli1 is a target of Sonic hedgehog that induces ventral neural tube development. *Development* **124**, 2537-52.
Lee, J. J., Ekker, S. C., von Kessler, D. P., Porter, J. A., Sun, B. I. and Beachy, P. A. (1994). Autoproteolysis in hedgehog protein biogenesis. *Science* **266**, 1528-37.
Lee, K. J. and Jessell, T. M. (1999). The specification of dorsal cell fates in the vertebrate central nervous system. *Annu Rev Neurosci* **22**, 261-94.
Lei, Q., Zelman, A. K., Kuang, E., Li, S. and Matise, M. P. (2004). Transduction of graded Hedgehog signaling by a combination of Gli2 and Gli3 activator functions in the developing spinal cord. *Development* **131**, 3593-604.
Levitt, M., Spector, S., Sjoerdsma, A. and Udenfriend, S. (1965). Elucidation of the Rate-Limiting Step in Norepinephrine Biosynthesis in the Perfused Guinea-Pig Heart. *J Pharmacol Exp Ther* **148**, 1-8.
Lewis, P. M., Dunn, M. P., McMahon, J. A., Logan, M., Martin, J. F., St-Jacques, B. and McMahon, A. P. (2001). Cholesterol modification of sonic hedgehog is required for long-range signaling activity and effective modulation of signaling by Ptc1. *Cell* **105**, 599-612.
Li, J. Y. and Joyner, A. L. (2001). Otx2 and Gbx2 are required for refinement and not induction of mid-hindbrain gene expression. *Development* **128**, 4979-91.
Li, M., Pevny, L., Lovell-Badge, R. and Smith, A. (1998). Generation of purified neural precursors from embryonic stem cells by lineage selection. *Curr Biol* **8**, 971-4.
Licata, F., Li Volsi, G., Di Mauro, M., Fretto, G., Ciranna, L. and Santangelo, F. (2001). Serotonin modifies the neuronal inhibitory responses to gamma-aminobutyric acid in the red nucleus: a microiontophoretic study in the rat. *Exp Neurol* **167**, 95-107.
Liem, K. F., Jr., Tremml, G. and Jessell, T. M. (1997). A role for the roof plate and its resident TGFbeta-related proteins in neuronal patterning in the dorsal spinal cord. *Cell* **91**, 127-38.
Liem, K. F., Jr., Tremml, G., Roelink, H. and Jessell, T. M. (1995). Dorsal differentiation of neural plate cells induced by BMP-mediated signals from epidermal ectoderm. *Cell* **82**, 969-79.
Lin, J. C. and Rosenthal, A. (2003). Molecular mechanisms controlling the development of dopaminergic neurons. *Semin Cell Dev Biol* **14**, 175-80.
Litingtung, Y. and Chiang, C. (2000a). Control of Shh activity and signaling in the neural tube. *Dev Dyn* **219**, 143-54.
Litingtung, Y. and Chiang, C. (2000b). Specification of ventral neuron types is mediated by an antagonistic interaction between Shh and Gli3. *Nat Neurosci* **3**, 979-85.
Litingtung, Y., Dahn, R. D., Li, Y., Fallon, J. F. and Chiang, C. (2002). Shh and Gli3 are dispensable for limb skeleton formation but regulate digit number and identity. *Nature* **418**, 979-83.
Liu, A. and Joyner, A. L. (2001a). Early anterior/posterior patterning of the midbrain and cerebellum. *Annu Rev Neurosci* **24**, 869-96.
Liu, A. and Joyner, A. L. (2001b). EN and GBX2 play essential roles downstream of FGF8 in patterning the mouse mid/hindbrain region. *Development* **128**, 181-91.
Liu, A., Li, J. Y., Bromleigh, C., Lao, Z., Niswander, L. A. and Joyner, A. L. (2003). FGF17b and FGF18 have different midbrain regulatory properties from FGF8b or activated FGF receptors. *Development* **130**, 6175-85.
Liu, A., Losos, K. and Joyner, A. L. (1999). FGF8 can activate Gbx2 and transform regions of the rostral mouse brain into a hindbrain fate. *Development* **126**, 4827-38.
Liu, Q. S., Pu, L. and Poo, M. M. (2005). Repeated cocaine exposure in vivo facilitates LTP induction in midbrain dopamine neurons. *Nature* **437**, 1027-31.

Lo, L. C., Johnson, J. E., Wuenschell, C. W., Saito, T. and Anderson, D. J. (1991). Mammalian achaete-scute homolog 1 is transiently expressed by spatially restricted subsets of early neuroepithelial and neural crest cells. *Genes Dev* **5**, 1524-37.
Logan, C. Y. and Nusse, R. (2004). The Wnt signaling pathway in development and disease. *Annu Rev Cell Dev Biol* **20**, 781-810.
Loonstra, A., Vooijs, M., Beverloo, H. B., Allak, B. A., van Drunen, E., Kanaar, R., Berns, A. and Jonkers, J. (2001). Growth inhibition and DNA damage induced by Cre recombinase in mammalian cells. *Proc Natl Acad Sci U S A* **98**, 9209-14.
Lum, L., Yao, S., Mozer, B., Rovescalli, A., Von Kessler, D., Nirenberg, M. and Beachy, P. A. (2003a). Identification of Hedgehog pathway components by RNAi in Drosophila cultured cells. *Science* **299**, 2039-45.
Lum, L., Zhang, C., Oh, S., Mann, R. K., von Kessler, D. P., Taipale, J., Weis-Garcia, F., Gong, R., Wang, B. and Beachy, P. A. (2003b). Hedgehog signal transduction via Smoothened association with a cytoplasmic complex scaffolded by the atypical kinesin, Costal-2. *Mol Cell* **12**, 1261-74.
Ma, Q., Fode, C., Guillemot, F. and Anderson, D. J. (1999). Neurogenin1 and neurogenin2 control two distinct waves of neurogenesis in developing dorsal root ganglia. *Genes Dev* **13**, 1717-28.
Mallamaci, A., Mercurio, S., Muzio, L., Cecchi, C., Pardini, C. L., Gruss, P. and Boncinelli, E. (2000). The lack of Emx2 causes impairment of Reelin signaling and defects of neuronal migration in the developing cerebral cortex. *J Neurosci* **20**, 1109-18.
Marigo, V., Davey, R. A., Zuo, Y., Cunningham, J. M. and Tabin, C. J. (1996a). Biochemical evidence that patched is the Hedgehog receptor. *Nature* **384**, 176-9.
Marigo, V., Scott, M. P., Johnson, R. L., Goodrich, L. V. and Tabin, C. J. (1996b). Conservation in hedgehog signaling: induction of a chicken patched homolog by Sonic hedgehog in the developing limb. *Development* **122**, 1225-33.
Marigo, V. and Tabin, C. J. (1996). Regulation of patched by sonic hedgehog in the developing neural tube. *Proc Natl Acad Sci U S A* **93**, 9346-51.
Marti, E., Bumcrot, D. A., Takada, R. and McMahon, A. P. (1995a). Requirement of 19K form of Sonic hedgehog for induction of distinct ventral cell types in CNS explants. *Nature* **375**, 322-5.
Marti, E., Takada, R., Bumcrot, D. A., Sasaki, H. and McMahon, A. P. (1995b). Distribution of Sonic hedgehog peptides in the developing chick and mouse embryo. *Development* **121**, 2537-47.
Martin, R. M., Leonhardt, H. and Cardoso, M. C. (2005). DNA labeling in living cells. *Cytometry A* **67**, 45-52.
Martinez-Barbera, J. P., Signore, M., Boyl, P. P., Puelles, E., Acampora, D., Gogoi, R., Schubert, F., Lumsden, A. and Simeone, A. (2001). Regionalisation of anterior neuroectoderm and its competence in responding to forebrain and midbrain inducing activities depend on mutual antagonism between OTX2 and GBX2. *Development* **128**, 4789-800.
Martinez, S., Crossley, P. H., Cobos, I., Rubenstein, J. L. and Martin, G. R. (1999). FGF8 induces formation of an ectopic isthmic organizer and isthmocerebellar development via a repressive effect on Otx2 expression. *Development* **126**, 1189-200.
Marusich, M. F., Furneaux, H. M., Henion, P. D. and Weston, J. A. (1994). Hu neuronal proteins are expressed in proliferating neurogenic cells. *J Neurobiol* **25**, 143-55.
Massion, J. (1967). The mammalian red nucleus. *Physiol Rev* **47**, 383-436.
Massion, J. (1988). Red nucleus: past and future. *Behav Brain Res* **28**, 1-8.

Matise, M. P., Epstein, D. J., Park, H. L., Platt, K. A. and Joyner, A. L. (1998). Gli2 is required for induction of floor plate and adjacent cells, but not most ventral neurons in the mouse central nervous system. *Development* **125**, 2759-70.
Matsunaga, E., Katahira, T. and Nakamura, H. (2002). Role of Lmx1b and Wnt1 in mesencephalon and metencephalon development. *Development* **129**, 5269-77.
Maves, L., Jackman, W. and Kimmel, C. B. (2002). FGF3 and FGF8 mediate a rhombomere 4 signaling activity in the zebrafish hindbrain. *Development* **129**, 3825-37.
Maxwell, S. L., Ho, H. Y., Kuehner, E., Zhao, S. and Li, M. (2005). Pitx3 regulates tyrosine hydroxylase expression in the substantia nigra and identifies a subgroup of mesencephalic dopaminergic progenitor neurons during mouse development. *Dev Biol* **282**, 467-79.
Maxwell, S. L. and Li, M. (2005). Midbrain dopaminergic development in vivo and in vitro from embryonic stem cells. *J Anat* **207**, 209-18.
McEvilly, R. J., Erkman, L., Luo, L., Sawchenko, P. E., Ryan, A. F. and Rosenfeld, M. G. (1996). Requirement for Brn-3.0 in differentiation and survival of sensory and motor neurons. *Nature* **384**, 574-7.
McMahon, A. P. and Bradley, A. (1990). The Wnt-1 (int-1) proto-oncogene is required for development of a large region of the mouse brain. *Cell* **62**, 1073-85.
McMahon, A. P., Joyner, A. L., Bradley, A. and McMahon, J. A. (1992). The midbrain-hindbrain phenotype of Wnt-1-/Wnt-1- mice results from stepwise deletion of engrailed-expressing cells by 9.5 days postcoitum. *Cell* **69**, 581-95.
Melis, M., Spiga, S. and Diana, M. (2005). The dopamine hypothesis of drug addiction: hypodopaminergic state. *Int Rev Neurobiol* **63**, 101-54.
Menezes, J. R. and Luskin, M. B. (1994). Expression of neuron-specific tubulin defines a novel population in the proliferative layers of the developing telencephalon. *J Neurosci* **14**, 5399-416.
Meyer, N. P. and Roelink, H. (2003). The amino-terminal region of Gli3 antagonizes the Shh response and acts in dorsoventral fate specification in the developing spinal cord. *Dev Biol* **257**, 343-55.
Meyers, E. N., Lewandoski, M. and Martin, G. R. (1998). An Fgf8 mutant allelic series generated by Cre- and Flp-mediated recombination. *Nat Genet* **18**, 136-41.
Millen, K. J., Wurst, W., Herrup, K. and Joyner, A. L. (1994). Abnormal embryonic cerebellar development and patterning of postnatal foliation in two mouse Engrailed-2 mutants. *Development* **120**, 695-706.
Millet, S., Campbell, K., Epstein, D. J., Losos, K., Harris, E. and Joyner, A. L. (1999). A role for Gbx2 in repression of Otx2 and positioning the mid/hindbrain organizer. *Nature* **401**, 161-4.
Mo, R., Freer, A. M., Zinyk, D. L., Crackower, M. A., Michaud, J., Heng, H. H., Chik, K. W., Shi, X. M., Tsui, L. C., Cheng, S. H. et al. (1997). Specific and redundant functions of Gli2 and Gli3 zinc finger genes in skeletal patterning and development. *Development* **124**, 113-23.
Montero, C. (2003). The antigen-antibody reaction in immunohistochemistry. *J Histochem Cytochem* **51**, 1-4.
Morin, X., Cremer, H., Hirsch, M. R., Kapur, R. P., Goridis, C. and Brunet, J. F. (1997). Defects in sensory and autonomic ganglia and absence of locus coeruleus in mice deficient for the homeobox gene Phox2a. *Neuron* **18**, 411-23.
Motoyama, J., Liu, J., Mo, R., Ding, Q., Post, M. and Hui, C. C. (1998). Essential function of Gli2 and Gli3 in the formation of lung, trachea and oesophagus. *Nat Genet* **20**, 54-7.

Motoyama, J., Milenkovic, L., Iwama, M., Shikata, Y., Scott, M. P. and Hui, C. C. (2003). Differential requirement for Gli2 and Gli3 in ventral neural cell fate specification. *Dev Biol* **259**, 150-61.
Muir, G. D. and Whishaw, I. Q. (2000). Red nucleus lesions impair overground locomotion in rats: a kinetic analysis. *Eur J Neurosci* **12**, 1113-22.
Muller, F., Albert, S., Blader, P., Fischer, N., Hallonet, M. and Strahle, U. (2000). Direct action of the nodal-related signal cyclops in induction of sonic hedgehog in the ventral midline of the CNS. *Development* **127**, 3889-97.
Muller, M., Jabs, N., Lorke, D. E., Fritzsch, B. and Sander, M. (2003). Nkx6.1 controls migration and axon pathfinding of cranial branchio-motoneurons. *Development* **130**, 5815-26.
Nagatsu, T., Levitt, M. and Udenfriend, S. (1964a). Conversion of L-tyrosine to 3,4-dihydroxyphenylalanine by cell-free preparations of brain and sympathetically innervated tissues. *Biochem Biophys Res Commun* **14**, 543-9.
Nagatsu, T., Levitt, M. and Udenfriend, S. (1964b). Tyrosine Hydroxylase. The Initial Step in Norepinephrine Biosynthesis. *J Biol Chem* **239**, 2910-7.
Nakamura, H., Katahira, T., Matsunaga, E. and Sato, T. (2005). Isthmus organizer for midbrain and hindbrain development. *Brain Res Brain Res Rev* **49**, 120-6.
Nathan, P. W. and Smith, M. C. (1982). The rubrospinal and central tegmental tracts in man. *Brain* **105**, 223-69.
Nelson, E. L., Liang, C. L., Sinton, C. M. and German, D. C. (1996). Midbrain dopaminergic neurons in the mouse: computer-assisted mapping. *J Comp Neurol* **369**, 361-71.
Nestler, E. J. (2001). Molecular basis of long-term plasticity underlying addiction. *Nat Rev Neurosci* **2**, 119-28.
Neumann, C. J., Grandel, H., Gaffield, W., Schulte-Merker, S. and Nusslein-Volhard, C. (1999). Transient establishment of anteroposterior polarity in the zebrafish pectoral fin bud in the absence of sonic hedgehog activity. *Development* **126**, 4817-26.
Nieoullon, A., Vuillon-Cacciuttolo, G., Dusticier, N., Kerkerian, L., Andre, D. and Bosler, O. (1988). Putative neurotransmitters in the red nucleus and their involvement in postlesion adaptive mechanisms. *Behav Brain Res* **28**, 163-74.
Norton, W. H., Mangoli, M., Lele, Z., Pogoda, H. M., Diamond, B., Mercurio, S., Russell, C., Teraoka, H., Stickney, H. L., Rauch, G. J. et al. (2005). Monorail/Foxa2 regulates floorplate differentiation and specification of oligodendrocytes, serotonergic raphe neurones and cranial motoneurones. *Development* **132**, 645-58.
Novitch, B. G., Chen, A. I. and Jessell, T. M. (2001). Coordinate regulation of motor neuron subtype identity and pan-neuronal properties by the bHLH repressor Olig2. *Neuron* **31**, 773-89.
Nunes, I., Tovmasian, L. T., Silva, R. M., Burke, R. E. and Goff, S. P. (2003). Pitx3 is required for development of substantia nigra dopaminergic neurons. *Proc Natl Acad Sci U S A* **100**, 4245-50.
Nusse, R. and Varmus, H. E. (1982). Many tumors induced by the mouse mammary tumor virus contain a provirus integrated in the same region of the host genome. *Cell* **31**, 99-109.
Odenthal, J., van Eeden, F. J., Haffter, P., Ingham, P. W. and Nusslein-Volhard, C. (2000). Two distinct cell populations in the floor plate of the zebrafish are induced by different pathways. *Dev Biol* **219**, 350-63.
Ogden, S. K., Ascano, M., Jr., Stegman, M. A., Suber, L. M., Hooper, J. E. and Robbins, D. J. (2003). Identification of a functional interaction between the

transmembrane protein Smoothened and the kinesin-related protein Costal2. *Curr Biol* **13**, 1998-2003.
Osumi, N., Hirota, A., Ohuchi, H., Nakafuku, M., Iimura, T., Kuratani, S., Fujiwara, M., Noji, S. and Eto, K. (1997). Pax-6 is involved in the specification of hindbrain motor neuron subtype. *Development* **124**, 2961-72.
Pabst, O., Herbrand, H. and Arnold, H. H. (1998). Nkx2-9 is a novel homeobox transcription factor which demarcates ventral domains in the developing mouse CNS. *Mech Dev* **73**, 85-93.
Pabst, O., Rummelies, J., Winter, B. and Arnold, H. H. (2003). Targeted disruption of the homeobox gene Nkx2.9 reveals a role in development of the spinal accessory nerve. *Development* **130**, 1193-202.
Padel, Y., Angaut, P., Massion, J. and Sedan, R. (1981). Comparative study of the posterior red nucleus in baboons and gibbons. *J Comp Neurol* **202**, 421-38.
Paillard, J. (1978). The pyramidal tract: two millions fibres in search of a function. *J Physiol (Paris)* **74**, 155-62.
Pankratz, N. and Foroud, T. (2004). Genetics of Parkinson disease. *NeuroRx* **1**, 235-42.
Park, H. L., Bai, C., Platt, K. A., Matise, M. P., Beeghly, A., Hui, C. C., Nakashima, M. and Joyner, A. L. (2000). Mouse Gli1 mutants are viable but have defects in SHH signaling in combination with a Gli2 mutation. *Development* **127**, 1593-605.
Parras, C. M., Schuurmans, C., Scardigli, R., Kim, J., Anderson, D. J. and Guillemot, F. (2002). Divergent functions of the proneural genes Mash1 and Ngn2 in the specification of neuronal subtype identity. *Genes Dev* **16**, 324-38.
Patten, I., Kulesa, P., Shen, M. M., Fraser, S. and Placzek, M. (2003). Distinct modes of floor plate induction in the chick embryo. *Development* **130**, 4809-21.
Patten, I. and Placzek, M. (2000). The role of Sonic hedgehog in neural tube patterning. *Cell Mol Life Sci* **57**, 1695-708.
Pattyn, A., Hirsch, M., Goridis, C. and Brunet, J. F. (2000). Control of hindbrain motor neuron differentiation by the homeobox gene Phox2b. *Development* **127**, 1349-58.
Pattyn, A., Morin, X., Cremer, H., Goridis, C. and Brunet, J. F. (1997). Expression and interactions of the two closely related homeobox genes Phox2a and Phox2b during neurogenesis. *Development* **124**, 4065-75.
Pazos, A., Cortes, R. and Palacios, J. M. (1985). Quantitative autoradiographic mapping of serotonin receptors in the rat brain. II. Serotonin-2 receptors. *Brain Res* **346**, 231-49.
Pazos, A. and Palacios, J. M. (1985). Quantitative autoradiographic mapping of serotonin receptors in the rat brain. I. Serotonin-1 receptors. *Brain Res* **346**, 205-30.
Perrone-Capano, C., Da Pozzo, P. and di Porzio, U. (2000). Epigenetic cues in midbrain dopaminergic neuron development. *Neurosci Biobehav Rev* **24**, 119-24.
Perrone-Capano, C. and Di Porzio, U. (2000). Genetic and epigenetic control of midbrain dopaminergic neuron development. *Int J Dev Biol* **44**, 679-87.
Persson, M., Stamataki, D., te Welscher, P., Andersson, E., Bose, J., Ruther, U., Ericson, J. and Briscoe, J. (2002). Dorsal-ventral patterning of the spinal cord requires Gli3 transcriptional repressor activity. *Genes Dev* **16**, 2865-78.
Pfaff, S. L., Mendelsohn, M., Stewart, C. L., Edlund, T. and Jessell, T. M. (1996). Requirement for LIM homeobox gene Isl1 in motor neuron generation reveals a motor neuron-dependent step in interneuron differentiation. *Cell* **84**, 309-20.

Pierani, A., Brenner-Morton, S., Chiang, C. and Jessell, T. M. (1999). A sonic hedgehog-independent, retinoid-activated pathway of neurogenesis in the ventral spinal cord. *Cell* **97**, 903-15.
Pierani, A., Moran-Rivard, L., Sunshine, M. J., Littman, D. R., Goulding, M. and Jessell, T. M. (2001). Control of interneuron fate in the developing spinal cord by the progenitor homeodomain protein Dbx1. *Neuron* **29**, 367-84.
Pinson, K. I., Brennan, J., Monkley, S., Avery, B. J. and Skarnes, W. C. (2000). An LDL-receptor-related protein mediates Wnt signalling in mice. *Nature* **407**, 535-8.
Placzek, M. and Briscoe, J. (2005). The floor plate: multiple cells, multiple signals. *Nat Rev Neurosci* **6**, 230-40.
Placzek, M., Dodd, J. and Jessell, T. M. (2000). Discussion point. The case for floor plate induction by the notochord. *Curr Opin Neurobiol* **10**, 15-22.
Placzek, M., Jessell, T. M. and Dodd, J. (1993). Induction of floor plate differentiation by contact-dependent, homeogenetic signals. *Development* **117**, 205-18.
Placzek, M., Tessier-Lavigne, M., Jessell, T. and Dodd, J. (1990a). Orientation of commissural axons in vitro in response to a floor plate-derived chemoattractant. *Development* **110**, 19-30.
Placzek, M., Tessier-Lavigne, M., Yamada, T., Jessell, T. and Dodd, J. (1990b). Mesodermal control of neural cell identity: floor plate induction by the notochord. *Science* **250**, 985-8.
Placzek, M., Yamada, T., Tessier-Lavigne, M., Jessell, T. and Dodd, J. (1991). Control of dorsoventral pattern in vertebrate neural development: induction and polarizing properties of the floor plate. *Development* **Suppl 2**, 105-22.
Platt, K. A., Michaud, J. and Joyner, A. L. (1997). Expression of the mouse Gli and Ptc genes is adjacent to embryonic sources of hedgehog signals suggesting a conservation of pathways between flies and mice. *Mech Dev* **62**, 121-35.
Poh, A., Karunaratne, A., Kolle, G., Huang, N., Smith, E., Starkey, J., Wen, D., Wilson, I., Yamada, T. and Hargrave, M. (2002). Patterning of the vertebrate ventral spinal cord. *Int J Dev Biol* **46**, 597-608.
Polymeropoulos, M. H., Lavedan, C., Leroy, E., Ide, S. E., Dehejia, A., Dutra, A., Pike, B., Root, H., Rubenstein, J., Boyer, R. et al. (1997). Mutation in the alpha-synuclein gene identified in families with Parkinson's disease. *Science* **276**, 2045-7.
Porter, J. A., Ekker, S. C., Park, W. J., von Kessler, D. P., Young, K. E., Chen, C. H., Ma, Y., Woods, A. S., Cotter, R. J., Koonin, E. V. et al. (1996a). Hedgehog patterning activity: role of a lipophilic modification mediated by the carboxy-terminal autoprocessing domain. *Cell* **86**, 21-34.
Porter, J. A., von Kessler, D. P., Ekker, S. C., Young, K. E., Lee, J. J., Moses, K. and Beachy, P. A. (1995). The product of hedgehog autoproteolytic cleavage active in local and long-range signalling. *Nature* **374**, 363-6.
Porter, J. A., Young, K. E. and Beachy, P. A. (1996b). Cholesterol modification of hedgehog signaling proteins in animal development. *Science* **274**, 255-9.
Prakash, N., Brodski, C., Naserke, T., Puelles, E., Gogoi, R., Hall, A., Panhuysen, M., Echevarria, D., Sussel, L., Weisenhorn, D. M. et al. (2006). A Wnt1-regulated genetic network controls the identity and fate of midbrain-dopaminergic progenitors in vivo. *Development* **133**, 89-98.
Price, S. R. and Briscoe, J. (2004). The generation and diversification of spinal motor neurons: signals and responses. *Mech Dev* **121**, 1103-15.
Przedborski, S. and Jackson-Lewis, V. (1998). Mechanisms of MPTP toxicity. *Mov Disord* **13 Suppl 1**, 35-8.

Puelles, E., Acampora, D., Lacroix, E., Signore, M., Annino, A., Tuorto, F., Filosa, S., Corte, G., Wurst, W., Ang, S. L. et al. (2003). Otx dose-dependent integrated control of antero-posterior and dorso-ventral patterning of midbrain. *Nat Neurosci* **6**, 453-60.

Qiu, M., Shimamura, K., Sussel, L., Chen, S. and Rubenstein, J. L. (1998). Control of anteroposterior and dorsoventral domains of Nkx-6.1 gene expression relative to other Nkx genes during vertebrate CNS development. *Mech Dev* **72**, 77-88.

Ramon y Cajal, S. (1906). Nobel Lecture, Physiology or Medicine 1901-1921: The Structure and Connexions of Neurons: Elsevier, Amsterdam.

Rastegar, S., Albert, S., Le Roux, I., Fischer, N., Blader, P., Muller, F. and Strahle, U. (2002). A floor plate enhancer of the zebrafish netrin1 gene requires Cyclops (Nodal) signalling and the winged helix transcription factor FoxA2. *Dev Biol* **252**, 1-14.

Rhinn, M., Dierich, A., Shawlot, W., Behringer, R. R., Le Meur, M. and Ang, S. L. (1998). Sequential roles for Otx2 in visceral endoderm and neuroectoderm for forebrain and midbrain induction and specification. *Development* **125**, 845-56.

Richardson, W. D., Smith, H. K., Sun, T., Pringle, N. P., Hall, A. and Woodruff, R. (2000). Oligodendrocyte lineage and the motor neuron connection. *Glia* **29**, 136-42.

Riddle, R. and Pollock, J. D. (2003). Making connections: the development of mesencephalic dopaminergic neurons. *Brain Res Dev Brain Res* **147**, 3-21.

Riddle, R. D., Ensini, M., Nelson, C., Tsuchida, T., Jessell, T. M. and Tabin, C. (1995). Induction of the LIM homeobox gene Lmx1 by WNT7a establishes dorsoventral pattern in the vertebrate limb. *Cell* **83**, 631-40.

Riddle, R. D., Johnson, R. L., Laufer, E. and Tabin, C. (1993). Sonic hedgehog mediates the polarizing activity of the ZPA. *Cell* **75**, 1401-16.

Rieger, D. K., Reichenberger, E., McLean, W., Sidow, A. and Olsen, B. R. (2001). A double-deletion mutation in the Pitx3 gene causes arrested lens development in aphakia mice. *Genomics* **72**, 61-72.

Roelink, H., Augsburger, A., Heemskerk, J., Korzh, V., Norlin, S., Ruiz i Altaba, A., Tanabe, Y., Placzek, M., Edlund, T., Jessell, T. M. et al. (1994). Floor plate and motor neuron induction by vhh-1, a vertebrate homolog of hedgehog expressed by the notochord. *Cell* **76**, 761-75.

Roelink, H., Porter, J. A., Chiang, C., Tanabe, Y., Chang, D. T., Beachy, P. A. and Jessell, T. M. (1995). Floor plate and motor neuron induction by different concentrations of the amino-terminal cleavage product of sonic hedgehog autoproteolysis. *Cell* **81**, 445-55.

Rosen, B. and Beddington, R. (1994). Detection of mRNA in whole mounts of mouse embryos using digoxigenin riboprobes. *Methods Mol Biol* **28**, 201-8.

Rosen, B. and Beddington, R. S. (1993). Whole-mount in situ hybridization in the mouse embryo: gene expression in three dimensions. *Trends Genet* **9**, 162-7.

Rowitch, D. H., B, S. J., Lee, S. M., Flax, J. D., Snyder, E. Y. and McMahon, A. P. (1999). Sonic hedgehog regulates proliferation and inhibits differentiation of CNS precursor cells. *J Neurosci* **19**, 8954-65.

Rubenstein, J. L., Shimamura, K., Martinez, S. and Puelles, L. (1998). Regionalization of the prosencephalic neural plate. *Annu Rev Neurosci* **21**, 445-77.

Rubia, K., Overmeyer, S., Taylor, E., Brammer, M., Williams, S. C., Simmons, A. and Bullmore, E. T. (1999). Hypofrontality in attention deficit hyperactivity disorder during higher-order motor control: a study with functional MRI. *Am J Psychiatry* **156**, 891-6.

Ruel, L., Rodriguez, R., Gallet, A., Lavenant-Staccini, L. and Therond, P. P. (2003). Stability and association of Smoothened, Costal2 and Fused with Cubitus interruptus are regulated by Hedgehog. *Nat Cell Biol* **5**, 907-13.
Ruiz i Altaba, A. (1998). Combinatorial Gli gene function in floor plate and neuronal inductions by Sonic hedgehog. *Development* **125**, 2203-12.
Ruiz i Altaba, A. (1999). Gli proteins encode context-dependent positive and negative functions: implications for development and disease. *Development* **126**, 3205-16.
Ruiz i Altaba, A., Cox, C., Jessell, T. M. and Klar, A. (1993). Ectopic neural expression of a floor plate marker in frog embryos injected with the midline transcription factor Pintallavis. *Proc Natl Acad Sci U S A* **90**, 8268-72.
Ruiz i Altaba, A., Jessell, T. M. and Roelink, H. (1995a). Restrictions to floor plate induction by hedgehog and winged-helix genes in the neural tube of frog embryos. *Mol Cell Neurosci* **6**, 106-21.
Ruiz i Altaba, A., Palma, V. and Dahmane, N. (2002). Hedgehog-Gli signalling and the growth of the brain. *Nat Rev Neurosci* **3**, 24-33.
Ruiz i Altaba, A., Placzek, M., Baldassare, M., Dodd, J. and Jessell, T. M. (1995b). Early stages of notochord and floor plate development in the chick embryo defined by normal and induced expression of HNF-3 beta. *Dev Biol* **170**, 299-313.
Sakurada, K., Ohshima-Sakurada, M., Palmer, T. D. and Gage, F. H. (1999). Nurr1, an orphan nuclear receptor, is a transcriptional activator of endogenous tyrosine hydroxylase in neural progenitor cells derived from the adult brain. *Development* **126**, 4017-26.
Sampath, K., Rubinstein, A. L., Cheng, A. M., Liang, J. O., Fekany, K., Solnica-Krezel, L., Korzh, V., Halpern, M. E. and Wright, C. V. (1998). Induction of the zebrafish ventral brain and floorplate requires cyclops/nodal signalling. *Nature* **395**, 185-9.
Sander, M., Paydar, S., Ericson, J., Briscoe, J., Berber, E., German, M., Jessell, T. M. and Rubenstein, J. L. (2000). Ventral neural patterning by Nkx homeobox genes: Nkx6.1 controls somatic motor neuron and ventral interneuron fates. *Genes Dev* **14**, 2134-9.
Sasaki, H. and Hogan, B. L. (1993). Differential expression of multiple fork head related genes during gastrulation and axial pattern formation in the mouse embryo. *Development* **118**, 47-59.
Sasaki, H. and Hogan, B. L. (1994). HNF-3 beta as a regulator of floor plate development. *Cell* **76**, 103-15.
Sasaki, H., Hui, C., Nakafuku, M. and Kondoh, H. (1997). A binding site for Gli proteins is essential for HNF-3beta floor plate enhancer activity in transgenics and can respond to Shh in vitro. *Development* **124**, 1313-22.
Sasaki, H., Nishizaki, Y., Hui, C., Nakafuku, M. and Kondoh, H. (1999). Regulation of Gli2 and Gli3 activities by an amino-terminal repression domain: implication of Gli2 and Gli3 as primary mediators of Shh signaling. *Development* **126**, 3915-24.
Saucedo-Cardenas, O. and Conneely, O. M. (1996). Comparative distribution of NURR1 and NUR77 nuclear receptors in the mouse central nervous system. *J Mol Neurosci* **7**, 51-63.
Saucedo-Cardenas, O., Quintana-Hau, J. D., Le, W. D., Smidt, M. P., Cox, J. J., De Mayo, F., Burbach, J. P. and Conneely, O. M. (1998). Nurr1 is essential for the induction of the dopaminergic phenotype and the survival of ventral mesencephalic late dopaminergic precursor neurons. *Proc Natl Acad Sci U S A* **95**, 4013-8.

Schambra, U. B., Lauder, J. M., Petrusz, P. and Sulik, K. K. (1990). Development of neurotransmitter systems in the mouse embryo following acute ethanol exposure: a histological and immunocytochemical study. *Int J Dev Neurosci* **8**, 507-22.
Schapira, A. H. (1997). Pathogenesis of Parkinson's disease. *Baillieres Clin Neurol* **6**, 15-36.
Schauerte, H. E., van Eeden, F. J., Fricke, C., Odenthal, J., Strahle, U. and Haffter, P. (1998). Sonic hedgehog is not required for the induction of medial floor plate cells in the zebrafish. *Development* **125**, 2983-93.
Schier, A. F., Neuhauss, S. C., Harvey, M., Malicki, J., Solnica-Krezel, L., Stainier, D. Y., Zwartkruis, F., Abdelilah, S., Stemple, D. L., Rangini, Z. et al. (1996). Mutations affecting the development of the embryonic zebrafish brain. *Development* **123**, 165-78.
Schimmang, T., Lemaistre, M., Vortkamp, A. and Ruther, U. (1992). Expression of the zinc finger gene Gli3 is affected in the morphogenetic mouse mutant extra-toes (Xt). *Development* **116**, 799-804.
Scholpp, S., Lohs, C. and Brand, M. (2003). Engrailed and Fgf8 act synergistically to maintain the boundary between diencephalon and mesencephalon. *Development* **130**, 4881-93.
Schwarz, M., Alvarez-Bolado, G., Urbanek, P., Busslinger, M. and Gruss, P. (1997). Conserved biological function between Pax-2 and Pax-5 in midbrain and cerebellum development: evidence from targeted mutations. *Proc Natl Acad Sci U S A* **94**, 14518-23.
Semina, E. V., Murray, J. C., Reiter, R., Hrstka, R. F. and Graw, J. (2000). Deletion in the promoter region and altered expression of Pitx3 homeobox gene in aphakia mice. *Hum Mol Genet* **9**, 1575-85.
Semina, E. V., Reiter, R. S. and Murray, J. C. (1997). Isolation of a new homeobox gene belonging to the Pitx/Rieg family: expression during lens development and mapping to the aphakia region on mouse chromosome 19. *Hum Mol Genet* **6**, 2109-16.
Shamim, H., Mahmood, R., Logan, C., Doherty, P., Lumsden, A. and Mason, I. (1999). Sequential roles for Fgf4, En1 and Fgf8 in specification and regionalisation of the midbrain. *Development* **126**, 945-59.
Shi, S. R., Cote, R. J. and Taylor, C. R. (1997). Antigen retrieval immunohistochemistry: past, present, and future. *J Histochem Cytochem* **45**, 327-43.
Shoji, H., Ito, T., Wakamatsu, Y., Hayasaka, N., Ohsaki, K., Oyanagi, M., Kominami, R., Kondoh, H. and Takahashi, N. (1996). Regionalized expression of the Dbx family homeobox genes in the embryonic CNS of the mouse. *Mech Dev* **56**, 25-39.
Silver, D. P. and Livingston, D. M. (2001). Self-excising retroviral vectors encoding the Cre recombinase overcome Cre-mediated cellular toxicity. *Mol Cell* **8**, 233-43.
Simeone, A. (2000). Positioning the isthmic organizer where Otx2 and Gbx2meet. *Trends Genet* **16**, 237-40.
Simeone, A., Gulisano, M., Acampora, D., Stornaiuolo, A., Rambaldi, M. and Boncinelli, E. (1992). Two vertebrate homeobox genes related to the Drosophila empty spiracles gene are expressed in the embryonic cerebral cortex. *Embo J* **11**, 2541-50.
Simon, H. H., Bhatt, L., Gherbassi, D., Sgado, P. and Alberi, L. (2003). Midbrain dopaminergic neurons: determination of their developmental fate by transcription factors. *Ann N Y Acad Sci* **991**, 36-47.
Simon, H. H., Saueressig, H., Wurst, W., Goulding, M. D. and O'Leary, D. D. (2001). Fate of midbrain dopaminergic neurons controlled by the engrailed genes. *J Neurosci* **21**, 3126-34.

Smidt, M. P., Asbreuk, C. H., Cox, J. J., Chen, H., Johnson, R. L. and Burbach, J. P. (2000). A second independent pathway for development of mesencephalic dopaminergic neurons requires Lmx1b. *Nat Neurosci* **3**, 337-41.

Smidt, M. P., Smits, S. M., Bouwmeester, H., Hamers, F. P., van der Linden, A. J., Hellemons, A. J., Graw, J. and Burbach, J. P. (2004a). Early developmental failure of substantia nigra dopamine neurons in mice lacking the homeodomain gene Pitx3. *Development* **131**, 1145-55.

Smidt, M. P., Smits, S. M. and Burbach, J. P. (2003). Molecular mechanisms underlying midbrain dopamine neuron development and function. *Eur J Pharmacol* **480**, 75-88.

Smidt, M. P., Smits, S. M. and Burbach, J. P. (2004b). Homeobox gene Pitx3 and its role in the development of dopamine neurons of the substantia nigra. *Cell Tissue Res* **318**, 35-43.

Smidt, M. P., van Schaick, H. S., Lanctot, C., Tremblay, J. J., Cox, J. J., van der Kleij, A. A., Wolterink, G., Drouin, J. and Burbach, J. P. (1997). A homeodomain gene Ptx3 has highly restricted brain expression in mesencephalic dopaminergic neurons. *Proc Natl Acad Sci U S A* **94**, 13305-10.

Solanto, M. V. (2002). Dopamine dysfunction in AD/HD: integrating clinical and basic neuroscience research. *Behav Brain Res* **130**, 65-71.

Spencer, R. F., Wenthold, R. J. and Baker, R. (1989). Evidence for glycine as an inhibitory neurotransmitter of vestibular, reticular, and prepositus hypoglossi neurons that project to the cat abducens nucleus. *J Neurosci* **9**, 2718-36.

Stamataki, D., Ulloa, F., Tsoni, S. V., Mynett, A. and Briscoe, J. (2005). A gradient of Gli activity mediates graded Sonic Hedgehog signaling in the neural tube. *Genes Dev* **19**, 626-41.

Stern, C. D. (2001). Initial patterning of the central nervous system: how many organizers? *Nat Rev Neurosci* **2**, 92-8.

Stone, D. M., Hynes, M., Armanini, M., Swanson, T. A., Gu, Q., Johnson, R. L., Scott, M. P., Pennica, D., Goddard, A., Phillips, H. et al. (1996). The tumour-suppressor gene patched encodes a candidate receptor for Sonic hedgehog. *Nature* **384**, 129-34.

Stoykova, A. and Gruss, P. (1994). Roles of Pax-genes in developing and adult brain as suggested by expression patterns. *J Neurosci* **14**, 1395-412.

Strahle, U., Blader, P., Henrique, D. and Ingham, P. W. (1993). Axial, a zebrafish gene expressed along the developing body axis, shows altered expression in cyclops mutant embryos. *Genes Dev* **7**, 1436-46.

Strahle, U., Blader, P. and Ingham, P. W. (1996). Expression of axial and sonic hedgehog in wildtype and midline defective zebrafish embryos. *Int J Dev Biol* **40**, 929-40.

Strahle, U., Lam, C. S., Ertzer, R. and Rastegar, S. (2004). Vertebrate floor-plate specification: variations on common themes. *Trends Genet* **20**, 155-62.

Strominger, N. L., Truscott, T. C., Miller, R. A. and Royce, G. J. (1979). An autoradiographic study of the rubroolivary tract in the rhesus monkey. *J Comp Neurol* **183**, 33-45.

Sun, X., Meyers, E. N., Lewandoski, M. and Martin, G. R. (1999). Targeted disruption of Fgf8 causes failure of cell migration in the gastrulating mouse embryo. *Genes Dev* **13**, 1834-46.

Sund, N. J., Ang, S. L., Sackett, S. D., Shen, W., Daigle, N., Magnuson, M. A. and Kaestner, K. H. (2000). Hepatocyte nuclear factor 3beta (Foxa2) is dispensable for maintaining the differentiated state of the adult hepatocyte. *Mol Cell Biol* **20**, 5175-83.

Sund, N. J., Vatamaniuk, M. Z., Casey, M., Ang, S. L., Magnuson, M. A., Stoffers, D. A., Matschinsky, F. M. and Kaestner, K. H. (2001). Tissue-specific deletion of Foxa2 in pancreatic beta cells results in hyperinsulinemic hypoglycemia. *Genes Dev* **15**, 1706-15.

Suzuki, T., Fujikura, K., Higashiyama, T. and Takata, K. (1997). DNA staining for fluorescence and laser confocal microscopy. *J Histochem Cytochem* **45**, 49-53.

Swanson, J., Castellanos, F. X., Murias, M., LaHoste, G. and Kennedy, J. (1998). Cognitive neuroscience of attention deficit hyperactivity disorder and hyperkinetic disorder. *Curr Opin Neurobiol* **8**, 263-71.

Taguchi, J., Kuriyama, T., Ohmori, Y. and Kuriyama, K. (1989). Immunohistochemical studies on distribution of GABAA receptor complex in the rat brain using antibody against purified GABAA receptor complex. *Brain Res* **483**, 395-401.

Taipale, J. and Beachy, P. A. (2001). The Hedgehog and Wnt signalling pathways in cancer. *Nature* **411**, 349-54.

Taipale, J., Chen, J. K., Cooper, M. K., Wang, B., Mann, R. K., Milenkovic, L., Scott, M. P. and Beachy, P. A. (2000). Effects of oncogenic mutations in Smoothened and Patched can be reversed by cyclopamine. *Nature* **406**, 1005-9.

Taipale, J., Cooper, M. K., Maiti, T. and Beachy, P. A. (2002). Patched acts catalytically to suppress the activity of Smoothened. *Nature* **418**, 892-7.

Tanabe, Y., William, C. and Jessell, T. M. (1998). Specification of motor neuron identity by the MNR2 homeodomain protein. *Cell* **95**, 67-80.

Teillet, M. A., Lapointe, F. and Le Douarin, N. M. (1998). The relationships between notochord and floor plate in vertebrate development revisited. *Proc Natl Acad Sci U S A* **95**, 11733-8.

ten Donkelaar, H. J. (1988). Evolution of the red nucleus and rubrospinal tract. *Behav Brain Res* **28**, 9-20.

Tian, J., Yam, C., Balasundaram, G., Wang, H., Gore, A. and Sampath, K. (2003). A temperature-sensitive mutation in the nodal-related gene cyclops reveals that the floor plate is induced during gastrulation in zebrafish. *Development* **130**, 3331-42.

Tiveron, M. C., Hirsch, M. R. and Brunet, J. F. (1996). The expression pattern of the transcription factor Phox2 delineates synaptic pathways of the autonomic nervous system. *J Neurosci* **16**, 7649-60.

Trojanowski, J. Q., Goedert, M., Iwatsubo, T. and Lee, V. M. (1998). Fatal attractions: abnormal protein aggregation and neuron death in Parkinson's disease and Lewy body dementia. *Cell Death Differ* **5**, 832-7.

Tzschentke, T. M. (2000). The medial prefrontal cortex as a part of the brain reward system. *Amino Acids* **19**, 211-9.

Tzschentke, T. M. and Schmidt, W. J. (2000). Functional relationship among medial prefrontal cortex, nucleus accumbens, and ventral tegmental area in locomotion and reward. *Crit Rev Neurobiol* **14**, 131-42.

Ungless, M. A., Whistler, J. L., Malenka, R. C. and Bonci, A. (2001). Single cocaine exposure in vivo induces long-term potentiation in dopamine neurons. *Nature* **411**, 583-7.

Vaidya, C. J., Austin, G., Kirkorian, G., Ridlehuber, H. W., Desmond, J. E., Glover, G. H. and Gabrieli, J. D. (1998). Selective effects of methylphenidate in attention deficit hyperactivity disorder: a functional magnetic resonance study. *Proc Natl Acad Sci U S A* **95**, 14494-9.

van den Munckhof, P., Luk, K. C., Ste-Marie, L., Montgomery, J., Blanchet, P. J., Sadikot, A. F. and Drouin, J. (2003). Pitx3 is required for motor activity and for survival of a subset of midbrain dopaminergic neurons. *Development* **130**, 2535-42.
van der Kooy, D. (1979). The organization of the thalamic, nigral and raphe cells projecting to the medial vs lateral caudate-putamen in rat. A fluorescent retrograde double labeling study. *Brain Res* **169**, 381-7.
van Straaten, H. W. and Hekking, J. W. (1991). Development of floor plate, neurons and axonal outgrowth pattern in the early spinal cord of the notochord-deficient chick embryo. *Anat Embryol (Berl)* **184**, 55-63.
van Straaten, H. W., Hekking, J. W., Thors, F., Wiertz-Hoessels, E. L. and Drukker, J. (1985a). Induction of an additional floor plate in the neural tube. *Acta Morphol Neerl Scand* **23**, 91-7.
van Straaten, H. W., Thors, F., Wiertz-Hoessels, L., Hekking, J. and Drukker, J. (1985b). Effect of a notochordal implant on the early morphogenesis of the neural tube and neuroblasts: histometrical and histological results. *Dev Biol* **110**, 247-54.
Vernay, B., Koch, M., Vaccarino, F., Briscoe, J., Simeone, A., Kageyama, R. and Ang, S. L. (2005). Otx2 regulates subtype specification and neurogenesis in the midbrain. *J Neurosci* **25**, 4856-67.
Vollrath, D., Jaramillo-Babb, V. L., Clough, M. V., McIntosh, I., Scott, K. M., Lichter, P. R. and Richards, J. E. (1998). Loss-of-function mutations in the LIM-homeodomain gene, LMX1B, in nail-patella syndrome. *Hum Mol Genet* **7**, 1091-8.
Wakamatsu, Y. and Weston, J. A. (1997). Sequential expression and role of Hu RNA-binding proteins during neurogenesis. *Development* **124**, 3449-60.
Wallen, A. and Perlmann, T. (2003). Transcriptional control of dopamine neuron development. *Ann N Y Acad Sci* **991**, 48-60.
Wallen, A., Zetterstrom, R. H., Solomin, L., Arvidsson, M., Olson, L. and Perlmann, T. (1999). Fate of mesencephalic AHD2-expressing dopamine progenitor cells in NURR1 mutant mice. *Exp Cell Res* **253**, 737-46.
Wan, H., Kaestner, K. H., Ang, S. L., Ikegami, M., Finkelman, F. D., Stahlman, M. T., Fulkerson, P. C., Rothenberg, M. E. and Whitsett, J. A. (2004a). Foxa2 regulates alveolarization and goblet cell hyperplasia. *Development* **131**, 953-64.
Wan, H., Xu, Y., Ikegami, M., Stahlman, M. T., Kaestner, K. H., Ang, S. L. and Whitsett, J. A. (2004b). Foxa2 is required for transition to air breathing at birth. *Proc Natl Acad Sci U S A* **101**, 14449-54.
Wang, M. Z., Jin, P., Bumcrot, D. A., Marigo, V., McMahon, A. P., Wang, E. A., Woolf, T. and Pang, K. (1995). Induction of dopaminergic neuron phenotype in the midbrain by Sonic hedgehog protein. *Nat Med* **1**, 1184-8.
Wassarman, K. M., Lewandoski, M., Campbell, K., Joyner, A. L., Rubenstein, J. L., Martinez, S. and Martin, G. R. (1997). Specification of the anterior hindbrain and establishment of a normal mid/hindbrain organizer is dependent on Gbx2 gene function. *Development* **124**, 2923-34.
Weigel, D. and Jackle, H. (1990). The fork head domain: a novel DNA binding motif of eukaryotic transcription factors? *Cell* **63**, 455-6.
Weigel, D., Jurgens, G., Kuttner, F., Seifert, E. and Jackle, H. (1989). The homeotic gene fork head encodes a nuclear protein and is expressed in the terminal regions of the Drosophila embryo. *Cell* **57**, 645-58.
Weinstein, D. C., Ruiz i Altaba, A., Chen, W. S., Hoodless, P., Prezioso, V. R., Jessell, T. M. and Darnell, J. E., Jr. (1994). The winged-helix transcription factor HNF-3 beta is required for notochord development in the mouse embryo. *Cell* **78**, 575-88.

Wijgerde, M., McMahon, J. A., Rule, M. and McMahon, A. P. (2002). A direct requirement for Hedgehog signaling for normal specification of all ventral progenitor domains in the presumptive mammalian spinal cord. *Genes Dev* **16**, 2849-64.
Wilkinson, D. G., Bailes, J. A. and McMahon, A. P. (1987). Expression of the proto-oncogene int-1 is restricted to specific neural cells in the developing mouse embryo. *Cell* **50**, 79-88.
Wilson, L. and Maden, M. (2005). The mechanisms of dorsoventral patterning in the vertebrate neural tube. *Dev Biol* **282**, 1-13.
Wong, A. H. and Van Tol, H. H. (2003). Schizophrenia: from phenomenology to neurobiology. *Neurosci Biobehav Rev* **27**, 269-306.
Wood, H. B. and Episkopou, V. (1999). Comparative expression of the mouse Sox1, Sox2 and Sox3 genes from pre-gastrulation to early somite stages. *Mech Dev* **86**, 197-201.
Wuenschell, C. W., Mori, N. and Anderson, D. J. (1990). Analysis of SCG10 gene expression in transgenic mice reveals that neural specificity is achieved through selective derepression. *Neuron* **4**, 595-602.
Wurst, W., Auerbach, A. B. and Joyner, A. L. (1994). Multiple developmental defects in Engrailed-1 mutant mice: an early mid-hindbrain deletion and patterning defects in forelimbs and sternum. *Development* **120**, 2065-75.
Wurst, W. and Bally-Cuif, L. (2001). Neural plate patterning: upstream and downstream of the isthmic organizer. *Nat Rev Neurosci* **2**, 99-108.
Xiang, M., Gan, L., Zhou, L., Klein, W. H. and Nathans, J. (1996). Targeted deletion of the mouse POU domain gene Brn-3a causes selective loss of neurons in the brainstem and trigeminal ganglion, uncoordinated limb movement, and impaired suckling. *Proc Natl Acad Sci U S A* **93**, 11950-5.
Xie, J., Murone, M., Luoh, S. M., Ryan, A., Gu, Q., Zhang, C., Bonifas, J. M., Lam, C. W., Hynes, M., Goddard, A. et al. (1998). Activating Smoothened mutations in sporadic basal-cell carcinoma. *Nature* **391**, 90-2.
Xu, P. Y., Liang, R., Jankovic, J., Hunter, C., Zeng, Y. X., Ashizawa, T., Lai, D. and Le, W. D. (2002). Association of homozygous 7048G7049 variant in the intron six of Nurr1 gene with Parkinson's disease. *Neurology* **58**, 881-4.
Yamada, T., Pfaff, S. L., Edlund, T. and Jessell, T. M. (1993). Control of cell pattern in the neural tube: motor neuron induction by diffusible factors from notochord and floor plate. *Cell* **73**, 673-86.
Yamada, T., Placzek, M., Tanaka, H., Dodd, J. and Jessell, T. M. (1991). Control of cell pattern in the developing nervous system: polarizing activity of the floor plate and notochord. *Cell* **64**, 635-47.
Ye, W., Bouchard, M., Stone, D., Liu, X., Vella, F., Lee, J., Nakamura, H., Ang, S. L., Busslinger, M. and Rosenthal, A. (2001). Distinct regulators control the expression of the mid-hindbrain organizer signal FGF8. *Nat Neurosci* **4**, 1175-81.
Ye, W., Shimamura, K., Rubenstein, J. L., Hynes, M. A. and Rosenthal, A. (1998). FGF and Shh signals control dopaminergic and serotonergic cell fate in the anterior neural plate. *Cell* **93**, 755-66.
Zappone, M. V., Galli, R., Catena, R., Meani, N., De Biasi, S., Mattei, E., Tiveron, C., Vescovi, A. L., Lovell-Badge, R., Ottolenghi, S. et al. (2000). Sox2 regulatory sequences direct expression of a (beta)-geo transgene to telencephalic neural stem cells and precursors of the mouse embryo, revealing regionalization of gene expression in CNS stem cells. *Development* **127**, 2367-82.

Zervas, M., Blaess, S. and Joyner, A. L. (2005). Classical embryological studies and modern genetic analysis of midbrain and cerebellum development. *Curr Top Dev Biol* **69**, 101-38.
Zervas, M., Millet, S., Ahn, S. and Joyner, A. L. (2004). Cell behaviors and genetic lineages of the mesencephalon and rhombomere 1. *Neuron* **43**, 345-57.
Zetterstrom, R. H., Solomin, L., Jansson, L., Hoffer, B. J., Olson, L. and Perlmann, T. (1997). Dopamine neuron agenesis in Nurr1-deficient mice. *Science* **276**, 248-50.
Zetterstrom, R. H., Williams, R., Perlmann, T. and Olson, L. (1996). Cellular expression of the immediate early transcription factors Nurr1 and NGFI-B suggests a gene regulatory role in several brain regions including the nigrostriatal dopamine system. *Brain Res Mol Brain Res* **41**, 111-20.
Zhang, X. M., Ramalho-Santos, M. and McMahon, A. P. (2001). Smoothened mutants reveal redundant roles for Shh and Ihh signaling including regulation of L/R symmetry by the mouse node. *Cell* **106**, 781-92.
Zhao, S., Maxwell, S., Jimenez-Beristain, A., Vives, J., Kuehner, E., Zhao, J., O'Brien, C., de Felipe, C., Semina, E. and Li, M. (2004). Generation of embryonic stem cells and transgenic mice expressing green fluorescence protein in midbrain dopaminergic neurons. *Eur J Neurosci* **19**, 1133-40.
Zheng, K., Heydari, B. and Simon, D. K. (2003). A common NURR1 polymorphism associated with Parkinson disease and diffuse Lewy body disease. *Arch Neurol* **60**, 722-5.
Zhou, Q. and Anderson, D. J. (2002). The bHLH transcription factors OLIG2 and OLIG1 couple neuronal and glial subtype specification. *Cell* **109**, 61-73.
Zhou, Q., Choi, G. and Anderson, D. J. (2001). The bHLH transcription factor Olig2 promotes oligodendrocyte differentiation in collaboration with Nkx2.2. *Neuron* **31**, 791-807.
Zhou, Q., Wang, S. and Anderson, D. J. (2000). Identification of a novel family of oligodendrocyte lineage-specific basic helix-loop-helix transcription factors. *Neuron* **25**, 331-43.
Zhou, Q. Y. and Palmiter, R. D. (1995). Dopamine-deficient mice are severely hypoactive, adipsic, and aphagic. *Cell* **83**, 1197-209.
Zhou, Q. Y., Quaife, C. J. and Palmiter, R. D. (1995). Targeted disruption of the tyrosine hydroxylase gene reveals that catecholamines are required for mouse fetal development. *Nature* **374**, 640-3.
Zhu, A. J., Zheng, L., Suyama, K. and Scott, M. P. (2003). Altered localization of Drosophila Smoothened protein activates Hedgehog signal transduction. *Genes Dev* **17**, 1240-52.